BNL-72331-2004
FORMAL REPORT

RIKEN BNL Research Center

New Discoveries at RHIC
-- The Strongly Interactive QGP

Brookhaven National Laboratory
Upton, New York

April 5, 2004

RBRC Scientific Articles

Volume 9

Building 510A, Brookhaven National Laboratory, Upton, N.Y 11973-5000, USA

OFFICIAL FILE COPY

DISCLAIMER

This report was prepared as an account of work sponsored by an agency of the United States Government. Neither the United States Government nor any agency thereof, nor any of their employees, nor any of their contractors, subcontractors or their employees, makes any warranty, express or implied, or assumes any legal liability or responsibility for the accuracy, completeness, or any third party's use or the results of such use of any information, apparatus, product, or process disclosed, or represents that its use would not infringe privately owned rights. Reference herein to any specific commercial product, process, or service by trade name, trademark, manufacturer, or otherwise, does not necessarily constitute or imply its endorsement, recommendation, or favoring by the United States Government or any agency thereof or its contractors or subcontractors. The views and opinions of authors expressed herein do not necessarily state or reflect those of the United States Government or any agency thereof.

FOR UNCLASSIFIED, UNLIMITED STI PRODUCTS

Available electronically at-

OSTI:

http://www.osti.gov/bridge

Available for a processing fee to U.S. Department of Energy and its contractors, in paper from-

U.S. Department of Energy
Office of Scientific and Technical Information
P.O. Box 62
Oak Ridge, TN 37831
(865) 576-8401
Facsimile: (865) 576-5728
E-mail: reports@adonis.osti.gov

National Technical Information Service (NTIS):

Available for sale to the public from-

U.S. Department of Commerce
National Technical Information Service
5285 Port Royal Road
Springfield, VA 22131
(800) 553-6847
Facsimile: (703) 605-6900
Online ordering: http://www.ntis.gov/ordering.htm

Printed on recycled paper

Preface to the Series

The RIKEN BNL Research Center (RBRC) was established in April 1997 at Brookhaven National Laboratory. It is funded by the "Rikagaku Kenkyusho," (RIKEN) The Institute of Physical and Chemical Research, of Japan. The Center is dedicated to the study of strong interactions, including hard QCD/spin physics, lattice QCD and RHIC (Relativistic Heavy Ion Collider) physics through nurturing of a new generation of young physicists. The first Director of RBRC (1997 – 2003) was Professor T. D. Lee.

A Memorandum of Understanding between RIKEN and BNL was signed on April 30, 2002 extending this collaboration and the RIKEN BNL Research Center (RBRC) for another five years.

Since its inception the Center has now matured with both a strong theoretical and experimental group. These consist of Fellows, Postdocs, RBRC Physics/University Fellows and an active group of Consultants/Collaborators. Computing capabilities consist of a 0.6 teraflops parallel processor computer operational since August 1998. It was awarded the Supercomputer 1998 Gordon Bell Prize for price performance. This is expected to be augmented by a ten teraflops QCDOC computer in JFY 2004. The Center also organizes an extensive series of workshops on specific topics in strong interactions with an accompanying series of published proceedings.

Members and participants of RBRC on occasion will develop articles in the nature of a status report, a general review, and/or an overview of special events, such as this one.

N. P. Samios
Director, RIKEN BNL Research Center

*Work performed under the auspices of U.S.D.O.E. Contract No. DE-AC02-98-CH10886.

CONTENTS

Preface to the Series i

Forward 1

Experimental Results from the Early Measurements at RHIC; Hunting for the Quark Gluon Plasma
Thomas W. Ludlam 3

Theoretical Analysis:

New Forms of QCD Matter Discovered at RHIC
Miklos Gyulassy and Larry McLerran 23

Strongly Coupled Quark-Gluon Plasma
Edward Shuryak 61

Hadronic Signals of Deconfinement at RHIC
Berndt Müller 79

Discovery of Jet Quenching and Beyond
Xin-Nian Wang 89

Collective Flow Signals the Quark Gluon Plasma
Horst Stöcker 103

Searching Evidence for the Color Glass Condensate at RHIC
J.-P. Blaizot and F. Gelis 133

Other RBRC Scientific Articles Proceedings Volumes

Forward

Recent experiments at RHIC have produced matter at energy densities at least 20 times that of atomic nuclei and perhaps an order of magnitude even larger. At such extremely high energy densities, strongly interacting matter is composed of quarks and gluons. The extraordinary discoveries of jet quenching, strong elliptic flow and other properties at RHIC established that this matter strongly interacts with itself.

The purpose of this special volume is to highlight and summarize these published experimental discoveries from RHIC so far, and to pinpoint their physics implications from our present theoretical understanding. Since the volume deals with published experimental results and their implications, the same results already exist in the literature. Yet, we feel strongly that there are urgent needs and great merit for such a timely compilation of experts' views and summaries from the leaders in the field.

The present success of RHIC is the culmination of intense efforts by many physicists through more than three decades. In the earlier time, whenever the term Quark Gluon Plasma (QGP) was used, the underlying idea was quite often a weakly interactive plasma, much like the electron plasma. For such a weakly interactive plasma, Debye length would play a most fundamental role. Yet, what has been discovered at RHIC is a strongly interactive QGP, quite different from the old preconceptions. Many of the properties of this strongly interactive plasma are unexpected, and much of its characteristics are yet to be discovered. This is truly an exciting time for physics.

We are indebted to the contributors of this volume for their effort, and we sincerely hope this RBRC publication can be a useful service to the physics community at large.

T. D. Lee
N. P. Samios

Experimental Results from the Early Measurements at RHIC; Hunting for the Quark Gluon Plasma

Thomas W. Ludlam

Experimental Results from the Early Measurements at RHIC; Hunting for the Quark Gluon Plasma

T. Ludlam
Physics Department
Brookhaven National Laboratory

Abstract

This is a short survey of key measurements that have driven the exciting new physics results from the first years of RHIC operation. The focus is on those data that relate to the question of whether new forms of matter, e.g. the quark gluon plasma, can be explored with heavy ion collisions at RHIC. Only published, publicly available data are considered.

Prologue: A very brief history of relativistic heavy ion experiments

The first ideas for experiments to search for the quark gluon plasma came hard on the heels of the deep-inelastic scattering experiments of the 1970's that convinced us of the physical reality of quarks, and the subsequent rapid development of QCD as a theory to describe the concepts of quark confinement and asymptotic freedom. By the late 1970's an equation of state was discussed for nuclear matter in which a postulated "quark phase" appeared at temperatures and densities that seemed to be accessible to experiments via high energy collisions of heavy nuclei.

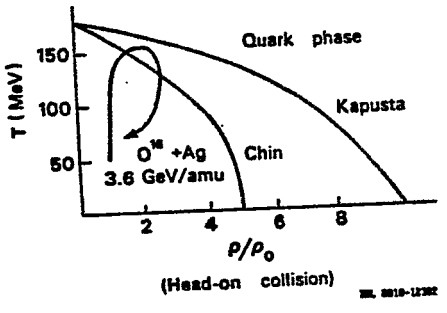

Figure 1: An early (c. 1979) phase diagram for nuclear matter showing a possible trajectory for exploring the quark phase with heavy ion collisions. The calculation for oxygen-silver collisions was done with a cascade code. [Ref. 1]

The search began at the Bevalac, at Lawrence Berkeley Lab, with nuclear beams in the range of a few GeV/u. Much was learned in this era of studies at LBL. Experiments showed that temperatures deduced from proton and pion spectra at 90° rose steadily with collision energies through the Bevalac range, and began to plateau near the Hagedorn temperature [2]. The phenomenon of flow in nuclear matter was developed as

a concept and established experimentally in the Bevalac program [3], as was the application of Hanbury-Brown Twiss interferometry to nuclear systems [4].

By 1980 it was clear that much higher collision energies were called for, and LBL developed a design for a heavy ion collider, VENUS, using the Bevalac as injector [5]. VENUS would have achieved beam energies of 20 GeV/u for heavy ions. At the same time efforts began, led by many in the Bevalac community, to promote the possibility of heavy ion collisions in the CERN PS, SPS, and ISR [6]. Brookhaven began exploring a possible heavy ion program at Isabelle, which was then under construction [7].

In the summer of 1983 a BNL-organized Task Force on Relativistic Heavy Ion Physics, including theorists, experimenters and accelerator physicists, presented a report to BNL Director Nick Samios with recommendations for the design parameters of a Relativistic Heavy Ion Collider that could be built in the footprint of the Isabelle/CBA project, whose fate had been sealed only weeks earlier [8]. Key specifications for RHIC at that time were that the facility be capable of accelerating ion species over the full range of nuclear masses (including protons), that it be able to provide proton-nucleus collisions, and that it be operational over a wide range of collision energies – leaving no large gap between the top energy of the forthcoming SPS data and the range covered by RHIC.

It was during this same summer of 1983 that the ten-year Long Range Plan for Nuclear Physics, carried out by the DOE/NSF Nuclear Science Advisory Committee, identified a high-energy colliding beams facility such as RHIC as the "highest priority new scientific opportunity in our field" [9].

With this impetus, a program began immediately to accelerate ions for experiments in the AGS just as similar plans were going ahead for the CERN SPS. The first experiments in the AGS, with oxygen and silicon ions accelerated to ~10 GeV/u, began in 1984. These were soon followed by gold beams. Experiments in the SPS, with sulfur and then lead beams at 160 GeV/u began in 1985. The fixed-target experiments at Brookhaven and CERN provided the first opportunity for extensive studies of heavy-nucleus interactions in the energy regime associated with high-energy particle production.

Helped by significant advances in detector and computing technology, the AGS and SPS heavy ion experiments made measurements of the abundances and spectra of many species of particles produced in these collisions. In particular, measurements were made at CERN of the production of the J/ψ resonance, a bound state of charm and anti-charm quarks, with results clearly indicating that the nucleus-nucleus collisions at high energy are very different from a simple superposition of nucleon-nucleon interactions. These, and many other measurements showed that nuclear collisions are indeed capable of producing the conditions needed for the existence of hot, compressed nuclear matter [10].

In 2000, after 15 years of ground-breaking experiments with the fixed-target ion beams, and the SPS heavy ion program nearing completion, CERN scientists assessed the

combined results from the seven large experiments participating in the lead beam program. [11] They concluded that a "multitude" of different observations gave results which, taken together, could not be explained with models based on ordinary hadronic interactions, while on the other hand the data showed several of the expected indicators for a quark-gluon plasma. Having built a strong case of circumstantial evidence, the community expressed confidence that definitive observation of the elusive new state of matter would come with next generation of collision energies about to become available. In the words of Director General Luciano Maiani at a CERN press conference in February 2000, "The challenge now passes to the Relativistic Heavy Ion Collider at Brookhaven, and later to CERN's Large Hadron Collider."

The Collider era begins: surveying the new landscape

The RHIC construction project was formally completed in 1999, and the first data-taking runs began in the summer of 2000, with full participation by all four experiments: BRAHMS, PHENIX, PHOBOS, and STAR. [12]. The run modes for RHIC operation to date are shown in Table 1.

Year	Beam Configurations	Sample	Physics
2000	Au-Au at 130 GeV/u	~5 μb^{-1} (5wk)	First look at HI collisions in the new energy range
2001-2002	Au-Au at 200 GeV/u	~50 μb^{-1} (14wk)	Global properties; particle spectra; first look at hard scat.
	Au-Au at 19 GeV/u	<1 μb^{-1} (1 day)	Global connection to SPS energy
	p-p at 200 GeV	~0.8 μb^{-1} (5wk)	Comparison data; first spin data
2003	d-Au at 200 GeV/u	~10 nb^{-1} (11wk)	Comparison data for Au-Au analysis.
	p-p at 200 GeV	~5 pb^{-1} (3wk)	Spin data & commissioning
2004	Au-Au at 200 GeV/u	~1.2 nb^{-1} (10wk)	"Long run" for high statistics
	Au-Au at 62.4 GeV	~ 20 μb^{-1} (1wk)	Energy scan
	p-p at 200 GeV	(5 wk)	Development run

Table 1. Overview of RHIC Physics runs from 2000 to 2004.

As the sample sizes in this table indicate, the early RHIC runs were marked by a rapid increase in the machine performance. By the end of Run-2 (2001-2002) the design luminosity for full-energy Au+Au collisions had been achieved. This rapid development is graphically illustrated in Figure 2, which shows the rate at which Au+Au data were collected by the four experiments over three running periods.

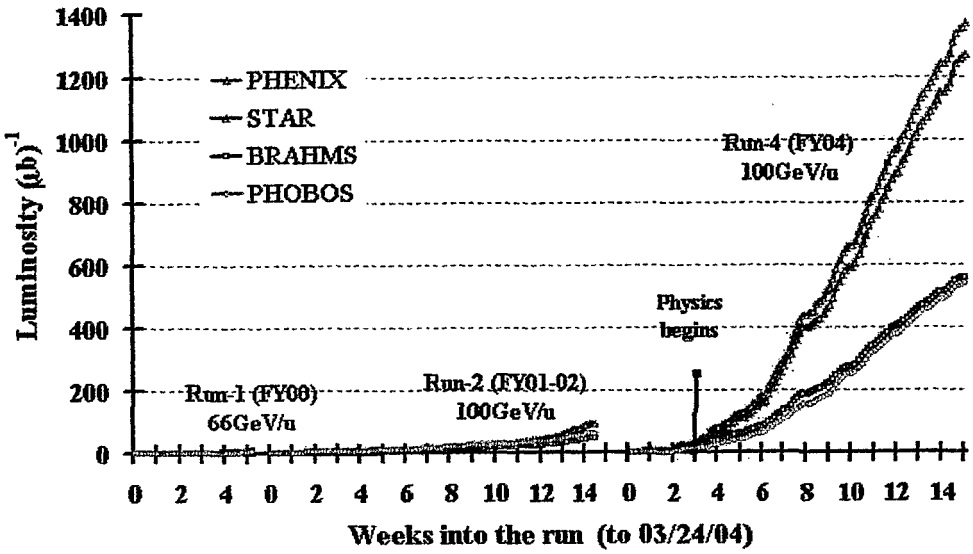

Figure 2. The integrated luminosity delivered to each of the four experiments during the three Au+Au running periods to date.

Also evident in Table 1 is the importance of the flexibility built into the machine to operate in many modes. The ability to operate the collider in six different modes of beam species/collision energy during the first four physics runs has been a critical factor in making possible the extraordinary wealth of physics results that have come out so quickly.

The first Au-Au run at RHIC, at sqrt(S_{nn}) = 130 GeV, quickly showed that the gross features of the data are consistent with monotonically increasing energy densities with increasing collision energy. The measured transverse energy spectrum in the PHENIX central spectrometer arms revealed unprecedented energy deposition in the central region of rapidity for the most central events (**Figure 3**) [13].

In treating these early data, all four experiments came together to provide consistent, precisely defined centrality classes based on particle multiplicities and zero-degree calorimenters, and using a consistent set of Glauber-type calculations to extract the number of participating nucleons, N_{part}, and the number of binary nucleon-nucleon collisions, N_{coll}, for each centrality class (see, for example, Fig. 3).

Multiplicity data for the most central collisions, first published by PHOBOS [14], show a corresponding logaraithmic increase of particle density with collision energy (**Figure 4a**). The multiplicity density per interacting nucleon pair significantly exceeds

that measured in nucleon-nucleon collider data. Nonetheless, as discussed in Ref. 14, the measured multiplicity densities fall at the low end of the spectrum of pre-RHIC theoretical predictions. Also, significantly, the multiplicity density saturates with increasing centrality (N_{part}), as seen in **Figure 4b.**

These E_T and multiplicity results provide the basis for the first estimates of the energy density achieved in the RHIC collisions. The energy density obtained by PHENIX from the E_T data, using the straightforward Bjorken formulation for central events, is $\varepsilon_{BJ} = 4.6$ GeV/fm^3 at sqrt(S_{nn}) = 130 GeV [13]. The corresponding number at 200 GeV is $\varepsilon_{BJ} = 5.0$ GeV/fm^3. These estimates assume a formation time of 1 fm/c. More aggressive estimates, invoking smaller formation times, are often quoted as 15 GeV/fm^3 or larger. Calculations of energy loss of high pT particles support the larger values (see later), as do the (model dependent) hydrodynamic calculations of initial conditions based on particle spectra and flow data. In any event, data indicate energy densities that well exceed the value inside a nucleon (~1 GeV/fm^3).

Another important early result from the RHIC data was the rapid publication of well-measured spectra for identified particles at mid-rapidity, including mesons, baryons, and hyperons. From these data it was quickly learned that the statistical thermal models that had previously been applied to the AGS and SPS heavy ion data work very well in the RHIC energy range. As shown in **Figure 5**, the relative abundances of observed particle types are very well described by a statistical system with an equilibrium temperature at chemical freeze-out of T = 177 MeV, and a baryochemical potential μ_B = 29 MeV [15]. The near-zero value for the baryon density is a qualitatively new feature of the RHIC results, when compared to the lower-energy data. That the RHIC collisions closely approximate the ideal of a "baryon free" central rapidity region is nicely illustrated in the BRAHMS data shown in **Figure 6** [16]. The net baryons represent ~1% of the particle density at mid-rapidity in central collisions.

The HBT interferometry results from RHIC provided an early surprise, and remain a puzzle. The measured source sizes grow with centrality, and decrease with transverse momentum. But, as seen in **Figure 7**, the HBT parameters exhibit a very weak dependence on collision energy, spanning the range of AGS, SPS, and RHIC data [17]. The anomalously large radii and emission durations that had been predicted as a consequence of HBT formation are not seen.

The RHIC Harvest: Major new results

Flow and hydrodynamics

Having established that the Au-Au collisions produce high temperature and energy density over an apparently large volume, an essential question is whether or not this is a manifestation of a self-interacting medium. Is the hot volume in, or near, thermal equilibrium?

Among the first, surprising results from the early Au-Au data was the strength of the observed elliptic flow, and the degree to which the flow measurements agree with the calculations of models based on "ideal" hydrodynamics [18, 19]. This is illustrated in **Figure 8**, which shows measured charged-particle v_2, the asymmetry with respect to the reaction plane that defines elliptic flow, as a function of centrality (**Fig 8a**), and also a compilation (**Fig. 8b**) that graphically illustrates the saturation of hydrodynamic effects in RHIC energy range. It has, of course, been pointed out that the linear increase of the strength of elliptic flow shown in Fig. 8b shows no sign of actually saturating at the calculated hydro limit!

A convincing demonstration of the relevance of the observed flow behavior to hydrodynamic phenomena is shown in **Figure 9** [19, 20], where the measured flow parameter, v_2, is plotted as a function of transverse momentum for identified mesons and baryons. For soft particles, p_T less than ~1GeV/c, the dependence of flow on particle mass is described with remarkable accuracy by the hydrodynamic calculations. This is a strong indicator of bulk collective flow.

At large p_T, strong azimuthal correlations are still seen, but show a saturation for p_T above ~ 3 GeV/c, with values that decrease systematically with increasing centrality (**Figure 10**) [21]. This is a departure from nondissipative hydrodynamics, which predicts a monotonically increasing v_2 with increasing p_T.

Hard scattering at RHIC: Jet Quenching

The RHIC collision energy brings heavy-ion physics into the realm of hard-scattering QCD phenomena for the first time, and the first time, and the first look through this new window quickly revealed a qualitatively new phenomenon: In central Au-Au collisions the rate of particle production at large p_T does not scale with the number of nucleon-nucleon collisions in the interaction, but is dramatically suppressed in comparison with extrapolation from proton-proton collision data.
The comparison is made in terms of the "nuclear modification function",

$$R_{AA}(p_T) = \frac{d^2N^{AA} / dp_T d\eta}{T_{AA} d^2\sigma^{NN} / dp_T d\eta}$$

Where T_{AA} is the scaled number of binary nucleon-nucleon collisions, obtained from Glauber calculations for each centrality class. The suppression, seen in **Figure 11** [22], is in sharp contrast with the enhancement seen in the previous, lower energy heavy ion data, which exhibit the "Cronin effect" familiar from high-energy proton-nucleus data.

In subsequent measurements at 200 GeV/u, all four of the RHIC experiments have obtained well-measured spectra, as a function of centrality, for charged particles over transverse momenta out to $p_T > 10$ GeV/c. PHENIX has measured π^0s over this range as well. Importantly, all four experiments have directly measured p-p comparison

data at sqrt(S) = 200 GeV in their own detectors. Some representative data are shown in **Figure 12** [23-25].

The published RHIC data now map out in considerable detail the systemmatics of high-p_T suppression. **Figure 13a** shows R_{AA} for charged hadrons vs. transverse momentum, as a function of centrality (STAR) [23]. **Figure 13b** shows R_{AA} vs. p_T for π^0 data measured by PHENIX [25]. In both cases the suppression seen in central Au-Au events appears to saturate at $R_{AA} \approx 0.2$, extending to the highest measured p_T. Charged hadron data appear to behave differently from the π^0 data at intermediate p_T. Indeed, data from both PHENIX and STAR indicate that the degree of suppression in the p_T range from ~2 – 5 GeV/c depends very much on the type of observed particle, with pronounced differences in the behavior of mesons and baryons in this range [20, 26]. See **Figure 14.**

The observed high-p_T particles are generally assumed to be the products of jet production... the fragmentation of hard-scattered partons in the collision. Hence the observed suppression of high-p_T particles is readily associated with the phenomenon of "jet quenching", the predicted energy loss of hard-scattered partons in a dense final-state medium [27]. An important development in the analysis of the Au-Au data at RHIC has been the direct identification of jet structure through azimuthal correlations among high-p_T particles, as illustrated in **Figure 15** [28].

The Color Glass Alternative; deuteron-gold data

The observation of jet quenching is a powerful argument for the existence of a dense, thermalized final-state medium. Furthermore, if this medium is quark-gluon matter described by QCD, then energy-loss mechanisms can be calculated, and quantitative measurements of the modified high-p_T spectra can become an important probe of the properties of deconfined matter.

First, however, it became important to verify the energy-loss interpretation, in light of the recent theoretical work on the role of initial-state gluon saturation: the color glass condensate [29]. From this perspective, the paucity of jets in nuclear collisions may be purely an initial-state effect, resulting from the fact that the wavefunction of a nucleus during a high-energy collision differs significantly from a simple superposition of nucleon wavefunctions. The results on multiplicity density, noted above, are in general agreement with the color glass condensate scenario of strong coherence and extreme shadowing in the initial, formative stages of the collision.

The RHIC deuteron-gold run, carried out from January to March in 2003, was undertaken to discriminate between these two interpretations of the jet quenching results. In these collisions of a large nucleus with a small one, the color glass condensate mechanism should be operative, while there should be no significant volume of hot matter in the final state to slow down the hard-scattered partons.

By June 2003 the striking results of these measurements were presented by all four of the RHIC experiments. **Figure 16** shows the comparison of R_{AA} vs. p_T for d-Au and Au-Au collisions from BRAHMS [30], PHENIX [31], PHOBOS [32], and STAR [33]. The suppression at high pT seen in central Au-Au data is absent in the d-Au data. The result is further illustrated in the high-p_T correlation data shown in **Figure 17**, comparing Au-Au central, d-Au central, and p-p collisions. The recoil jet peak, absent in the Au-Au data, is clearly present in both d-Au and p-p collisions.

These data, presented simultaneously by the four collaborations on June 18, 2003, provide a conclusive experimental determination that the jet quenching effects seen in Au-Au collisions at mid-rapidity are in fact the result of final-state interactions, as expected from the formation of a hot, dense medium of deconfined matter.

Outlook

The published data from RHIC, through the 2003 runs, give convincing evidence that high-energy collisions of heavy nuclei produce a hot, dense state of matter characterized by strong collective interactions. This state has the earmarks of the long-postulated quark gluon plasma, and the details of this identification are now coming into focus [34]. In several important ways, the exploration of this new state of matter has taken a different course from what was envisioned when RHIC was first proposed. Instead of "smoking gun" signatures among the remnants of quark gluon plasma found in the collision debris, we have found a silver bullet in the ability to probe deconfined matter directly with high-p_T signals that can be calculated from the theory of QCD, rather than relying on phenomenological models.

RHIC may also be giving us a window on yet another elemental form of matter predicted by QCD: the color glass condensate. Although the d-Au results have ruled out color glass effects as the origin of jet quenching at mid-rapidity, there are many global features of the Au-Au data that support the hypothesis of strong saturation effects at early times in the collision. Furthermore, results reported by BRAHMS, PHENIX, and PHOBOS at the recent Quark Matter 2004 conference [38] indicate suppression of high-p_T production in d-Au data at large rapidity, where smaller values of Feynman-x are sampled than at mid-rapidity.

Thus, there are strong indications for an emerging picture in which the formation of quark-gluon plasma is preceded by an initial state described by color glass condensate, and that both of these states can be explored experimentally at RHIC. The stage is now set for a detailed understanding of these new phenomena and their relationship to the nature and origins of hadronic matter. The sensitive new probes involve measurements of rare processes, requiring large data samples. As illustrated in figure 2, the first step toward these precision measurements has been taken: The 2004 data samples, now being analyzed, have benefited from rapidly improving accelerator performance and exceed the previous statistics for Au-Au collisions by more than an order of magnitude.

References

1. K. Gudima and V. Toneev, Dubna Report E2-12624, 1979

2. These data are reviewed by H. Stocker et al., Int. Conf. On Extreme States in Nuclear Systems, Dresden (1980), p. 104

3. See, for example: H. Pugh, *"Equilibration, Compression and Flow at the Bevalac"*, Quark Matter '84 Proceedings, K. Kajantie, ed., Springer Verlag (1984), p. 143

4. Early HBT reference

5. The VENUS Project, LBL Pub-5025 (1979)

6. See H.G. Pugh, Proc. Workshop on Future Relativistic Heavy Ion Experiments, GSI Darmstadt, GSI 81-6 (1981), p. 1

7. CBA proposal (1982)

8. Report of the Task Force for Relativistic Heavy Ion Physics, reprinted in Proc. Quark Matter '83, Nucl. Phys. A418, (1984) p. 657c

9. DOE/NSF NSAC Long Range Plan, 1983

10. For recent surveys of results with heavy ion beams at the AGS and SPS accelerators, see C.A. Ogilvie, Nuclear Physics A 698 (2002), 3c; C. Lourenco, Nuclear Physics A 698 (2002), 13c.

11. M. Jacob and U. Heinz, "Evidence for a New State of Matter: an Assessment of the Results from the CERN Lead Beam Programme", CERN Press Office, *available online at www.cern.ch/CERN/Announcements/2000/NewStateMatter/science.html*

12. "The Relativistic Heavy Ion Collider Project: RHIC and its Detectors", M. Harrison et al, ed., Nuclear Instruments and Methods in Physics Research A 499 (2003).

13. PHENIX, K. Adcox et al., Phys. Rev. Lett. **87**, 052301 (2001)

14. PHOBOS, B.Back et al., PRL **88**, 022302 (2002); B. Back et al. Phys. Rev. **C65**, 061901R (2002)

15. P. Braun-Munzinger et al., Phys. Lett. **B518**, 41 (2001), and references therein

16. BRAHMS, I.G. Bearden et al., Phys. Rev. Lett. **90**, 102301 (2003)

17. STAR, C. Adler et al., Phys. Rev. Lett. **87**, 082301 (2001)

18. STAR, K.H. Ackermann et al., Phys. Rev. Lett. **86**, (2001), p. 402; C. Adler et al., Phys. Rev. **C66**, 034904 (2002)

19. PHENIX, S. Adler et al., Phys. Rev. Lett. **91**, 172301 (2003)

20. STAR, J. Adams et al., Phys. Rev. Lett. **92**, 052302 (2004)

21. STAR, C. Adler et al., Phys. Rev. Lett. **90**, 032301 (2003)

22. PHENIX, K. Adcox et al., Phys. Rev. Lett. **88**, 022301 (2002)

23. STAR, J. Adams et al., Phys. Rev. Lett. **91**, 172302 (2003)

24. PHENIX, S. Adler et al, Phys. Rev. Lett. **91**, 241803 (2003)

25. PHENIX, S. Adler et al., Phys. Rev. Lett. **91**, 072301 (2003)

26. PHENIX, S. Adler et al., Phys. Rev. Lett. **91**, 172301 (2003)

27. For a review, see: M. Gyulassy, I. Vitev, X.N. Wang, B.W. Zhang, "Jet Quenching and Radiative Energy Loss in Dense Nuclear Matter", published in *Quark Gluon Plasma 3*, R.C. Hwa and X. N. Wang, editors, World Scientific, Singapore, 2003.

28. STAR, C. Adler et al., Phys. Rev. Lett. **90**, 082302 (2003)

29. For a review, see: E. Iancu and R. Venugopalan, "The Color Glass Condensate and High-Energy Scattering in QCD", published in *Quark Gluon Plasma 3*, R.C. Hwa and X. N. Wang, editors, World Scientific, Singapore, 2003.

30. PHOBOS, B. Back et al., Phys. Rev. Lett. **91**, 072302 (2003)

31. PHENIX, S. Adler et al., Phys. Rev. Lett. **91**, 072303 (2003)

32. STAR, J. Adams et al., Phys. Rev. Lett. **91**, 072304 (2003)

33. BRAHMS, I. Arsene et al., Phys. Rev. Lett. **91**, 072305 (2003)

34. Very recent discussions can be found in the proceedings of this workshop.

35. Quark Matter 2004, Oakland, Ca., January 2004, proceedings to be published. The program is available on-line at http://qm2004.lbl.gov/

Figure 3

a. *Transverse energy spectrum at mid-rapidity measured by PHENIX in Au-Au collisions at 130 GeV. The solid curve shows minimum-bias data. The dashed curves show the top four centrality classes [Ref. 13]*

b. *Transverse energy spectrum from STAR, presented at the Quark Matter 2004, Oakland Ca, January 2004.*

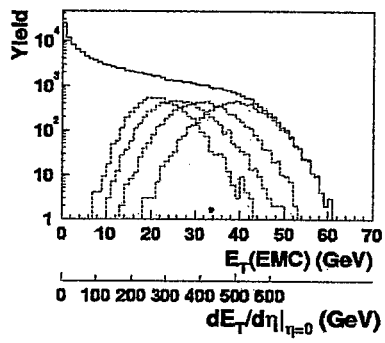

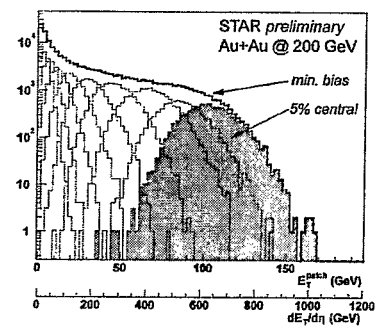

Figure 4a

Charged particle multiplicity density per interacting nucleon pair vs. collision energy. Central collision data from nucleus-nucleus interactions are compared with proton-antiproton collider data. Ref. 14

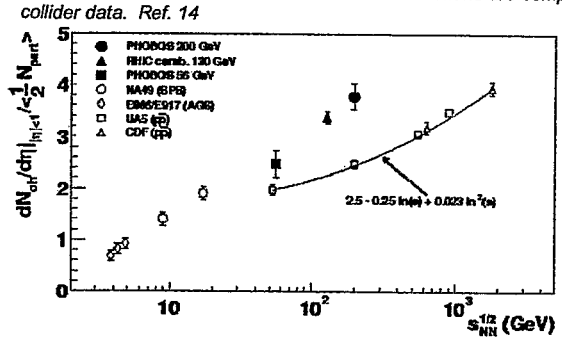

Figure 4b
PHOBOS measurement of multiplicity density as a function of centrality (Npart) Ref. 14

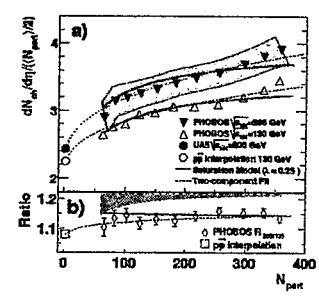

Figure 5
Measured particle abundance ratios at RHIC compared with statistical thermal model calculation. Ref. 15

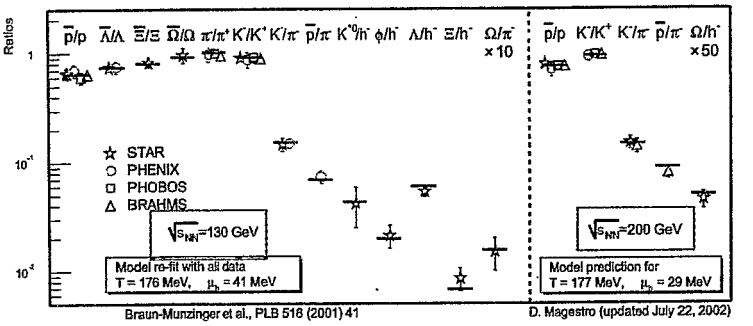

Figure 6

a. *The measured antiparticle/particle ratios as a function of rapidity, for central Au-Au collisions at sqrt(S_{nn}) = 200 GeV. BRAHMS, Ref. 16*

b. *The corresponding dn/dy spectra.*

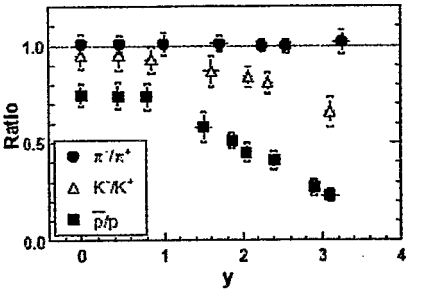

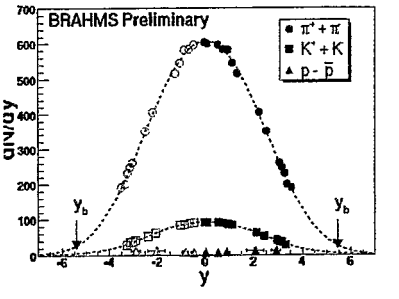

Figure 7

Measured HBT parameters as a function of (a.) collision energy and (b.) transverse momentum at the RHIC energy. [Ref. 17]

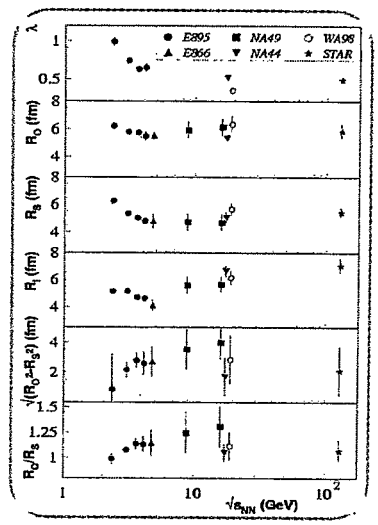

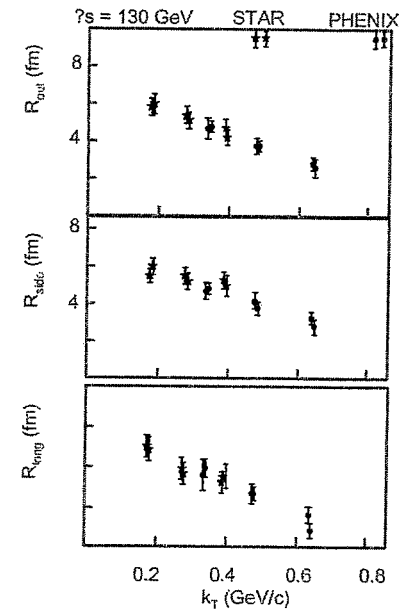

Figure 8a

The measured elliptic flow asymmetry Parameter as a function of centrality for 130 GeV/u Au-Au collisions (data points). The open rectangles show the range of values expected in the hydrodynamic limit. [Ref. 18]

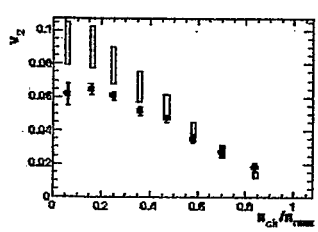

Figure 8b

The strength of elliptic flow a function of the density of particles in the collision overlap region [Ref. 18]. Here, ε measures the initial spatial eccentricity, and S is the area of the overlap region.

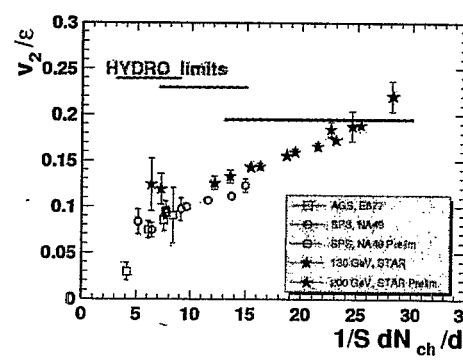

Figure 9

The elliptic flow parameter vs. transverse momentum for different particle species. Data from Ref.s 19, 20.
Hydro calculations: Huovinen et al., Phys. Lett. B 503 58 (2001)

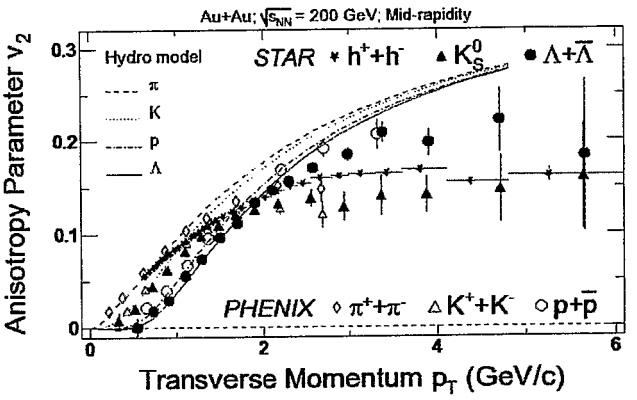

Figure 10

The reaction-plane asymmetry parameter as a function of transverse momentum, for different centralities in Au-Au collisions at 130 GeV/u. [Ref. 21]

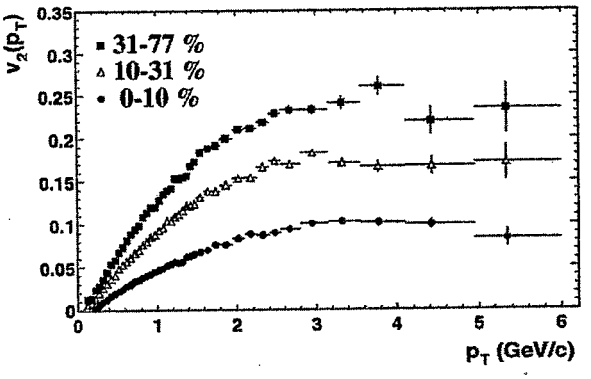

Figure 11

The nuclear modification ratio R_{AA} for charged hadrons an neutral pions in central Au-Au collisions. The band shows the range of values measured at the SPS, ssqrt(S_{nn}) = 17 GeV. Ref. 22.

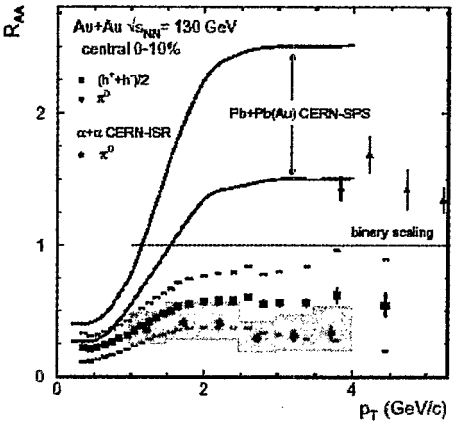

Figure 12

12a

Charged particle spectra from Au-Au and p-p collisions at 200 GeV/u in STAR, showing centality classes. [Ref. 23]

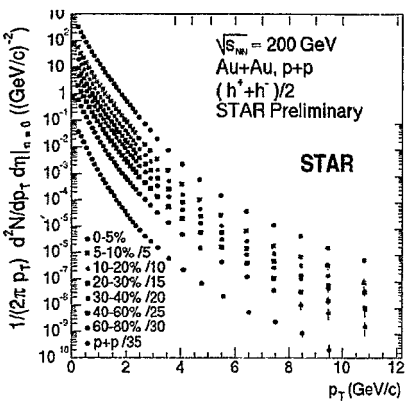

12b

π^0 spectra from p–p and central Au-Au collisions at 200 GeV/u in PHENIX. [Ref. 24, 25]

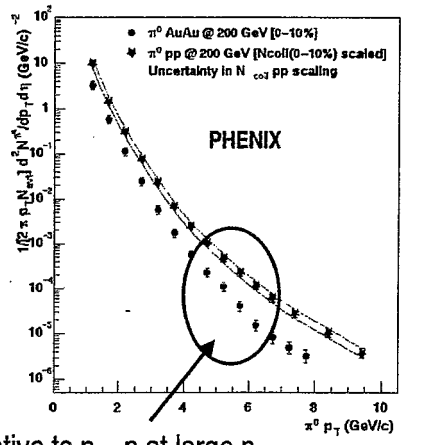

Clear suppression in central Au-Au relative to p – p at large p_t

Figure 13a
The nuclear modification function, R_{AA}, vs. transverse momentum for charged hadrons, as a function of centrality. STAR, Ref. 23

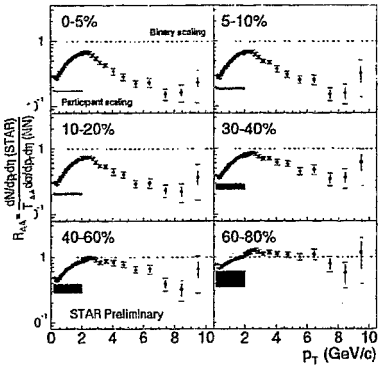

Figure 13b
R_{AA} vs. p_T for central and peripheral π^0s. PHENIX, Ref. 25.

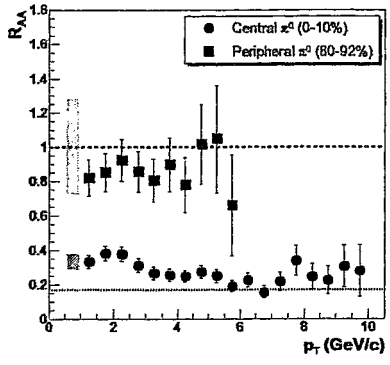

Note: vertical axis is logarithmic for STAR data, linear for PHENIX data.

Figure 14
Suppression data, measuring the ratio of yeilds in central to peripheral collisions, for identified mesons and baryons as a function of transverse momentum.

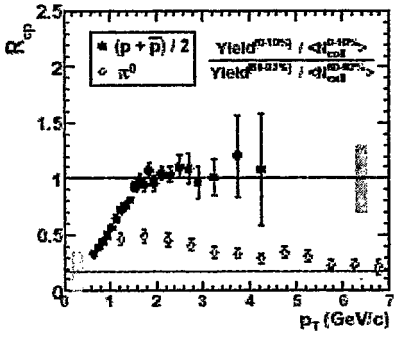

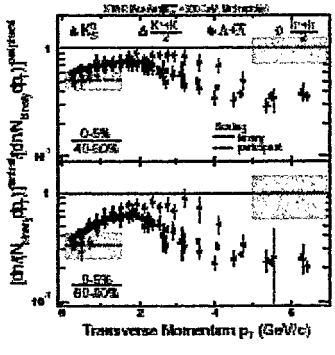

PHENIX: Ref. 26

STAR: Ref. 20

Figure 15

Two particle correlations at high p_T

The top panel shows azimuthal correlations between a "trigger" particle with $p_T > 4$ GeV/c and all other particles in the event with $p_T > 2$ GeV/c. The open circles are the estimated contribution from flow effects. The difference, shown in the lower panel, shows a jet peak at $\varphi = 0$. STAR, Ref. 28.

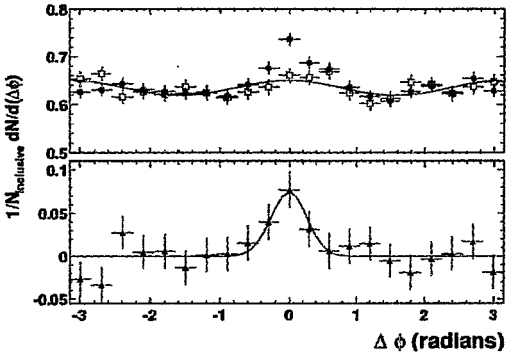

Figure 16a,b

Deuteron-gold data at $\sqrt{S_{nn}}$ = 200 GeV recorded Jan – Mar 2003, compared with Au-Au suppression results.

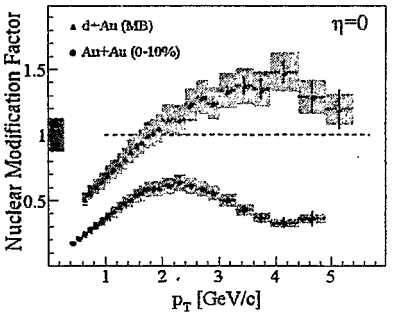

BRAHMS data: Ref. 30

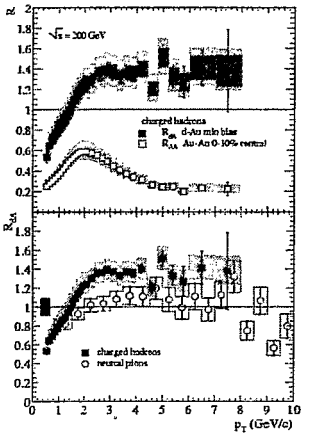

PHENIX data: Ref. 31

Figure 16 b,c
Deuteron-gold data at $\sqrt{S_{nn}}$ = 200 GeV recorded Jan – Mar 2003, compared with Au-Au suppression results.

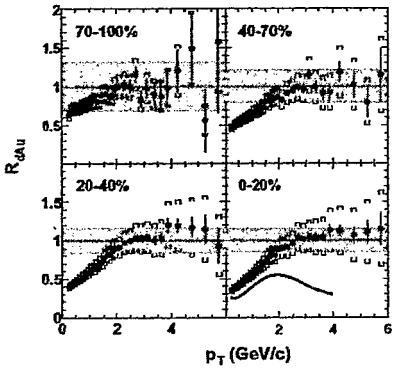

PHOBOS data: Ref. 32

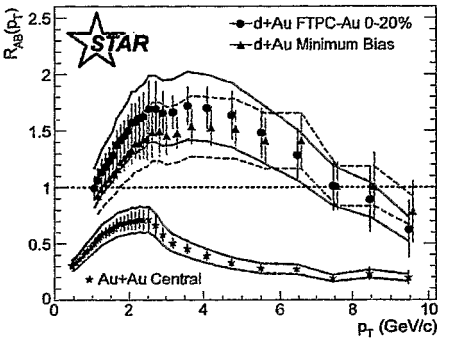

STAR data: Ref. 33

Figure 17
High-pT correlation data for p-p, central d-Au, central Au-Au at sqrt(S_{nn}) = 200 GeV, Showing trigger jet peaks at 0 degrees and recoil jet peaks at 180 degrees.
STAR data: Ref. 33

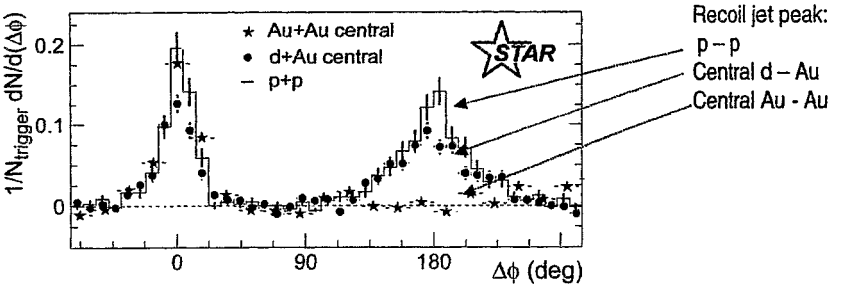

New Forms of QCD Matter Discovered at RHIC

Miklos Gyulassy and Larry McLerran

New Forms of QCD Matter Discovered at RHIC.

Miklos Gyulassy[a] and Larry McLerran[b]

[a]*Physics Department, Columbia UniversityNew York, NY USA*

[b]*Physics Department POB 5000 Brookhaven National Laboratory Upton, NY 11973 USA*

Abstract

We discuss two special limiting forms of QCD matter which may be produced at RHIC. We conclude from the available empirical evidence that an equilibrated, but strongly coupled Quark Gluon Plasma has been made in such collisions. We also discuss the growing body of evidence that its source is a Color Glass Condensate.

1 Introduction

Thirty years ago[1], T.D. Lee suggested that it would be interesting to explore new phenomena "by distributing high energy or high nucleon density over a relatively large volume." In this way one could temporarily restore broken symmetries of the physical vacuum and possibly create novel abnormal dense states of nuclear matter[2]. W. Greiner and collaborators pointed out that the required high densities could be achieved via relativistic heavy ion collisions[3]. Concurrently, Collins and Perry and others[4] realized that the asymptotic freedom property of Quantum Chromodynamics (QCD) implies the existence of an ultra-dense form of matter with deconfined quarks and gluons, called later the Quark-Gluon Plasma (QGP)[5]. In 1982 J.D. Bjorken developed a relativistic hydrodynamic theory[6] of the novel "inside-out" evolution of the central low baryon density regions of ultra-relativistic heavy ion collisions. While many signatures of QGP formation were proposed, he suggested that "if the quark-gluon plasma is produced, it will manifest itself in experimental signatures as yet unforeseen. The system is after all a complicated relativistic fluid subject to highly nonlinear forces. ... If very interesting and novel phenomena will be seen in ion-ion collisions, theory must develop the capability to interpret them, if not to predict them".

With this theoretical background, the 1983 DOE/NSAC Long Range Plan set in motion plans that led to the construction of the Relativistic Heavy Ion Collider (RHIC) [7] to explore properties of ultra-dense matter above the deconfinement transition point. Now, after its first three years of operation, a vast data base[8] on $p+p, D+Au$, and $Au+Au$ at $\sqrt{s} = 20-200$ AGeV has been harvested from RHIC. The published data are available through 22 (4 PRL) publications from BRAMHS[9], 92 (15 PRL) from PHENIX[10], 34 (6 PRL) from PHOBOS[11], and 127 (21 PRL) from STAR[12]. This body of data extends and builds upon the knowledge gained about dense hadronic matter measured at the SPS/CERN (publications include 108 NA49/35, 69 NA50/38, 26

CERES/NA45, 79 WA98/80, 32 na57/wa97) at $\sqrt{s} \leq 20$ AGeV The SPS heavy ion data already displayed several signatures that hinted at the onset of QGP formation[13]. Based on the SPS data and theoretical predictions, RHIC with its factor of 10 increase in the center of mass energy to 200 AGeV was assured to create matter well above the deconfinement transition point. The fourth year run of RHIC with Au+Au at 200 AGeV has just concluded with a gain of about another factor ~ 20 integrated luminosity ($\sim 1400/\mu$b). These and future RHIC data with significantly upgraded detectors will provide even higher resolution measurements of the detailed properties of the new forms of matter discovered at RHIC.

While there naturally remain many open questions and unsolved puzzles, a striking set of new phenomena have been conclusively discovered at RHIC. Those phenomena furthermore can now be readily interpreted and predicted from significant advances in theory and from the empirical information gained from the past 30 years from the Bevalac, SIS, AGS, and SPS experiments.

In this report, we discuss[14, 15] the evidence that at least one and possibly two new forms of QCD matter have been discovered at RHIC. We consider the Quark Gluon Plasma, which is a form of matter characterized by a thermal equilibrium density matrix of a system of quarks and gluons. We also consider the Color Glass Condensate (CGC), which is a form of matter characterized by a universal initial density matrix which describes high energy strongly interacting particles - including nuclei. The QGP is the incoherent thermal limit of QCD matter at high temperatures while the CGC is the coherent limit of QCD at high energies. Since the QGP has to be created at RHIC from the interaction of initial nuclear enhanced coherent chromo electric magnetic fields, both limiting forms of QCD matter need to be considered at RHIC.

The first 275 published experimental papers from RHIC have of course only barely scratched the surface of the new physics of these forms of matter, but the data are so striking and decisive that several strong physics conclusions can already be drawn. They establish empirically that a special form of strongly interacting QGP (sQGP) exists with remarkable properties. In addition, there is growing evidence that its source is well described by a saturated gluon CGC initial state. These RHIC discoveries and those at the SPS/CERN pave a clear path for future systematic studies of these new forms of matter in the laboratory.

We begin in section 2 by describing the basic ingredients of the QGP hypothesis. The hypothesis concerning the existence and properties of this form of matter has a firm basis in QCD. Much is known about its theoretical properties on the basis of numerical computation within QCD (lattice gauge theory). In section 3 we review the CGC hypothesis, which is newer but is also based firmly in QCD. The CGC hypothesis can be tested in a wide range of experimental environments (HERA, RHIC,LHC,eRHIC) not restricted to heavy ion collisions. It is newer, and because of this, somewhat more tenuous than is the QGP hypothesis.

The scientific method is based on the paradigm that theories are tested by falsification. This is an important concept, since simple models with many adjustable parameters are often used to "fit" heavy ion data. However, one of the most compelling motivations for extending studies of heavy ion physics into the ultra-relativistic RHIC energy frontier $\sqrt{s} \sim 20-200$ AGeV, is that predictions, based on the QCD theory itself, of new physics under extreme conditions of temperature and energy can be tested. For RHIC and higher energies controlled QCD theoretic approximations and methods have been developed that are applicable to a wide class of observables.

At lower energies, BEVALAC, SIS, AGS, and SPS, the physics of nuclear collisions is now known to be dominated by the non-equilibrium dynamics of the confined *intermediate* phase of QCD, known as hadronic resonance matter[16]. Unfortunately, even lattice QCD methods are

not yet powerful enough to predict the dynamics or thermodynamics of this intermediate form of matter. For low temperature nuclear matter, effective quantum hadro-dynamic theories (QHD, Chiral Perturbation Theory) have successfully been constructed incorporating the known (Lorentz and Chiral) symmetries of QCD. However, at moderate temperatures where matter is in the hadron resonance excitation region (below the deconfinement temperature) no quantitative theory yet exists. This handicaps the interpretation of data at such lower energies in terms of fundamental QCD properties. Many phenomenological hadronic dynamical models have been advanced to help interpret data at lower energies, but as yet they have not evolved into a consistent effective theory. The existing huge data base from lower energies provides valuable information for further development of such an effective theory. However, RHIC energies provide for the first time the possibility of exploring a qualitatively new kinematic regime where the uncertainties due to our as yet incomplete understanding of the intermediate hadronic resonance phase of QCD may be minimized.

The case that we present in this report, based on the published data from RHIC, about the Quark Gluon Plasma and the Color Glass Condensate is predicated by the firm root of these concepts in first principles in QCD. As such, these concepts must be tested thoroughly through a wide array of observables to see whether they are consistent with available measurements, and that they are robust in their predictions. It was a priori not at all obvious whether any observables exist at RHIC that can be described quantitatively by the QGP or CGC concepts. This is where a healthy bit of experimental "luck" was essential in order to find the "needles in the haystack" that are least distorted by uncertain non-equilibrium hadronic final state dynamics. We make the case in this report that a few sharp needles have been found through three convergent lines of empirical evidence that point to the discovery of a new strongly coupled QGP and its source, the saturated CGC.

It is also important to understand when an approximation to the QCD theory breaks down. Only special limits of QCD can be quantitatively predicted at this time: (1) long wavelength QCD thermodynamics, (2) very short wavelength pQCD, and (3) very high energy CGC coherence. New quark coalescence techniques are being developed to address the intermediate wavelength observables. Any breakdown of a given approximation must be understood for solid reasons. One case in point is applying the QGP hypothesis to observables (such as radial flow) which are strongly influenced by the uncertain late time dynamics of hadronic matter in heavy ion collisions. Another case is at the earliest formation times, when the description changes between the initial coherent CGC and the produced thermal QGP. In the latter case, one needs to determine directly from careful control experiments, which approximation to QCD is better suited to the phenomena under study. In this report we will discuss both the strengths and limitations of the present theoretical understanding of the RHIC discoveries.

2 What is the Quark Gluon Plasma?

Quantum Chromodynamics (QCD) predicts the existence of a deconfined form of matter called a Quark Gluon Plasma (QGP), in which the quark and gluon degrees of freedom normally confined within hadrons are mostly liberated[4]. This transition occurs when the energy density of matter is of the order of that of matter inside a proton. This density is about an order of magnitude larger than the energy density inside of atomic nuclei, that is about $1 - 10\ GeV/Fm^3$.

To get a more accurate determination of the energy of this transition to a Quark Gluon Plasma, QCD can be numerically studied using numerical methods[17]-[20]. Such computations show that there is a rapid rise of the energy density, $\epsilon(T)$, of matter when the temperature reaches $T \approx T_c \sim 160$ MeV. The energy density changes by about an order of magnitude in a narrow range of temperatures $\Delta T \sim 10 - 20\ MeV$ as can be seen from Fig. 1.

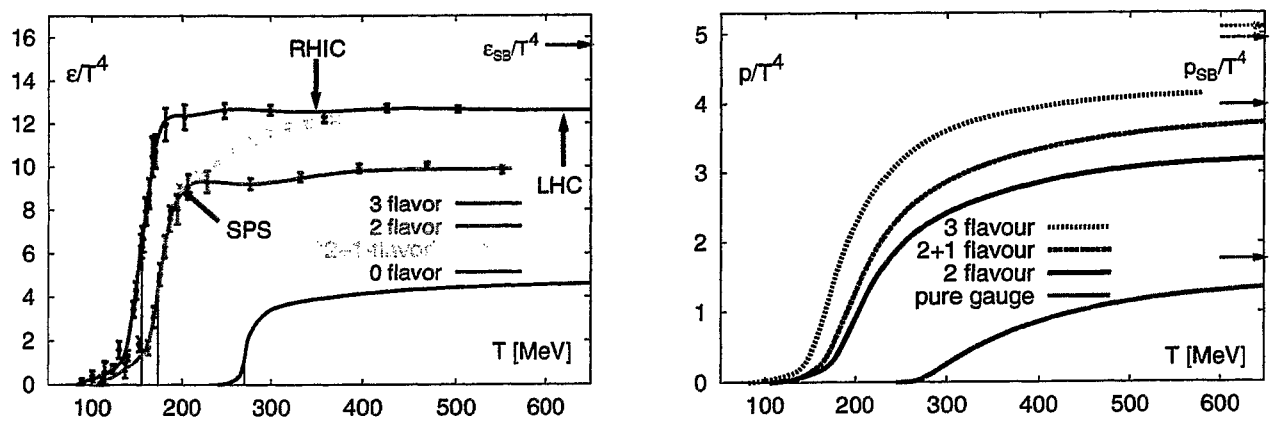

Figure 1: (a) The energy density as a function of temperature scaled by T^4 from lattice QCD [17]. Various number of species of quarks are considered. The realistic case is for $2+1$ flavors. An estimate of the typical temperature reached at SPS and RHIC, and estimated for LHC is included in the figure.(b) The pressure as a function of temperature scaled by T^4. Note that the pressure is continuous in the region where there is a sharp change in the energy density.

One can understand this transition as a change in the number of degrees of freedom of the system. Far below T_c, the active hadronic degrees of freedom are limited to three, corresponding to a dilute gas of 3 charge states of pions. Above T_c, 8 colors of gluons times two helicity degrees of freedom become activated. In addition, there are $N_f(T) \approx 2 - 3$ active light flavors of quarks (for T not far above T_c). Each flavor has equal number of quarks and antiquarks when the chemical potentials vanish, and each have two spin states and three colors. Therefore, there are $g_{q\bar{q}}(T) \approx 24 - 36$ quark degrees of freedom in a QGP. In the quark gluon plasma phase, there are then about 40 - 50 internal degrees of freedom in the temperature range $(1-3)T_c$, while the low temperature and vanishing chemical potentials the pion gas has 3. Since the energy density, pressure and entropy are all roughly proportional to the number of degrees of freedom, one understands this rapid change in the energy density over a narrow range of temperature as a change in the degrees of freedom between the confined and deconfined worlds.

The system above T_c is called a plasma because the degrees of freedom carry the non-Abelian analog of charge as in ordinary plasmas. Just as there are different regimes of ordinary plasmas, the QGP plasma also has weakly coupled and strongly coupled limits. At extremely high temperatures, the asymptotic freedom property of QCD predicts that it will be weakly coupled[4]. For moderate temperatures $(1-3)T_c$ accessible at RHIC, on the other hand, the plasma is predicted by nonperturbative lattice techniques to be strongly coupled - even though the thermodynamic variables are near the ideal Stefan Boltzmann limit. Thus, nonperturbative correlations beyond

dielectric phenomena persist in the QGP well beyond T_c.

The transition between the confined hadronic world and the deconfined QGP world may or may not be a phase transition in the strict statistical mechanical sense. Stricly speaking, a phase transition requires a mathematical discontinuity in the energy density or one of its derivatives in the infinite volume limit. The QGP transition may in fact be a "crossover", or rapid change, as is suggested numerical computation and a number of theoretical arguments. Nevertheless, the change as measured in numerical computation is very abrupt as seen in Fig. 1.

We shall refer to matter in the transition region as a "mixed phase". If there were a strict statistical mechanical first order phase transition, then matter in this region would be a mixture of hadronic gas phase and quark gluon plasma domains, as is the case when there is phase coexistence between water and ice. If there is a rapid crossover, then many of the bulk properties of the system, which are determined by the relation between energy density and pressure, are to a good approximation similar to those when there is a strict phase transition.

In the transition region, the energy density changes by roughly an order of magnitude, but the pressure is continuous and varies slowly. The sound velocity, $c_S^2 = dP/d\epsilon$ must therefore become very small in this range of energy densities[18, 19]. It is very difficult to generate pressure gradients and do mechanical work in the mixed phase region, since as we vary the energy density we generate little change in pressure. We will call a relation between energy density and pressure (an equation of state) stiff when the sound velocity is big (c_s of order the speed of light) and soft when it is small. The quark gluon plasma equation of state is stiff at high temperature, but becomes soft near T_c. The sound velocity as a function of temperature as determined by numerical computation is shown in Fig. 2a. It is expected that hadronic matter again becomes stiffer below T_c, and eventually softens as the temperature tends to zero. Unfortunately, lattice QCD is still not powerful enough to predict accurately the thermodynamic properties of hadronic matter below T_c. Preliminary results[21] (still with rather large pion mass $\sim$ 700 MeV) are roughly consistent with a heavy hadronic resonance gas equation of state, but the thermodynamics of the confined phase of QCD remains an open problem. This fact again underscores the necessity of concentrating on those (few) observables that are least influenced by the poorly known hadronic phase dynamics.

The relationship between the energy density and pressure determines the evolution of matter from a given initial condition *IF* local equilibrium is maintained. This then can determine experimentally by measuring "barometric" observables. The softening of the QGP equation of state near T_c is the key feature that can be looked for in the collective hydrodynamic flow patterns produced when the plasma expands.

Another distinctive feature of the QGP phase diagram is shown in the right panel in Fig.(2). Recent numerical calculations[20] have begun to show evidence that the QGP may have a phase transition in the strict statistical mechanical sense, if one also allows the system to have a high baryon number density as well as high temperature. [22, 23] In the plot on the right hand side of Fig. 2, the possible phases of QCD are shown as a function of both temperature and a measure of the baryon number density, μ_B. At low baryon number density, there is probably a rapid crossover from the low density hadronic world to that of the quark gluon plasma. At higher baryon number density, there is quite likely a first order phase transition. The computations on this issue are still work in progress and extrapolation to realistic quark masses are very difficult, so the position of the endpoint of first order phase transitions is still rather uncertain. There is an ongoing program at the SPS concentrating on lower energies to search for possible signatures of high baryon density quark plasma transition.

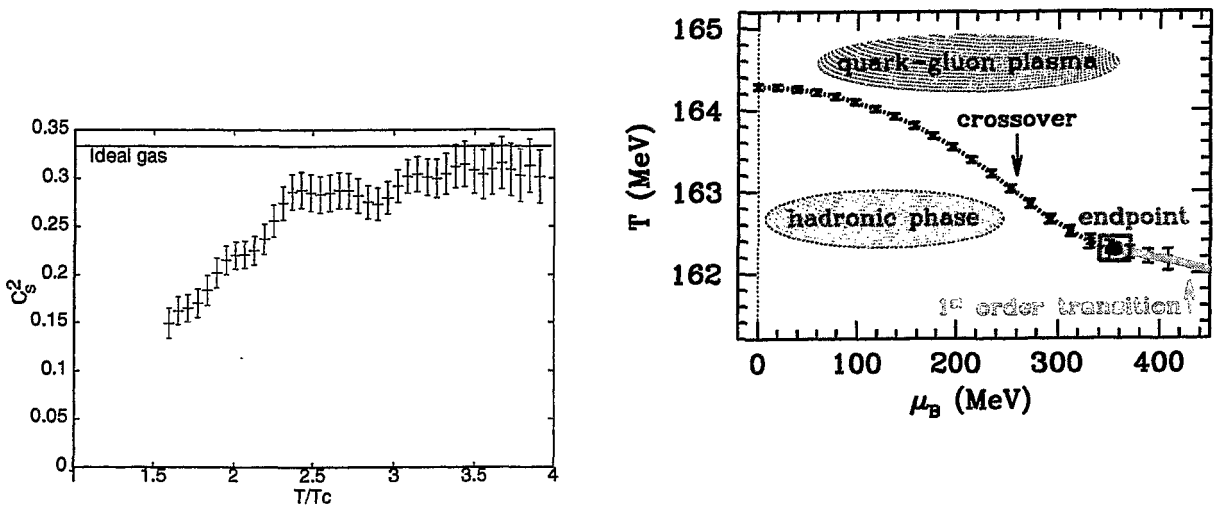

Figure 2: Important features of the QGP equation of state. (a) The speed of sound[18, 19] $c_s^2 = d\epsilon/dP$ drops below 1/3 for $T < 2T_c \approx 300$ MeV. (b) Right panel shows a current estimate of the location of the tri-critical point at finite baryon density[20]

The quark gluon plasma has the property that quarks and gluons are no longer confined inside of hadrons. This is unlike zero temperature and baryon number density QCD. The transition between the confined and deconfined world may provide us insights into the nature of confinement.

In the QCD equations of motion the small mass of the "light" u,d quarks can be neglected and the system possesses a special chiral symmetry. This chiral symmetry prevails at high temperature, in spite of the fact that quarks acquire a collective dynamical mass $\sim gT$ as do gluons. Below T_c, not only do quarks and gluons become confined into hadrons, but the chiral symmetry of QCD is also broken as manifested by the appearance of the 3 light pion degrees of freedom while the quarks are bound in heavy nucleons.

The Quark Gluon Plasma is important to search for at RHIC because:

- It is the ultimate, primordial form of QCD matter at high temperature or baryon number density (at least up to the electro weak scale at about $T_{EW} \sim 10^3 T_c$).
- It was present during the first few microseconds of the Big Bang according to current cosmology.
- It may occur naturally in supernovae, gamma ray bursts and neutron stars as matter at high baryon number density and relatively low temperature.
- It provides an example of phase transitions which may occur at a variety of higher temperature scales in the early universe.
- It may provide us important information concerning the origin of mass for matter, and how quarks are confined into hadrons.

3 What is the Color Glass Condensate?

The ideas for the Color Glass Condensate are motivated by HERA data on the gluon distribution function shown in Fig. 3(a) [24]. The gluon density , $xG(x, Q^2)$, rises rapidly as a function

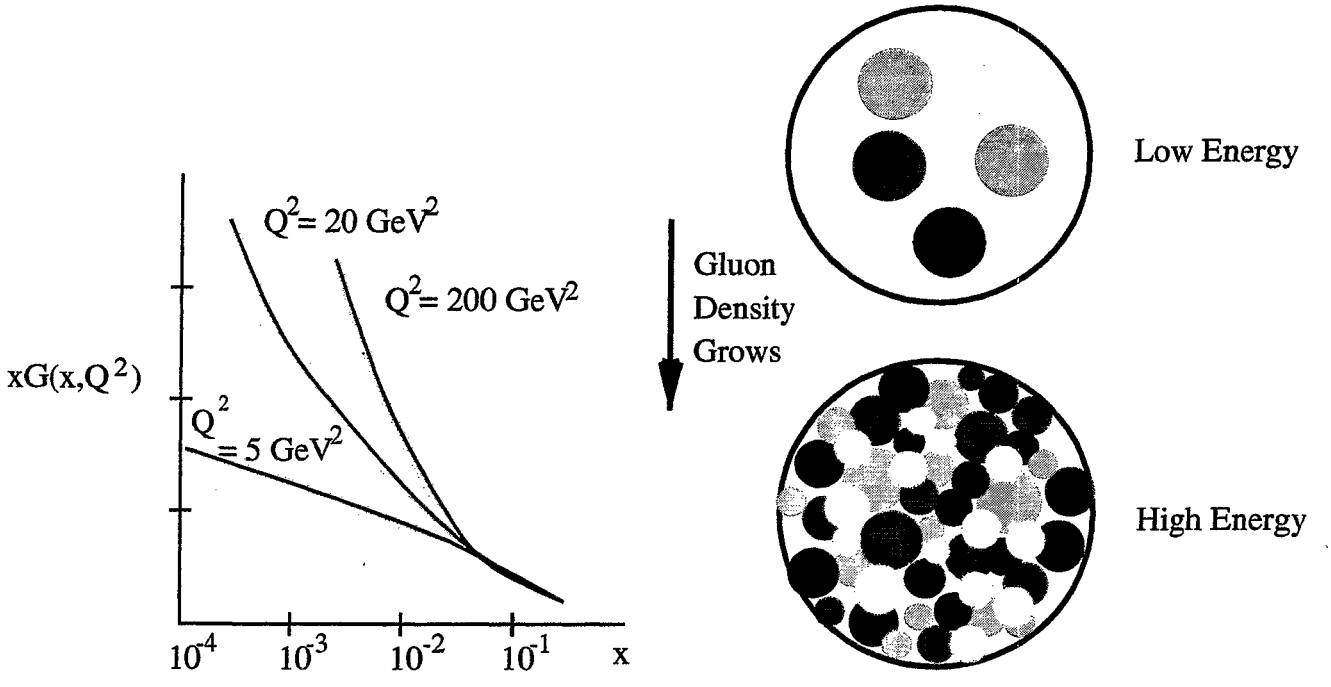

Figure 3: (a)The HERA data for the gluon distribution function as a function of x for various values of Q^2. (b) A physical picture of the low x gluon density inside a hadron as a function of energy

of decreasing fractional momentum, x, or increasing resolution, Q. This rise in the gluon density ultimately owes its origin to the non-Abelian nature of QCD and that the gluons carry color charge. At higher and higher energies, smaller x and larger Q become kinematically accessible. The rapid rise with $\log(1/x)$ was expected in a variety of theoretical works[25]-[27]. Due to the intrinsic non-linearity of QCD, gluon showers generate more gluon showers - producing an exponential avalanche toward small x. The physical consequence of this exponential growth is that the density of gluons per unit area per unit rapidity of any hadron including nuclei must increase rapidly as x decreases [28]. This follows because the transverse size, as seen via the total cross sections, rise more slowly at high energies than the number of gluons. This is illustrated in Fig. 3(b). The non-linearity of gluon interactions, however, led to the conjecture that the transverse density of gluons measured at some fixed Q^2 resolution scale should eventually become limited , that is, there is gluon saturation at sufficiently high energies. [25]-[26], [28]

The low x gluons are closely packed together in the transverse direction, therefore, as in the thermal case at extreme temperatures or chemical potentials, the strong interaction strength must become weak, $\alpha_S \ll 1$. Weakly coupled systems should be possible to understand from first principles in QCD [28].

This dense but weakly coupled system is called a Color Glass Condensate for reasons we now enumerate:[29]

- **Color** The gluons which make up this matter are colored.
- **Glass** The gluons at small x are generated from gluons at larger values of x. In the infinite momentum frame, these larger momentum gluons travel very fast and their natural time scales are Lorentz time dilated. This time dilated scale is transferred to the low x degrees of freedom which therefore evolve very slowly compared to natural time scales. This is the property of a glass.
- **Condensate** The dimensionless transverse phase space density

$$\rho = \frac{1}{\pi R^2} \frac{dN}{dy d^2 p_T} \tag{1}$$

saturates at a value $\rho = c/\alpha_S(Q_s)$, where c is a constant of order unity. Saturation is due to the competition between extra gluon radiation originating from the source current, $\propto \rho$, and non-linear gluon fusion, $\propto -\alpha_S \rho^2$, that reduces the number of gluons at high density. Because $\alpha_S << 1$, this means that the quantum mechanical states of the system associated with the condensate are multiply occupied. They are highly coherent, and share some properties of Bose condensates. The gluon occupation factor is very high, of order $1/\alpha_S$, but it is only slowly (logarithmically) increasing when further increasing the energy, or decreasing the transverse momentum. This provides saturation and cures the infrared problem of the traditional BFKL approach [30].

There is a critical momentum scale, $Q_s(x, A)$, which controls the occupation number through $1/\alpha_S(Q_s)$. This is called the CGC saturation scale. The transverse phase space density, ρ, is constant only up to $p_T < Q_s(x, A)$. For wavelengths, $1/p_T$, much smaller than $1/Q_s$, the coupling becomes even weaker and perturbative QCD predicts that $\rho \propto \alpha(p_T)/(R^2 p_T^2)$.

Note that Q_s plays a role in the CGC form of matter similar to what T_c plays in the QGP form of matter. Both delineate two different phases of matter. However, in the QGP case, the critical scale, $T_c \sim \Lambda_{QCD}$, is small and the matter on both sides of the transition remain in the strong coupling sector of QCD! In the CGC case, on the other hand, it is possible to find kinematic regimes of x that depend on A, where the CGC can be weakly coupled but in nonlinear regime due to high occupation numbers.

The crux of the search for the CGC therefore is to locate those kinematic regimes where the corrections to the weak coupling methods can be controlled. The non-linear dependence of Q_s on x and A will be discussed further in section 6. We note here only that both as x becomes small and A becomes large, Q_s grows. The saturation momentum itself does not saturate. The gluon distribution function for resolution scale $Q \leq Q_s$ grows slowly and saturates, while the gluon distribution function for $Q \geq Q_s$ grows rapidly. The physics is easy to understand: As more gluons are added to the hadron, they have to go to the unsaturated region since the saturated region is already densely packed.

The Color Glass Condensate is important to search for at RHIC because:

- It represents the universal form of high energy QCD wavefunctions at small x, not only of hadrons but heavy nuclei as well.
- It is a new form of matter because the gluons inside the hadron are separated by distance scales small compared to the hadron size, they evolve on time scales long compared to microphysics time scales, and the CGC itself is specified by a special new density matrix that encodes the non-linear virtual fields of QCD in the high energy limit.

- It already begins to become important at $x \sim 10^{-2}$ in protons at HERA, and and should begin to become important at comparable values of x at RHIC.
- It provides a rigorous QCD theoretical description of the initial state in $A + A$ from which the QGP must evolve.
- It can be tested directly at RHIC via $p + A$ or $D + A$, where no final state interactions and hence no QGP formation can occur.

4 The Space-Time Picture of Ultra-Relativistic Nuclear Collisions

Heavy ion collisions at ultrarelativistic energies are visualized in Fig. 4 as the collision of two sheets of colored glass.[31] The nuclei appear as sheets at ultrarelativistic energies because of Lorentz contraction. The CGC gluons are shown as vectors which represent the polarization of the gluons, and by colors corresponding to the various colors of gluons.

At ultrarelativistic energies, these sheets pass through one another. In their wake is left melting colored glass, which eventually materializes as quarks and gluons. These quarks and gluons would naturally form in their rest frame on some natural microphysics time scale. For the saturated color glass, this proper formation time scale, τ_0, is of order the inverse saturation momentum. At RHIC, $1/Q_s \sim 0.2$ fm/c $\sim 5 \times 10^{-25}$ sec. Note that 0.2 fm/c is also comparable to the natural crossing time of two 10 fm nuclei, each contracted by a gamma factor 100, in the center of mass frame at RHIC. For particles with a large momentum or rapidity along the beam axis, this time scale is Lorentz dilated. This means that the slow (smaller rapidity) particles are produced first towards the center of the collision regions and the fast (larger rapidity) particles are produced later further away from the collision region.

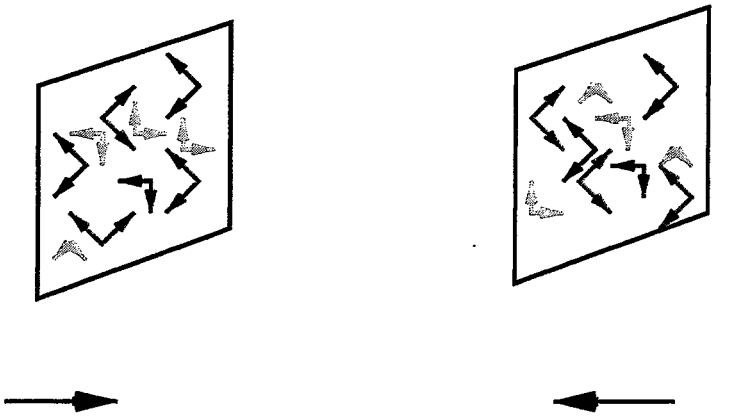

Figure 4: The collision of two sheets of colored glass. The arrows represent the polarization vectors for the gluons which live on the sheets, and their colors correspond to the different colors of gluons

This Bjorken "inside-out" correlation[6] between space and momentum is similar to what happens to matter in Hubble expansion in cosmology. The stars which are further away have larger

outward velocities. This means that the matter produced at RHIC, like the universe in cosmology is born expanding. One important difference is that the "mini-bang" at RHIC is born with one dimensional Hubble flow along the collision axis, while the Big-Bang is three dimensional. This is shown in Fig. 5

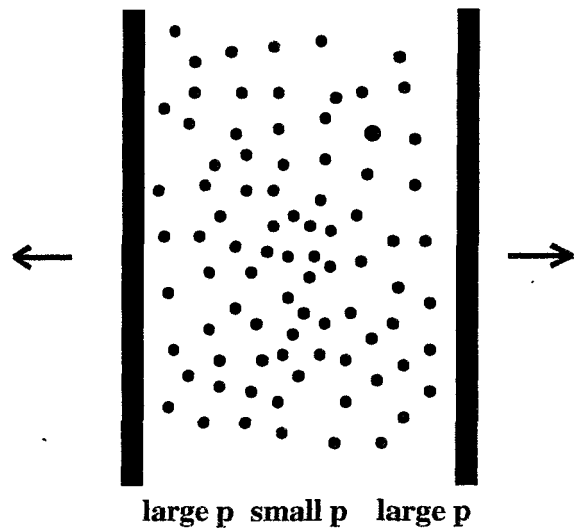

Figure 5: Particles being produced after the collision of two nuclei.

As this system expands, it cools. On some time scale $\tau_{eq} > \tau_0$ the produced quarks and gluons may thermalize. It is by no means obvious that local equilibrium can be reached on the short time scale $\sim (1-2)R/c \sim 10$ fm/c available in nuclear collisions. *IF* local equilibrium is reached early with $\tau_{eq} < 1$ fm/c , then the QGP can develop collective flow according to the laws of hydrodynamics. In any case, when the energy density decreases due to expansion below about 1 GeV/fm^3, the QGP must begin to hadronize through some mixture of hadrons and quarks and gluons. Eventually, all the quarks and gluons must become confined into hadrons that may still interact as hadronic matter before being detected.

The particle multiplicity as a function of energy has been measured at RHIC[32], as shown in Fig. 6. Combining the multiplicity data together with the measurements of transverse energy or of typical particle transverse momenta, one can determine the energy density of the matter when it decouples.[33] One can then extrapolate backwards in time using 1 dimensional (Bjorken) expansion, since decoupling occurs soon after the matter begins to expands three dimensionally. We can extrapolate backwards only until τ_0, when the matter is formed from the "shattered" Color Glass.

To do this extrapolation we use that the proper density of particles falls as $N/V \sim 1/\tau$ during 1 dimensional expansion. If the particles expand without interaction and work, then the energy per particle remains constant (and $E/V(\tau_0) \approx (dE_T/dy)/(\tau_0 \pi R^2)$ in terms of the final observed transverse energy per unit rapidity). If the particles thermalize, then $E/N(\tau) \sim 3T(\tau)$, and the *entropy* rather than the energy per particle remains constant. For a massless gas, the temperature then falls as $T \sim \tau^{-1/3}$. For a gas which is not massless or not in perfect equilibrium, the temperature falls somewhere in the range $T_o > T(\tau) > T_o(\tau_{eq}/\tau)^{1/3}$ This 1 dimensional expansion

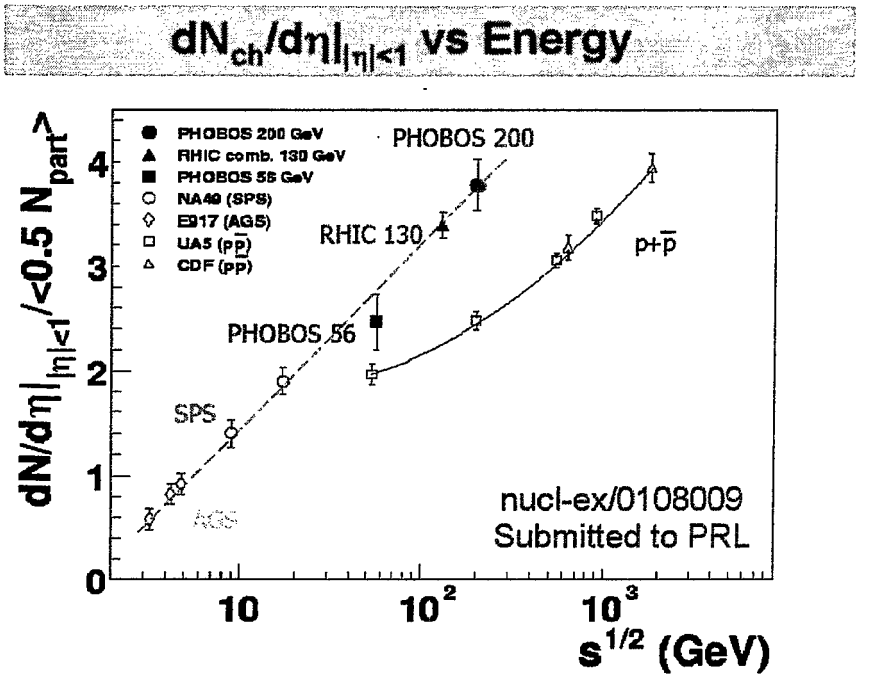

Figure 6: The particle multiplicity as a function of c.m. energy, $\sqrt{s}$, per nucleon pair at RHIC[32] and lower AGS and SPS energies.

continues until the system begins to feel the effects of finite size in the transverse direction, and then rapidly cools through three dimensional expansion. We shall take a conservative overestimate of this time to be of order $t_0 \sim 0.3$ fm/c The extrapolation of the energy density backwards is bounded by $\epsilon_f(t_f/t) < \epsilon(t) < \epsilon_f(t_f/t)^{4/3}$. The lower bound is that assuming that the particles do not thermalize and their typical energy is frozen. The upper bound assumes that the system thermalizes as an ideal massless gas. These bounds on the energy density is shown in Fig. 7. On the left axis is the energy density and on the bottom axis is time. The system begins as a coherent Color Glass Condensate, then melts to Quark Gluon Matter which may eventually thermalize to a Quark Gluon Plasma. At a time $\sim 3Fm/c$, the plasma becomes a mixture of quarks, gluons and hadrons which further expand together.

At a time of about 10 Fm/c, the system falls apart and decouples. At a time of $t \sim 1$ Fm/c, the estimate we make is identical to the Bjorken energy density estimate, and this provides a lower bound on the energy density achieved in the collision. (All estimates agree that by a time of order 1 Fm/c, matter has been formed.) The upper bound corresponds to assuming that the system expands as a massless thermal gas from a melting time of .3 Fm/c. (If the time was reduced, the upper bound would be increased yet further.) The bounds on the initial energy density are therefore

$$2 - 3\ GeV/Fm^3 \lesssim \epsilon \lesssim 20 - 30\ GeV/Fm^3 \tag{2}$$

where we included a greater range of uncertainty in the upper limit because of the uncertainty associated with the formation time. The energy density of nuclear matter is about 0.15 GeV/Fm^3,

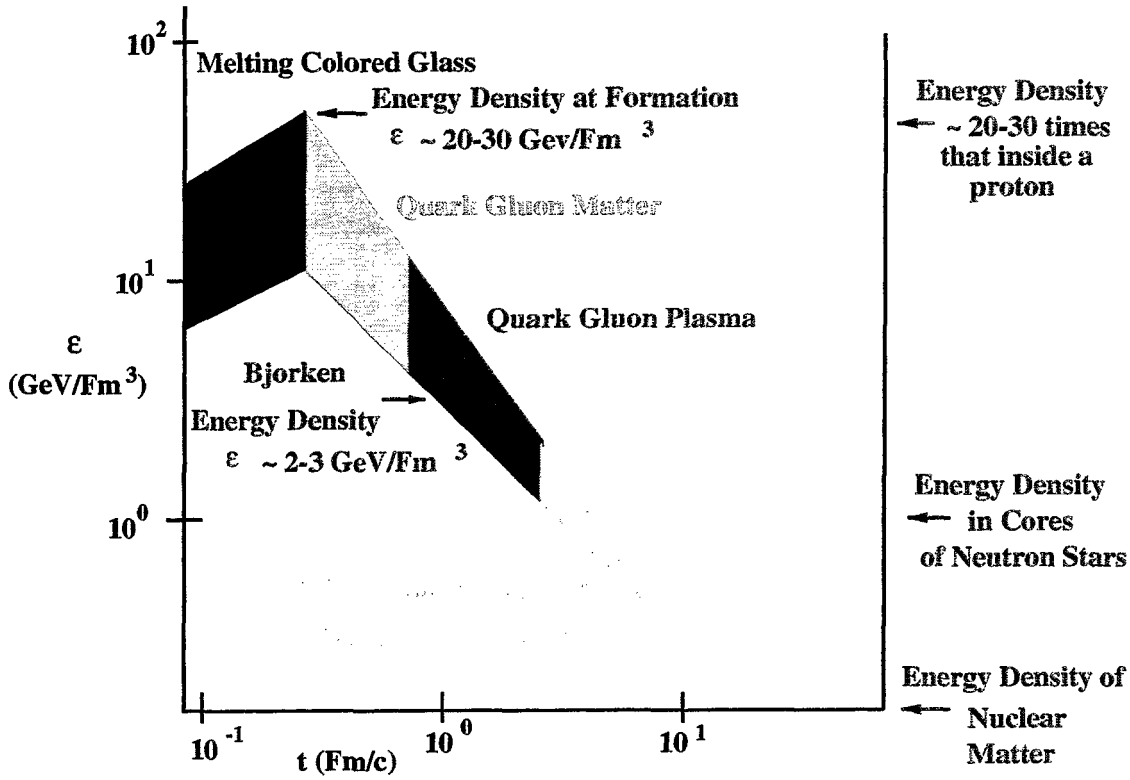

Figure 7: Bounds on the energy density as a function of time in heavy ion collisions.

and even the lowest energy densities in these collisions is in excess of this. At late times, the energy density is about that of the cores of neutron stars, $\epsilon \sim 1\ GeV/Fm^3$.

We conclude that based on the observed multiplicity at RHIC alone, the initial energy densities achieved in RHIC collisions can be high enough to produce a quark gluon plasma.

5 Empirical Evidence for QGP at RHIC

In this section, we discuss RHIC data which show that the matter produced in central collisions in RHIC becomes well thermalized, and behaving in a way consistent with theoretical expectations from QCD.

5.1 Collective Flow

The identification of a new form of "bulk matter" requires the observation of novel and uniquely different collective properties from ones seen before. In heavy ion reactions the flow pattern of thousands of produced hadrons is the primary observable used to look for novel collective

phenomena[3], [34]- [37]. The collective flow properties test two of the conditions necessary for the validity of the QGP hypothesis.

The first is the degree of thermalization. Nothing is yet known from lattice QCD about far off equilibrium dynamics of a QGP. However, the evolution of matter from some initial condition can be computed via the equations of viscous relativistic hydrodynamics if local equilibrium is maintained. These equations can be further approximated by perfect (Euler) fluid equations when the corrections due to viscosity can be neglected. Such viscous corrections can be neglected when scattering mean free paths are small compared to the scale of spatial gradients of the fluid.

The second condition is the validity of the numerically determined equation of state or relationship between energy density and pressure. The required input for perfect fluid hydrodynamical equations is the equation of state. With a specific initial boundary condition, the future evolution of the matter can be then predicted. We shall show that the data on elliptic flow confirms the idea that to a very good approximation, local thermal equilibrium is reached at RHIC energy and that the flow pattern is entirely consistent with numerical determinations of the equation of state from QCD.

The different types of collective flows are conveniently quantified in terms of the first few Fourier components of the azimuthal angle (angle around the beam axis for the collision) distribution. [38, 39], $v_n(y, p_T, N_p, h)$, of the centrality selected triple differential inclusive distribution of hadrons, h. The centrality or impact parameter range is usually specified by a range of associated multiplicities, from which the average number of participating nucleons, N_p, can be deduced. The azimuthal angle of the hadrons are measured relative to a globally determined estimate for the collision reaction plane angle $\Phi(M)$. The "directed" v_1 and "elliptic" v_2 flow components [37]-[39], [40]-[47] are readily identified from azimuthal dependence

$$\begin{aligned}\frac{dN_h(N_p)}{dydp_T^2d\phi} = \frac{dN_h(N_p)}{dydp_T^2}\frac{1}{2\pi}(1 &+ 2v_1(y, p_T, N_p, h)\cos\phi \\ &+ 2v_2(y, p_T, N_p, h)\cos 2\phi + \cdots) \ . \end{aligned} \tag{3}$$

The first term in the above equation also contains information about flow. Produced particles should have their momentum spectrum broadened in heavy ion collisions relative to the case for proton-proton collisions. Because flow is due to a collective velocity, the flow effects should be largest for the most massive particles, and therefore the mass dependence is a powerful diagnostic tool.

Figure (8) shows the striking bulk collectivity elliptic flow signature of QGP formation at RHIC. Unlike at SPS and lower energies, the observed large elliptic deformation ($(1+2v_2)/(1-2v_2) \sim 1.5$) of the final transverse momentum distribution agrees for the first time with non-viscous hydrodynamic predictions [48]-[60] at least up to about $p_T \sim 1$ GeV/c. However, the right panel shows that when the local rapidity density per unit area [40, 41] drops below the values achieved at RHIC $\sim 30/\text{fm}^2$, then the elliptic flow (scaled by the initial spatial ellipticity, $\epsilon = \langle (y^2 - x^2)/(y^2 + x^2) \rangle$) falls below the perfect fluid hydrodynamic predictions. We will discuss in more detail the origin of the large discrepancy at SPS energies in the next section.

The most impressive feature in Fig.(8) is the agreement of the observed hadron mass dependence of the elliptic flow pattern for all hadron species, π, K, p, Λ, with the hydrodynamic predictions below 1 GeV/c. This is the QGP fingerprint that shows that there is a common bulk collective azimuthally asymmetric flow velocity field, $u^\mu(\tau, r, \phi)$. Such good agreement with the hadron mass dependence of the $v_2(p_T, m_h)$ data is furthermore only found when the input equation

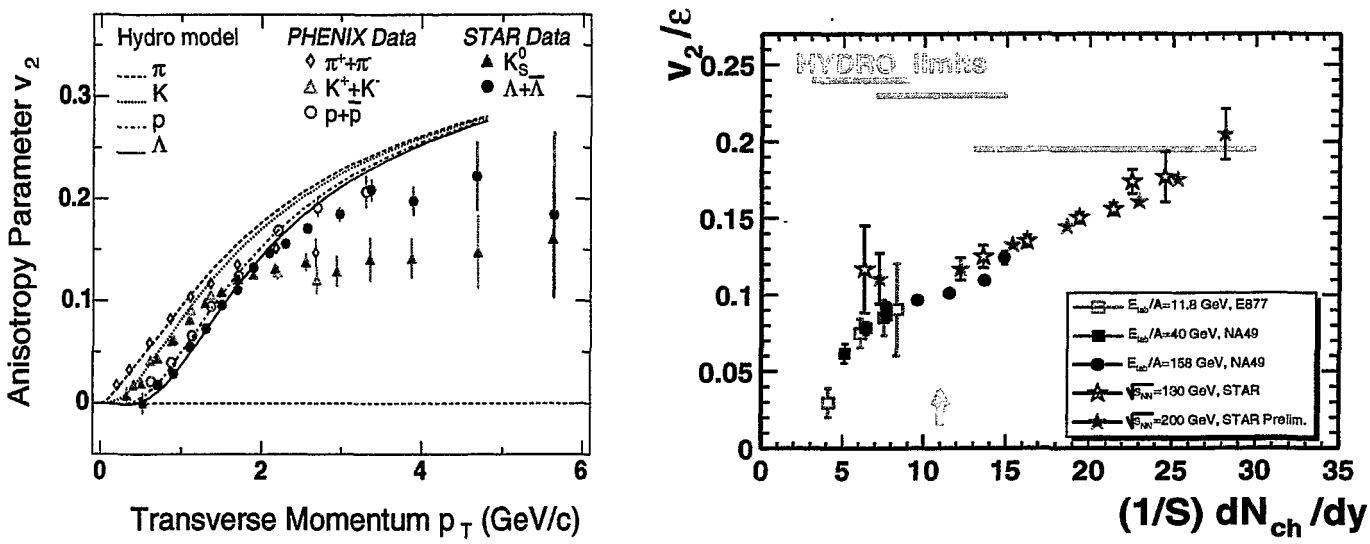

Figure 8: First line of evidence: Bulk collective flow is the barometric signature of QGP production. Left figure combines STAR [43]-[46] and PHENIX [47] measurements of the azimuthal elliptic flow ($v_2(p_T)$) of π, K, p, Λ in Au+Au at 200 AGeV. The predicted hydrodynamic flow pattern from [48]-[52] agrees well with observations in the bulk $p_T < 1$ GeV domain. Right figure from [41] shows v_2 scaled to the initial elliptic spatial anisotropy, ϵ, as a function of the charge particle density per unit transverse area. The bulk hydrodynamic limit is only attained at RHIC.

of state has the characteristic "softest point" near T_c as predicted by lattice QCD [48]-[60]. When equations of state without the predicted drop of speed of sound near T_c were used as input, the flow velocity field, especially that of the heavy baryon, was over estimated.

The flow velocity and temperature fields of a perfect (non-viscous) fluid obeys the hydrodynamic equations:

$$\partial_\mu \left\{[\epsilon_{QCD}(T(x)) + P_{QCD}(T(x))]u^\mu(x)u^\nu(x) - g^{\mu\nu}P_{QCD}(T(x))\right\} = 0 \,, \tag{4}$$

where $T(x)$ is the local temperature field, $P_{QCD}(T)$ is the QGP equation of state, and $\epsilon_{QCD}(T) = (TdP/dT - P)_{QCD}$ is the local proper energy density. The above equations apply in the rapidity window $|y| < 1$, where the baryon chemical potential can be neglected. Eq.(4) provides the barometric connection between the observed flow velocity and the theoretical properties of the QGP.

We note that in any hydrodynamic treatment of collective flow there is a tradeoff between the combined effects due to the initial state boundary condition, the equation of state of the matter, and dissipation effects. In order to use the flow pattern to constrain the equation of state the initial condition must be constrained from other measurements and dissipation must be negligible. Here is where the measurements of the global multiplicity systematics[32, 33] are so important. The remarkably weak energy and centrality dependence of the bulk entropy observed via the $dNdy$ plays a pivotal role as perhaps the most convincing test of the CGC initial condition hypothesis

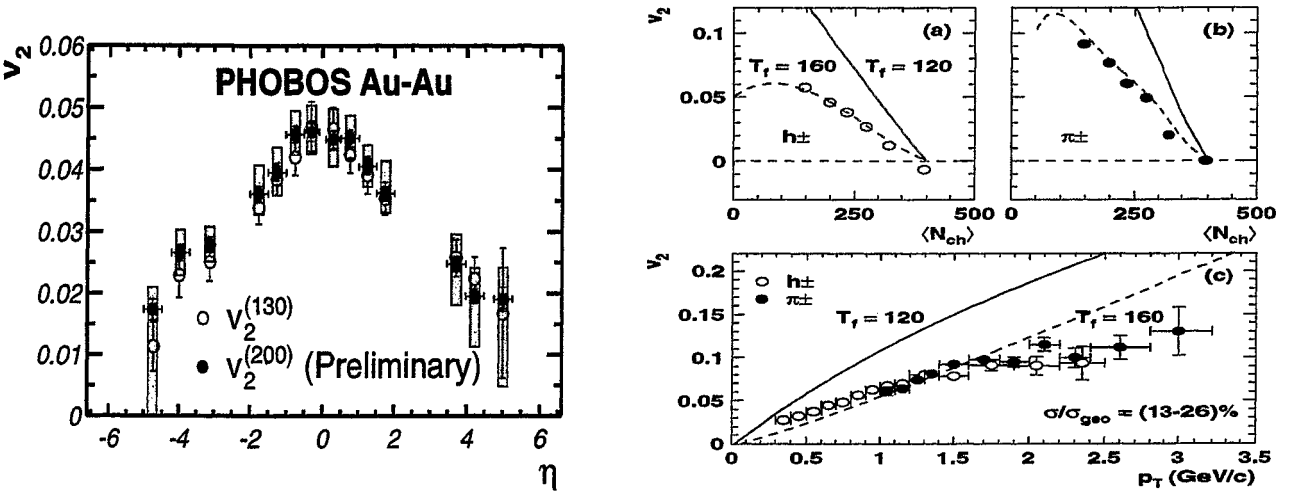

Figure 9: Left figure shows the pseudo rapidity dependence of elliptic from PHOBOS [62]. Right figure is CERES[63] data on elliptic flow at SPS. It is well below hydrodynamic predictions with freeze-out $T_f = 120$ MeV required to reproduce the single inclusive radial flow. Early freeze-out with $T_f = 160$ MeV, simulating effects of dissipation, is needed to reproduce the data.

at RHIC[61]. Without such an experimental and theoretical constraint on the initial condition no meaningful constraint on the QGP equation of state could have been found.

The study of the interplay between the equation of state and dissipative phenomena is more difficult and can only be untangled through detailed systematics of the flow pattern as a function of beam energy, centrality, and rapidity dependence. Here the detailed systematics from AGS and SPS data have played a pivotal role in helping sorting out the different viscous effects in hadronic and QGP matter as we discuss in the next section.

Why is v_2 more emphasized than v_1 or radial flow as a signature of QGP formation? The primary reason is that elliptic flow is generated mainly during the highest density phase of the evolution before the initial geometric spatial asymmetry of the plasma disappears. It comes from the azimuthal dependence of the pressure gradients, which can be studied by varying the centrality of the events [39]. Detailed parton transport [64] and hydrodynamic [54] calculations show that most of the v_2 at RHIC is produced before 3 fm/c and that elliptic flow is relatively insensitive to the late stage dissipative expansion of the hadronic phase. The reason for the generation of v_2 at relatively early times is that it is very difficult to convert the spatial anisotropy of the matter distribution into a momentum space anisotropy once the system cools into the mixed phase, since in the mixed phase pressure gradients cannot be set up. Actually, it was a surprise how well the observed collective flow agrees with perfect fluid hydrodynamic predictions. Ideal fluid flow requires very strong interactions of the quarks and gluons in the plasma at early times $\tau \gtrsim \tau_{eq} \approx 0.6$ fm/c.

In contrast, radial flow has been observed at all energies [65] and has been shown to be mainly sensitive to late time "pion wind" radial pressure gradients [16, 66], which continue to blow long after the QGP condenses into hadronic resonances.

5.2 The Breakdown of Bulk Collectivity

It is important to point out that no detailed 3+1D hydrodynamic calculation [56]-[60] has yet been able to reproduce the rapid decrease of $v_2(|\eta| > 1)$ observed by PHOBOS in Fig.(9). This is most likely due to the increasing role *hadronic* dissipation effects in the "corona" when the comoving density decreases with increasing y. The volume of the QGP shrinks while the hadronic corona thickens as the rapidity density dN/dy is reduced within a fixed nuclear geometry away from midrapidity. From the right panel of Fig.(8), we see that a decrease of the local transverse density from midrapidity RHIC conditions leads to an increasing deviation from the perfect fluid limit. The initial density was also observed to decrease at RHIC as $|y|$ increases [67]. Therefore, from the known SPS data, we should expect deviations from the perfect fluid limit away from the midrapidity region.

Another set of RHIC data that show deviations from perfect fluid hydrodynamic predictions is the centrality dependence of v_2. The observed $v_2(b)$ decreases relative to hydrodynamic predictions also when the impact parameter increases toward the more peripheral collisions. This is again due to the fact that the produced multiplicity, $dN/dy \propto N_p(b)$, decreases with increasing b. The hadronization time decreases with b since the QGP is formed with smaller initial density and the hadronic fluid is less efficient in transferring pressure into collective flow.

To elaborate further on this important point, Fig.9 shows CERES data [63] on $v_2(p_T)$ at SPS energy $\sqrt{s} = 17$ AGeV. In agreement with the NA49 data shown in the right panel of Fig.(8), the CERES data falls well below the hydrodynamic predictions. At even lower energies, AGS and BEVALAC, the v_2 even becomes *negative* and this "squeeze out" of plane [36] is now well understood in terms of low energy non-equilibrium nuclear transport theory [42, 68].

In order to account for the smallness of v_2 at SPS, hydrodynamics has to be frozen out at unphysically high densities and temperatures, $T_f \approx T_c$. However, the observed radial flow rules out this simple fix. The reduction of v_2 while maintaining radial flow can be approximately understood in approaches [54] that combined perfect fluid QGP hydrodynamics with dissipative final state hadronic evolution.

In light of the above discussion on the breakdown of collectivity due to hadronic dissipation at high rapidity and large impact parameters at RHIC and even at midrapidity at SPS and lower energies, the smallness of dissipative corrections in the central regions of RHIC is even more surprising. At mid-rapidities, the lack of substantial dissipation in the QGP phase is in itself a remarkable and unexpected discovery [69] at RHIC. Calculations based on parton transport theory [64] predicted large deviations from the ideal non-viscous hydrodynamic limit even in a QGP. Instead, the data show that the QGP at RHIC is almost a perfect fluid. A Navier Stokes analysis [55] of the RHIC data also indicates that the viscosity of the QGP must be about ten times smaller than expected if the QGP were a weakly interactive conventional Debye screened plasma. This unexpected feature of the QGP must be due to strong coupling QCD physics that persists to at least $3T_c$. (See [14, 69, 70] and refs therein for further discussion).

Summarizing this section: Elliptic flow measurements confirm that the quark-gluon matter produced at RHIC is to a very good approximation in local thermal equilibrium up to about 3 fm/c. In addition, the final hadron mass dependence of the flow pattern is remarkably consistent with numerical QCD computations of the equation of state. Viscous corrections furthermore appear to be surprisingly small

during this early evolution. The produced Quark Gluon Plasma must therefore be very strongly interacting. Such behavior was not seen at lower energy because the highly dissipative hadronic fluid component masked the QGP flow signals. The perfect fluid behavior is also masked at RHIC at higher rapidities and in more peripheral reactions again due to the increased role of the dissipative hadronic "corona".

5.3 Perturbative QCD and Jet Quenching

In addition to the breakdown of perfect fluid collectivity at high rapidity seen in Fig.(9), Fig.(8) clearly shows that hydrodynamics also breaks down at very short wavelengths and high transverse momenta, $p_T > 2$ GeV. Instead of continuing to rise with p_T, the elliptic asymmetry stops growing and the difference between baryon vs meson v_2 even reverses sign. Between $2 < p_T < 5$ GeV the baryon $v_2^B(p_T)$ exceeds the meson $v_2^M(p_T)$ by approximately 3/2. For such short wavelength components of the QGP, local equilibrium simply cannot be maintained due the fundamental asymptotic freedom property of QCD, i.e. the coupling strength becomes too weak.

In this section, we concentrate on the $p_T > 2$ GeV meson observables that can be readily understood in terms of QGP modified perturbative QCD (pQCD) dynamics [71, 72]. (Baryons at intermediate $2\ GeV \leq p_T \leq 5\ GeV$ are outside the range of a perturbative treatment and several competing mechanisms have been proposed and are under theoretical development[73, 74, 75].)

The quantitative study of short wavelength partonic pQCD dynamics focuses on the rare high p_T power law tails that extend far beyond the typical (long wavelength) scales $p < 3T \sim 1$ GeV of the bulk QGP. The second major discovery at RHIC is that the non-equilibrium power law high p_T jet distributions remain power law like but are strongly quenched [76]-[84]. Furthermore, the quenching pattern has a distinct centrality, p_T, azimuthal angle, and hadron flavor dependence that can be used to test the underlying dynamics in many independent ways.

Below RHIC energies, there is an enhancement of moderately high p_T tails that was observed in central $Pb+Pb$ reactions at the SPS. (Very recent reanalysis of the WA98 data shows a somewhat weaker enhancement at SPS [85]) This enhancement was expected as a consequence of the Cronin enhancement: now understood as an initial state effect[86]t which is also seen in pA collisions. Since the Cronin enhancement is an effect of the initial state nuclear wavefunction, it plays a role in the Color Glass Condensate, but we wish to isolate final state effects for our study of the Quark Gluon Plasma. In contrast, at RHIC a large suppression, by a factor of 4-5, was discovered in central $Au + Au$ that extends beyond 10 GeV for π^0.

Jet quenching in $A + A$ was proposed in [87, 88] as a way to study the dense matter produced at RHIC energies. As noted before, the pQCD jet production rates finally become large enough to measure yields up to high $p_T > 10$ GeV. Order of magnitude suppression effects were predicted based on simple estimates of induced gluon radiative energy loss. Ordinary, elastic energy loss [89] was known by that time to be too small to lead to significant attenuation.

As reviewed in [71, 72] refinements in the theory since then have opened the possibility of using the observed jet quenching pattern as a tomographic tool [90] to probe the parton densities in a QGP. The right panel of Fig.10 shows a recent jet tomographic analysis [91] of the PHENIX π^0 data [76, 77] based on the GLV opacity formalism [92]. This analysis concludes that the initial gluon rapidity density required to account for the observed jet quenching pattern must be $dN_g/dy \sim 1000 \pm 200$.

This jet tomographic measure of the initial dN_g/dy is in remarkable agreement with three

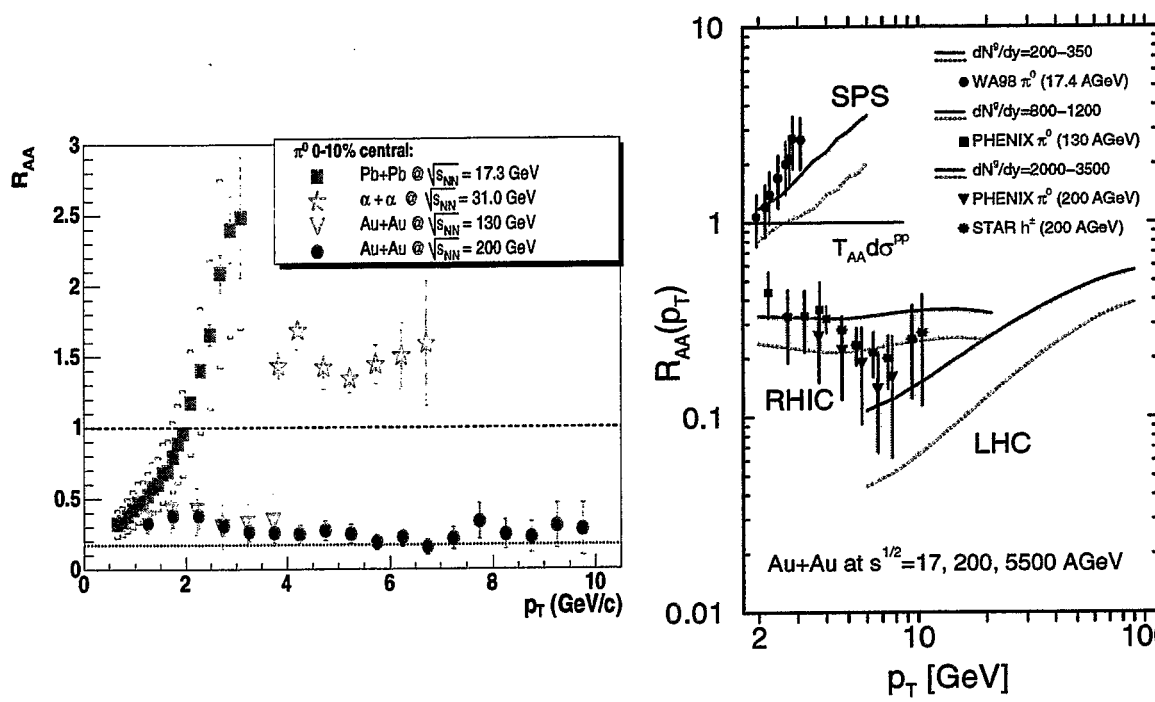

Figure 10: Jet Quenching at RHIC. Left [93] shows the jet quenching pattern of π^0 discovered by PHENIX [76, 77] at RHIC compared to previous observation of high p_T enhancement at ISR and SPS energies The nuclear modification factor $R_{AA} = dN_{AA}/T_{AA}(b)d\sigma_{pp}$ measures the deviation of AA spectra from factorized pQCD. Right shows predictions [91] of the $\sqrt{s}$ and p_T dependence from SPS, RHIC, LHC based on the GLV theory [92] of radiative energy loss.

other independent sources: (1) the initial entropy deduced via the Bjorken formula from the measured multiplicity, (2) the initial condition of the QGP required in hydrodynamics to produce the observed elliptic flow, and (3) the estimate of the maximum gluon rapidity density bound from the CGC gluon saturated initial condition, (which will be described later).

These four independent measures make it possible to estimate the maximal initial energy density in central collisions

$$\epsilon_0 = \epsilon(\tau \sim 1/p_0) \approx \frac{p_0^2}{\pi R^2}\frac{dN_g}{dy} \approx 20\frac{\text{GeV}}{\text{fm}^3} \sim 100 \times \epsilon_A \tag{5}$$

where $p_0 \approx Q_{sat} \approx 1.0 - 1.4$ GeV is the mean transverse momentum of the initial produced gluons from the incident saturated virtual nuclear CGC fields[15, 61, 94]. This scale controls the formation time $\hbar/p_0 \approx 0.2$ fm/c of the initially out-of-equilibrium (mostly gluonic) QGP. The success of the hydrodynamics requires that local equilibrium be achieved on a fast proper time scale $\tau_{eq} \approx (1-3)/p_0 < 0.6$ fm/c. The temperature at that time is $T(\tau_{eq}) \approx (\epsilon_0/(1-3) \times 12)^{1/4} \approx 2T_c$.

In HIJING model[95], the mini-jet cutoff is $p_0 = 2 - 2.2$ GeV limits the number of mini-jets to well below 1000. The inferred opacity of the QGP is observed to be much higher and consistent with the CGC[61] and EKRT[94] estimates.

5.3.1 I_{AA} and Di-Jet Tomography

Measurements of near side and away side azimuthal angle correlations of di-jet fragments provide the opportunity to probe the evolution of the matter produced at RHIC in even more detail. Fig.(11) show the discovery [81, 82, 83] of mono-jet production [87] in central collisions at RHIC. In peripheral collisions, the distribution $dN/d\Delta\phi$ of the azimuthal distribution of $p_T \sim 2$ GeV

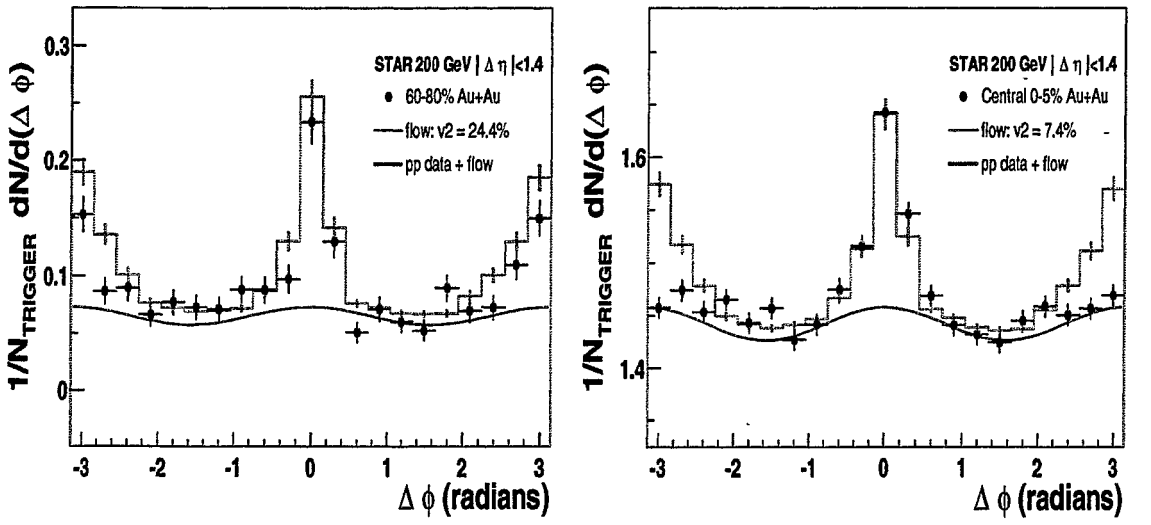

Figure 11: Monojets at RHIC from STAR [82, 83, 81]. Strongly correlated back-to-back di-jet production in pp and peripheral $AuAu$ left side is compared to mono-jet production discovered in central $AuAu$.

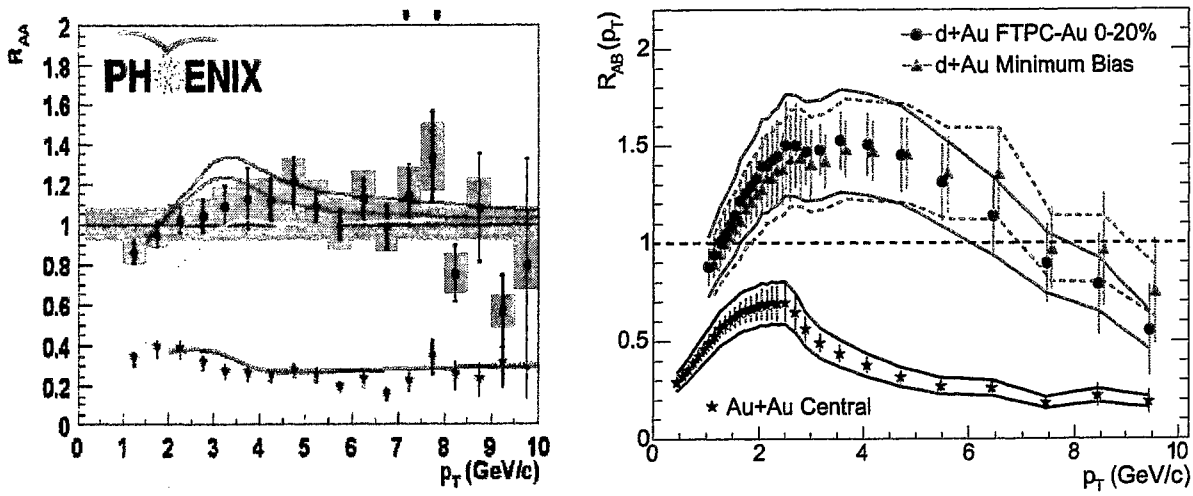

Figure 12: The **dA** control: PHENIX [96] π^0 and STAR [97] $h^{\pm}$ data compare R_{DAu} to R_{AuAu}. These and BRAHMS [98] and PHOBOS [99] data prove that jet quenching in $Au + Au$ must be due to final state interactions. Curves for π^0 show predictions from [91] for $AuAu$ and from [103] DAu. The curves for DAu show the interplay between different gluon shadow parameterizations (EKS, none, HIJING) and Cronin enhancement and are similar to predictions in [101, 102, 103]. In lower panel, the unquenching of charged hadrons is also seen in $D + Au$ relative to $Au + Au$ at high p_T.

hadrons relative to a tagged $p_T \sim 4$ GeV leading jet fragment shows the same near side and away side back-to-back jetty correlations as measured in $p + p$. This is strong evidence that the kinematic range studied tests the physics of pQCD binary parton collision processes. For central collisions, on the other hand, away side jet correlations are almost completely suppressed.

The published data are as yet limited to $y_1 \approx y_2 \approx 0$, broad p_T cuts: $p_{T1} > 4$ GeV and $p_T \sim 2$ GeV, two bins of $\phi_1 - \phi_2$, and of course averaged over Φ_b. The measured modification of di-jet correlations is obtained by subtracting out the correlations due to bulk elliptic flow, and this introduces some uncertainty. Analysis of present and future data at higher transverse momenta for a variety of rapidities will allow better tests of the underlying perturbative QCD dynamics.

Only one year ago [100] the interpretation of high p_T suppression was under intense debate because it was not yet clear how much of the quenching was due to initial state saturation (shadowing) of the gluon distributions and how much due to jet quenching discussed in the previous section. There was only one way to find out - eliminate the QGP final state interactions by substituting a Deuterium beam for one of the two heavy nuclei. In fact, it was long ago anticipated [88] that such a control test would be needed to isolate the unknown nuclear gluon shadowing contribution to the A+A quench pattern. In addition $D + Au$ was required to test predictions of possible initial state Cronin multiple interactions [86, 101, 102, 103, 104]. In contrast, one model of CGC [105] predicted a substantial suppression in $D + Au$ collisions. The data [96, 97, 98, 99] conclusively rule out large initial shadowing as the cause of the $x_{BJ} > 0.01$ quenching in Au+Au.

The I_{DAu} measurement from STAR [97] shows clearly how the suppression disappears in $D+Au$ collisions. The return of back-to-back jet correlation in $D + Au$ to the level observed in pp is seen in Fig.13. The data appear to be entirely consistent with jet quenching as a final state effect in

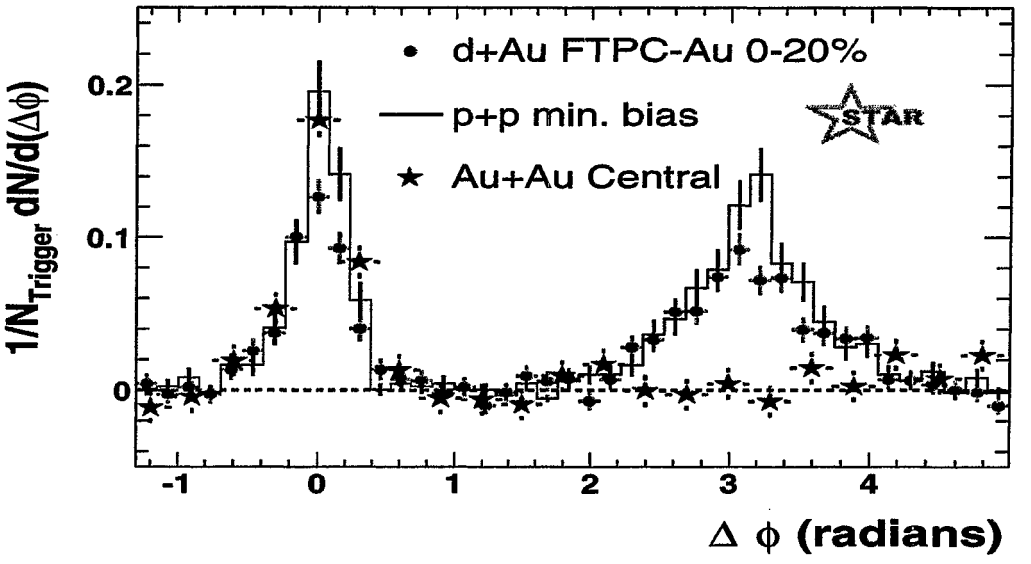

Figure 13: The **dA** "Return of the Jeti": Dijet fragment azimuthal correlations from STAR [97] in DAu are unquenched relative to the mono jet correlation observed in central $AuAu$.

$AuAu$ with little initial state effect in $D+Au$. These $D+Au$ data support the conclusion [106, 107] that the observed jet quenching in $AuAu$ is due to parton energy loss.

Theoretical analysics of jet quenching confirm the energy density estimates determined from measurements of particle multiplicity. They give large energy losses for jets propagating through the matter produced at RHIC, and strengthen the case for multliple strong interactions of the quark and gluon constituents of the matter made at RHIC.

6 Empirical Evidence for the Color Glass Condensate

In this section, the accumulated evidence for the Color Glass Condensate hypothesis is discussed[15]. The evidence rests in a variety of measurements done at different accelerators with different type of particles scattering. The discussion of the results from RHIC will be emphasized here, but it is first important to briefly review the results from HERA involving electron proton scattering.

6.1 Results from Electron-Hadron Scattering

Electron-hadron scattering provide information about the wavefunction of a hadron. The Color Glass Condensate describes the contribution to this wavefunction which have very many gluons in them. These pieces of the wavefunction control the physics at very small x, typically $x \leq 10^{-2}$. The various pieces of experimental information which support the CGC hypothesis come largely from ep scattering experiments at HERA:

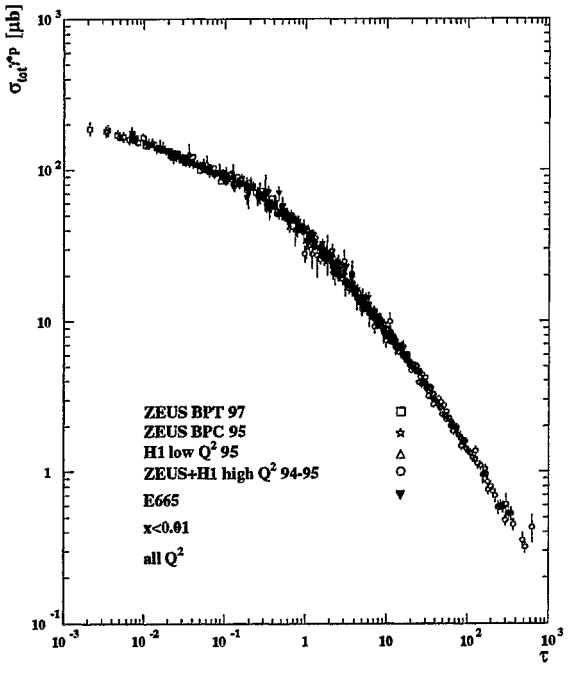

Figure 14: The cross section $\sigma^{\gamma^* p}$ as a function of the scaling variable $\tau = Q^2/Q^2_{sat}$.[109]

- Geometrical Scaling

  Geometrical scaling is the observation[108]-[109] that the deep inelastic cross section for virtual photon scattering as a function of Q^2 and x is really only a function of

$$\sigma^{\gamma^* p} \sim F(Q^2/Q^2_{sat}) \tag{6}$$

where the saturation momentum increases as the fractional momentum, x, of the gluon tends to zero as

$$Q^2_{sat}(x) \sim (x_0/x)^{\lambda}\ 1GeV^2 \tag{7}$$

with $\lambda \sim 0.3$ and $x_0 \sim 10^{-4}$. This scaling with $\tau = Q^2/Q^2_{sat}$ works for $x \leq 10^{-2}$ and over the available Q^2 range at HERA as shown in Fig. 14.

It is straightforward to understand why this scaling works for the small $Q^2 \leq Q^2_{sat}$. This is the region of the CGC, and there is only one dimensionful scale which characterizes the system: the saturation momentum.[110] The surprise is that there is an extended scaling window for $Q^2_{sat} \leq Q^2 \leq Q^4_{sat}/\Lambda^2_{QCD}$.[111] This can be proven analytically. As well, one now has reliable computation of the dependence on x of the saturation momentum, that is, one knows the exponent λ to about 15% accuracy, and it agrees with what is seen from the geometrical scaling curve.[112] What is not determined from the theory of the CGC is the scale x_0, and this must be found by experiment. This comes from the boundary conditions for the renormalization group equations.

- The Structure Function F_2

  Using the dipole description of the virtual photon wavefunction, the structure function F_2 can be related to the gluon distribution function which arises from the CGC. The results for the description of the data are remarkably good for $x \leq 10^{-2}$ and $Q^2 \leq 45\ GeV^2$. One should note that this description includes both the high and low Q^2 data. Descriptions based on DGLAP evolution can describe the large Q^2 points. The CGC description is very economical in the number of parameters which are used [113].

- Diffraction and Quasi-Elastic Processes

  The CGC provides a description of the underlying structure of gluonic matter inside a hadron. As such, it should be sensitive to probes of the transverse extent of this matter, which can be experimentally studied in diffraction and related quasi-elastic particle production.[114]-[118]

  Diffractive scattering can be computed in the CGC description for small inclusive masses of produces particles. The CGC agrees both with generic features of the data, and provides a reasonably good quantitative description.

  There are additional computations of quasi-elastic ρ meson production and J/Ψ production[119]-[120]. Again, up to uncertainties associated with the overall normalization (which arises from imprecise knowledge of hadronic wavefunctions), the CGC hypothesis provides a reasonably good quantitative description.

6.2 Heavy Ion Collisions

The collision of two ultrarelativistic heavy ions can be visualized as the scattering of two sheets of colored glass, as shown in Fig. 4. [121]-[124]

At very early times after the collision the matter is at very high energy density and in the form of a CGC. As time goes on, the matter expands. As it expands the density of gluons decreases, and gluons begin to propagate with little interaction. At later times, the interaction strength increases and there is sufficient time for the matter to thermalize and form a Quark Gluon Plasma. This scenario is shown in Fig. 7, with realistic estimates for energy density and time scales appropriate for the RHIC heavy ion accelerator.

6.3 The Multiplicity

The CGC allows for a direct computation of the particle multiplicity in hadronic collisions. If one naively tries to compute jet production, the total multiplicity is infrared divergent. This follows because of the $1/p_T^4$ nature of the perturbative formula for gluon production

$$\frac{1}{\pi R^2}\frac{dN}{dyd^2p_T} \sim \frac{1}{\alpha_S}\frac{Q_{sat}^4}{p_T^4} \tag{8}$$

In the CGC, when $p_T \leq Q_{sat}$, this divergence is cutoff and the total gluon multiplicity goes as

$$\frac{1}{\pi R^2}\frac{dN}{dy} \sim \frac{1}{\alpha_S}\, Q_{sat}^2 \tag{9}$$

One can compute the proportionality constant and before the RHIC data appeared, predictions were made for the gluon multiplicity. In Fig. 15, the predictions for the first RHIC run are presented. The CGC correctly predicted the multiplicity.

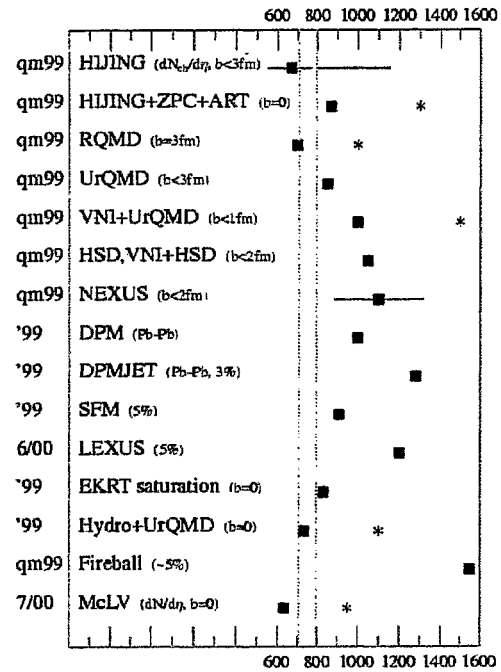

Figure 15: Predictions for the total multiplicity as measured at RHIC. The band is the experimentally measured region. The CGC prediction is marked McLV.

Also, the dependence of the multiplicity on the number of participants can also be computed, realizing that the saturation momentum squared should be (for not too small x) proportional $N_{part}^{1/3}$. This leads to

$$\frac{1}{N_{part}}\frac{dN}{dy} \sim \frac{1}{\alpha_S(Q_{sat}^2)} \sim \log N_{part} \tag{10}$$

so that a very slow logarithmic dependence on the number of participants is predicted in agreement with experiment, as shown in Fig. 16.[125]-[128]

One can go much further[59] and compute the dependence of the multiplicity on rapidity and centrality, and the transverse momentum distribution of produced hadrons by using CGC initial conditions matched together with a hydrodynamic calculation which evolves the matter through the Quark Gluon Plasma[60]. At high $p_T \gtrsim 2$ GeV, jet quenching of the small is pQCD power law tails is also taken into account. This combined hydrodynamic calculation of Nara and Hirano accounts very well for many important features of the data at RHIC. [129],[76]

We emphasize the importance of constraining the QGP hydrodynamics with a QCD theoretic initial condition, the CGC. At SPS energies, the uncertainty about initial conditions together with failure of hydrodynamics to account for the highly dissipative hadronic flow are in remarkable contrast to situation at RHIC. If the initial condition were not well constrained at RHIC, then the conclusion that a QGP was formed could not be sustained. Hydrodynamics is a dynamical mapping of a given given initial condition to final spectra that depends on the equation of state.

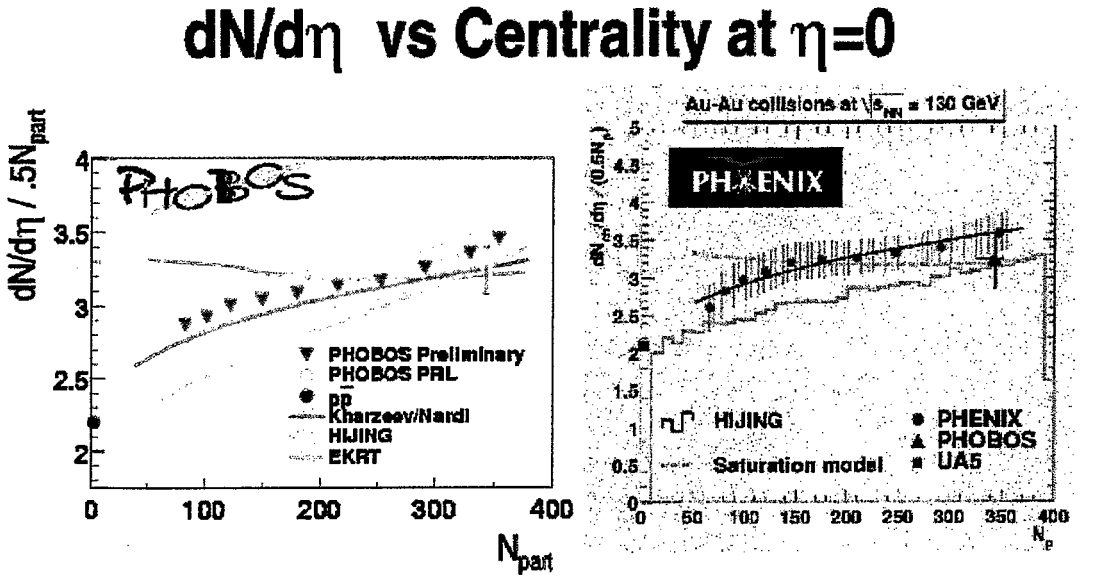

Figure 16: The total multiplicity as a function of the number of participants as measured by Phobos and Phenix.

Only with a known or predicted initial state does that mapping have the power to falsify the QCD equation of state.

In Figs 15 and 16, one can see that several phenomenological models, such as HIJING[95], could also account qualitatively for some of the global multiplicity observables. However, the surprising very weak centrality and beam energy dependence observed[62, 129, 67, 130] is most satisfactory explained and predicted by the CGC as arising from the slow $1/\alpha_S \sim \log Q^2_{sat}(N_{part}, \sqrt{s})$ in eqs.(9,10). This is one of the strongest lines of empirical evidence from RHIC that the CGC initial state (with its predicted N_{part} and $\sqrt{s}$ dependence) is formed and that it is the seed of the QGP that evolves from it.

6.4 High p_T Particles

The early results from RHIC on gold-gold collisions revealed that the high p_T production cross sections were almost an order of magnitude below that expected for jet production arising from incoherent parton-parton scattering.[131] This could be either due to initial state shadowing of the gluon distribution inside the nuclei,[132] or to final state jet quenching.[133] For centrally produced jets, the x of the parton which produces a 5-10 GeV particle is of order 10^{-1}, and this is outside the region where on the basis of the HERA data one expects the effects of the CGC to be important. Nevertheless, nuclei might be different than protons, so it is not a priori impossible.

The crucial test of these two different mechanisms is the comparison of dA scattering to pp. If there is suppression of jet in dA collisions, then it is an initial state effect. The experiments were

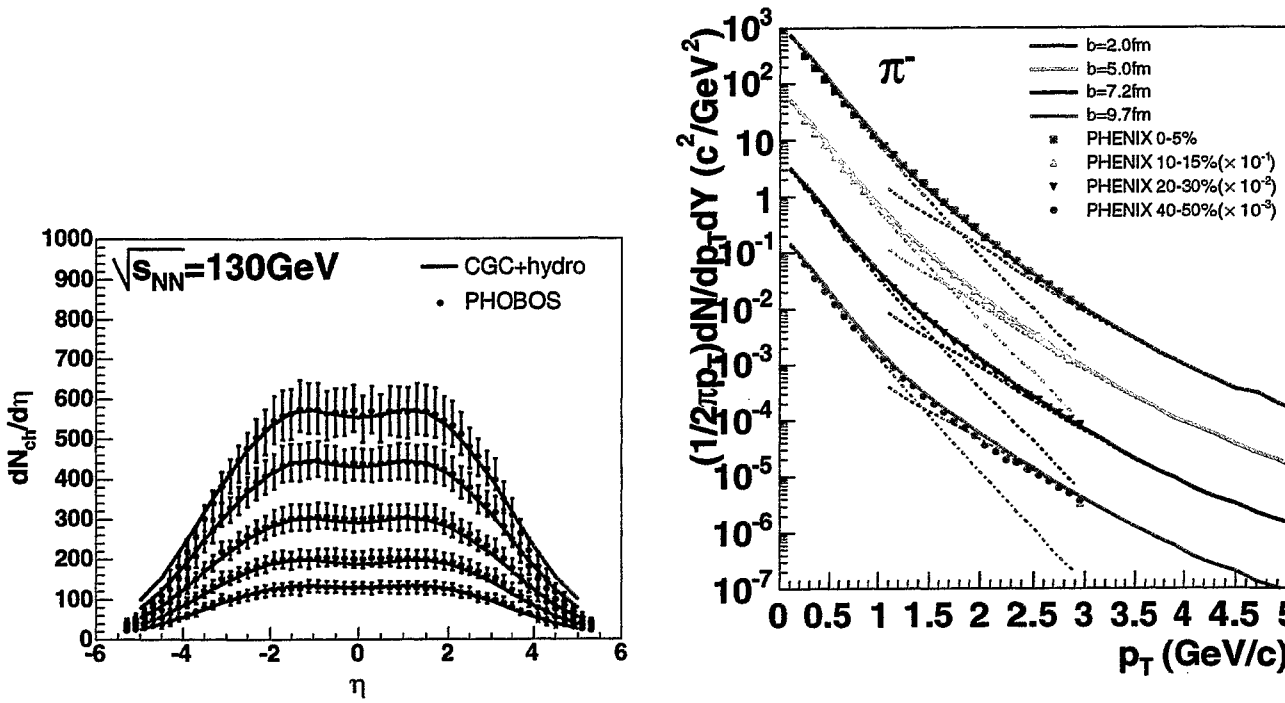

Figure 17: Results of hydrodynamic calculations[60] with a CGC initial condition. Left is the centrality dependence of the rapidity density from PHOBOS[129]. Right shows the transverse momentum distribution at zero rapidity for different centralities from PHENIX[76]. For $p_T > 2$ GeV jet quenching through the evolving QGP is also taken into account.

performed, and all there is little initial state effect for centrally produced jets.[134] The suppression of centrally produced jets in AA collisions at RHIC is indeed due to final state interactions, that is jet quenching.

This is not in contradiction with the existence of a CGC. The particles which control the multiplicity distribution in the central region are relatively soft, and arise from $x \sim 10^{-2}$. To probe such small x degrees of freedom at high transverse momentum at RHIC requires that one go to the forward region.[135]-[136]

If one uses naive Glauber theory to compute the effects of shadowing by multiple scattering, one expects that if one goes into the forward region of the deuteron, the probe propagates through more matter in the nucleus. This is because we probe all of the gluons with x greater than the minimum x of the nucleus which can be seen by the deuteron. Going more forward makes this minimum x smaller. Now multiple scattering will produce more particles at some intermediate value of p_T. (At very high p_T, the effects of multiple scattering will disappear.) This is the source of the Cronin peak and it is expected to occur at p_T of $2-4$ GeV. Clearly the height of this peak should increase as one goes more forward on the side of the deuteron, and should increase with the centrality of the collision.[137] A result of such a computation is shown in Fig. 18.

Classical rescattering effects are included in the computation of the properties of the CGC. There is another effect however and that is quantum evolution generated by the renormalization

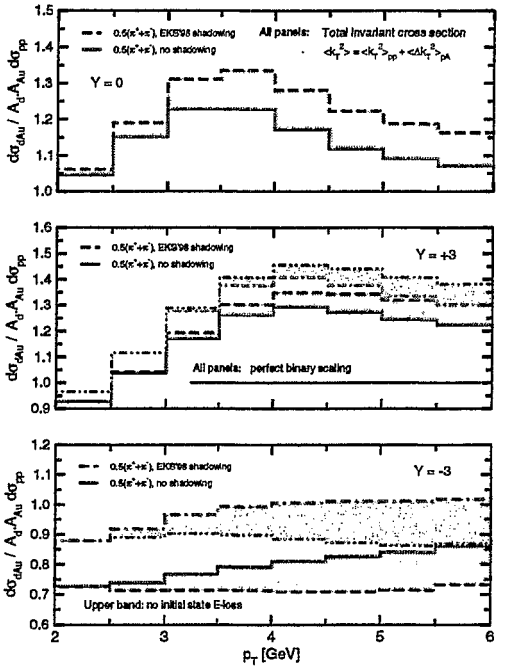

Figure 18: The expectations of classical multiple scattering for the rapidity and p_T dependence (with and without shadowing) for the p_T distribution in $D + Au$ collisions from [103].

group equations. It was a surprise that when one computed the evolution of the gluon distribution function including both effects, the quantum evolution dominated. This means that the height of the Cronin peak, and the overall magnitude of the gluon distribution decreased as one went from backwards to forward angles.[138]- [140] The results of one such computation are shown in Fig. 19

It was also a surprise how rapid the effect set in.

The Brahms experiment at RHIC recently presented data[141] on the ratio of central to peripheral transverse momentum distributions.The ratio R_{CP} is defined in such a way that if the processes were due to incoherent production of jets, then $R_{CP} = 1$. A value less than one indicates suppression, and a value larger than one indicates a Cronin type enhancement. The results for a variety of forward angles for R_{CP} as a function of p_T is shown in Fig. 20 a. There is clearly a decrease in R_{CP} as one goes to forward angles, in distinction from the predictions of classical multiple scattering. The effect is very rapid in rapidity, as was expected from computations of the CGC. In Fig. 20, the ratio R_{CP} is shown as a function of p_T for the forward pseudorapidity $\eta \sim 3$ for less central and more central events. The ratio decreases for more central collisions, against the expectation of classical multiple scattering and consistent with the CGC hypothesis.

Preliminary data[142]-[144] from all four experiments on the rapidity dependence of the transverse distributions in $D + Au$ suggest striking effects consistent with CGC. This is a very active area of research both theoretically and experimentally at this time.

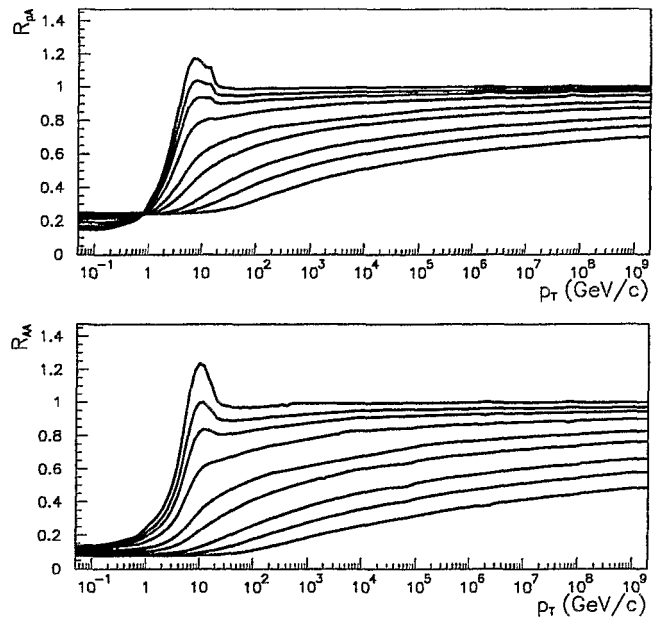

Figure 19: The gluon intrinsic gluon distribution function as a function of p_T for different pseudo-rapidities.

This data suggest a Cronin enhancement on the gold side and the depletion on the deuteron side, and as well a definite dependence on centrality. When these $D + Au$ data become finalized, they could prove that classical multiple scattering dominates on the gold side (large $x > 0.01$), but quantum evolution - i.e., deep gluon shadowing- on the deuteron side (small $x < 0.01$).

By a "happy coincidence", these effects nearly cancel in the mid-rapidity region, making RHIC well suited for studying QGP effects at midrapidity for hard probes.

6.5 The Developing Case for the CGC

In addition to the results described above, the Color Glass Condensate will be the subject of further experimental study at RHIC, LHC and eRHIC. At RHIC, one can study forward backward correlations in the forward direction in analogy with what was done for centrally produced jets. At LHC, in the forward region one measures relatively large p_T jets at $x \sim 10^{-6}$. This provides a direct measurement of the very small x gluon distribution function. Eventually eRHIC would be required to provide precision measurements of quark and gluon distribution functions at small x in a variety of nuclei.

The Color Glass Condensate hypothesis describes remarkably well generic features of *ep* measurements of properties of protons at small x. It also successfully predicted the the previously unexpected slow growth of multiplicity of produced particles with $\sqrt{s}$ and centrality at RHIC. The data from Brahms on the forward particle production appear to be qualitatively in accord with prediction of the CGC, and

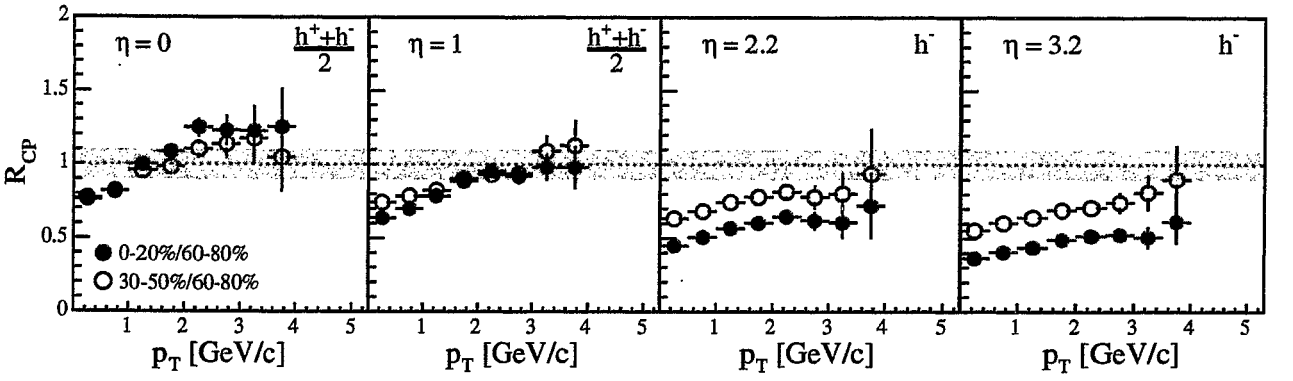

Figure 20: The central to peripheral charged and negative hadron ratios R_{CP} as a function of p_T for various forward pseudorapidities in 200 AGeV $D + Au$ from BRAHMS[141].

the preliminary data from Phobos, Star and RHIC on this subject await submission for publication. While the CGC hypothesis successfully describes the data from disparate experimental measurements, it can be further tested in a variety of new environments.

7 Conclusions

Our criteria for the discovery of the Quark Gluon Plasma at RHIC are:

- **Matter at energy densities so large that the simple degrees of freedom are quarks and gluons. This energy density is that predicted by lattice gauge theory for the existence of a QGP in thermal systems, and is about 2 GeV/Fm^3**
- **The matter must be to a good approximation thermalized.**
- **The properties of the matter associated with the matter while it is hot and dense must follow from QCD computations based on hydrodynamics, lattice gauge theory results, and perturbative QCD for hard processes such as jets**

All of the above are satisfied from the published data at RHIC. A surprise is the degree to which the computations based on hydrodynamics agree so well with elliptic flow data. This leads us to conclude that the matter produced at RHIC is a strongly interacting Quark Gluon Plasma, contrary to naive expectation based on weakly coupled plasma estimates.

The case for the Color Glass Condensate is rapidly evolving into a compelling case. Much of the exciting new data from RHIC presented at QM2004 has not yet been published. Nevertheless, the data from HERA taken together with the data on particle multiplicities, and the data submitted for publication by Brahms make a strong case, which may become compelling with further reinforcement from results from the other experiments at RHIC, and future experimental tests at LHC and eRHIC. This area is rapidly evolving both experimentally and theoretically.

Although in our opinion, the case for the QGP at RHIC is now overwhelming, there are of course many important scientific issues not yet addressed in the first three years of data. The

experiments have demonstrated that a new form of matter, the sQGP, exists. The harder long term task of mapping out its properties can now be confidently continued at RHIC.

8 Acknowledgments

This work was supported by the Director, Office of Energy Research, Office of High Energy and Nuclear Physics, Division of Nuclear Physics, of the U.S. Department of Energy under Contracts DE-FG-02-93ER-40764 and DE-AC02-98H10886.

References

[1] *Report of the workshop on BeV/nucleon collisions of heavy ions – how and why*, Bear Mountain, New York, Nov. 29 – Dec. 1, 1974 (BNL-AUI, 1975); G. Baym, Nucl. Phys. A **698**, XXIII (2002) [arXiv:hep-ph/0104138].

[2] T. D. Lee and G. C. Wick, Phys. Rev. D **9**, 2291 (1974).

[3] J. Hofmann, H. Stocker, W. Scheid and W. Greiner, Bear Mountain Workshop, New York, Dec 1974; H. G. Baumgardt *et al.*, Z. Phys. A **273**, 359 (1975).

[4] J. C. Collins and M. J. Perry, Phys. Rev. Lett. **34**, 1353 (1975); G. Baym and S. A. Chin, Phys. Lett. B **62** (1976) 241; B. A. Freedman and L. D. McLerran, Phys. Rev. D **16**, 1169 (1977); G. Chapline and M. Nauenberg, Phys. Rev. D **16**, 450 (1977).

[5] E. V. Shuryak, Phys. Lett. B **78**, 150 (1978); O. K. Kalashnikov and V. V. Klimov, Phys. Lett. B **88**, 328 (1979); J. I. Kapusta, Nucl. Phys. B **148** (1979) 461.

[6] J. D. Bjorken, FERMILAB-CONF-83-070-T; Phys. Rev. D **27**, 140 (1983).

[7] RHIC: http://www.bnl.gov/rhic/default.htm

[8] For a complete list of RHIC publications see QPIRES: http://www.slac.stanford.edu/spires/hep/ using "find cn brahms or cn phobos or cn star or cn phenix and ps published"

[9] BRAHMS exp. homepage: http://www4.rcf.bnl.gov/brahms/WWW/brahms.html

[10] PHENIX exp. homepage: http://www.phenix.bnl.gov/

[11] PHOBOS exp. homepage: http://www.phobos.bnl.gov/

[12] STAR exp. homepage: http://www.star.bnl.gov/

[13] CERN symposium, Feb. 10, 2000. See, e.g, CERN Courier **40** (May 2000) 13; B. Schwarzschild, Phys. Today **53** (May 2000) 20.

[14] M. Gyulassy, Proc. NATO/ASI: Structure and Dynamics of Elementary Matter (Kemer, Turkey, 2003, ed. W. Greiner), arXiv:nucl-th/0403032.

[15] L. McLerran, Proc. NATO/ASI: Structure and Dynamics of Elementary Matter (Kemer, Turkey, 2003, ed. W. Greiner), arXiv:hep-ph/0402137.

[16] S. A. Bass, M. Gyulassy, H. Stocker and W. Greiner, J. Phys. G **25**, R1 (1999) [arXiv:hep-ph/9810281].

[17] C. R. Allton et al, Phys. Rev. D **68**, 014507 (2003) [arXiv:hep-lat/0305007]. F. Karsch, E. Laermann and A. Peikert, Phys. Lett. B **478**, 447 (2000) [arXiv:hep-lat/0002003]. F. Karsch, Lect. Notes Phys. **583**, 209 (2002) [arXiv:hep-lat/0106019].

[18] C. W. Bernard *et al.* [MILC Collaboration], Phys. Rev. D **55**, 6861 (1997) [arXiv:hep-lat/9612025].

[19] S. Gupta, Pramana **61**, 877 (2003) [arXiv:hep-ph/0303072].

[20] Z. Fodor and S. D. Katz, arXiv:hep-lat/0402006. F. Csikor et al arXiv:hep-lat/0401022.

[21] F. Karsch, K. Redlich and A. Tawfik, Phys. Lett. B **571**, 67 (2003) [arXiv:hep-ph/0306208].

[22] M. A. Halasz et al, Phys. Rev. D **58**, 096007 (1998) [arXiv:hep-ph/9804290]. M. A. Stephanov, K. Rajagopal and E. V. Shuryak, Phys. Rev. Lett. **81**, 4816 (1998) [arXiv:hep-ph/9806219].

[23] D. H. Rischke, Prog. Part. Nucl. Phys. **52**, 197 (2004) [arXiv:nucl-th/0305030].

[24] J. Breitweg et. al. *Eur. Phys. J.* **67**, 609 (1999).

[25] L. V. Gribov, E. M. Levin and M. G. Ryskin, *Phys. Rept.* **100**, 1 (1983).

[26] A. H. Mueller and Jian-wei Qiu, *Nucl. Phys.* **B268**, 427 (1986); J.-P. Blaizot and A. H. Mueller, *Nucl. Phys.* **B289**, 847 (1987).

[27] L.N. Lipatov, *Sov. J. Nucl. Phys.* **23** (1976), 338;
E.A. Kuraev, L.N. Lipatov and V.S. Fadin, *Sov. Phys. JETP* **45** (1977), 199;
Ya.Ya. Balitsky and L.N. Lipatov, *Sov. J. Nucl. Phys.* **28** (1978), 822.

[28] L. D. McLerran and R. Venugopalan, *Phys. Rev.* **D49**, 2233(1994); 3352 (1994); **D50**, 2225 (1994).

[29] E. Iancu, A. Leonidov and L. D. McLerran, *Nucl. Phys.* **A692**, 583 (2001); E. Ferreiro E. Iancu, A. Leonidov and L. D. McLerran, *Nucl. Phys.* bf A710,373 (2002).

[30] E. Iancu and L. McLerran, *Phys.Lett.* **B510**, 145 (2001).

[31] A. Kovner, L. D. McLerran and H. Weigert, *Phys. Rev.* **D52**, 6231 (1995); 3809 (1995); A. Krasnitz and R. Venugopalan, *Phys. Rev. Lett* **84**, 4309 (2000); *Nucl. Phys.* **B557**, 237 (1999); A. Krasnitz, Y. Nara and R. Venugopalan, *Phys. Rev. Lett.* **87** , 192302 (2001).

[32] B. B. Back *et al.* [PHOBOS Collaboration], Phys. Rev. Lett. **88**, 022302 (2002) [arXiv:nucl-ex/0108009].

[33] B. B.Back et. al. [PHOBOS], *Phys. Rev. Lett.* **85**, 3100 (2000);

[34] H. Stocker, J. A. Maruhn and W. Greiner, Z. Phys. A **293**, 173 (1979); Phys. Rev. Lett. **44**, 725 (1980); L. Csernai and H. Stocker, Phys. Rev. C **25**, 3208 (1981).

[35] H. Stocker *et al.*, Phys. Rev. C **25**, 1873 (1982).

[36] H. Stocker and W. Greiner, Phys. Rept. **137**, 277 (1986).

[37] W. Reisdorf and H. G. Ritter, Ann. Rev. Nucl. Part. Sci. **47**, 663 (1997).

[38] S. Voloshin and Y. Zhang, Z. Phys. C **70**, 665 (1996) [arXiv:hep-ph/9407282].

[39] J. Y. Ollitrault, Phys. Rev. D **46**, 229 (1992).

[40] S. A. Voloshin and A. M. Poskanzer, Phys. Lett. B **474**, 27 (2000) [arXiv:nucl-th/9906075].

[41] C. Alt *et al.* [NA49 Collaboration], Phys. Rev. C **68**, 034903 (2003) [arXiv:nucl-ex/0303001].

[42] G. Stoicea *et al.*, arXiv:nucl-ex/0401041.

[43] J. Adams *et al.* [STAR Collaboration], arXiv:nucl-ex/0310029, Phys. Rev. Lett. 92 (2004) 062301.

[44] P. R. Sorensen, hadronization of the bulk partonic matter created in Au + Au collisions at arXiv:nucl-ex/0309003. Ph.D. thesis.

[45] J. Adams *et al.* [STAR Collaboration], arXiv:nucl-ex/0306007, Phys. Rev. Lett. 92 (2004) 052302

[46] C. Adler *et al.* [STAR Collaboration], Phys. Rev. C **66**, 034904 (2002) [arXiv:nucl-ex/0206001].

[47] S. S. Adler *et al.* [PHENIX Collaboration], Phys. Rev. Lett. **91**, 182301 (2003) [arXiv:nucl-ex/0305013].

[48] P. F. Kolb, P. Huovinen, U. W. Heinz and H. Heiselberg, Phys. Lett. B **500**, 232 (2001).

[49] P. Huovinen, P. F. Kolb, U. W. Heinz, P. V. Ruuskanen and S. A. Voloshin, Phys. Lett. B **503**, 58 (2001).

[50] P. F. Kolb, U. W. Heinz, P. Huovinen, K. J. Eskola and K. Tuominen, Nucl. Phys. A **696**, 197 (2001).

[51] P. Huovinen, arXiv:nucl-th/0305064.

[52] P. F. Kolb and U. Heinz, arXiv:nucl-th/0305084.

[53] D. Teaney, J. Lauret and E. V. Shuryak, nucl-th/0104041.

[54] D. Teaney, J. Lauret and E. V. Shuryak, arXiv:nucl-th/0110037.

[55] D. Teaney, Phys. Rev. C **68**, 034913 (2003). D. Teaney, arXiv:nucl-th/0301099.

[56] T. Hirano and Y. Nara, Phys. Rev. Lett. **91**, 082301 (2003) [arXiv:nucl-th/0301042].

[57] T. Hirano and Y. Nara, Phys. Rev. C **68**, 064902 (2003) [arXiv:nucl-th/0307087].

[58] T. Hirano and Y. Nara, arXiv:nucl-th/0307015.

[59] T. Hirano, arXiv:nucl-th/0403042.

[60] T. Hirano and Y. Nara, arXiv:nucl-th/0403029.

[61] E. Iancu and R. Venugopalan, arXiv:hep-ph/0303204. L. D. McLerran and R. Venugopalan, Phys. Rev. D **49**, 2233 (1994) [arXiv:hep-ph/9309289]. D. Kharzeev and E. Levin, Phys. Lett. B **523**, 79 (2001) [arXiv:nucl-th/0108006].

[62] B. B. Back *et al.* [PHOBOS collaboration], Nucl. Phys. A **715**, 65 (2003) [arXiv:nucl-ex/0212009].

[63] G. Agakichiev *et al.* [CERES/NA45 Collaboration], arXiv:nucl-ex/0303014.

[64] D. Molnar and M. Gyulassy, Nucl. Phys. A **697**, 495 (2002) [Erratum-ibid. A **703**, 893 (2002)] [arXiv:nucl-th/0104073]. B. Zhang, M. Gyulassy and C. M. Ko, Phys. Lett. B **455**, 45 (1999) [arXiv:nucl-th/9902016].

[65] Y. Cheng, F. Liu, Z. Liu, K. Schweda and N. Xu, Phys. Rev. C **68**, 034910 (2003). N. Xu *et al.* [NA44 Collaboration], Nucl. Phys. A **610**, 175C (1996).

[66] S. A. Bass and A. Dumitru, Phys. Rev. C **61**, 064909 (2000) [arXiv:nucl-th/0001033].

[67] I. G. Bearden *et al.* [BRAHMS Collaboration], Phys. Rev. Lett. **88**, 202301 (2002) [arXiv:nucl-ex/0112001].

[68] P. Danielewicz, R. Lacey and W. G. Lynch, Science **298**, 1592 (2002) [arXiv:nucl-th/0208016].

[69] G. Brown et al, arXiv:hep-ph/0402068; E. Shuryak, RBRC report, this volume

[70] P. Danielewicz and M. Gyulassy, Phys. Rev. D **31** (1985) 53.

[71] M. Gyulassy, I. Vitev, X. N. Wang and B. W. Zhang, arXiv:nucl-th/0302077. M. Gyulassy, Lect. Notes Phys. **583**, 37 (2002) [arXiv:nucl-th/0106072].

[72] R. Baier, D. Schiff and B. G. Zakharov, Ann. Rev. Nucl. Part. Sci. **50**, 37 (2000) [arXiv:hep-ph/0002198].

[73] D. Kharzeev, Phys. Lett. B **378**, 238 (1996) [arXiv:nucl-th/9602027]. S. E. Vance et al, Phys. Lett. B **443**, 45 (1998) [arXiv:nucl-th/9806008]. I. Vitev and M. Gyulassy, Phys. Rev. C **65**, 041902 (2002) [arXiv:nucl-th/0104066].

[74] P. Csizmadia, et al J. Phys. G **25**, 321 (1999) [arXiv:hep-ph/9809456]. R. J. Fries, B. Muller, C. Nonaka and S. A. Bass, Phys. Rev. Lett. **90**, 202303 (2003) [arXiv:nucl-th/0301087]. D. Molnar and S. A. Voloshin, Phys. Rev. Lett. **91**, 092301 (2003) [arXiv:nucl-th/0302014]. V. Greco, C. M. Ko and P. Levai, Phys. Rev. C **68**, 034904 (2003) [arXiv:nucl-th/0305024]. Z. W. Lin and D. Molnar, Phys. Rev. C **68**, 044901 (2003) [arXiv:nucl-th/0304045].

[75] B. Muller, RBRC report, this volume.

[76] K. Adcox *et al.*, Phys. Rev. Lett. **88**, 022301 (2002); P. Levai *et al.*, Nucl. Phys. A **698**, 631 (2002).

[77] K. Adcox *et al.* [PHENIX Collaboration], Phys. Lett. B **561**, 82 (2003) [arXiv:nucl-ex/0207009].

[78] S. S. Adler *et al.* [PHENIX Collaboration], Phys. Rev. Lett. **91**, 072301 (2003) [arXiv:nucl-ex/0304022].

[79] J. Adams *et al.* [STAR Collaboration], Phys. Rev. Lett. **91**, 172302 (2003) [arXiv:nucl-ex/0305015].

[80] C. Adler *et al.*, [STAR Collaboration] Phys. Rev. Lett. **89**, 202301 (2002) [arXiv:nucl-ex/0206011].

[81] P. Jacobs and J. Klay [STAR Collaboration], arXiv:nucl-ex/0308023.

[82] C. Adler *et al.* [STAR Collaboration], Phys. Rev. Lett. **90**, 082302 (2003) [arXiv:nucl-ex/0210033].

[83] D. Hardtke [The STAR Collaboration], Nucl. Phys. A **715**, 272 (2003) [arXiv:nucl-ex/0212004].

[84] C. Adler *et al.* [STAR Collaboration], Phys. Rev. Lett. **90**, 032301 (2003).

[85] D. d'Enterria, arXiv:nucl-ex/0403055.

[86] A. Accardi, "Cronin effect in pA : A survey of theoretical models," arXiv:hep-ph/0212148.

[87] M. Gyulassy and M. Plumer, Nucl. Phys. A **527**, 641 (1991). M. Gyulassy, M. Plumer, M. Thoma and X. N. Wang, Nucl. Phys. A **538**, 37C (1992)

[88] X. Wang and M. Gyulassy, Phys. Rev. Lett. **68**, 1480 (1992).

[89] J. D. Bjorken, FERMILAB-PUB-82-059-THY and erratum (unpublished); M. H. Thoma and M. Gyulassy, Nucl. Phys. B **351**, 491 (1991); E. Braaten and M. H. Thoma, Phys. Rev. D **44**, 2625 (1991); M. H. Thoma, J. Phys. G **26**, 1507 (2000) [arXiv:hep-ph/0003016].

[90] M. Gyulassy, P. Levai, and I. Vitev, Phys. Lett. B **538**, 282 (2002): E. Wang and X.-N. Wang, Phys. Rev. Lett. **89**, 162301 (2002); C. A. Salgado and U. A. Wiedemann, Phys. Rev. Lett. **89**, 092303 (2002);

[91] I. Vitev and M. Gyulassy, Phys. Rev. Lett. **89**, 252301 (2002) [arXiv:hep-ph/0209161].

[92] M. Gyulassy, P. Levai and I. Vitev, Nucl. Phys. B **594**, 371 (2001) [arXiv:nucl-th/0006010]. Phys. Rev. Lett. **85**, 5535 (2000) [arXiv:nucl-th/0005032]; Phys. Rev. D **66**, 014005 (2002) [arXiv:nucl-th/0201078]; Nucl. Phys. B **571**, 197 (2000) [arXiv:hep-ph/9907461].

[93] D. d'Enterria [PHENIX Collaboration], arXiv:nucl-ex/0401001.

[94] K. J. Eskola, K. Kajantie, P. V. Ruuskanen and K. Tuominen, Phys. Lett. B **543**, 208 (2002) [arXiv:hep-ph/0204034]; Phys. Lett. B **532**, 222 (2002) [arXiv:hep-ph/0201256]; *Nucl. Phys.* **B570**, 379 (2000); *Phys. Lett.* **B497**, 39 (2001).

[95] V. Topor Pop *et al.*, Phys. Rev. C **68**, 054902 (2003) [arXiv:nucl-th/0209089]. X. N. Wang and M. Gyulassy, Phys. Rev. D **44**, 3501 (1991).

[96] S. S. Adler *et al.* [PHENIX Collaboration], Phys. Rev. Lett. **91**, 072303 (2003) [arXiv:nucl-ex/0306021].

[97] J. Adams *et al.* [STAR Collaboration], Phys. Rev. Lett. **91**, 072304 (2003) [arXiv:nucl-ex/0306024].

[98] I. Arsene *et al.* [BRAHMS Collaboration], suppression," Phys. Rev. Lett. **91**, 072305 (2003) [arXiv:nucl-ex/0307003].

[99] B. B. Back *et al.* [PHOBOS Collaboration], Phys. Rev. Lett. **91**, 072302 (2003) [arXiv:nucl-ex/0306025].

[100] Transverse Dynamics at RHIC, BNL March 6-8, 2003, "http://www.phenix.bnl.gov/phenix/WWW/publish/rak/workshop/int/program_TD.htm"

[101] X. N. Wang, Phys. Rev. C **61**, 064910 (2000) [arXiv:nucl-th/9812021].

[102] X. N. Wang, Phys. Rept. **280**, 287 (1997) [arXiv:hep-ph/9605214].

[103] I. Vitev, Phys. Lett. B **562**, 36 (2003) [arXiv:nucl-th/0302002]; X. N. Wang, Phys. Lett. B **565**, 116 (2003) [arXiv:nucl-th/0303004]; A. Accardi and M. Gyulassy, arXiv:nucl-th/0308029; P. Levai, G. Papp, G. G. Barnafoldi and G. I. Fai, arXiv:nucl-th/0306019.

[104] J. w. Qiu and I. Vitev, arXiv:hep-ph/0309094; arXiv:hep-ph/0401062.

[105] D. Kharzeev, E. Levin and L. McLerran, Phys. Lett. B **561**, 93 (2003) [arXiv:hep-ph/0210332].

[106] X. N. Wang, arXiv:nucl-th/0305010.

[107] X. N. Wang, Phys. Lett. B **579**, 299 (2004) [arXiv:nucl-th/0307036].

[108] D. Schildknecht and Bernd Surrow, *Phys. Lett.* **B499**, 116 (2001)

[109] A. M. Stasto, K. Golec-Biernat and J. Kwiecinski, *Phys. Rev. Lett.*, **86**, 596 (2001).

[110] E. Levin and K. Tuchin, *Nucl. Phys.* **A691**, 779 (2001)

[111] E. Iancu, K. Itakura and L. McLerran, Nucl. Phys. A **708**, 327 (2002).

[112] A. H. Mueller and V. N. Triantafyllopoulos, *Nucl.Phys.* **B640**, 331 (2002). D. N. Triantafyllopoulos, Nucl. Phys. B **648**, 293 (2003).

[113] E. Iancu, K. Itakura, and S. Munier, to be published in *Phys. Lett. B*, hep-ph/0310338

[114] L. Frankfurt, V. Guzey, M. McDermott, *Phys.Rev.Lett.* **87**, 192301 (2001) L. Frankfurt, M. Strikman and M. Zhalov, *Phys.Lett.* **B537**, 51 (2002); T. Rogers, V. Guzey, M. Strikman and Z. Xu, hep-ph/0309099.

[115] K. Golec-Biernat and M. Wüsthoff, *Phys. Rev.* **D59** (1999), 014017; *ibid.* **D60** (1999), 114023; *Eur. Phys. J.* **C20** (2001) 313.

[116] W. Buchmuller and A. Hebecker, *Nucl.Phys.* **B476**, 203 (1996). W. Buchmuller, T. Gehrmann and A. Hebecker, *Nucl.Phys.* **B537**, 477 (1999)

[117] Y. Kovchegov and L. McLerran, *Phys.Rev.* **D60**, 054025 (1999).

[118] J. Bartels, K. Golec-Biernat and H. Kowalski, *Phys.Rev.* **D66**, 014001 (2002);

[119] A. H. Mueller, S. Munier and A. Stasto *Nucl.Phys.* **B603**, 427 (2001)

[120] H. Kowalski and D. Teaney, *Phys. Rev.* **D68**,114005 (2003).

[121] A. Kovner, L. McLerran and H. Weigert, Phys. Rev **D52** 3809 (1995); **D52** 6231 (1995).

[122] A. Krasnitz and R. Venugopalan, Nucl. Phys. **B557** 237 (1999); *Phys. Rev. Lett.* **84** (2000), 4309; Phys. Rev. Lett. **86** (2001).

[123] T. Lappi, *Phys. Rev.* **C67**, 054903 (2003).

[124] A. Krasnitz, Y. Nara, and R. Venugopalan, *Phys. Rev. Lett.* **87** (2001) 192302.

[125] K. Eskola, K. Kajantie and K. Tuominen, *Phys. Lett.* **B497**, 39 (2001).

[126] D. Kharzeev and M. Nardi, *Phys. Lett.* **B507**, 121 (2001); D. Kharzeev, E. Levin, *Phys. Lett.* **B523**, 79 (2001).

[127] B.B. Back et al [PHOBOS] *Phys. Rev.* **C65**, 31901R (2002).

[128] K. Adcox et. al. *Phys. Rev. Lett.* **86**, 3500 (2001)

[129] B. B. Back *et al.* [PHOBOS Collaboration], Phys. Rev. Lett. **85**, 3100 (2000) [arXiv:hep-ex/0007036].

[130] K. Adcox *et al.* [PHENIX Collaboration], Phys. Rev. Lett. **88**, 242301 (2002) [arXiv:nucl-ex/0112006].

[131] B. Back. et. al. *Phys. Lett.* **B578**, 297 (2004); C. Adler et. al. *Phys. Rev. Lett.* **89** 202301, (2002).

[132] D. Kharzeev, E. Levin and L. McLerran, *Phys. Lett.* **B561**, 93 (2003)

[133] J. D. Bjorken, Fermilab-Pub-82-059-THY; D. Appell, *Phys. Rev.* **D33**, 717 (1986);M. Gyulassy and M. Plumer, *Phys. Lett.* **B243**, 432 (1990); M. Gyulassy, M. Plumer, M. Thoma and X. N. Wang, *Nucl. Phys.* **A538**, 37C (1992);

[134] I. Arsene et. al. *Phys. Rev. Lett.* **91**, 072305 (2003); B. Back et. al. *Phys. Rev. Lett.* **91**, 072302 (2003); S.S. Adler et al., *Phys. Rev. Lett.* **91** , 072303 (2003); J. Adams, *Phys. Rev. Lett.* **91**, 072304 (2003); M. Gyulassy, I. Vitev and X. N. Wang, *Phys. Rev. Lett.* **86**, 2537 (2001)

[135] A. Dumitru and J. Jalilian-Marian, *Phys.Lett.* **B547**, 15 (2002); *Phys.Rev.Lett.***89**,022301(2002)

[136] F. Gelis and J. Jalilian-Marian, *Phys.Rev.* **D67**, 074019 (2003).

[137] I. Vitev and M. Gyulassy, *Phys. Rev. Lett.* **89**, 252 (2002); M. Gyulassy, P. Levai and I. Vitev, *Phys. Rev.* **D66**, 014005 (2002); *Nucl. Phys.* **B594**, 371 (2001); *Nucl. Phys.* **B571**, 197 (2000) I. Vitev, *Phys. Lett.* **B562**, 36 (2003).

[138] D. Kharzeev, Y. Kovchegov and K. Tuchin, *Phys.Rev.* **D68**, 094013 (2003).

[139] R. Baier, A. Kovner and U. Wiedemann, *Phys.Rev.* **D68**, 054009 (2003).

[140] J. Albacete, N. Armesto, A. Kovner, C. Salgado and U. Wiedemann, hep-ph/0307179

[141] I. Arsene *et al.* [BRAHMS Collaboration], arXiv:nucl-ex/0403005.

[142] Zhangbu Xu for the Star Collaboration at Quark Matter 2004.

[143] Rachid Noucier for the Phobos Collaboration;

[144] Talks presented at Quark Matter 2004: R. G de Cassagnac for the Phenix Collaboration at Quark Matter 2004, M. X. Liu for the Phenix Collaboration;

Strongly Coupled Quark-Gluon Plasma

Edward Shuryak

Strongly coupled Quark-Gluon Plasma

Edward Shuryak
Department of Physics and Astronomy,
University at Stony Brook, NY 11794, USA

Abstract

We start with brief summary of the main experimental discoveries made at RHIC, and then proceed to why we think quark-gluon plasma at RHIC is in strong coupling regime. The robust collective flow phenomena are well described by ideal hydrodynamics, with the Equation of State (EoS) predicted by lattice simulations. However the transport properties turned out to be unexpected, with rescattering cross section one-to-two orders of magnitude larger than expected from perturbative QCD. These and other theoretical developments indicate that Quark-Gluon Plasma (QGP) produced at RHIC, and probably in a wider temperature region $T_c < T < 4T_c$, is not at all a weakly coupled quasiparticle gas, but is rather in a strongly coupled regime, sQGP for short. After reviewing two other "strongly coupled systems", (i) the strongly coupled supersymmetric theories studied via Maldacena duality; (ii) trapped ultra-cold atoms with very large scattering length, we return to sQGP. We show that one can get a consistent picture unifying lattice results about quasiparticle masses, their interactions, correlation functions and thermodynamics. Its main new element is the existence of hundreds of bound states, most them colored. We then discuss the implications of this picture on the EoS, viscosity and jet quenching.

1 Two sets of major discoveries made at RHIC

The Relativistic Heavy Ion Collider at Brookhaven is the largest facility dedicated to heavy ion physics, built *to produce and study the properties of new form of matter*, the Quark-Gluon Plasma (QGP). Let me emphasize from the onset that this goal of the RHIC project has been met with widely spread skepticism, especially by people with a high energy physics background. It was argued that even if a large number of quarks and gluons be created at RHIC, it will simply fizzle into a firework of multiple jets and mini-jets, with small (and calculable by pQCD) deviations from a set of independent multiple pp collisions.

RHIC just completed its Run-4, in which a record number of events $\sim 10^9$ per detector was recorded. Obviously our experimental colleagues are eager to have a look at it now. However, let us all make a break from ever continuing stream of work and have a look back, summarizing what have we learned from the data of Runs 1-3 and recent theory development and comparing it with the original picture we had in mind many years ago.

The goal "to produce QGP" via certain set of signals, new flavor, dileptons and photons, vector meson melting including J/ψ, together with the name itself, was first formulated in my papers [1]. They followed earlier theoretical ideas that very high temperature QCD should be weakly coupled [2], in which the color charge should not be confined but rather screened [1] (thus "plasma"). So QGP was thought to be a "normal phase" of QCD, and expected to be much simpler in its structure than the "QCD vacuum", with its chiral symmetry breaking and (still mysterious) confinement, leading to

thousands of quark bound states filling the particle data tables. It was widely expected (for about 3 decades!) that a simple perturbative approach to QGP properties, similar to that used e.g. for QED plasmas, would adequately describe its properties right from $T = T_c$, at least qualitatively.

But, when one penetrates into the domain never studied before, one may always find quite unexpected things[1]. The same happened at RHIC. Not only the skeptics have been proved wrong about "matter" production and robust collective phenomena seen there, but the whole view of QGP structure underwent a major revision in the last year or so.

I will start with a list of major discoveries [2], which I will group into 2 sets, those related with soft $p_t < 2\,GeV$ and hard $p_t > 2\,GeV$ parts of the observed particle spectra.

Discoveries related with the bulk of secondaries ($p_t < 2\,GeV$)**:** are obviously about the properties of the matter produced. We learned that:
(i) like at CERN, particle composition is quite well equilibrated, including strangeness;
(ii) the multiplicity does not grow very rapidly with energy, as binary scaling for hard collisions would suggest, so there is some coherence in production;
(iii) the magnitude of the radial flow velocity is reaching about .7 of speed of light, is larger than at SPS and its effect extends to higher $p_t \sim 1.5 - 2\,GeV$.
(iv) Especially impressive are data on the so called *elliptic flow*, observed for non-central (and even rather peripheral) collisions. It is significantly stronger than at CERN.
(v) Both radial and elliptic flows are correctly described by hydrodynamics, including their dependence on collision energy, centrality and – last but not least – the particle type. It gave good quantitative description of about 99% of the spectra for all secondaries[3] (except for the hard part at $p_t > 2\,GeV$), essentially without any parameters other than (lattice-based) EoS.

RHIC collisions are sometimes called the *Little Bangs*, and they are obviously quite different from a fizzle predicted by pQCD.

Discoveries related with the hard tail of the spectra $p_t > 2\,GeV$, naturally came from runs 2 and 3.
(i) Already the first data on high transverse momentum tail of the spectrum, from the second RHIC run, have shown its suppression by a factor ~ 5, exceeding expectations of the naive parton model. Including such initial state effects as Cronin effect, one finds that actual jet quenching is closer to a factor 10 suppression.
(ii) The puzzle became more intense when it was found that even the large p_t particles are emitted very anisotropically in the azimuthal angle.
(iii) Observation of the 2-particle correlations at large p_t have confirmed that in these region (of not-so-large p_t) the secondaries still originated from jets. The shadowing of the away-side jets confirmed the strong quenching, as it also reaches about an order of magnitude suppression .
(iv) Further clarification came from the run 3, when a control experiment with deuteron-gold (dAu) collisions has confirmed that at mid-rapidity[4] the suppression is *not* due to the initial state shadowing, but is instead indeed a final state absorption.

The original intention [4] was to use jet quenching in order to get a kind of a tomographic picture of the QGP cluster. However, the data available so far (up to about $p_t = 12\,GeV$ mostly show that a produced matter is so black – up to 90% of produced jets are absorbed – that only jets from the surface

[1]Recall that this very country was "accidentally" discovered by Columbus, searching only another passage to well known India.

[2]I am certainly not in the position to comment on which experiment was the first on which particular observations, and use more or less random set of data, with a reference to the collaboration. (It is possible to use data from any one of them due to quite remarkable level of consistency between RHIC data.) A real experimental summary done by collaborations are expected soon.

[3]Modulo the remaining disagreement with HBT radii, on the level of 30-40 percents.

[4]The latest dAu data from BRAHMS experiment indicate much stronger initial state effects in the forward region, hopefully an expected gluon saturation signal.

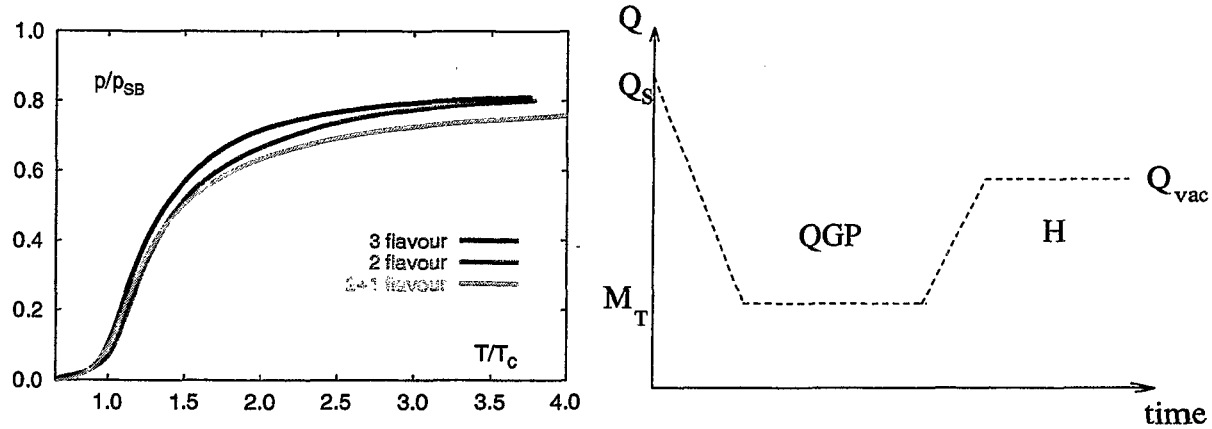

Figure 1: (a) The pressure (divided by that for free gas) versus the temperature T/T_c, from lattice thermodynamics studied by Bielefeld group. (b) Schematic plot of the cut-off scales during the evolution of the system with time, from [15]. At the collision time=0 the scale is presumably the saturation scale Q_s in the incoming nuclei, which grows with the collision energy. Then the cutoff decreases reaching some nearly constant value in QGP at $T > T_c$, the thermal gluon mass M_T (??) and stay at this value till it rises again in the mixed phase to its vacuum value in the hadronic (H) phase $Q_{vac} \sim 1\,GeV$.

is escaping. Clearly a drive to larger p_t is still very much needed.

In this brief report I would not discuss the large p_t physics, except of mentioning some new ideas about the mechanism of jet quenching, but will try to summarize in more detail the physics implications of the data at smaller p_t on the QGP production and properties. Before we go into specifics, let me summarize the successes and surprises we have seen on the way.

Brief summary of QGP properties, as it is extracted from data: The thermodynamics at chemical freezeout tells us that it occurs at a universal temperature $T_c \approx 170\,MeV$ which coincides with the expected critical temperature. The hydrodynamics tells us parameters of the EoS: it has not yet been very precisely mapped (we need an energy scan for that), but e.g. the *latent heat* of the QCD transition is fixed by these works to be about 800 MeV/fm^3, the same value as it was predicted by the lattice QCD. Furthermore, the expected EoS (pressure as a function of the energy density) above the transition region is also confirmed to be roughly $p \approx \epsilon/3$.

In contrast to that, the transport properties (viscosity) of QGP turned out to be completely unexpected. The rescattering of constituents needed to sustain the observed degree of collectivity is one to two orders stronger than it was predicted on the basis of pQCD. The ratio of the QGP viscosity relative to its entropy density $\eta/s \sim 1/10$, making it *the most ideal fluid ever observed.* (In particularly: water would not flow, if only few thousands molecules would be put together.)

2 Evolving theoretical views on QGP properties

Since 1970's till quite recently Quark Gluon Plasma (QGP) was viewed as a gas of quasiparticles (dressed quarks and gluons) which interact relatively weakly with each other. A significant amount of theoretical work has been invested on refining the perturbative high-T calculations, to thermodynamics and kinetics of QGP, see e.g. my book [5] for more details. We now know all perturbatively calculable corrections to free gas expressions, $O(g^2, g^3, g^4, g^5, g^6 log(g))$, making in total 7 terms of the weak coupling series (see e.g. [6]). Although they are not converging, unless $T \sim 10^6 GeV$ or so, hopes remained that some clever re-summation will get all the physics right.

The non-perturbative results which came from lattice QCD, such as pressure shown in Fig.1(a), seemed to support this view. Indeed, the ratio of the calculated pressure to that at zero coupling gets

to about 0.8 soon after the phase transition, so it was tempting to assume that the deviation, $\sim .2$, is a good measure of the interaction corrections.

As I will argue below in more detail, this simple reasoning turned out to be very misleading, and it managed to fool us all for decades. Only recently had we learned that in two other examples of very strongly interaction matter – (i) the CFT gauge theory at comparable coupling; and (ii) trapped atoms at the Feshbach resonances – the same ratio also about .8. (And I will argue by the end of this paper, one can explain this .8 for QGP at $T = 2T_c$ in a radically new picture, with only half of pressure coming from a quasiparticle gas and the rest from *hundreds* of bound states.)

The breakthrough in our thinking [27] came basically from 3 different sources:
(i) a general idea that while confinement and chiral breaking disappear at $T > T_c$ and there is not much free charge to generate large Debye mass yet, the sizes of states and scale at which the coupling is defined should be rather low at $T = (1-2)T_c$, see e.g. Fig.1 (b).
(ii) Triumph of hydro[5] , compared with apparent failure of weak coupling "parton cascades" of various kinds. For example, Gyulassy and Molnar [7] concluded that the elliptic flow can only by reproduced by a gluon cascade if the cross section be enhanced by a factor of about 50. That forced us to think hard *Why is the Quark-Gluon Plasma at RHIC such an ideal fluid ?* Important paper by Policastro, Son and Starinets [19] was a radical step in this direction.
(iii) The last ringing bell came from the lattice practitioners. Surprisingly to all, recent works in Japan and Bielefeld [8] have found that the lowest charmonium states are not melting at T_c, as was believed previously, but actually persist to at least $T = 2T_c$. Then came similar evidences that mesonic bound states made of light quarks survive we into the QGP phase as well [9].

All these developments provided a hint, that the QGP quasiparticles at $T \sim few\, T_c$ have much stronger interaction than previously expected, we have found a *strongly coupled QGP.*

After more details about hydro and brief discussion of two other strongly coupled examples we will return below to recent attempts to understand what exactly sQGP is.

3 Collective flows, EoS and transport properties

Is hadronic matter really produced in heavy ion collisions? Is there something qualitatively new in AA collisions, never seen in "elementary"[6] pp or $e+e-$ collisions?

Indeed, the original motivation for heavy ion program is not just increase the number of secondary particles produced per event (up to several thousands at RHIC), but to reach a *qualitatively different* dynamical regime. characterized by a small microscopic scale l (e.g. mean free path) as compared to the macro scale L (the system's size): $l \ll L$. If this is achieved, the fireball produced in heavy ion collisions should be treated as a macroscopic body, with thermo and hydrodynamics.

Statistical models do indeed work remarkably well for heavy ion collisions, even at energies lower than RHIC. But they also work for pp or e^+e^- (and we still do not know why). end to it. In contrast to that, pp or e^+e^- show no sign of flow effects, see early attempts to see them [10]. So, a multi-body excited systems produced in these case are *not* macroscopically large. It is not "matter" but just a bunch of particles.

[5]In fact the hydrodynamics with its "non-ideal" expansion in powers of the mean free path is the oldest example of a *strong coupling* expansion, including the *inverse* powers of the cross section.

[6]Apart of the large-p_t tail, described by the parton model plus pQCD corrections, it is very far from being elementary and is very poorly understood. One may argue that heavy ion collisions, described well by hydro/thermodynamics, are in fact even much simpler.

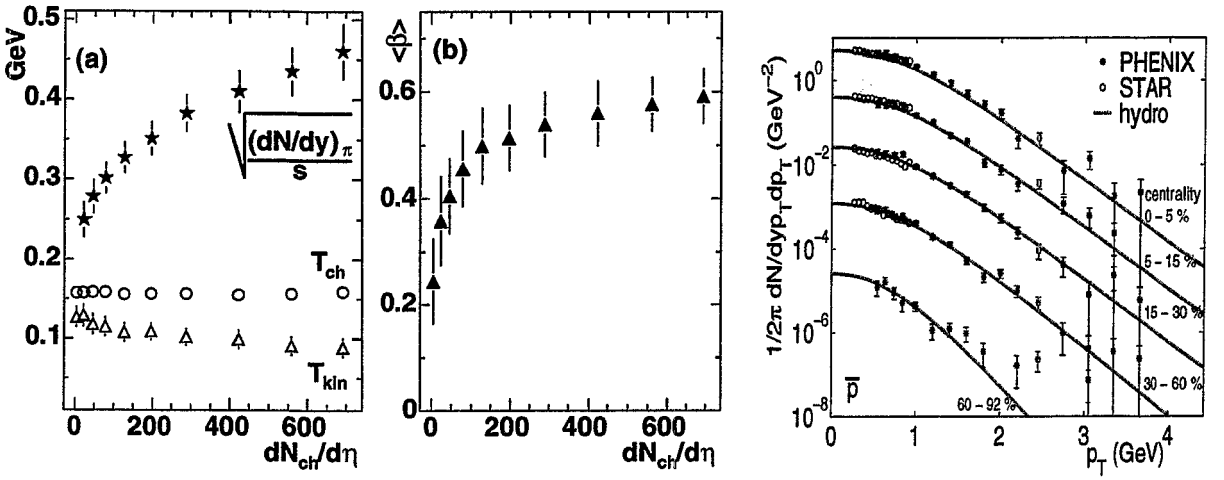

Figure 2: (a) The "blast model" fits to STAR collaboration data. The values of the and freezeout temperatures are shown in (a) and the mean collective velocity. (b) Comparison between STAR and PHENIX data for protons with hydro calculation by Kolb and Rapp [12] (which correctly incorporates chemical freezeout).

3.1 Transverse flow

Heavy ion collisions, on the other hand, showed a variety of *"flows"* since very low energies, but not all of them are indeed a collective expansion.

Let me start with a historic comment. First attempts to connect the experimental information with the collective transverse flow were made independently by Siemens and Rasmussen [11] for low energy (BEVALAC) and by Zhirov and myself [10] for high energy pp collisions at CERN ISR around 1979. The idea of both papers was exactly the same: collective expansion boosts spectra of various secondaries differently, depending on their mass. Pions are light and their spectrum remains exponential, with a "blue shifted" temperature, while for heavy particles the effect is different. Fortunately it is easily calculable and depends on the value of the particle mass only.

Siemens and Rasmussen found the expected difference for pions and protons produced by heavy ions at $E \sim 1GeV/N$ fitted them with two parameters, the freezeout temperature $T_f \sim 30\,MeV$ and the velocity of what they have called the "blast wave". (Long discussion afterwords shown that ideal hydro is not really applicable in this case, however.). Zhirov and myself [10] found no flow in pp data from ISR: the $\pi, K.N$ spectra from pp showed the same m_t-slope. All of us had to wait for heavy ion collisions at high energies, and only at SPS and now at RHIC we have seen real hydrodynamical flow, radial and especially elliptic.

Let me jump years ahead and show a modern version of the blust wave fit to RHIC data, shown in Fig.2 as a function of centrality. Two basic parameters are the freezeout temperature T_{kin} and the mean flow velocity $< \beta >$. T_{kin} decreases and the velocity increases for more central collisions, displaying an expected conversion of the internal energy into flow. Note also that the temperature of chemical equilibration T_{ch} seem to be completely independent of the centrality: the interpretation of it is that it is in fact the *QCD critical temperature.*

Fig.2 is an example of a hydro prediction for the proton p_t spectra. Note that no parameters (other than total entropy and EoS) are used, and the agreement of the predicted shape is very good, both in normalization and shape.

At RHIC (rather unexpectedly) we found that different flow-related slopes for pion and nucleons holds till rather large $p_t \sim 2\,GeV$, making both spectra to cross. As a result there are more baryons than pions above this point (till about $p_t \sim 5\,GeV$). Observation of that lead to a very good question:

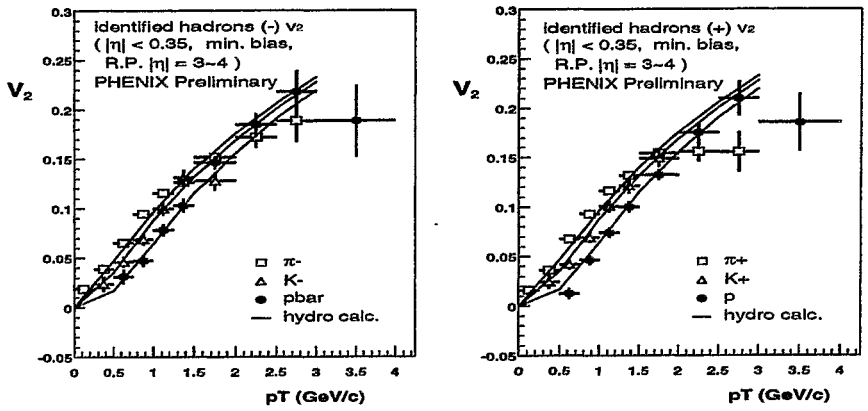

Figure 3: The p_t-differential elliptic flow $v_2(p_t)$ from minimum bias Au+Au collisions at RHIC, for different identified hadron species (PHENIX). with negative (left) and positive (right) charge.The curves are hydrodynamic calculations.

how far down the spectrum the hydrodynamics should be trusted?

3.2 Elliptic Flow

Non-central heavy ion collisions produced fireball which has an almond shape. It would not matter for independently produced secondaries, but in a collective expansion the shape matters, leading to "elliptic" flow pattern. This is quantified by v_i harmonics defined as

$$\frac{dN}{d\phi} = \frac{v_0}{2\pi} + \frac{v_2}{\pi}\cos(2\phi) + \frac{v_4}{\pi}\cos(4\phi) + \cdots \tag{1}$$

Each of v_i is a function of centrality (the impact parameter b), rapidity y, transverse momentum p_t and, last but not least, the particle type. By now v_1, v_2, v_4 have been studied. The important feature of elliptic flow is *self-quenching*, as a result of which the elliptic flow develops earlier than the radial one. This is why it is especially important for understanding the EOS of the QGP.

The ellipticity depends on a particle mass, again in a predictable way [13]. Let me show few plots from Kolb and Heinz review [14] to convince the reader that the elliptic flow is a hydrodynamical effects.

The next Fig.4 makes use of one important fact: centrality dependence of v_2 is basically a response to the initial *spatial* anisotropy of the system, quantified by the parameter $\epsilon = \langle y^2 - x^2\rangle / \langle y^2 + x^2\rangle$, and so plotting v_2/ϵ one basically eliminates the geometry of the problem and finds all points at some universal curve, see[7] Fig.4(a).

The main message of this figure is that v_2 grows with multiplicity[8] . The parts (b,c) of the figure shows how the v_2 magnitude was expected to depend on the collision energy[9], from Teaney et al [13].

We will not have time to discuss details of the hydrodynamics calculations, which reproduce these data. Let me only tell why RHIC energy range is special. Due to the QCD phase transition, the matter is very soft in the so called "mixed phase" energy density region. That is why at SPS energies there was no substantial v_2 contribution, which only happen at RHIC due to "stiff QGP".

[7]The horizontal band on this figure marked "hydro limit" refers to some hydro with ideal gas EoS and simplistic freezeout. It supposed to hold at very large entropy density.

[8]This theoretical prediction was made at QM99 by Teaney and myself, as well as Kolb and Heinz, prior to RHIC.

[9]Other authors such as Ollitraught and Heinz et al have used fixed freezeout predicted a different energy dependence of v_2.

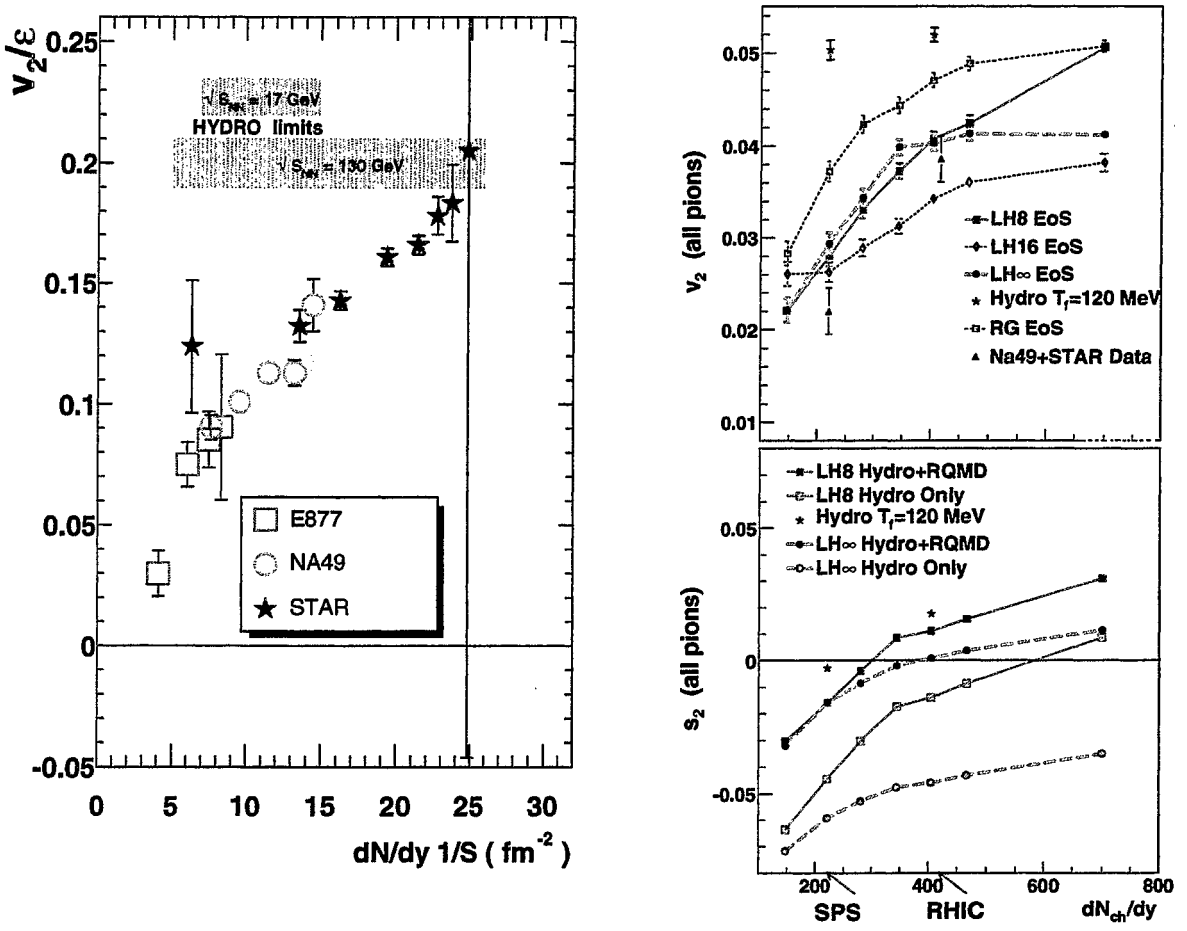

Figure 4: (a) The compilation of elliptic flow (the ratio of v_2/ϵ) dependence on collision energy (represented by the particle multiplicity). (b,c) Energy dependence of the elliptic flow predicted by hydro calculation by Teaney et al [13] for different EoS. The curve with the latent heat (LH) =800 MeV/fm^3 is the closest to the lattice EoS, and it is also the best fit to all flow data at SPS and RHIC

3.3 The limits to ideal hydro

The ideal hydrodynamics is *not* just a bunch of conservation laws, but the local parameterization of the stress tensor

$$T^{\mu\nu} = (\epsilon + p)u^\mu u^\nu - pg^{\mu\nu} \tag{2}$$

Here ϵ is the energy density, p is the pressure, and $u^\mu = \gamma(1, \mathbf{v})$ is the proper velocity of the fluid.

Inclusion of dissipative effects, to the first order in l/L, is possible via the following corrections to the stress tensor

$$\delta T_{\mu\nu} = \eta(\nabla_\mu u_\nu + \nabla_\nu u_\mu - \frac{2}{3}\Delta_{\mu\nu}\nabla_\rho u_\rho) + \xi(\Delta_{\mu\nu}\nabla_\rho u_\rho) \tag{3}$$

where the coefficients η, ξ are called the shear and the bulk viscosities. In this equation the following projection operator onto the matter rest frame was used: $\nabla_\mu \equiv \Delta_{\mu\nu}\partial_\nu$, $\Delta_{\mu\nu} \equiv g_{\mu\nu} - u_\mu u_\nu$. It is further useful to normalize the magnitude of the viscosity coefficient η to the entropy density s, forming a dimensionless ratio. For example a sound wave have dispersion law

$$\omega = c_s q - \frac{i}{2}\mathbf{q}^2\Gamma_s, \qquad \Gamma_s \equiv \frac{4}{3T}\frac{\eta}{s} \tag{4}$$

Let us now discuss what is the value of QGP viscosity, following Teaney [16]. He argued that relative deviations from ideal case should be $\sim (\eta/s)p_t^2$, and shown that such deviations are indeed seen in real data. In Fig.5 we show it for the elliptic flow parameter v_2. Since its value is determined at sufficiently early times – about 3 fm/c – the deviation should correspond to the QGP phase. The results for different Γ_s/τ shown in Fig.5 deviate from ideal hydro curve at $p_\perp \approx 1.6\,GeV$ which indicates $\Gamma_s/\tau \sim 0.05$ or so. Substituting here the relevant time $\tau \sim 3fm/c$ we get $\Gamma_s \sim .15fm$. Strong coupling result for typical $T \sim 200\,MeV$ at the time gives $\Gamma_s \sim 0.1fm$, while weak coupling one would predict much larger value $\Gamma_s \sim 2fm$ or so. About the same value follows from the gluon cascade with the enhance cross section by Molnar and Gyulassy [7] mentioned above.

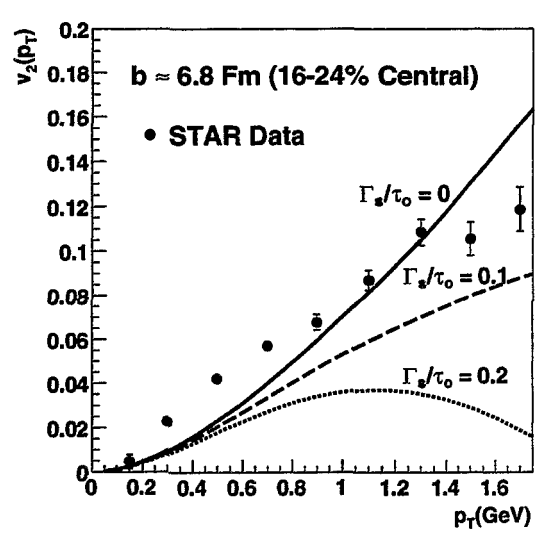

Figure 5: Elliptic flow v_2 as a function of p_T for different values of Γ_s/τ_o. The data points are four particle cumulants data from the STAR collaboration. Only statistical errors are shown.

4 Other strongly couples systems

4.1 Finite T N =4 supersymmetric gauge field theory at strong coupling

To find a gauge theory in which strong coupling limit makes sense is a nontrivial task. Furthermore, to develop tools which would allow a systematic expansion in *inverse* coupling constant is even more challenging. However both problems have been solved during 1990's, first for a specific – 4 times supersymmetric – gauge theory, and then for some other examples (we would not discuss).

It is a Conformal Field Theory (CFT), with a non-running coupling. Its finite-T version is in the QGP-like phase at *any* coupling, from weak to strong. As a result of long development by string theorists based on "holography" and "duality" ideas, the so called AdS/CFT correspondence [17] was shown, which states that *CFT in strong coupling is dual to a weakly coupled string theory*, albeit in 10 dimensions in a particular gravity field. The finite-T version has a gravity metrics with a *black hole*, and it is its Hawking radiation which heats up our Universe[10], represented by a 4-d surface at some distance from the black hole.

For a non-string theorist like myself to follow the duality arguments and gravity-based arguments is a fascinating, near magical experience. On the other hand, as I am not really interested in string theory and consequences of supersymmetry, but rather in generic effects of any strong coupling, it is imperative to find a meaning for gravity-based calculations and results *inside the gauge theory itself.* This work has just started (see below) and we of course have a lot of problems to solve.

This CFT has gluons with N_c colors, which for technical reasons is considered large, 4 types of fermions (gluinos) and 6 scalars. The gauge coupling is always combined with the color factor $\lambda \equiv g^2 N_c$, and can be either small or large. In the former case one has standard Feynman calculus on a gauge side, in the latter it is better to used the gravity formulation. For instance, a potential between two static quark-like charges is then described by a string between them, which is not straight as in QCD but stretched by gravity into 5-th dimension. The result is a modified Coulomb's law for strong coupling ($\lambda \gg 1$) [17], which has the same r-dependence but $\sqrt{\lambda}$ instead of λ

$$V(r) = -\frac{4\pi^2}{\Gamma(1/4)^4}\frac{\sqrt{\lambda}}{r} \tag{5}$$

times a very strange coefficient including Euler Gamma function.

The strong-coupling results for finite T include:

(i) bulk thermodynamics resulted in[18] It was found that the free energy in this limit is $\mathbf{F}(T, N_c, \lambda) = \left((3/4) + O(1/\lambda^{3/2})\right)\mathbf{F}(T, N_c, 0)$ where $\mathbf{F}(T, N_c, 0) \approx N_c^2 T$ is the free (zero coupling) result, analogous to Stephan-Boltzmann result for blackbody radiation.

(ii) the heavy quark potential is totally screened for a Debye radius of order $1/T$ [20] and leads to quasiparticle masses of the order $M \sim \sqrt{\lambda}T$

(iii) viscosity of strongly coupled matter was found to be unusually small, leading to a rather good liquid with hydrodynamical behavior even at small spatial scales. In particular, the viscosity to entropy ratio was found to be [19]

$$\frac{\eta}{s} = \frac{1}{4\pi} \tag{6}$$

which is probably the smallest possible value, as it is obtained for an infinite coupling.

One thing that became clear to us [21] is the meaning of the black hole. Thinking about strongly coupled gauge theory one cannot avoid noticing that in particular partial waves particles fall at each

[10] As Sun worms the Earth.

other, propagating indefinitely toward small distances. This for example happens in Klein-Gordon eqn. for $\alpha > 1/2$. In equilibrium, there must also be waved propagating back, from small to large distances: this constant pair production is a kind of Hawking radiation.

Another is that the interaction is transfered by gluons with a superluminal speed, $v \sim \lambda^{1/4} >> 1$, which may justify potential type ladder diagrams even for relativistic bound states.

Furthermore, as I will try to show, it explained the puzzle of why thermodynamics can be nearly independent on the value of the coupling λ in strong coupling, while the composition of matter drastically changes when it changes from weak to strong. In a naive picture of a quasiparticle gas, one would expect the Boltzmann factors for quasiparticles to be $exp(-M/T) \sim exp(-\sqrt{\lambda}) \ll 1$, while $p \sim T^4$ clearly demands the light particles with masses $M \sim T$ at any coupling. What those states may be?

Zahed and myself [21] proposed an explanation: these light states are deeply bound binary composites, in which the supercritical Coulomb is balanced by the centrifugal force. The argument is rather involved and cannot be given here. Let me just say that the key is the derivation of the modified Coulomb law via ladder diagrams is possible, revealing that virtual gluons in this regime must fly with super-luminal velocity $v \approx \lambda^{1/4} \gg 1$. Therefore even for relativistically moving quasiparticles the interaction can be described by a potential. Solving the Klein-Gordon (or Dirac or Yang-Mills) equations for scalars (or spinors or gluons) in yields **towers of deeply bound states**, extending from large quasiparticle masses $m/T \approx \sqrt{(\lambda)}$ all the way to small ones $E/T \approx \lambda^0$ that are independent of the coupling constant. More specifically the spectrum is

$$E_{nl} = \pm m \left[1 + \left(\frac{C}{n + 1/2 + \sqrt{(l+1/2)^2 - C^2}} \right)^2 \right]^{-1/2} . \tag{7}$$

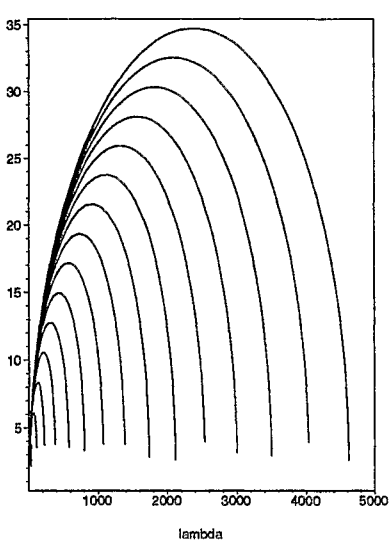

Figure 6: The spectrum of the states versus the 'tHooft coupling constant λ. for the levels with fixed $n_r = 0$ and the orbital momentum $l = 1..15$. One can see that there are light bound states at any coupling.

In weak coupling $C = g^2 N = \lambda$ is small and the bound states energies are close to $\pm m$. Specifically [11] $E_{nl} - m \approx -\frac{C^2 m}{2(n+l+1)^2}$, which is the known Balmer formulae. All of that, including the expression above, was known since 1930's.

New view on this formula, in the (opposite) strong coupling limit, gives the following. If the Coulomb law coefficient is large $C = (4\pi^2/\Gamma(1/4)^4)\sqrt{\lambda} \gg 1$, the quantized energies are imaginary *unless the square root gets balanced by a sufficiently large angular momentum.* In this regime, one may ignore the 1 in (7) and obtain the **equi-distant** spectrum of deeply bound states

$$E_{nl} \approx \frac{m}{C} \left[(n + 1/2) + \left((l+1/2)^2 - C^2 \right)^{1/2} \right] \tag{8}$$

Rather unexpectedly, we have also found that even though the trajectory of any particular Coulomb bound state depends critically on the coupling λ, their average density remains about λ-independent constant. This explains puzzling results obtained using the string theory. Although each level energy, and even its existence, depend on the coupling, the partition function is nearly independent of it.

[11] The fact that only the combination $n + l$ appears, i.e. principle quantum number, is a consequence of the known Coulomb degeneracy. This is no longer the case in the relativistic case.

5 Strongly coupled trapped atoms

If the previous section is too theoretical to some readers, here is a table-top experiment. Exciting recent development took place at the frontier of low temperature physics, with trapped Li^6 (fermionic) atoms. Using magnetic field one can use the so called Feshbach resonances and make a pair of atoms nearly degenerate with their bound state (usually called a molecule but actually a Cooper pair). This results in so large scattering length a, than a qualitatively new type of matter – *strongly coupled fermi and bose gases* – is observed. In particular, this very dilute systems start to behave hydrodynamically, displaying elliptic flow very similar to that in non-central heavy ion collisions.

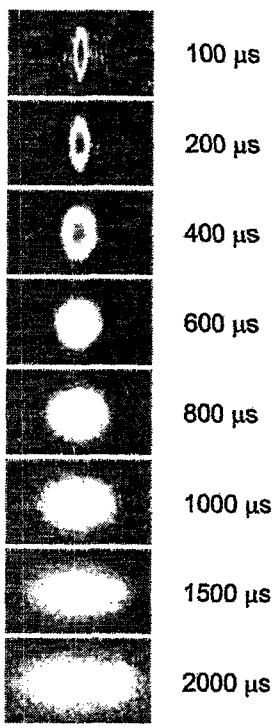

Figure 7: Hydrodynamical expansion of trapped Li^6, from [22].

More generally, studies of strongly coupled many-body problems, in which the binary scattering length diverges, is being studied in at least two other settings: (i) a dilute gas of neutrons, with the famous virtual level; (ii) trapped atomic Li atoms in which the scattering length can be tuned till practically infinite values, plus or minus, by applying a magnetic field which shifts the Feshbach resonances.

Remarkably, for its fermionic version it was indeed found very recently that a strong coupling leads to a hydrodynamical behavior [22]. The way it was demonstrated is precisely the same "elliptic flow" as discussed above. One can start with a deformed trap. Normally the gas is so dilute $an^{1/3} \ll 1$ that atoms just fly away isotropically, but when tuning to strong coupling regime is done the expansion is anisotropic and can be described hydrodynamically.

A number of other spectacular experimental discoveries with trapped Li^6 were also made later. It was found [23] that an adiabatic crossing through the resonance converts nearly all atoms into very loosely bound (but remarkably stable) "Cooper pairs", which can also Bose-condense [24] if the temperature is low enough. Since in heavy ion collisions the system also crosses the zero binding lines adiabatically, various bound pairs of quarks and gluons should also be generated this way. That is probably why we do not observe large fluctuations predicted for systems crossing the QGP-hadronic matter boundary.

6 New picture of QGP, with multiple bound states

The viscosity argument made above is only one of three arguments for sQGP. Two others are (i) the idea that smaller overall scale leads to a coupling which runs more and becomes stronger [27], and (ii) bound states seen on the lattice. We suddenly realized that we were in the position similar to trying to understand properties of the ordinary matter ignoring existence of atoms.

Naively, the deconfinement was expected to guarantee that no hadronic bound states would survive at $T > T_c$, except perhaps $\bar{b}b$ states bound by color Coulomb forces. The earliest suggested QGP signal was a disappearance of familiar hadronic peaks – ρ, ω, ϕ mesons – in the dilepton spectra [1]. Moreover, even small-size deeply-bound $\bar{c}c$ states, $\eta_c, J/\psi$, were expected to melt at $T \approx T_c$ [25, 26]. However, as we already mentioned in the Introduction, there are indications from the lattice that charmonium and light quarks do create meson-like states at $T > T_c$.

In the first paper by Zahed and myself on the issue[27] we related presence of loosely bound pairs

channel	rep.	charge factor	no. of states
gg	1	9/4	9_s
gg	8	9/8	$9_s * 16$
$qg + \bar{q}g$	3	9/8	$3_c * 6_s * 2 * N_f$
$qg + \bar{q}g$	6	3/8	$6_c * 6_s * 2 * N_f$
$\bar{q}q$	1	1	$4_s * N_f^2$
$qq + \bar{q}\bar{q}$	3	1/2	$4_s * 3_c * 2 * N_f^2$

Table 1: Binary attractive channels discussed in this work, the subscripts s,c,f mean spin,color and flavor, $N_f = 3$ is the number of relevant flavors.

of quasiparticles with large rescattering and hydro regime of QGP[12]. Indeed, the scattering lengths are supposed to diverge at the *zero binding lines* on the phase diagram (see Fig.8(a)), introduced in [27]. Those line are separate sQGP from wQGP, in which there are no bound states.

In our paper [29] we investigate the relationship between four (previously disconnected) lattice results: **i.** spectral densities from MEM analysis of correlators; **ii.** static quark free energies $F(R)$; **iii.** quasiparticle masses; **iv.** bulk thermodynamics $p(T)$. We found high degree of consistency among them not known before. The potentials $V(R)$ derived from $F(R)$ lead to large number of binary bound states, mostly colored, in gq, qq, gg, on top of the usual $\bar{q}q$ mesons. Using the Klein-Gordon equation and **(ii-iii)** we evaluate their binding energies and locate the zero binding endpoints on the phase diagram, which happen to agree with (**i**). We then estimate the contribution of all states to the bulk thermodynamics in agreement with (**iv**).

The bound states of $\bar{q}q$ can only be colorless mesons (the octet channel is repulsive), but in QGP there can be *colored* bound states. Quite famous are quark Cooper pairs qq which drive the color superconductivity at sufficiently high density and low T: but pairs themselves should exist outside this region as well. Gluons can form a number of states with attraction, and there can also be gq hybrids. A generic reason why we think all of them exist is that at T close to T_c all quasiparticles are very heavy.

Using a singlet $\bar{q}q$ as a standard benchmark (the only one studied so far on the lattice), one can summarize the list of all attractive channels in the following small Table1, indicating the relative strength of the Coulomb potential and also a number of states. One can see, there are many hundreds of attractive channels which can support bound states.

In another paper, by Brown et al [28], the fate of the $\bar{q}q$ bound states is traced to $T \approx T_c$, where the Nambu-Goldstone and Wigner-Weyl modes meet. The pion binding at total zero mass is very difficult to reach from the sQGP side, and it can only be accomplished by the combination of (i) the color Coulomb interaction, (ii) the relativistic effects, and (iii) the interaction induced by the instanton-anti-instanton molecules. The spin-spin forces turned out to be small. While near T_{zb} all mesons are large-size nonrelativistic objects bound by Coulomb attraction, near T_c they get much more tightly bound, with many-body collective interactions becoming important and making the σ and π masses approach zero (in the chiral limit). The wave function at the origin grows strongly with binding, and the near-local four-Fermi interactions induced by the instanton molecules play an increasingly more important role as the temperature moves downward toward T_c.

With all of it included, Zahed and myself [29] had evaluated the contribution of all these binary bound states into the partition function. The results for masses of the bound states are shown in Fig.9(a), and the resulting pressure in Fig.9(b). We have shown that as the level closes toward its endpoint, its contribution to pressure becomes partially compensated by a repulsive effective interaction between the unbound quasiparticles. The contribution of the virtual level above zero quickly disappear. Assembling

[12]We suggested this mechanism for large rescattering before we learned about Feshbach resonances for atoms, which proves that this mechanism works.

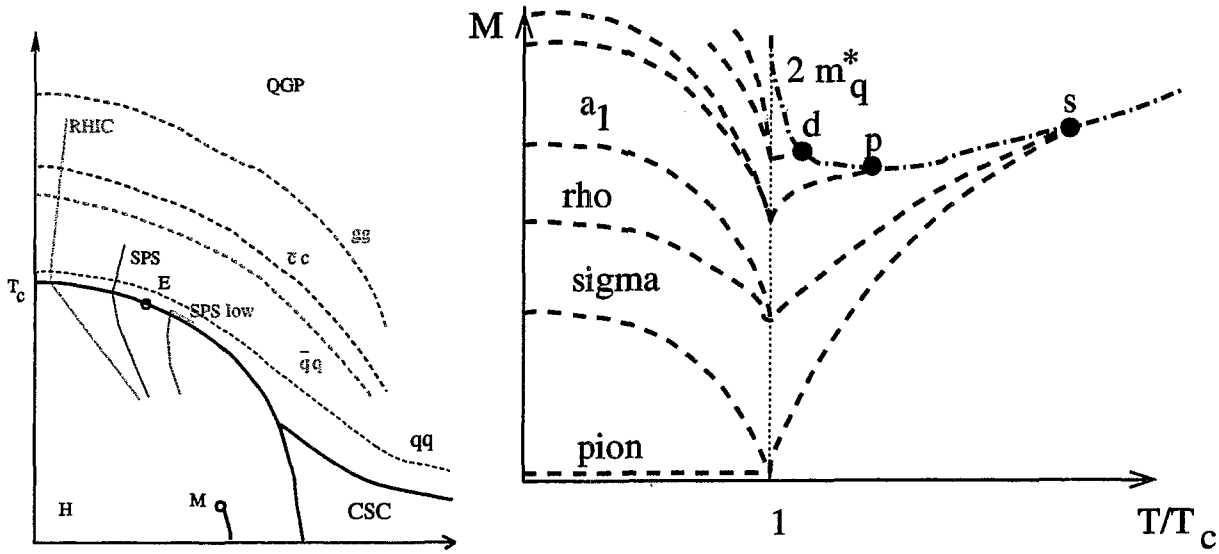

Figure 8: Schematic position of several zero binding lines on the QCD phase diagram (a) and of specific hadronic masses on temperature T (b). In the latter the dash-dotted line shows twice the (chiral) effective mass of a quark. Black dots marked s, p, d correspond to the points where the binding vanishes for states with orbital momentum $l = 0, 1, 2....$

all these ingredients together, we have found that all pieces fit together nicely, reproducing total pressure as calculated on the lattice. Hundreds of exotic bound states are tamed by small Boltzmann factors, contributing (at RHIC) up to about a half of the pressure.

How one can observe these states experimentally? One rather direct way is provided by dileptons, which directly tells us about $\bar{q}q$ relative placements in the vector channels. If there are bound states for ρ, ω, ϕ at $T > T_c$ one may hope to see some enhancement above the free-quasiparticle rate, in 1-2 GeV mass region. Even if there are no bound states, at high enough T, there is still some effect of the attractive potential visible in the dilepton rates.

Quite recently we have noticed [30] one more important role that binary bound states may play in sQGP: "ionization" of them by passing jets can contribute to jet quenching. Indeed, in QED we know it to be dominant at not-too-large gamma factors $\gamma = 1 - 100$. One motivation is that at SPS the density is not that much different from RHIC, and yet there is no jet quenching. One obvious difference with radiative mechanism is that the lost energy is *not* to be found in the forward cone.

7 Brief summary and outlook

There is no question that with the RHIC project we got very lucky: we have not found exactly what we expect, but got instead much more. RHIC experiments have shown that the QGP at $T = (1-2)T_C$ is not a weakly interacting gas of quasiparticles, being instead a *strongly coupled QGP*.

Not only the expected energy density is reached, as planned well above the critical region, but we have indeed created a *well-equilibrated matter*, behaving as it should in a bulk. Surprisingly, this is true not only for most central collisions, but also for relatively peripheral ones (but not most peripheral, of course). That means that few hundred of particles is already enough, even for very specific hydrodynamical effects like elliptic flow. This is truly surprising: it would not work for a small drop containing only few hundreds of water molecules!

What exactly sQGP is we start to understand only now. A lot of experience with two other strongly coupled systems was emphasized in this summary: those are (i) ultra-cold trapped cold atoms in a large scattering length regime; and (ii) the N =4 supersymmetric Yang-Mills theory, or CFT. Both show that

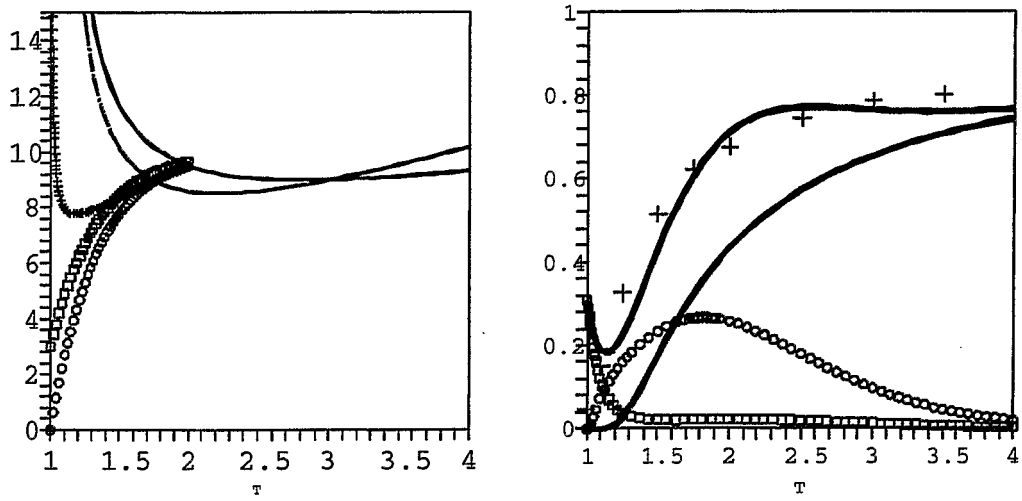

Figure 9: (a) The lines show twice the effective masses for quarks and gluons versus temperature T/T_c. Note that for $T < 3T_c$ $M_q > M_g$. Circles and squares indicate estimated masses of the pion-like and rho-like $\bar{q}q$ bound states, while the crosses stand for all colored states. (b) Pressure (in units of that for a gas of massless and noninteracting quasiparticles) versus the temperature T/T_c. The crosses correspond to the $N_f = 2$ lattice results, from Fig.1(a). The lower solid curve is the contribution of unbound quasiparticles, the upper includes also that of all bound states. Squares are for the pion-like and rho-like $\bar{q}q$ bound states combined, and circles for all the colored bound states.

strong coupling does indeed lead to a hydrodynamical behavior and small viscosity. Both teach us a lesson, that small deviation of EoS from ideal gas does not really mean the matter is weakly interacting. Both show that resonances between bound and unbound states seem to play a key role in hydro flow.

The next notable theoretical achievement is that quantitative predictions of lattice QCD, on T_c value, the magnitude of the "latent heat" and also overall EoS were justified by data. Together with hydrodynamics (and details like knowledge of the initial shape of the overlap region and final freezeout conditions) it provided essentially parameter free theory, which was exactly on the mark as far as all flows (spectra) are concerned. (I think the remaining discrepancies with HBT radii will be worked out.)

There are plenty of other open questions and even known experimental puzzles. Is charm floating with all other flavors, or not? What happens with charmonium, is it enhanced or depleted? Why are there so many baryons at $p_t = 2-5\,GeV$? Why the ellipticity is so large even at very large $p_t \sim 10GeV$? Can we see some of the bound states in sQGP in a dilepton signal? What role the bound state play in jet quenching?

And a super-question is: which part of what we have learned at RHIC would still be applicable at LHC? Will it still be a bang, or not? Stay tuned...

References

[1] E. V. Shuryak, *Phys.Lett.* **B78** (1978) 150, (full version *Yadernaya Fizika* **28** (1978) 796), *Phys.Rep.* **61** (1980) 71.

[2] J. C. Collins and M J Perry, Phys. Rev Lett. 34(1975)1336

[3] E. V. Shuryak, Zh.E.T.F **74** (1978) 408, (Sov. Phys. JETP **47** (1978) 212),

[4] D. A. Appel, Phys. Rev. D **33**, 717 (1986). J. P. Blaizot and L. D. McLerran, Phys. Rev. D **34**, 2739 (1986). M. Gyulassy and M. Plumer, Phys. Lett. B **243**, 432 (1990). X. N. Wang, M. Gyulassy and M. Plumer, Phys. Rev. D **51**, 3436 (1995) [hep-ph/9408344].

[5] E.V.Shuryak, The QCD vacuum, hadrons and superdense matter. WSPC. 1st edition 1987, 2nd edition 2004.

[6] K. Kajantie, M. Laine, K. Rummukainen and Y. Schroder, Phys. Rev. D **67**, 105008 (2003) [arXiv:hep-ph/0211321].

[7] D. Molnar and M. Gyulassy, Nucl. Phys. **A697** (2002) 495; [Erratum-ibid. **A703** (2002) 893]

[8] S. Datta, F. Karsch, P. Petreczky and I. Wetzorke, hep-lat/0208012. M. Asakawa and T. Hatsuda, Nucl. Phys. **A715** (2003) 863c; hep-lat/0308034;

[9] F. Karsch et al Nucl. Phys. **B715** (2003) 701.

[10] E. V. Shuryak and 0. V. Zhirov, *Phys.Lett.* B89 (1979) 253

[11] P. J. Siemens and J. 0. Rasmussen, Phys. Rev Lett. 42(1979)880

[12] P. F. Kolb and R. Rapp, Phys. Rev. C **67**, 044903 (2003) [arXiv:hep-ph/0210222].

[13] D. Teaney, J. Lauret and E.V. Shuryak, Phys. Rev. Lett. **86** (2001) 4783, more details in nucl-th/0110037. P.F. Kolb, P.Huovinen, U. Heinz, H. Heiselberg, Phys. Lett. **B500** (2001) 232.

[14] P. F. Kolb and U. Heinz, arXiv:nucl-th/0305084.

[15] E.V. Shuryak, Nucl.Phys.A717:291-321,2003

[16] D.Teaney nucl-th/0301099

[17] J.M. Maldacena, Adv.Theor.Math.Phys.2:231-252,1998,hep-th/9711200.

[18] G.T. Horowitz and A. Strominger, Nucl. Phys. **B360** (1991) 197. S.S.Gubser, I.R.Klebanov and A.A. Tseytlin, Nucl. Phys. **B534** (1998) 202

[19] G. Policastro, D. T. Son and A. O. Starinets, Phys. Rev. Lett. **87** (2001) 081601.

[20] S.-J. Rey, S.Theisen and J.-T. Yee,Nucl.Phys.B527:171-186,1998, hep-th/9803135

[21] E.V. Shuryak and I. Zahed, Phys. Rev. D **69**, 014011 (2004), hep-th/0307103.

[22] K.M.O'Hara et al, Science 298,2179, 2002; T.Bourdel et al, Phys.Rev.Lett.91 (2003) 020402.

[23] J.Cubizolles et al, cond-mat/0308018, K.Strecker et al,cond-mat/0308318

[24] M.W. Zwierlein et al, cond-mat/0311617

[25] T. Matsui and H. Satz, Phys. Lett. **B178** (1986) 416.

[26] F. Karsch, M. T. Mehr and H. Satz, Z. Phys. **C37** (1988) 617.

[27] E. V. Shuryak and I. Zahed, arXiv:hep-ph/0307267. Submitted to PRL

[28] G. E. Brown, C. H. Lee, M. Rho and E. Shuryak, "The anti-q q bound states and instanton molecules at t approx. ¿= T(C)," arXiv:hep-ph/0312175.

[29] E. V. Shuryak and I. Zahed,Toward the Theory of Binary Bound States in Quark-Gluon Plasma, hep-ph/0403127, submitted to PRD.

[30] G. E. Brown, E. V. Shuryak and I. Zahed,Jet Quenching due to Ionization of Binary Bound States in Quark-Gluon Plasma, in progress,

Hadronic Signals of Deconfinement at RHIC

Berndt Müller

Hadronic Signals of Deconfinement at RHIC

Berndt Müller
Department of Physics, Duke University, Durham, NC 27708-0305, USA

This article reviews (soft) hadronic signals of deconfinement and chiral symmetry restoration in hot QCD matter in the light of the results from the first three years of the experimental program at the Relativistic Heavy Ion Collider.

I. INTRODUCTION

Quantum mechanics dictates that even "empty" space is not empty, but rather filled with quantum fluctuations of all possible kinds. In many contexts, such as in atomic physics, these vacuum fluctuations are subtle effects which can only be observed by precision experiments. In other situations, especially when interactions of sufficient strength are involved, the vacuum fluctuations can be of substantial magnitude and even "condense" into a nonvanishing expectation value of some quantum field. These vacuum condensates can act as a medium [1], which influences the properties of particles propagating through it.

An important example of such a vacuum condensate is the Higgs vacuum, which is introduced in the Standard Model of particle physics to generate the masses of quarks, leptons, and the gauge bosons of the weak interaction. The vacuum expectation value of the Higgs field, $\langle\phi\rangle = 246$ GeV, is uniquely determined in the Standard Model; the quark and lepton masses differ from one another only due to the different strength of the coupling of each fermion to the Higgs field. The quark masses receive additional contributions from the quark and gluon condensates in the QCD vacuum, which have been measured to be:

$$\langle\bar{q}q\rangle = (235\text{MeV})^3,$$
$$\langle g^2 G_{\mu\nu}G^{\mu\nu}\rangle = (840\text{MeV})^4. \qquad (1)$$

In fact, the contribution of the QCD vacuum condensates to the masses for the three light quark flavours u, d, s considerably exceed the mass believed to be generated by the Higgs field see Fig. 1).

If the vacuum acts as a medium and influences the properties of fundamental particles and their interactions, its properties can conceivably change. This idea has important implications in cosmology (inflation [2]) and in modern versions of the anthropic cosmological principle [3, 4], which invoke the concept of multiple universes with different phenomenological properties due to the realization of different vacuum states. The most promising candidate for the fundamental theory of spacetime, superstring theory, promises to sustain an almost unlimited number of vacuum states [5], lending some credence to this concept. These theoretical speculations call for an experimental verification of the existence of multiple vacuum states and the possibility of transitions among them under the influence of external constraints.

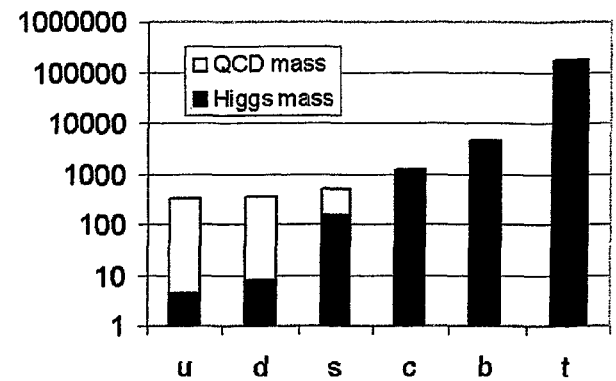

FIG. 1: Masses of the six quark flavors. The masses generated by electroweak symmetry breaking (current quark masses) are shown in dark blue; the additional masses of the light quark flavors generated by spontaneous chiral symmetry breaking in QCD (constituent quark masses) are shown in light yellow. Note the logarithmic mass scale.

Because of the energy scales involved, only the QCD vacuum is amenable to modification at energies accessible with present technologies. The Relativistic Heavy Ion Collider (RHIC) was built to explore these questions by creating conditions in the laboratory under which the structure of the QCD vacuum would change and the properties of particles and forces of the strong interactions would be modified. The beam energy of RHIC was chosen to be high enough to generate temperatures commensurate with the energy scale of the QCD vacuum condensates and thus to affect the structure of the QCD vacuum.

Numerical simulations of lattice QCD predict that a dramatic change in the QCD vacuum state occurs around the critical temperature $T_c \approx 160$ MeV, where the quark and gluon condensates melt, and the vacuum takes on a simpler structure. The part of the light quark masses that is induced by the quark condensate disappears above T_c and only the much smaller masses generated by the electroweak Higgs field remain. The degrees of freedom corresponding to independently propagating gluons, which are frozen in the normal QCD vacuum, are also liberated above T_c. This pattern is visible in Fig. 2, which shows the dramatic jump in the scaled energy density $\epsilon(T)/T^4$ at the critical temperature.

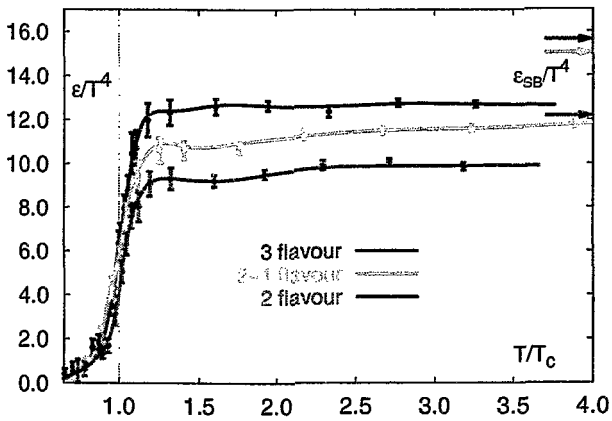

FIG. 2: Scaled energy density ϵ/T^4 for thermal lattice-QCD with two and three light quark flavors and for two light and one heavier flavor (from Karsch [47]).

II. HADRONIC PROBES OF DECONFINEMENT

Which observables allow us to confirm that the predicted transformation of the QCD vacuum actually occurs? Here we focus on signals involving light (u, d, s) quarks, the primary constituents of the medium. This restriction is not intended to minimize the importance of other observables, such as hard probes, covered in different contributions to this volume [7]. In fact, the strong quenching of the emission of hadrons at large transverse momenta and the existence of a strong (anisotropic) collective flow are important prerequisites for the apparent dominance of quark recombination at momenta of a few GeV/c, which will be discussed below.

Two effects caused by the disappearance of the vacuum condensates stand out: The melting of the quark condensate lowers the effective mass of the s-quark from about 500 MeV to less than 150 MeV, making it easy to create s-quark pairs in copious quantities [8–10]. The dissolution of the gluon condensate and the concomitant screening of the long-range color force by thermal gluons allows light quarks to propagate outside of hadronic bound states. As the hot quark-gluon plasma (QGP) cools, hadrons should form by recombinant emission of quark-antiquark pairs (mesons) or color-singlet triplets of quarks (baryons) from the surface of the hot medium [11], preserving the collective flow pattern of their partonic constituents [12].

A. Flavor equilibration

Let us consider these arguments more quantitatively. The expectation that the formation of a deconfined quark-gluon plasma results in a substantial enhancement of the production of hadrons carrying strangeness is based on a comparison of energy thresholds and rates. In a hadronic environment, the energy required to excite strangeness is about 700 MeV, as in the reaction $\pi\pi \to K\bar{K}$, or about $4T_c$. In the QGP, the threshold for the dominant reaction $gg \to s\bar{s}$ is about 300 MeV, less than $2T_c$. Hadronic reactions producing multiply strange hadrons, such as the Ξ and Ω hyperons, are thus predicted to be slow under thermal equilibrium conditions and not leading to hadrochemical equilibrium within the time available in a heavy-ion reaction [13]. On the other hand, flavor equilibrium among u, d, s quarks is predicted to develop within a QGP on the available time scales [8]. Hadrons containing any number of strange quarks should, therefore, be produced in equilibrium abundances when a QGP is formed.

The prediction of a strong enhancement of the production of multi-strange baryons and antibaryons is independent of the details of the hadronization model, although the quantitative predictions for individual hadron yields may differ slightly [10, 14–17]. Extensive studies of final state effects on the chemical composition of the emitted hadrons have concluded that the abundances of multi-strange baryons are only slightly affected by inelastic rescattering [18]. The consistency of this scenario was confirmed recently once more in a systematic study of baryon pair production based on model independent rate equations, which showed that a strong enhancement of multi-strange baryon production requires the assumption of flavor equilibrium already at the start of the hadronic phase evolution [19, 20].

It is important to distinguish the chemical equilibrium distribution attained in a deconfined plasma phase from the statistical distribution of hadrons produced in e^+e^- or p+p reactions[21–23]. In those reactions, the production of hadrons carrying strange quarks is systematically suppressed. Although this phenomenon can be explained as an effect of flavor conservation in a small volume of hadronic size, it is precisely the *disappearance* of this suppression in heavy-ion collisions, corresponding to the transition from a canonical ensemble to a macrocanonical one, which is the signature of the creation of locally deconfined QCD matter.

The observation of a strong enhancement of multi-strange baryon and antibaryon emission in Pb+Pb collisions by experiment WA97 [24] formed an important pillar of the claim that evidence for a new state of matter had been found at the CERN-SPS [25]. The results were confirmed and extended to lower beam energies in recent years by the NA57 collaboration [26]. The conclusion that a deconfined phase is formed under the conditions created by Pb+Pb collisions at CERN-SPS energies is also supported by a recent comprehensive analysis of the data for several relevant observables in the framework of a schematic, but realistic model of the space-time evolution of the collisions [27].

As impressive as these results are, the evidence remains indirect and relies on the argument that a hadrochemical equilibrium cannot be established by interactions among

hadrons with confined quarks. The higher beam energies available at RHIC have made it possible to explore regions of phase space where the formation of hadrons from recombining quarks can be directly observed and the partonic origin of their collective flow pattern can be established. It is important to recognize that, in contrast to the strangeness enhancement itself, these phenomena were not quantitatively predicted before the observations were made. However, I will argue that the theoretical arguments, even if they were developed under the motivation of the first experimental results from RHIC, are sufficiently robust to provide compelling evidence for the formation of a deconfined quark phase, as more complete and statistically precise data are becoming available.

B. Quark recombination

Let us begin with a discussion of quark recombination (see Fig. 3a). The statistical coalescence of two or more particles to form a bound state is a widely used concept, which remains somewhat murky in many cases for two reasons. First, the formation of a bound state requires that either at least one of the two particles is off-shell or that another particle carries away the surplus energy. Second, the implicit reduction in the number of degrees of freedom during coalescence tends to conflict with the second law of thermodynamics, which dictates that the entropy cannot decrease. Fortunately, there are regions of phase space – hadrons emitted with highly epithermal momenta – where these concerns do not constitute serious obstacles. Hadrons emitted with a high momentum make an almost instantaneous transition from the dense medium into the surrounding vacuum. Another way to state this is to say that – observed from the fast moving hadron – the radiating surface appears highly Lorentz contracted and thus thin on a hadronic length scale. Energy conservation is therefore not an important constraint on the recombination process. Moreover, at high transverse momentum, the masses of quarks and hadrons can be neglected in first approximation with corrections of order $\mathcal{O}(m^2/p_T^2) \ll 1$. And finally, fast hadrons constitute only a very small fraction of all emitted particles, thus limiting possible violations of the second law of thermodynamics.

Denoting the quark phase-space distribution by $w_\alpha(p)$ (here α denotes color, flavor, and spin degrees of freedom) and employing light-cone coordinates along the direction of the emitted hadron, instantaneous recombination predicts the following meson and baryon spectra, respectively [28]:

$$E\frac{dN_M}{d^3P} = \int d\Sigma \frac{P\cdot u}{(2\pi)^3} \sum_{\alpha\beta} \int dx\, w_\alpha(xP^+)\bar{w}_\beta((1-x)P^+)|\phi^{(M)}_{\alpha\beta}(x)|^2, \tag{2}$$

$$E\frac{dN_B}{d^3P} = \int d\Sigma \frac{P\cdot u}{(2\pi)^3} \sum_{\alpha\beta\gamma} \int dx\, dx'\, w_\alpha(xP^+)w_\beta(x'P^+)w_\gamma((1-x-x')P^+)|\phi^{(B)}_{\alpha\beta\gamma}(x,x')|^2. \tag{3}$$

Here Σ stands for the freeze-out hypersurface, u^μ for the collective flow velocity of the partonic matter, and capital letters P denote hadron coordinates. For a thermal parton distribution, $w(p) = \exp(p\cdot u/T)$, the partonic factors in both equations combine to a single thermal distribution for the hadron, $w(P^+)$. In this case the integrations over the momentum fractions x, x' become trivial, and the end result is independent of the details of the hadron wavefunction ϕ. The prediction is that hadrons are emitted in thermal and chemical equilibrium abundances and acquire the collective radial flow velocity of the quarks. In fact, one can argue that the recombination mechanism provides the justification for applying the statistical model to describe ratios of hadron yields at up to momenta of several GeV/c.

In the absence of a thermal medium, energetic hadrons are created by the fragmentation of a fast quark or gluons (see Fig. 3b). This mechanism predicts a hadron spectrum of the form

$$E\frac{dN_h}{d^3P} = \int d\Sigma \frac{P\cdot u}{(2\pi)^3} \sum_{\alpha} \int dz\, z^{-3}\, w_\alpha(P^+/z) D_{\alpha\to h}(z), \tag{4}$$

where $z < 1$ denotes the momentum fraction carried by the hadron. It is easily shown that for large values of the momentum P^+ recombination always wins over fragmentation in the case of an exponentially falling momentum distribution, because $w(P^+/z)$ falls off faster than $w(P^+)$. On the other hand, fragmentation asymptotically dominates over recombination, when the parton distribution obeys a power law as it is always the case in QCD at sufficiently large momentum. In relativistic heavy ion collisions the power law tail is suppressed (in central Au+Au collisions at RHIC by about a factor 5) due to the energy loss of fast partons dur-

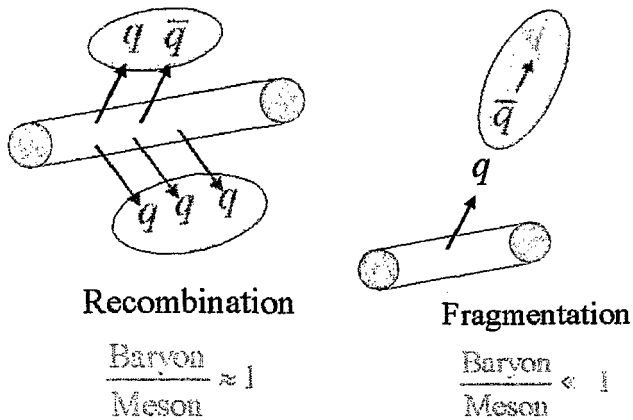

FIG. 3: (a) Left panel: Mesons and baryons formation by recombination of quarks and/or antiquarks from a thermal, deconfined medium predicts a baryon/meson ratio of order unity. (b) Right panel: Hadron production by fragmentation of an energetic parton favors meson over baryon production.

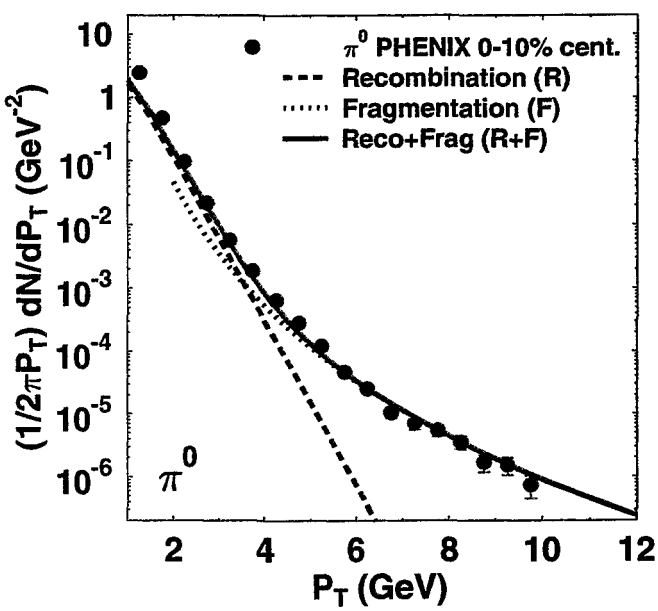

FIG. 4: Spectrum of pions emitted in central Au+Au collisions at RHIC for $\sqrt{s_{NN}} = 200$ GeV. The contributions from recombination and fragmentation are shown separately, together with the data from the PHENIX collaboration (from [28]).

ing their passage through the hot, dense matter. This mechanism delays the dominance of fragmentation over recombination to rather large transverse momenta, about 4 GeV/c for mesons and 6 GeV/c for baryons. This is illustrated in Fig. 4, which shows the two contributions to the pion spectrum in central Au+Au collisions at RHIC separately, together with the PHENIX data.

C. Collective flow of quarks

When the radial flow velocity of the QGP exhibits an azimuthal anisotropy, as in noncentral collisions of two nuclei, this anisotropy becomes imprinted on the hadrons formed by quark recombination. If the quark flow anisotropy has the form $[1+v_2(p)\cos 2\varphi_p]$, where φ_p is the emission angle with respect to the collision plane and $v_2(p)$ the so-called elliptic flow velocity, the elliptic flow parameter for a meson or baryon is (in the usual case where $v_2 \ll 1$):

$$\begin{aligned} v_2^{(M)}(P) &= v_2(xP) + v_2((1-x)P), \\ v_2^{(B)}(P) &= v_2(xP) + v_2(x'P) + v_2((1-x-x')P). \end{aligned} \tag{5}$$

In the limiting case of equal momentum fractions carried by the constituent quarks these relations simplify to [12, 28, 29]

$$\begin{aligned} v_2^{(M)}(P) &\approx 2v_2(P/2), \\ v_2^{(B)}(P) &\approx 3v_2(P/3). \end{aligned} \tag{6}$$

In the hydrodynamic regime, where the flow anisotropy grows roughly linearly with the momentum, $v_2(p) = \alpha p$, the scaling factors cancel, and mesons and baryons exhibit an equal v_2 at the same momentum. At large transverse momentum, however, where the anisotropy is limited by transparency effects, this is no longer the case, and a collective anisotropic flow carried by quarks can be distinguished from one carried by a hadronic fluid. Final state effects on the elliptic flow in the hadronic phase have been shown to be small [30].

D. Unified descriptions

These considerations based on general principles can be extended in several ways to cover a wider range of hadron momenta [31]. By choosing the medium rest frame instead of the light-cone frame of the emitted hadron, one can obtain a more traditional coalescence model description of the hadron spectrum down to $p_T = 0$ [32]. The price one pays for this extended coverage is the need to make specific assumptions about the internal wavefunction of the emitted hadrons, which are by necessity simplistic. A virtue of this approach is that one can incorporate final-state decays of unstable hadrons, such as the ρ-meson, which help to resolve the entropy problem and improve the description of pion spectra, especially at small momenta [33]. Effects due to hadron masses can also be treated more consistently in such models.

Another extension concerns the treatment of fragmentation processes. In the presence of a medium, a fast parton may form a hadron by picking up one or more constituents from the medium. This process has been called fast-slow recombination [32]. Depending on the

hadron wavefunction, it may contribute to hadron emission up to quite large transverse momenta extending into the $6-8$ GeV/c range. Alternatively, one can consider the process of hadron formation via fragmentation also as a recombination process acting on a primary distribution of fragmented shower partons [34, 35]. This approach gives a microscopic description of the fragmentation functions $D_{\alpha\to h}(z)$, allowing one to extend the calculation consistently, albeit model dependently, to hadron production by recombination involving partons from a thermal medium [36]. This model predicts a large baryon-to-meson ratio in the p_T-range of $3-8$ GeV/c, where the mixed recombination of thermal and shower partons dominates. This approach is also aplicable to hadron production in p+p and d+Au collisions, where it provides an explanation for the differences in the Cronin effect observed for mesons and baryons [37].

E. Principal signatures

These considerations suggest several critical signatures of the formation of a thermal quark-gluon plasma accompanied by a structural change in the QCD vacuum:

- Hadrons containing any number of strange quarks should be produced in near equilibrium abundances;
- Hadrons created by recombination of moderately energetic quarks should form the dominant mode of hadron emission at low and intermediate momenta;
- Baryons should be produced as abundantly as mesons at intermediate transverse momenta;
- The collective flow patterns of the emitted hadrons should reflect the collective flow of their constituent quarks.

As we will discuss in the next section, these characteristic phenomena have been observed in Au+Au collisions at RHIC.

III. RESULTS FROM RHIC

Fig. 5 shows that hadrons containing any number of s-quarks are produced according to the expectation that a chemically equilibrated quark-gluon plasma converts into hadrons maintaining flavor equilibrium near the critical temperature. The value deduced from the data ($T_{\rm ch}$ = 177 MeV [38]) is equal to T_c within the present theoretical uncertainties. There exist significant deviations from the predicted equilibrium abundances for some short-lived hadronic resonances, such as the $\Delta(1232)$, K^*, and the $\Lambda(1520)$. These deviations can be qualitatively understood as final state effects due to medium modifications of the resonance spectral function or absorption and regeneration effects [39].

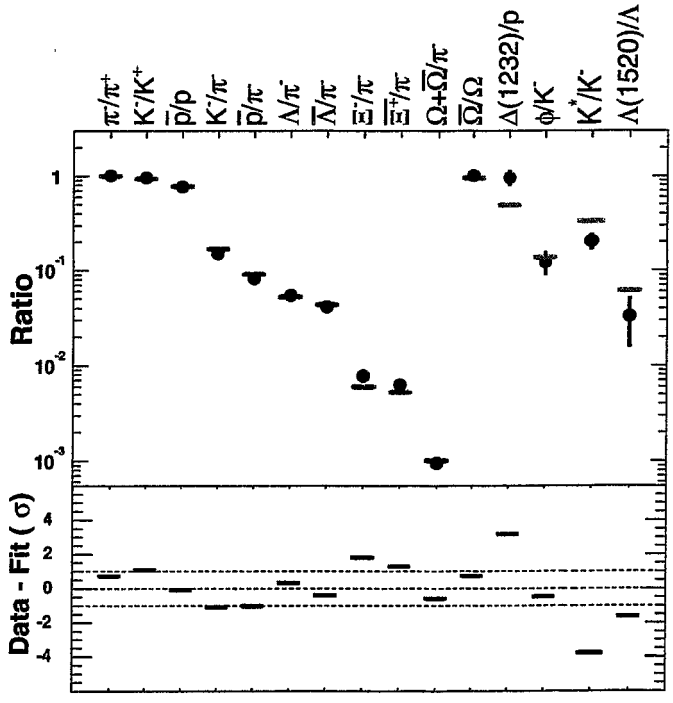

FIG. 5: Comparison of the ratios of observed yields of various hadrons at midrapidity in Au+Au collisions at RHIC with the ratios predicted in a thermal and chemical equilibrium model (from STAR).

The apparent lack of a nuclear suppression of protons [40] and Λ-hyperons [41] in Au+Au collisions in the transverse momentum range $2-4$ GeV/c, where pions are already suppressed by a factor $4-5$, came as a surprise. The measurements have been extended to other identified mesons and baryons, including the ϕ and the Ξ (see Fig. 6), confirming the baryon-meson dichotomy which is a generic feature of the recombination mechanism. The observed onset of nuclear suppression for the baryons between 4 and 6 GeV/c is in excellent agreement with the predictions by the Duke and Texas A&M models (see Fig. 7) and reflects the transition from a recombination dominated to a fragmentation dominated hadronization regime. The fall-off of the baryon/meson ratio at small p_T (see Fig. 7a) is due to mass effects.

Measurements of the flow patterns of the emitted hadrons provide essential additional evidence for the hypothesis that they are created directly from a phase of unconfined quarks and antiquarks. The experiment makes use of the fact that the region of heated vacuum in semiperipheral collisions between two nuclei is almond-shaped and thus sustains anisotropic pressure gradients. In the hydrodynamic limit this leads to an anisotropic expansion pattern called "elliptic flow" [44], which is characterized by the parameter v_2. As already mentioned, the flow anisotropy is an increasing function of the momentum of the emitted particle in the hydrodynamic regime and saturates when transparency effects set in at large transverse momenta.

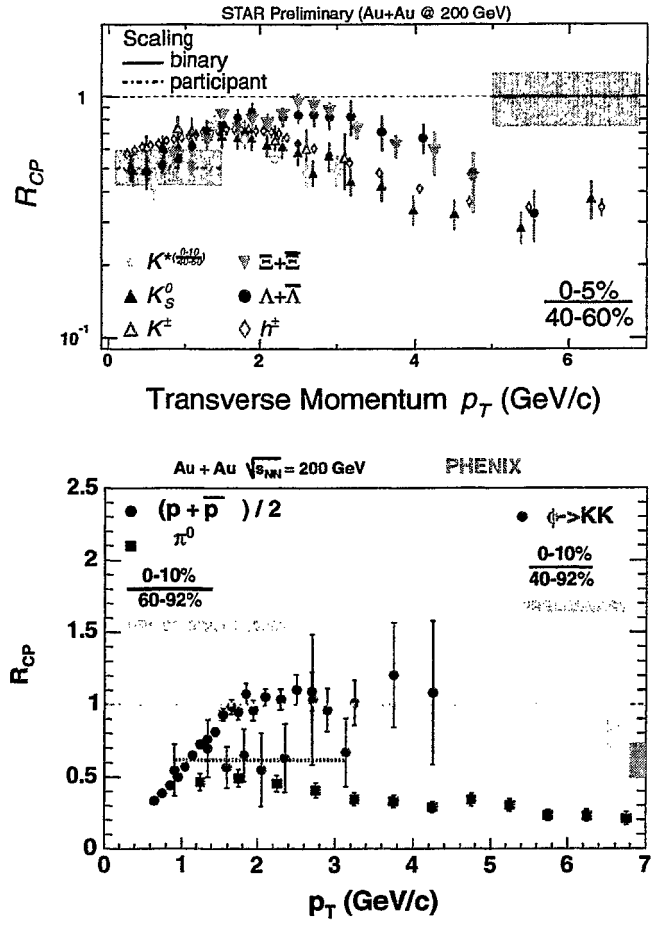

FIG. 6: Nuclear suppression observed in central (compared with peripheral) Au+Au collisions for various hadrons. (a) Upper panel: STAR [42]; (b) lower panel: PHENIX [43].

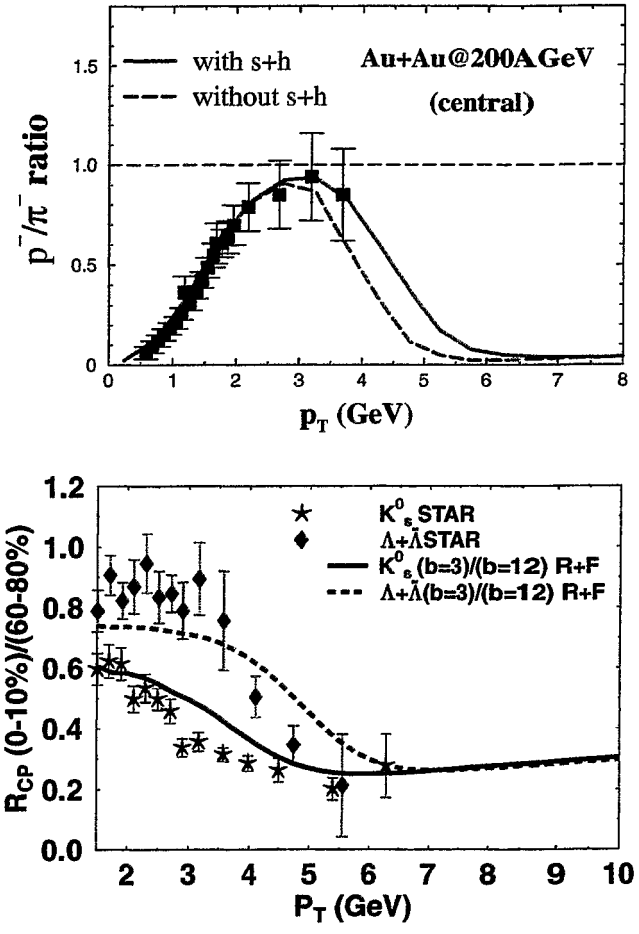

FIG. 7: Baryon enhancement as function of transverse momentum predicted by two different recombination models, in comparison with RHIC data. (a) Upper panel: Texas A&M model for p/π. (b) Lower panel: Nuclear suppression of Λ-hyperons and kaons in the Duke model.

The RHIC experiments have confirmed this expected behavior, but found that it varies sustantially from one hadron species to another (see Fig. 8a). However, when the constituent rescaling (6) is applied to these data, the flow patterns are found to collapse onto a common line (see Fig. 8b), suggesting that one observes the flow pattern of individual quarks, which coalesce into hadrons only at the end of the expansion [45]. The onset of saturation at a quark momentum $p_T \approx 1$ GeV/c is consistent with the transition between recombination and fragmentation observed in the baryon/meson ratios. The different behavior of mesons and baryons is characteristic of the quark recombination mechanism and reproduced in all model calculations [32, 46] (see Fig. 9).

IV. SUMMARY AND OUTLOOK

Experiments with relativistic heavy ions are allowing us, for the first time, to verify that a vacuum state can be modified under extreme conditions, causing dramatic changes in the properties of fundamental particles (quarks) and the strong forces among them. Hadrons emerging by recombination of the constituents of the hot QCD medium provide evidence for its flavor chemical equilibration and the deconfinement of (constituent) quarks. While flavor equilibration was already observed in experiments at the CERN-SPS, the characteristic momentum dependence of the baryon/meson ratios and the anisotropic collective flow patterns of hadrons have been observed at RHIC for the first time. Both features are model independent predictions of the quark recombination mechanism in a kinematic range where general arguments about the dominance of recombination apply if, and only if, a thermally and chemically equilibrated quark plasma hadronizes.

The present data and their theoretical descriptions leave a number of important questions unaddressed. One concerns two-body correlations among energetic hadrons. Recombination from a purely thermal medium only allows for quantum (HBT) correlations among hadrons,

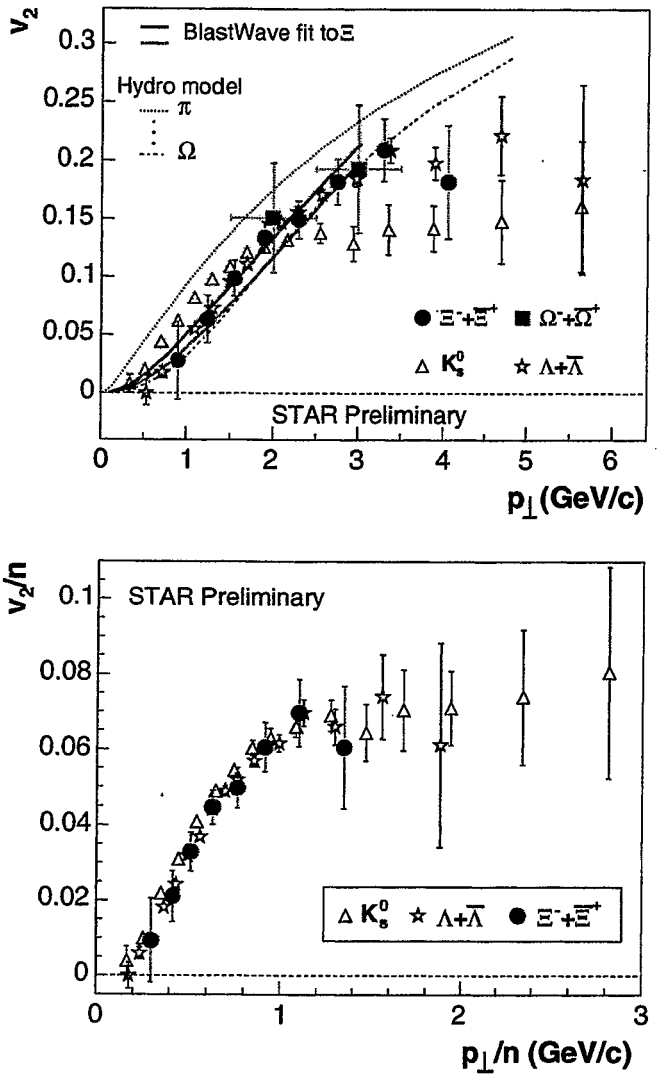

FIG. 8: (a) Upper panel: Elliptic flow parameter v_2 measured for various strange hadrons as function of transverse momentum p_T (STAR data). (b) Lower panel: Same data, but plotted in the scaled variables v_2/n and p_T/n, where $n = 2, 3$ is the number of constituent quarks in a hadron.

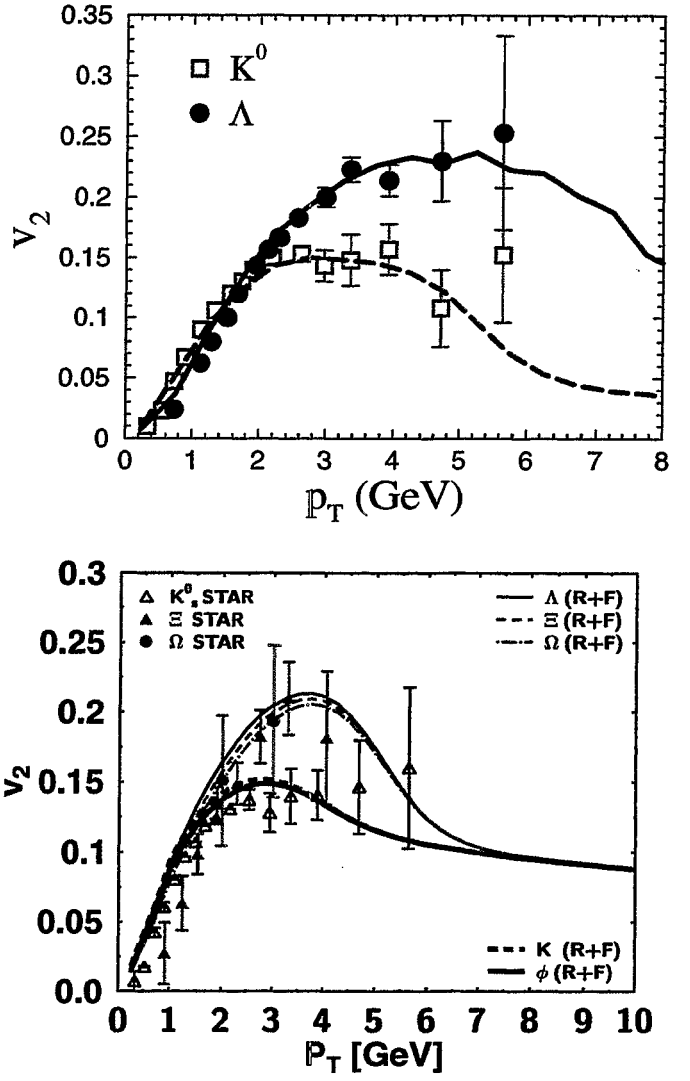

FIG. 9: Elliptic flow parameter v_2 as function of transverse momentum p_T together with the STAR data. (a) Upper panel: Kaons and Λ hyperons (Greco et al. [32]). (b) Lower panel: Kaons, Ξ and Ω hyperons (Nonaka et al. [46]).

but there is clear evidence in the data for the persistence of jet-like correlations into the kinematic regime where the recombination mechanism is thought to dominate. One explanation could be that these correlations are vestiges of the recombination of thermal and shower partons. Another explanation could be that the assumption of a completely thermal medium is a simplification, and that two-parton correlations become increasingly important with increasing p_T. These two explanations are likely just two faces of the same mechanism, because correlations among partons are probably caused by interactions of an energetic parton with constituents of the medium.

Another important puzzle is the apparent absence of gluonic degrees of freedom in the recombination mechanism. Does this indicate that gluons disappear as independent degrees of freedom as the plasma approaches the critical temperature from above? The precipitous drop in the Debye screening mass of a thermal plasma found in (quenched) lattice-QCD simulations near, but above T_c (see Fig. 8 of [47]) would suggest that this is, indeed, the case. One way to explain the absence of gluons is to argue that they fragment into quark-antiquark pairs prior to recombination [35].

The presence of strong dynamical correlations (clustering) among the constituents of the medium prior to hadronization, as suggested by theoretical considerations [48], would certainly serve to enhance the probability of recombination. This would be similar as the preformation of four-nucleon clusters facilitating the α-particle decay of heavy nuclei [49].

Acknowledgments

This work was supported in part by grant No. DE-FG02-96ER40945 from the U. S. Department of Energy. I thank Steffen Bass, Rainer Fries, Rudolph Hwa, Che-Ming Ko, and Thorsten Renk for valuable comments on the manuscript and Olga Barannikova, Rainer Fries, Vincenzo Greco, Chiho Nonaka, Richard Seto and Paul Sorensen for providing figures.

[1] T. D. Lee, *Trans. N.Y. Acad. Sci.* (Ser.2) **40**, 111 (1980).
[2] A. H. Guth, *Phys. Rev. D* **23**, 347 (1981); A. D. Linde, *Phys. Lett.* **108B**, 389 (1982); A. Albrecht and P. J. Steinhardt, *Phys. Rev. Lett.* **48**, 1220 (1982). For a concise review of inflationary cosmology see, e. g. A. H. Guth, *Inflation and Eternal Inflation*, arXiv:astro-ph/0002156.
[3] M. J. Rees, *Astrophys. & Space Sci.* **285**, 95 (2003);
[4] P. C. W. Davies, *Mod. Phys. Lett. A* **19**, 727 (2004).
[5] L. Susskind, *The anthropic landscape of string theory*, arXiv:hep-th/0302219.
[6] F. Karsch, *Nucl. Phys. A* **698**, 199 (2002).
[7] Evidence for the formation of a quark-gluon plasma in Au+Au collisions at RHIC from various other signature observables is discussed in various other articles in this volume.
[8] J. Rafelski and B. Müller, *Phys. Rev. Lett.* **48**, 1066 (1982).
[9] J. Rafelski, *Phys. Rept.* **88**, 331 (1982).
[10] P. Koch, B. Müller and J. Rafelski, *Phys. Rept.* **142**, 167 (1986).
[11] A. P. Vischer, P. J. Siemens and J. C. Parikh, *Phys. Rev. D* **43**, 271 (1991).
[12] S. A. Voloshin, *Nucl. Phys. A* **715**, 379 (2003).
[13] P. Koch and J. Rafelski, *Nucl. Phys. A* **444**, 678 (1985).
[14] T. S. Biro and J. Zimanyi, *Nucl. Phys. A* **395**, 525 (1983).
[15] H. W. Barz, B. L. Friman, J. Knoll and H. Schulz, *Nucl. Phys. A* **484**, 661 (1988).
[16] T. S. Biro, P. Levai and J. Zimanyi, *Phys. Lett. B* **347**, 6 (1995).
[17] J. Rafelski and J. Letessier, *Phys. Rev. Lett.* **85**, 4695 (2000).
[18] S. A. Bass and A. Dumitru, *Phys. Rev. C* **61**, 064909 (2000).
[19] J. Kapusta and I. Shovkovy, *Phys. Rev. C* **68**, 014901 (2003).
[20] P. Huovinen and J. I. Kapusta, *Phys. Rev. C* **69**, 014902 (2004).
[21] R. Hagedorn, *Nuovo Cim. Suppl.* **3**, 147 (1965); R. Hagedorn and J. Ranft, *ibid.* **6**, 169 (1968).
[22] F. Becattini, A. Giovannini and S. Lupia, *Z. Phys. C* **72**, 491 (1996).
[23] F. Becattini and U. W. Heinz, *Z. Phys. C* **76**, 269 (1997).
[24] E. Andersen *et al.* [WA97 Collab.], *Phys. Lett. B* **449**, 401 (1999).
[25] U. W. Heinz and M. Jacob, *Evidence for a new state of matter: An assessment of the results from the CERN lead beam programme*, arXiv:nucl-th/0002042.
[26] L. Sandor *et al.* [NA57 Collab.], *J. Phys. G* **30** (2004) S129.
[27] T. Renk, *A comprehensive description of multiple observables in heavy-ion collisions at SPS*, arXiv:hep-ph/0403239.
[28] R. J. Fries, B. Müller, C. Nonaka and S. A. Bass, *Phys. Rev. Lett.* **90**, 202303 (2003); *Phys. Rev. C* **68**, 044902 (2003).
[29] D. Molnar and S. A. Voloshin, *Phys. Rev. Lett.* **91**, 092301 (2003).
[30] Z. W. Lin and C. M. Ko, *Phys. Rev. C* **65**, 034904 (2002).
[31] An up-to-date survey of the various approaches to quark recombination can be found in: R. J. Fries, *Recombination models*, arXiv:nucl-th/0403036.
[32] V. Greco, C. M. Ko and P. Levai, *Phys. Rev. Lett.* **90**, 202302 (2003); *Phys. Rev. C* **68**, 034904 (2003).
[33] V. Greco and C. M. Ko, *Effect of resonance decays on hadron elliptic flows*, arXiv:nucl-th/0402020.
[34] K. P. Das and R. C. Hwa, *Phys. Lett. B* **68**, 459 (1977); Erratum *ibid.* **73**, 504 (1978).
[35] R. C. Hwa and C. B. Yang, *Phys. Rev. C* **66**, 025205 (2002); *Phys. Rev. C* **67**, 034902 (2003).
[36] R. C. Hwa and C. B. Yang, *Recombination of shower partons at high p_T in heavy-ion collisions*, arXiv:nucl-th/0401001.
[37] R. C. Hwa and C. B. Yang, *Final-state interaction as the origin of the Cronin effect*, arXiv:nucl-th/0403001.
[38] P. Braun-Munzinger, K. Redlich and J. Stachel, *Particle production in heavy ion collisions*, arXiv:nucl-th/0304013, in: *Quark Gluon Plasma 3*, eds. R. C. Hwa and X.-N. Wang (World Scientific, Singapore, 2004).
[39] H. B. Zhang [STAR Collab.], *Δ, K^* and ρ resonance production and their probing of freeze-out dynamics at RHIC*, arXiv:nucl-ex/0403010.
[40] K. Adcox *et al.* [PHENIX collab.], *Phys. Rev. Lett.* **88**, 242301 (2002); *Phys. Rev. C* **69**, 024904 (2004); S. S. Adler et al. [PHENIX collab.], *Phys. Rev. Lett.* **91**, 172301 (2003).
[41] C. Adler *et al.* [STAR collab.], *Phys. Rev. Lett.* **89**, 092301 (2002); J. Adams *et al.* [STAR Collab.], *Phys. Rev. Lett.* **92**, 052302 (2004).
[42] M. A. C. Lamont [STAR collab.], arXiv:nucl-ex/0403059.
[43] A. D. Frawley [PHENIX collab.], arXiv:nucl-ex/0404009.
[44] J. Y. Ollitrault, *Phys. Rev. D* **46**, 229 (1992).
[45] J. Adams *et al.* [STAR Collab.], *Phys. Rev. Lett.* **92**, 052302 (2004).
[46] C. Nonaka, R. J. Fries and S. A. Bass, *Phys. Lett. B* **583**, 73 (2004); C. Nonaka, B. Müller, M. Asakawa, S. A. Bass and R. J. Fries, *Phys. Rev. C* **69**, 031902 (2004)
[47] O. Kaczmarek, F. Karsch, E. Laermann and M. Lütgemeier, *Phys. Rev. D* **62**, 034021 (2000).
[48] E. V. Shuryak and I. Zahed, *Towards a theory of binary bound states in the quark gluon plasma*, arXiv:hep-ph/0403127.
[49] There exists an extensive literature addressing this problem. A representative example is: S. M. Lenzi, et al., *Phys. Rev. C* **48**, 1463 (1993).

Discovery of Jet Quenching and Beyond

Xin-Nian Wang

Discovery of Jet Quenching and Beyond

Xin-Nian Wang
Nuclear Science Division, MS 70R0319,
Lawrence Berkeley National Laboratory, Berkeley, CA 94720

Recent observation of high-p_T hadron spectra suppression and mono-jet production in central $Au + Au$ collisions and their absence in $d + Au$ collisions at RHIC have confirmed the long predicted phenomenon of jet quenching in high-energy heavy-ion collisions. Detailed analyses of the experimental data also show parton energy loss as the mechanism for the discovered jet quenching. Using a pQCD parton model that incorporates medium modified parton fragmentation functions and comparing to experimental data from deeply inelastic scattering off nuclei, one can conclude that the initial gluon (energy) density of the hot matter produced in central $Au + Au$ collisions that causes jet quenching at RHIC is about 30 (100) times higher than in a cold Au nucleus. Combined with data on bulk and collective properties of the hot matter, the observed jet quenching provides strong evidence for the formation of a strongly interacting quark gluon plasma in central $Au + Au$ collisions at RHIC.

I. INTRODUCTION

In the last three years, since the physics operation of the Relativistic Heavy-ion Collider (RHIC) at Brookhaven National Laboratory (BNL), one has witnessed tremendous progress in heavy-ion experimental physics and many milestones in the search for the elusive quark gluon plasma (QGP) that is expected to be formed in high-energy heavy-ion collisions. One of the most exciting phenomena observed at RHIC is jet quenching, or suppression of leading hadrons from fragmentation of hard partons due to their strong interaction with the dense medium. Such a phenomenon was long predicted by a pQCD-based model calculation [1], but was not seen in high-energy heavy-ion collisions until the first measurements in central $Au+Au$ collisions at $\sqrt{s} = 130$ GeV at RHIC [2,3]. The azimuthal distribution of high p_T hadrons was also found to display large anisotropy with respect to the reaction planes [4] of non-central $Au + Au$ collisions which was expected to be caused by the path-length dependence of jet quenching [5,6].

The measurements were confirmed and further extended to a larger p_T range in $Au + Au$ collisions at $\sqrt{s} = 200$ GeV, and the suppression was found to have a weak p_T-dependence at $p_T > 6$ GeV/c [7,8], independent of hadron species. At the same time, the back-side high-p_T two-hadron correlation in azimuthal angle, characteristic of high-p_T back-to-back jets in $p + p$ collisions, was found to disappear in central $Au+Au$ collisions [9], confirming the predicted mono-jet phenomenon of jet quenching [10].

The final milestone in the experimental discovery of jet quenching was achieved during the third year of the RHIC physics program, when both the single-hadron spectra [11–13] and the disappearance of away-side two-hadron correlation [12] were found to be absent in the same central rapidity region of $d + Au$ collisions at $\sqrt{s} = 200$ GeV. These $d + Au$ results prove that the observed high-p_T suppression patterns in $Au+Au$ collisions are not initial state effects encoded in the wavefunction of a beam nucleus, but are jet quenching caused by final state interaction of hard partons with the produced dense medium.

Following these three major experimental results, additional data—such as the dependence of away-side suppression on the azimuthal angle relative to the reaction plane [14], modification of the hadron distributions (fragmentation functions) both along and opposite the direction of the triggered high-p_T hadron [15], and absence of suppression in the direct photon spectra [16] in $Au + Au$ collisions—have now solidified the conclusion that the observed jet quenching is caused by parton multiple scattering and energy loss in the hot and dense medium. Furthermore, the splitting of baryon and meson spectra suppression and azimuthal anisotropy in the intermediate $p_T < 6$ GeV/c region [17–19] also point to non-trivial medium modification of hadronization that is indicative of dense partonic matter. Such a wealth of data affords one a quantitative phenomenological analysis of jet quenching and a tomographical picture of the hot and dense matter formed in heavy-ion collisions at RHIC.

In this report, we will first briefly review the recent progress in pQCD study of parton multiple scattering and induced radiative energy loss in a dense medium. Combining this with the pQCD parton model of high-p_T jet and hadron production, one can analyze the observed jet quenching phenomena to extract properties of the dense matter produced. One can combine the deduced properties with other information from analyses of bulk particle spectra such as collective flow and total multiplicity and energy production to present a collection of compelling evidence for the existence of a strongly interacting quark gluon plasma in $Au + Au$ collisions at RHIC. However, we will focus in this report only on the analysis of jet quenching data and the properties of the dense matter one can extract from these data.

II. PARTON ENERGY LOSS

One important step in establishing evidence of QGP formation is to characterize the properties of the produced dense medium, for example, the parton and energy density and current-current correlations, among many other characteristics. Traditionally, one can study the properties of a medium via scattering experiments with particles. In deeply inelastic scattering (DIS) experiments, for example, leptons scatter off the nucleon medium via photon exchange. The response function or the correlation function of the electromagnetic currents $j_\mu^{em}(x) = \sum_q e_q \bar{\psi}_q(x)\gamma_\mu \psi_q(x)$,

$$W_{\mu\nu}(q) = \frac{1}{4\pi}\int d^4x e^{iq\cdot x}\langle A \mid j_\mu^{em}(0) j_\nu^{em}(x) \mid A\rangle, \quad (1)$$

is a direct measurement of the quark distributions in a nucleon or nucleus. For a dynamic system in heavy-ion collisions, one can no longer use the technique of scattering with an external beam of particles in the conventional sense because of the transient nature of the matter. The lifetime of the system is very short, on the order of a few fm/c. The initial spatial size is only the size of the colliding nuclei, about 6 fm in diameter in the transverse dimension for the heaviest nuclei. The system expands very rapidly both in the longitudinal and the transverse direction. These characteristics make it impossible to use external probes to study the properties of the produced dense matter in high-energy heavy-ion collisions. One has to resort to internal probes such as the electromagnetic emission from the dynamic medium, whose rate is given by the thermal average of the above correlation function. The emission rate depends mainly on the local temperature or the parton density while the total yield also depends on the whole evolution history of the system. Therefore, a strongly interacting system can reveal its properties and dynamics through photon and dilepton emission. The same medium interaction should also cause attenuation of fast and energetic partons propagating through the medium. Such an effect is the underlying physics of the jet quenching [20,21] phenomenon and jet tomography technique for studying properties of dense matter in high-energy heavy-ion collisions.

Jet quenching as a probe of the dense matter in heavy-ion collisions takes advantage of the hard processes of jet production in high-energy heavy-ion collisions. Because large-p_T partons are produced very early in heavy-ion collisions, they can probe the early stage of the formed dense medium. Similar to the technology of computed tomography (CT), the study of these energetic particles, their initial production and interaction with the dense medium can yield critical information about the properties of the medium that is otherwise difficult to access through soft hadrons from the hadronization of the bulk matter. Though relatively rare with small cross sections, the jet production rate can be calculated perturbatively in QCD and agrees well with experimental measurements in high-energy $p + p(\bar{p})$ collisions. A critical component of the jet tomography is then to understand the jet's attenuation through dense matter as it propagates through the medium.

There have been many theoretical studies [22–24] of jet attenuation in a hot medium in recent years. The first attempt was by Bjorken [20] to calculate elastic energy loss of a parton via elastic scattering in the hot medium. A simple estimate can be given by the thermal averaged energy transfer $\nu_{\rm el} \approx q_\perp^2/2\omega$ of the jet parton to a thermal parton, with energy ω, and $q_\perp$ the transverse momentum transfer of the elastic scattering. The resultant elastic energy loss [25]

$$\frac{dE_{\rm el}}{dx} = C_2 \frac{3\pi\alpha_s^2}{2} T^2 \ln\left(\frac{3ET}{2\mu^2}\right) \quad (2)$$

is sensitive to the temperature of the thermal medium but is small compared to radiative energy loss. Here, μ is the Debye screening mass and C_2 is the Casimir coefficient of the propagating parton in its fundamental presentation. The elastic energy loss can also be calculated within finite temperature field theory of QCD [26] with a more careful and consistent treatment of the Debye screening effect.

Though there had been estimates of the radiative parton energy loss using the uncertainty principle [27], the first theoretical study of QCD radiative parton energy loss incorporating Landau-Pomeranchuk-Migdal interference effect [28] is by Gyulassy and Wang [29] where multiple parton scattering is modeled by a screened Coulomb potential model. Baier *et al.* (BDMPS) [30] later considered the effect of gluon rescattering which turned out to be very important for gluon radiation induced by multiple scattering in a dense medium. These two studies have ushered in many recent works on the subject, including a path integral approach to the problem [31], twist [32] or opacity expansion framework [33,34] which is more suitable for multiple parton scattering in a finite system. The radiative parton energy loss in the leading order of the twist or opacity expansion was found to have a simple form [33]

$$\frac{dE_{\rm rad}}{dx} \approx C_2 \frac{\alpha_s \mu^2}{4}\frac{L}{\lambda}\ln\left(\frac{2E}{\mu^2 L}\right), \quad (3)$$

for an energetic parton ($E \gg \mu$) in a static medium, where λ is the gluon's mean free path in the medium. The unique L-dependence of the parton energy loss, which was first discovered by BDMPS [30] is a consequence of the non-Abelian LMP interference effect in a QCD medium. In a dynamic system the total energy loss was found [6,35,36] to be proportional to a line integral of the gluon density along the parton propagation path.

Since gluons are bosons, there should also be stimulated gluon emission and absorption by the propagating parton in the presence of thermal gluons in the hot medium. Such detailed balance is crucial for parton thermalization and should also be important for calculating

the energy loss of an energetic parton in a hot medium. Taking into account such detailed balance in gluon emission, Wang and Wang [37] obtained an asymptotic behavior of the effective energy loss in the opacity expansion framework ,

$$\frac{\Delta E}{E} \approx \frac{\alpha_s C_2 \mu^2 L^2}{4\lambda E}\left[\ln\frac{2E}{\mu^2 L} - 0.048\right] - \frac{\pi\alpha_s C_F}{3}\frac{LT^2}{\lambda E^2}\left[\ln\frac{\mu^2 L}{T} - 1 + \gamma_E - \frac{6\zeta'(2)}{\pi^2}\right], \quad (4)$$

where the first term is from the induced bremsstrahlung and the second is due to gluon absorption in detailed balance, which effectively reduces the total parton energy loss in the medium. Though the effect of detailed balance is small at large energy ($E \gg \mu$), it changes the effective energy dependence of the energy loss in the intermediate energy region.

III. MODIFIED FRAGMENTATION FUNCTION

Because of color confinement in the vacuum, one can never separate hadrons fragmenting from the leading parton and particles materializing from the radiated gluons. The total energy in the conventionally defined jet cone in principle should not change due to induced radiation, assuming that most of the energy carried by radiative gluons remains inside the jet cone [38]. Additional rescattering of the emitted gluon with the medium could broaden the jet cone significantly, thus reducing the energy in a fixed cone. However, fluctuation of the underlying background in high-energy heavy-ion collisions makes it very difficult, if not impossible, to determine the energy of a jet on an event-by-event base with sufficient precision to discern a finite energy loss of the order of 10 GeV. Since high-p_T hadrons in hadronic and nuclear collisions come from fragmentation of high-p_T jets, energy loss naturally leads to suppression of high-p_T hadron spectra. This was why Gyulassy and Wang proposed [1] to measure the suppression of high-p_T hadrons to study parton energy loss in heavy-ion collisions.

Since parton energy loss effectively slows down the leading parton in a jet, a direct manifestation of jet quenching is the modification of the jet fragmentation function, $D_{a\to h}(z,\mu^2)$, which can be measured directly in events in which one can identify the jet via a companion particle like a direct photon [39] or a triggered high p_T hadron. This modification can be directly translated into the energy loss of the leading parton. Since inclusive hadron spectra are a convolution of the jet production cross section and the jet fragmentation function in pQCD, the suppression of inclusive high-p_T hadron spectra is a direct consequence of the medium modification of the jet fragmentation function caused by parton energy loss.

Since a jet parton is always produced via a hard process involving a large momentum scale, it should also have final state radiation with and without rescattering, leading to the DGLAP evolution of fragmentation functions. Such final state radiation effectively acts as a self-quenching mechanism, softening the leading hadron distribution. This process is quite similar to the induced gluon radiation and the two should have a strong interference effect. It is therefore natural to study jet quenching and modified fragmentation functions in the framework of modified DGLAP evolution equations in a medium [32].

To demonstrate medium modified fragmentation function and parton energy loss, we review here the twist expansion approach in the study of deeply inelastic scattering (DIS) eA [32,40]. While the results can be readily extended to the case of a hot medium, they also provide a baseline for comparison to parton energy loss in cold nuclei.

In the parton model with the collinear factorization approximation, the leading-twist contribution to the semi-inclusive cross section can be factorized into a product of parton distributions, parton fragmentation functions and the hard partonic cross section. Including all leading log radiative corrections, the lowest order contribution from a single hard $\gamma^* + q$ scattering can be written as

$$\frac{dW^S_{\mu\nu}}{dz_h} = \sum_q e_q^2 \int dx f_q^A(x,\mu_I^2) H^{(0)}_{\mu\nu}(x,p,q) D_{q\to h}(z_h,\mu^2),$$

where $H^{(0)}_{\mu\nu}(x,p,q)$ is the hard part of the process in leading order, ℓ_h the observed hadron momentum, $p = [p^+, 0, \mathbf{0}_\perp]$ the momentum per nucleon in the nucleus, $q = [-Q^2/2q^-, q^-, \mathbf{0}_\perp]$ the momentum transfer carried by the virtual photon. In the chosen frame, q^- is the quark momentum transferred from the virtual photon. The momentum fraction carried by the hadron is defined as $z_h = \ell_h^-/q^-$ and $x = x_B = Q^2/2p^+q^-$ is the Bjorken variable. μ_I^2 and μ^2 are the factorization scales for the initial quark distributions $f_q^A(x,\mu_I^2)$ in a nucleus and the fragmentation functions $D_{q\to h}(z_h,\mu^2)$, respectively.

In a nuclear medium, the propagating quark in DIS will experience additional scattering with other partons from the nucleus. The rescatterings may induce additional gluon radiation and cause the leading quark to lose energy. Such induced gluon radiations will effectively give rise to additional terms in a DGLAP-like evolution equation leading to the modification of the fragmentation functions in a medium. These are the so-called higher-twist corrections since they involve higher-twist parton matrix elements and are power-suppressed. The leading contributions involve two-parton correlations from two different nucleons inside the nucleus.

One can apply the generalized factorization [41] to these multiple scattering processes. In this approximation, the double scattering contribution to radiative correction can be calculated and the effective modified fragmentation function is [32]

$$\widetilde{D}_{q\to h}(z_h,\mu^2) \equiv D_{q\to h}(z_h,\mu^2) + \int_0^{\mu^2} \frac{d\ell_T^2}{\ell_T^2}\frac{\alpha_s}{2\pi}\int_{z_h}^1 \frac{dz}{z} \left[\Delta\gamma_{q\to qg}(z,x,x_L,\ell_T^2)\, D_{q\to h}(z_h/z) + \Delta\gamma_{q\to gq}(z,x,x_L,\ell_T^2) D_{g\to h}(z_h/z)\right], \quad (5)$$

in much the same form as the DGLAP correction in vacuum, where $D_{q\to h}(z_h,\mu^2)$ and $D_{g\to h}(z_h,\mu^2)$ are the leading-twist quark and gluon fragmentation functions. The modified splitting functions are given as

$$\Delta\gamma_{q\to qg}(z,x,x_L,\ell_T^2) = \left[\frac{1+z^2}{(1-z)_+} T_{qg}^A(x,x_L) + \delta(1-z)\Delta T_{qg}^A(x,\ell_T^2)\right] \frac{2\pi\alpha_s C_A}{\ell_T^2 N_c f_q^A(x,\mu_I^2)}, \quad (6)$$

$$\Delta\gamma_{q\to gq}(z,x,x_L,\ell_T^2) = \Delta\gamma_{q\to qg}(1-z,x,x_L,\ell_T^2). \quad (7)$$

Here, the fractional momentum $x = x_B$ is carried by the initial quark and $x_L = \ell_T^2/2p^+q^- z(1-z)$ is the additional momentum fraction carried either by the quark or gluon in the secondary scattering that is required for induced gluon radiation. The twist-four parton matrix element of the nucleus,

$$T_{qg}^A(x,x_L) = \int \frac{dy^-}{2\pi}\, dy_1^- dy_2^-\, e^{i(x+x_L)p^+y^-}\,(1-e^{-ix_Lp^+y_2^-}) \times(1-e^{-ix_Lp^+(y^--y_1^-)})\theta(-y_2^-)\theta(y^--y_1^-) \times\frac{1}{2}\langle A|\bar\psi_q(0)\,\gamma^+ F_\sigma{}^+(y_2^-)\, F^{+\sigma}(y_1^-)\,\psi_q(y^-)|A\rangle\ , \quad (8)$$

has a dipole-like structure which is a result of LPM interference in gluon bremsstrahlung.

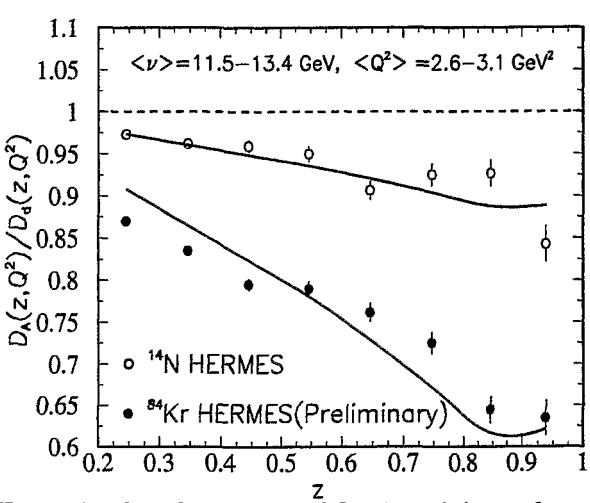

FIG. 1. Predicted nuclear modification of the jet fragmentation functions compared to the HERMES data [43] on ratios of hadron distributions between A and d targets in DIS.

Averaged over a Gaussian nuclear distribution, the interference will produce a factor $1-e^{-x_L^2/x_A^2}$ with $x_A = 1/MR_A$. Here R_A is the nuclear size and M is the nucleon mass. Using the factorization approximation [32,41,42], one can relate the twist-four parton matrix elements of the nucleus to the twist-two parton distributions of nucleons and the nucleus,

$$T_{qg}^A(x,x_L) \approx \frac{\widetilde{C}}{x_A}(1-e^{-x_L^2/x_A^2}) f_q^A(x), \quad (9)$$

where $\widetilde{C} \equiv 2Cx_T f_g^N(x_T)$ is considered a constant. One can identify $1/x_Lp^+ = 2q^-z(1-z)/\ell_T^2$ as the formation time of the emitted gluons. In the limit of collinear radiation ($x_L \to 0$) or when the formation time of the gluon radiation is much larger than the nuclear size, the above matrix element vanishes, demonstrating a typical LPM interference effect.

Since the LPM interference suppresses gluon radiation whose formation time ($\tau_f \sim Q^2/\ell_T^2p^+$) is larger than the nuclear size MR_A/p^+ (here in the infinite momentum frame), ℓ_T^2 should then have a minimum value of $\ell_T^2 \sim Q^2/MR_A \sim Q^2/A^{1/3}$. Therefore, the leading higher-twist contribution is proportional to $\alpha_s R_A/\ell_T^2 \sim \alpha_s R_A^2/Q^2$ due to double scattering and depends quadratically on the nuclear size R_A.

With the assumption of the factorized form of the twist-4 nuclear parton matrices, there is only one free parameter $\widetilde{C}(Q^2)$ which represents quark-gluon correlation strength inside nuclei. Once it is fixed, one can predict the z, energy and nuclear dependence of the medium modification of the fragmentation function. Shown in Fig. 1 are the calculated [35] nuclear modification factor of the fragmentation functions for ^{14}N and ^{84}Kr targets as compared to the recent HERMES data [43]. The predicted shape of the z-dependence agrees well with the experimental data. A remarkable feature of the prediction is the quadratic $A^{2/3}$ nuclear size dependence, which is verified for the first time by an experiment. By fitting the overall suppression for one nuclear target, one obtains the only parameter in the calculation, $\widetilde{C}(Q^2) = 0.0060$ GeV^2 with $\alpha_s(Q^2) = 0.33$ at $Q^2 \approx 3$ GeV^2. The predicted energy (ν) dependence also agrees with the experimental data as shown in Fig. 2. Note that the suppression goes away as the quark energy increases. This is in sharp contrast to the jet quenching in heavy-ion collisions.

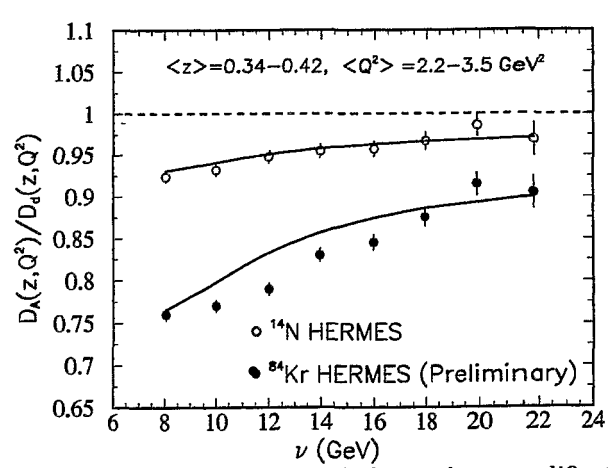

FIG. 2. Energy dependence of the nuclear modification compared with the HERMES data [43].

One can quantify the modification of the fragmentation by the quark energy loss which is defined as the momentum fraction carried by the radiated gluon,

$$\langle \Delta z_g \rangle = \int_0^{\mu^2} \frac{d\ell_T^2}{\ell_T^2} \int_0^1 dz \frac{\alpha_s}{2\pi} z \, \Delta\gamma_{q\to gq}(z, x_B, x_L, \ell_T^2)$$
$$= \widetilde{C} \frac{C_A \alpha_s^2}{N_c} \frac{x_B}{x_A Q^2} \int_0^1 dz \frac{1+(1-z)^2}{z(1-z)}$$
$$\times \int_0^{x_\mu} \frac{dx_L}{x_L^2} (1 - e^{-x_L^2/x_A^2}), \qquad (10)$$

where $x_\mu = \mu^2/2p^+q^- z(1-z) = x_B/z(1-z)$ if the factorization scale is set as $\mu^2 = Q^2$. When $x_A \ll x_B \ll 1$ the leading quark energy loss is approximately

$$\langle \Delta z_g \rangle (x_B, \mu^2) \approx \widetilde{C} \frac{C_A \alpha_s^2}{N_c} \frac{x_B}{Q^2 x_A^2} 6\sqrt{\pi} \ln \frac{1}{2x_B}. \qquad (11)$$

Since $x_A = 1/MR_A$, the energy loss $\langle \Delta z_g \rangle$ thus depends quadratically on the nuclear size.

In the rest frame of the nucleus, $p^+ = M$, $q^- = \nu$, and $x_B \equiv Q^2/2p^+q^- = Q^2/2M\nu$. One can get the averaged total energy loss as $\Delta E = \nu \langle \Delta z_g \rangle \approx \widetilde{C}(Q^2)\alpha_s^2(Q^2) M R_A^2 (C_A/N_c) 3\ln(1/2x_B)$. With the determined value of $\widetilde{C}$, $\langle x_B \rangle \approx 0.124$ in the HERMES experiment [43] and the average distance $\langle L_A \rangle = R_A\sqrt{2/\pi}$ for the assumed Gaussian nuclear distribution, one gets the quark energy loss $dE/dL \approx 0.5$ GeV/fm inside a Au nucleus.

IV. JET QUENCHING IN HOT MEDIUM

To extend the study of modified fragmentation functions to jets in heavy-ion collisions, one can assume $\langle k_T^2 \rangle \approx \mu^2$ (the Debye screening mass) and a gluon density profile $\rho(y) = (\tau_0/\tau)\theta(R_A - y)\rho_0$ for a 1-dimensional expanding system. Since the initial jet production rate is independent of the final gluon density, which can be related to the parton-gluon scattering cross section [44] $[\alpha_s x_T G(x_T) \sim \mu^2 \sigma_g]$, one has then

$$\frac{\alpha_s T_{qg}^A(x_B, x_L)}{f_q^A(x_B)} \sim \mu^2 \int dy \sigma_g \rho(y) [1 - \cos(y/\tau_f)], \qquad (12)$$

where $\tau_f = 2Ez(1-z)/\ell_T^2$ is the gluon formation time. The averaged fractional energy loss is then,

$$\langle \Delta z_g \rangle = \frac{C_A \alpha_s}{\pi} \int_0^1 dz \int_0^{Q^2/\mu^2} du \frac{1+(1-z)^2}{u(1+u)}$$
$$\times \int_{\tau_0}^{R_A} d\tau \sigma_g \rho(\tau) \left[1 - \cos\left(\frac{(\tau - \tau_0)\, u\, \mu^2}{2Ez(1-z)} \right) \right]. \qquad (13)$$

Keeping only the dominant contribution and assuming $\sigma_g \approx C_a 2\pi\alpha_s^2/\mu^2$ (C_a=1 for qg and 9/4 for gg scattering), one obtains the total energy loss,

$$\langle \Delta E \rangle \approx \pi C_a C_A \alpha_s^3 \int_{\tau_0}^{R_A} d\tau \rho(\tau)(\tau - \tau_0) \ln \frac{2E}{\tau \mu^2}. \qquad (14)$$

which has also be obtained in the opacity expansion approach [6,36] in a thin plasma.

In a static medium, the gluon density is independent of time and one can recover the quadratic lenghth dependence in Eq. (3). Neglecting the logarithmic dependence on τ, the averaged energy loss can be expressed as

$$\langle \frac{dE}{dL} \rangle_{1d} \approx (dE_0/dL)(2\tau_0/R_A) \qquad (15)$$

in a 1-dimensional expanding system, $\rho(\tau) = \rho_0\tau_0/\tau$. Here $dE_0/dL \propto \rho_0 R_A$ is the energy loss in a static medium with the same gluon density ρ_0 as in the 1-d expanding system at time τ_0. Because of the expansion, the averaged energy loss $\langle dE/dL \rangle_{1d}$ is suppressed as compared to the static case and does not depend linearly on the system size at a fixed value of initial gluon density.

One should emphasize now that the above simple logarithmic energy dependence of the parton energy loss in Eqs. (11) and (14) is only an asymptotic behavior. However, kinematic limits on induced gluon radiation from a parton with finite energy can result in a stronger energy dependence [33]. The effect of detailed balance with thermal absorption further increases the energy dependence [37], while reducing the effective parton energy loss for intermediate values of parton energy. Such a detailed balance effect sets the energy dependence of the energy loss in cold nuclei in DIS apart from the hot medium in heavy-ion collisions. If one parameterizes the energy dependence of the energy loss including the full kinematic limits and thermal absorption, one would get

$$\langle \frac{dE}{dL} \rangle_{1d} = \epsilon_0 (E/\mu - 1.6)^{1.2}/(7.5 + E/\mu). \qquad (16)$$

The threshold is the consequence of gluon absorption that competes with radiation and effectively shuts off the energy loss. The parameter μ is set to be 1.5 GeV in the following discussions. Such a detailed balance effect can also explain why the total hadron multiplicity that is dominated by soft hadrons does have significant enhancement over the $p+p$ collisions as result of induced gluon emission.

A. Single Spectra

To calculate the modified high-p_T spectra in $A+A$ collisions, we use a LO pQCD model [45],

$$\frac{d\sigma_{AA}^h}{dy d^2 p_T} = K \sum_{abcd} \int d^2b d^2r dx_a dx_b d^2k_{aT} d^2k_{bT}$$
$$\times t_A(r) t_A(|\mathbf{b} - \mathbf{r}|) g_A(k_{aT}, r) g_A(k_{bT}, |\mathbf{b} - \mathbf{r}|)$$
$$\times f_{a/A}(x_a, Q^2, r) f_{b/A}(x_b, Q^2, |\mathbf{b} - \mathbf{r}|)$$
$$\times \frac{D'_{h/c}(z_c, Q^2, \Delta E_c)}{\pi z_c} \frac{d\sigma}{dt}(ab \to cd), \qquad (17)$$

with medium modified fragmentation functions $D'_{h/c}$. Here, $z_c = p_T/p_{Tc}$, $y = y_c$, $\sigma(ab \to cd)$ are elementary parton scattering cross sections and $t_A(b)$ is the nuclear thickness function normalized to $\int d^2b t_A(b) = A$. The $K \approx 1.5$–2 factor is used to account for higher order pQCD corrections.

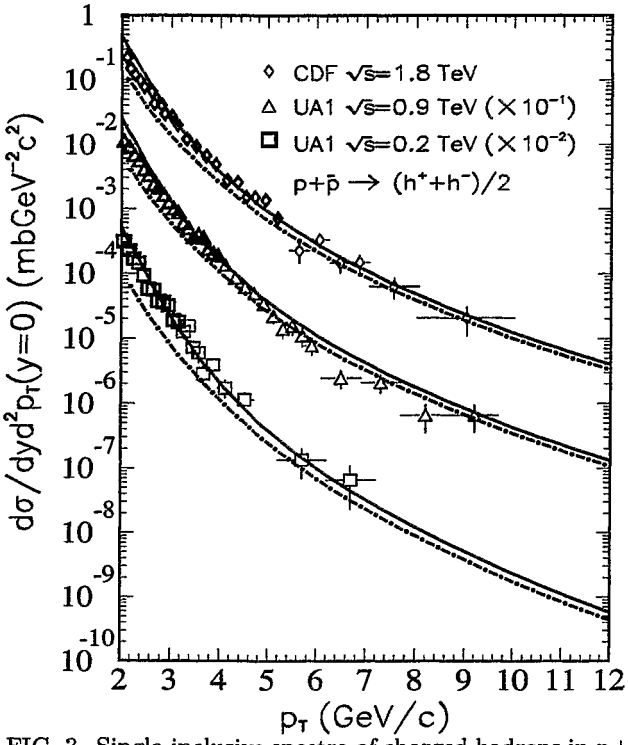

FIG. 3. Single-inclusive spectra of charged hadrons in $p+\bar{p}$ collisions at $\sqrt{s} = 200, 900, 1800$ GeV. The solid (dot-dashed) lines are parton model calculations with (without) intrinsic k_T. Experimental data are from Refs. [50,51].

To simplify the incorporation of the medium modification of the fragmentation function in the parton model, an effective model [39] can be used:

$$D'_{h/c}(z_c, Q^2, \Delta E_c) = e^{-\langle \frac{\Delta L}{\lambda} \rangle} D^0_{h/c}(z_c, Q^2) + (1 - e^{-\langle \frac{\Delta L}{\lambda} \rangle}) \times \left[\frac{z'_c}{z_c} D^0_{h/c}(z'_c, Q^2) + \langle \frac{\Delta L}{\lambda} \rangle \frac{z'_g}{z_c} D^0_{h/g}(z'_g, Q^2) \right] \quad (18)$$

where z'_c, z'_g are the rescaled momentum fractions after parton energy loss. This effective model is found [46] to reproduce the pQCD result from Eq.(5) very well, but only when $\Delta z = \Delta E_c/E$ is set to be $\Delta z \approx 0.6\langle z_g \rangle$. Therefore the actual averaged parton energy loss should be $\Delta E/E = 1.6\Delta z$, with Δz extracted from the effective model. The factor 1.6 is mainly caused by the unitarity correction effect in the pQCD calculation. The fragmentation functions in free space $D^0_{h/c}(z_c, Q^2)$ will be given by the BBK parameterization [47].

The parton distributions per nucleon $f_{a/A}(x_a, Q^2, r)$ inside the nucleus are assumed to be factorizable into the parton distributions in a free nucleon given by the MRSD$-'$ parameterization [48] and the impact-parameter dependent nuclear modification factor given by the new HIJING parameterization [49]. The initial transverse momentum distribution $g_A(k_T, Q^2, b)$ is assumed to have a Gaussian form with a width that includes both an intrinsic part in a nucleon and nuclear broadening. This parton model can describe high-p_T hadron spectra in $p + p(\bar{p})$ well, as shown in Fig. 3 that compares the parton model calculation [45] with the experimental data on the inclusive charged hadron spectra at different collider energies.

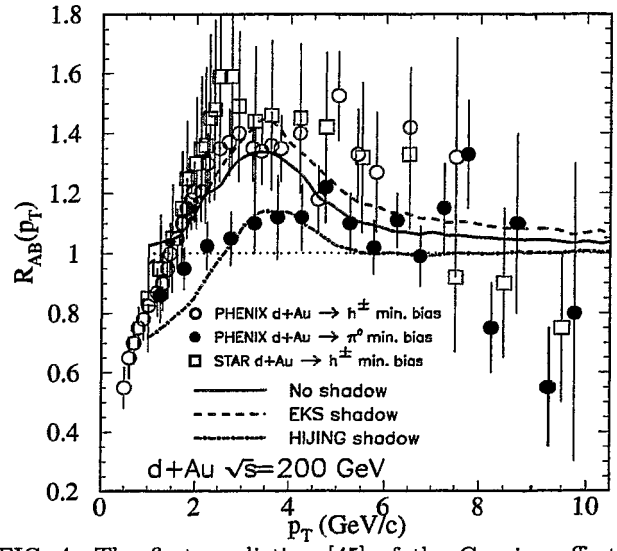

FIG. 4. The first prediction [45] of the Cronin effect in $p + Au$ collisions at $\sqrt{s} = 200$ GeV compared to the recent RHIC data from PHENIX [11] and STAR [12]. The dashed and dot-dashed lines correspond to HIJING [49] and EKS [52] parameterizations of nuclear parton distributions.

In $p + A$ collisions, this parton model incorporates both nuclear modification of the parton distributions and broadening of the initial transverse momentum. The initial momentum broadening leads to an enhancement, known as the Cronin effect, of the hadron spectra in the intermediate p_T region. The enhancement disappears at large p_T. The parameters have been fitted to the nuclear modification of the p_T spectra in $p + A$ collisions at up to the Fermilab energy $\sqrt{s} = 40$ GeV. Shown in Fig. 4 is the first prediction made in 1998 [45] of the Cronin effect at RHIC for $p + Au$ collisions at $\sqrt{s} = 200$ GeV as compared to the RHIC data on $d + Au$ collisions. As one can see, the initial multiple scattering in nuclei can give some moderate Cronin enhancement of the high-p_T spectra, though the details depend on the parameterization of the nuclear modification of parton distributions. Therefore, any observed suppression of the high-p_T spectra in $Au + Au$ collisions has to be caused by jet quenching.

In $A + A$ collisions, one has to consider medium modification of the fragmentation functions due to parton energy loss according to Eq. (18). Assuming a 1-dimensional expanding medium with a gluon density

$\rho_g(\tau, r)$ that is proportional to the transverse profile of participant nucleons, one can calculate the impact-parameter dependence of the energy loss,

$$\Delta E(b, r, \phi) \approx \langle \frac{dE}{dL} \rangle_{1d} \int_{\tau_0}^{\Delta L} d\tau \frac{\tau - \tau_0}{\tau_0 \rho_0} \rho_g(\tau, b, \vec{r} + \vec{n}\tau), \tag{19}$$

according to Eq. (14), where $\Delta L(b, \vec{r}, \phi)$ is the distance a jet, produced at $\vec{r}$, has to travel along $\vec{n}$ at an azimuthal angle ϕ relative to the reaction plane in a collision with impact-parameter b. Here, ρ_0 is the averaged initial gluon density at initial time τ_0 in a central collision and $\langle dE/dL \rangle_{1d}$ is the average parton energy loss over a distance R_A in a 1-d expanding medium with an initial uniform gluon density ρ_0. The corresponding energy loss in a static medium with a uniform gluon density ρ_0 over a distance R_A is [35] $dE_0/dL = (R_A/2\tau_0)\langle dE/dL \rangle_{1d}$. We will use the parameterization in Eq. (16) for the effective energy dependence of the quark energy loss.

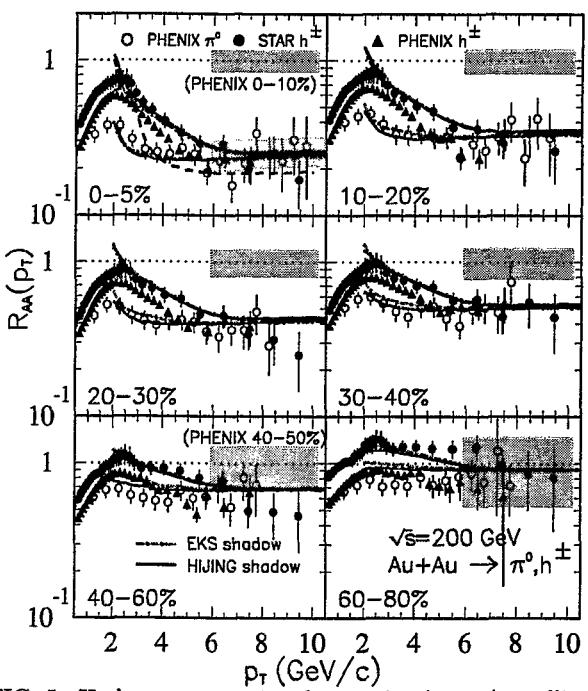

FIG. 5. Hadron suppression factors in $Au + Au$ collisions as compared to data from STAR [8] and PHENIX [7]. See text for a detailed explanation.

Shown in Fig. 5 are the calculated nuclear modification factors $R_{AB}(p_T) = d\sigma^h_{AB}/\langle N_{\text{binary}} \rangle d\sigma^h_{pp}$ for hadron spectra ($|y| < 0.5$) in $Au + Au$ collisions at $\sqrt{s} = 200$ GeV, as compared to experimental data [8,7]. Here, $\langle N_{\text{binary}} \rangle = \int d^2b d^2r t_A(r) t_A(|\vec{b} - \vec{r}|)$. To fit the observed π^0 suppression (solid lines) in the most central collisions, we have used $\mu = 1.5$ GeV, $\epsilon_0 = 1.07$ GeV/fm and $\lambda_0 = 1/(\sigma\rho_0) = 0.3$ fm in Eqs. (18) and (16). The hatched area (also in other figures in this report) indicates a variation of $\epsilon_0 = \pm 0.3$ GeV/fm. The hatched boxes around $R_{AB} = 1$ represent experimental errors of STAR data in overall normalization, including a constant factor of about 18% from the determination of total $p+p$ inelastic cross section. Nuclear k_T broadening and parton shadowing together give a slight enhancement of hadron spectra at intermediate $p_T = 2-4$ GeV/c without parton energy loss.

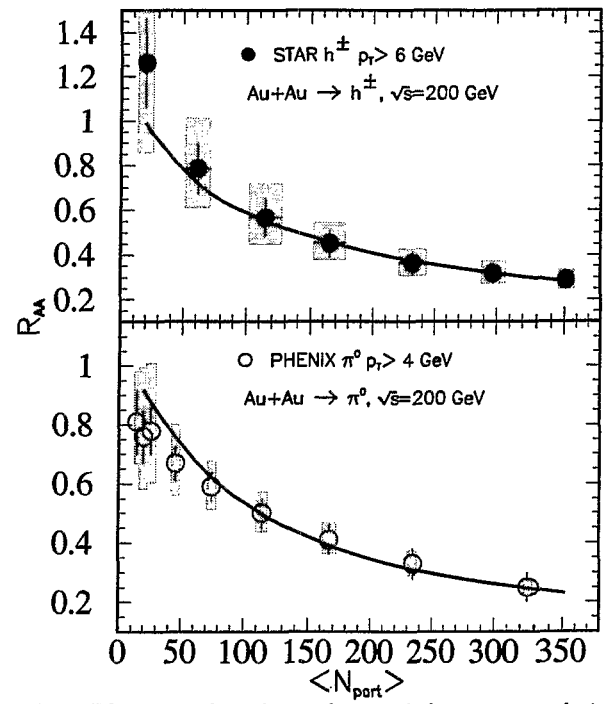

FIG. 6. The centrality dependence of the measured single inclusive hadron suppression [7,8] at high-p_T as compared to theoretical calculation with parton energy loss

The flat p_T dependence of the π^0 suppression is a consequence of the strong energy dependence of the parton energy loss as also noted in Refs. [53,54]. This is in sharp contrast to the energy dependence of the suppression in DIS as shown in Fig. 2 and should be a strong indication of the detailed balance effect in a thermal medium. Such an effect also causes the slight rise of R_{AB} at $p_T < 4$ GeV/c in the calculation. In this region, one expects the fragmentation picture to gradually lose its validity and to be taken over by other non-perturbative effects, especially for kaons and baryons. As a consequence, the $(K + p)/\pi$ ratio in central $Au + Au$ collisions is significantly larger than in peripheral $Au+Au$ or $p+p$ collisions [17]. This has been attributed to parton coalescence in the fragmentation of the leading parton [55–57]. The slight flavor dependence of the Cronin effect in $d + Au$ collisions as shown in Fig. 4 could also be attributed to the coalescence effect [59,58]. Such an effect, while providing interesting insight into the hadronization mechanism in the quark gluon plasma, will complicate the picture of jet quenching and introduce large uncertainties in the physics extracted from jet tomography analysis of the experimental data. Fortunately, the effect has been

shown to disappear at large $p_T > 5$ GeV/c both in the coalescence models and the experimental data. The suppression ratio of charged hadrons and π^0 and of Λ and K all converge [19] at large p_T. In the calculation shown in Fig. 5, a nuclear-dependent (proportional to $\langle N_{\rm binary}\rangle$) soft component was added to kaon and baryon fragmentation functions to take into account the coalescence effect, so that $(K+p)/\pi \approx 2$ at $p_T \sim 3$ GeV/c in the most central $Au+Au$ collisions and it approaches its $p+p$ value at $p_T > 5$ GeV/c. To demonstrate the sensitivity to the parameterized parton energy loss in the intermediate p_T region, we also show $R_{AA}^{h^\pm}$ in 0-5% centrality (dashed line) for $\mu = 2.0$ GeV and $\epsilon_0 = 2.04$ GeV/fm without the soft component.

The measured centrality dependence of the single hadron suppression in $Au+Au$ collisions, shown in Fig. 6, agrees very well with parton model with energy loss. This is the consequence of the centrality dependence of the averaged total energy loss in Eq. (14), which leads to an effective surface emission of the surviving jets. Jets produced around the core of the overlapped region are strongly suppressed, since they lose the largest amount of energy. The centrality dependence of the suppression is found to be more dominated by the geometry of the produced dense matter than the length dependence of the parton energy loss.

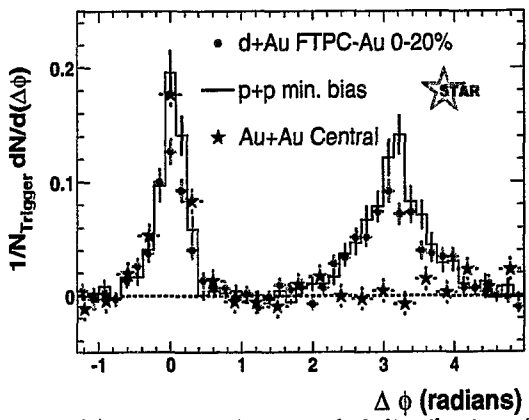

FIG. 7. (a) Two-particle azimuthal distributions for minimum bias and central $d+Au$ collisions, and for $p+p$ collisions [12]. (b) Comparison of two-particle azimuthal distributions for central d+Au collisions to those seen in p+p and central Au+Au collisions.

B. Di-hadron Spectra

Since jets are always produced in pairs in LO pQCD, two-hadron correlations in $p+p$ collisions should have unique characteristics pertaining to the back-to-back jet structure of the initial hard parton-parton scattering. Jet quenching should also modify this di-hadron correlation of the back-to-back jets. Shown in Fig. 7 are the two-hadron correlations in azimuthal angle as measured by STAR experiment in $p+p$, $d+Au$ and $Au+Au$ collisions at RHIC [12]. While the same-side correlation remains the same, the away-side correlation due to the back-side jet is strongly suppressed in central $Au+Au$ collisions. The energy loss that causes the suppression of the single inclusive hadron spectra should also be able to explain the disappearance of away-side correlation.

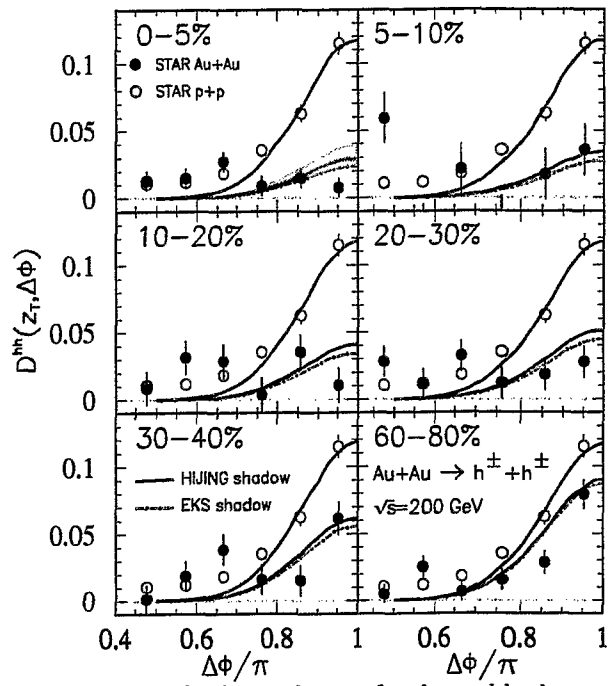

FIG. 8. Back-to-back correlations for charged hadrons with $p_T^{\rm trig} > p_T > 2$ GeV/c, $p_T^{\rm trig} = 4-6$ GeV/c and $|y| < 0.7$ in $Au+Au$ (lower curves) and $p+p$ (upper curves) collisions as compared to the STAR [9] data.

In the same LO pQCD parton model, one can calculate the spectra [60],

$$E_1E_2\frac{d\sigma_{AA}^{h_1h_2}}{d^3p_1d^3p_2} = \frac{K}{2}\sum_{abcd}\int d^2b d^2r dx_a dx_b d^2k_{aT} d^2k_{bT}$$
$$\times t_A(r)t_A(|\mathbf{b}-\mathbf{r}|)g_A(k_{aT},r)g_A(k_{bT},|\mathbf{b}-\mathbf{r}|)$$
$$\times f_{a/A}(x_a,Q^2,r)f_{b/A}(x_b,Q^2,|\mathbf{b}-\mathbf{r}|)$$
$$\times D_{h/c}(z_c,Q^2,\Delta E_c)D_{h/d}(z_d,Q^2,\Delta E_d)\frac{\hat{s}}{2\pi z_c^2 z_d^2}$$
$$\times \frac{d\sigma}{d\hat{t}}(ab\to cd)\delta^4(p_a+p_b-p_c-p_d), \qquad (20)$$

of two back-to-back hadrons from independent fragmentation of the back-to-back jets. Let us assume hadron h_1 is a triggered hadron with $p_{T1} = p_T^{\rm trig}$. One can define a hadron-triggered fragmentation function (FF) as the back-to-back correlation with respect to the triggered hadron:

$$D^{h_1h_2}(z_T,\phi,p_T^{\rm trig}) = p_T^{\rm trig}\frac{d\sigma_{AA}^{h_1h_2}/d^2p_T^{\rm trig}dp_Td\phi}{d\sigma_{AA}^{h_1}/d^2p_T^{\rm trig}}, \qquad (21)$$

similarly to the direct-photon triggered FF [39] in γ-jet events. Here, $z_T = p_T/p_T^{\rm trig}$ and integration over

$|y_{1,2}| < \Delta y$ is implied. In a simple parton model, two jets should be exactly back-to-back. The initial parton transverse momentum distribution in our model will give rise to a Gaussian-like angular distribution. In addition, we also take into account transverse momentum smearing within a jet using a Gaussian distribution with a width of $\langle k_\perp \rangle = 0.6$ GeV/c.

Shown in Fig. 8 are the calculated back-to-back correlations for charged hadrons in $Au + Au$ collisions as compared to STAR data [9]. The same energy loss that is used to calculate single hadron suppression can also describe well the observed away-side hadron suppression and its centrality dependence.

With cross sections integrated over ϕ, one obtains a hadron-triggered FF $D^{h_1 h_2}(z_T, p_T^{\rm trig})$. The suppression factor $I_{AA}(z_T, p_T^{\rm trig}) \equiv D_{AA}^{h_1 h_2}/D_{pp}^{h_1 h_2}$ defined by the STAR experiment [9] is just the medium modification factor of the hadron-triggered FF. The shape of the modification is predicted [60] to be very similar to that of the γ-triggered fragmentation functions [39].

C. High p_T Azimuthal Anisotropy

Another aspect of jet quenching is the azimuthal anisotropy of the spectra caused by parton energy loss which depends on the azimuthal angle according to Eq. (19). In non-central collisions, the average path length of parton propagation will vary with the azimuthal angle relative to the reaction plane. This leads to an azimuthal dependence of the total parton energy loss and therefore azimuthal asymmetry of high-p_T hadron spectra [5,6]. Such an asymmetry is another consequence of parton energy loss and yet it is not sensitive to effects of initial state interactions.

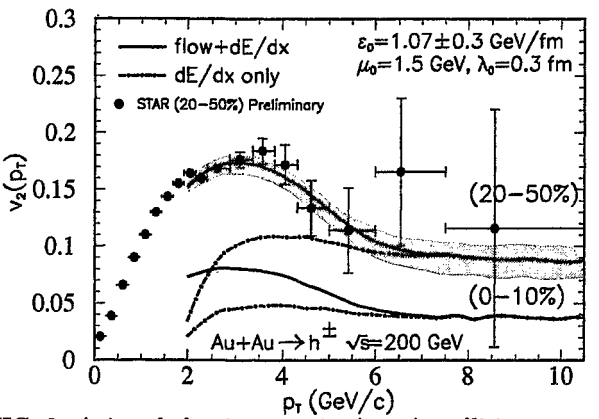

FIG. 9. Azimuthal anisotropy in Au+Au collisions as compared to the STAR [61] 4-particle cumulant result.

In the parton model, the azimuthal angle dependence of the parton energy loss will be given by Eq. (14) for non-central heavy-ion collisions. Using this anisotropic energy loss in the effective modified fragmentation functions in the pQCD parton model of high-p_T hadron spectra, one will obtain azimuthal anisotropic spectra. Shown in Fig. 9 is $v_2(p_T)$ (second Fourier coefficient of the azimuthal angle distribution) of charged hadrons generated from parton energy loss (dot-dashed) as compared to preliminary STAR data [61], using the 4-particle cumulant moments method [62] which is supposed to reduce non-geometrical effects such as inherent two-particle correlations from di-jet production [63]. The energy loss extracted from high-p_T hadron spectra suppression can also account for the observed azimuthal anisotropy at large p_T. At intermediate p_T, the observed v_2 is larger than the simple parton model calculation. Such discrepancy can also be attributed to effects of parton coalescence. If the difference is made up by kaons and baryons from the coalescence contribution, one finds that they must have $v_2 \approx 0.23$ (0.11) for 20-50% (0-10%) collisions. The total $v_2(p_T)$ is shown by the solid lines.

V. JET QUENCHING AND QGP

From both single and di-hadron spectra and their azimuthal anisotropy $v_2(p_T)$, the extracted average energy loss in the parton model calculation for a 10 GeV quark in the expanding medium is $\langle dE/dL \rangle_{1d} \approx 0.85 \pm 0.24$ GeV/fm, which is equivalent to $dE_0/dL \approx 13.8 \pm 3.9$ GeV/fm in a static and uniform medium over a distance $R_A = 6.5$ fm at an initial time $\tau_0 = 0.2$ fm. Compared to the energy loss extracted from HERMES data on DIS, this value is about 30 times higher than the quark energy loss in cold nuclei. Since the parton energy loss in the thin plasma limit is proportional to the gluon number density, one can conclude that the initial gluon density reached in the central $Au + Au$ collisions at 200 GeV should be about 30 times higher than the gluon density in a cold Au nucleus. This number is consistent with the estimate from the measured rapidity density of charged hadrons [64] using the Bjorken scenario [65] and assuming duality between the number of initial gluons and final charged hadrons. Given the measured total transverse energy $dE_T/d\eta \approx 540$ GeV or about 0.8 GeV per charged hadron [66] in central $Au + Au$ collisiona at $\sqrt{s} = 130$ GeV, the initial energy density in the formed dense matter is at least 100 times higher than in cold nuclear matter.

The above analyses of RHIC data on jet quenching are based on an assumption that the dominant mechanism of the jet quenching is parton energy loss before hadronization. It is reasonable to ask whether leading hadrons from the jet fragmentation could have strong interaction with the medium and whether hadron absorption could be the main cause for the observed jet quenching [67,68]. A detailed analysis of jet quenching data concludes [69] that the data are not compatible with such a scenario of hadronic absorption and that the observed patterns of jet quenching in heavy-ion collisions at RHIC are the consequences of parton energy loss.

In addition to the long hadron formation time (it could be about 30-70 fm/c for a 10 GeV pion) estimated from uncertainty principle, there are many patterns of the suppression that can rule out the scenario of hadron absorption. Foremost among them, the large v_2 at high-p_T and the same-side di-hadron correlation cannot be reconciled with the hadron absorption scenario.

Since the spectra azimuthal anisotropy is caused by the eccentricity of the dense medium, which decreases rapidly with time [70] due to transverse expansion, it has to happen at a very early time. By the time of a few fm/c before the formation of any hadron, the eccentricity is already reduced to a non-significant value. Any further interaction cannot produce much spectral anisotropy.

As shown in Fig. 7, while the away-side jet is suppressed in central $Au + Au$ collisions, the same-side di-hadron correlation remains almost the same as in $p + p$ and $d + Au$ collisions. This is clear evidence that jet hadronization takes place outside the dense medium with a reduced parton energy. A recent study [71] of the di-hadron fragmentation functions shows that the conditional (or triggered) di-hadron distribution at large z within a jet is quite stable against radiative evolution (or energy loss). On the other hand, a hadron absorption mechanism will suppress both the leading and secondary hadron in the same way and should lead to the suppression of the same-side correlation. One may argue that the jet whose leading hadron is the trigger hadron could be emitted from the surface and suffer no energy loss and therefore no suppression of the secondary hadron. This is not true. Even though the same-side jet is produced close to the surface due to trigger bias, the parton jet on the average still loses about 2 GeV energy [69], which should be carried by soft hadrons in the direction of the triggered hadron. If one collects all the energy from jet fragmentation for a fixed value of trigger hadron p_T, this energy in central $Au+Au$ collisions should be larger than in $p+p$ collisions by about 2 GeV. This has indeed been confirmed by preliminary data from STAR [15], as shown in Fig. 10, where the scalar sum of the p_T on the same side of the triggered hadron is indeed about 2 GeV larger in central $Au + Au$ than in $p+p$ collisions. The analysis [15] also sees modification of the fragmentation function both along and opposite the trigger hadron direction.

Finally, if hadron absorption can suppress high-p_T hadrons and jets, it would most likely happen in heavy-ion collisions at the SPS energy. Hadron spectra at this energy are very steep at high-p_T and are very sensitive to initial transverse momentum broadening and parton energy loss [45]. However, the measured π spectrum in central $Pb+Pb$ collisions only shows the expected Cronin enhancement [72,73] with no sign of significant suppression. More recent analysis of the $Pb+Pb$ data at the SPS energy also shows [74] that both same-side and back-side jet-like correlations are not suppressed, though the back-side distribution is broadened.

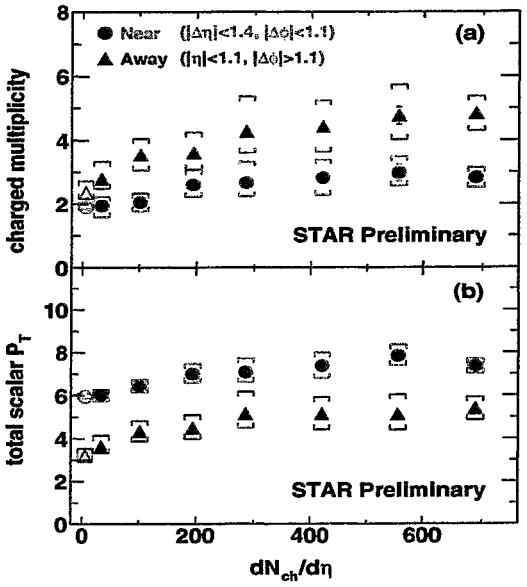

FIG. 10. Charged hadron multiplicity (a) and total scalar p_T (b) of the near and away side jet with $4 < p_T^{trig} < 6$ GeV/c and $0.15 < p_T < 4$ GeV/c in $p+p$ (open symbols) and $Au+Au$ collisions from STAR experiment [15].

VI. SUMMARY AND OUTLOOK

In summary, with the latest measurements of high-p_T hadron spectra and jet correlations in $p+p$, $d+Au$ and $Au+Au$ collisions at RHIC, the observed jet quenching in $Au+Au$ collisions has been established as a consequence of final-state interaction between jets and the produced dense medium. The collective body of data, suppression of high-p_T spectra and back-to-back jet correlation, high-p_T anisotropy and centrality dependence of the observables, points to parton energy loss as the culprit of the observed jet quenching. A simultaneous phenomenological study within a LO pQCD parton model incorporating the parton energy loss describes the experimental data of $Au + Au$ collisions very well. The extracted average energy loss for a 10 GeV quark in the expanding medium is equivalent to an energy loss in a static and uniform medium that is about 30 times larger than in a cold nucleus. This leads us to conclude that the initial gluon (energy) density is about 30 (100) times of that in a cold nuclear matter. It is inconceivable to imagine within our current understanding of QCD that any form of matter other than quark gluon plasma could exist at such a high energy density.

A vast collection of data on bulk properties of particle production in heavy-ion collisions provides further evidence of QGP formation at RHIC. Most striking among these data is the elliptic flow measurement [75] that was found to saturate the hydrodynamic limit and exhibit all the signature behaviors of a collective hydro flow, including the splitting in $v_2(p_T)$ of hadrons with different masses [18,19,76]. Together with jet quenching, they pro-

vide a collection of compelling evidence for the formation of a strongly interacting quark gluon plasma at RHIC.

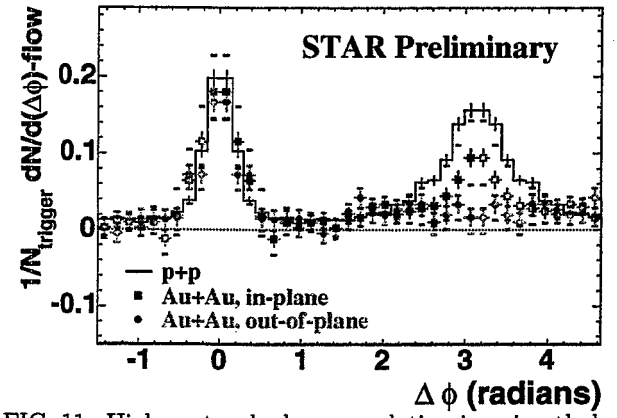

FIG. 11. High-p_T two-hadron correlation in azimuthal angle for different orientation of the trigger hadron with respect to the reaction [14].

The discovery of jet quenching and its central role in characterizing the strongly interacting quark gluon plasma will usher in another new era of studying the properties of the dense matter. With higher-precision data extending to higher p_T, one can find out the missing energy of the suppressed jet [77] and map out in detail the modification of the fragmentation functions and the energy dependence of the energy loss. The preliminary results from STAR [15] on modified fragmentation functions in $Au + Au$ collisions have already demonstrated the potential of the study and could even shed light on parton thermalization and hadronization. The ultimate measurement of a modified FF in heavy-ion collisions will be the direct-γ-triggered FF. Recent preliminary results from PHENIX [16] indicate that such a measurement will be within reach in the next few years.

One can also study the di-hadron correlations with respect to the reaction plane. Shown in Fig. 11 are the preliminary results from STAR [14] on di-hadron correlation in azimuthal angle for different orientations of the trigger hadron with respect to the reaction plane in $Au + Au$ collisions. This could eventually measure the length dependence of the parton energy loss. Measurements of charmed mesons can provide additional tests of the parton energy loss scenario of jet quenching, since recent theoretical studies [78–81] show many unique features of heavy quark energy loss that are different from those of light quarks and gluons.

ACKNOWLEDGEMENT

This work is supported by the Director, Office of Energy Research, Office of High Energy and Nuclear Physics, Divisions of Nuclear Physics, of the U.S. Department of Energy under Contract No. DE-AC03-76SF00098.

[1] X.-N. Wang and M. Gyulassy, Phys. Rev. Lett. **68**, 1480 (1992).
[2] K. Adcox *et al.*, Phys. Rev. Lett. **88**, 022301 (2002).
[3] C. Adler *et al.* [STAR Collaboration], Phys. Rev. Lett. **89**, 202301 (2002).
[4] C. Adler *et al.* [STAR Collaboration], Phys. Rev. Lett. **90**, 032301 (2003).
[5] X.-N. Wang, Phys. Rev. C **63**, 054902 (2001).
[6] M. Gyulassy, I. Vitev and X.-N. Wang, Phys. Rev. Lett. **86**, 2537 (2001).
[7] S. S. Adler *et al.*, Phys. Rev. Lett. **91**, 072301(2003). Phys. Rev. C **69**, 034910 (2004)
[8] J. Adams *et al.* [STAR Collaboration], Phys. Rev. Lett. **91**, 172302 (2003).
[9] C. Adler *et al.* [STAR Collaboration], Phys. Rev. Lett. **90**, 082302 (2003).
[10] M. Plümer, M. Gyulassy and X.-N. Wang, Nucl. Phys. A **590**, 511c (1995).
[11] S. S. Adler *et al.* [PHENIX Collaboration], Phys. Rev. Lett. **91**, 072303 (2003).
[12] J. Adams *et al.* [STAR Collaboration], Phys. Rev. Lett. **91**, 072304 (2003).
[13] B. B. Back *et al.* [PHOBOS Collaboration], Phys. Rev. Lett. **91**, 072302 (2003).
[14] K. Filimonov, in proceedings of 17th International Conference on Ultra Relativistic Nucleus-Nucleus Collisions, Oakland, California, 11-17 Jan 2004.
[15] F. Wang, in proceedings of 17th International Conference on Ultra Relativistic Nucleus-Nucleus Collisions, Oakland, California, 11-17 Jan 2004.
[16] J. Frantz, in proceedings of 17th International Conference on Ultra Relativistic Nucleus-Nucleus Collisions, Oakland, California, 11-17 Jan 2004.
[17] S. S. Adler *et al.* [PHENIX Collaboration], Phys. Rev. Lett. **91**, 172301 (2003).
[18] S. S. Adler *et al.* [PHENIX Collaboration], Phys. Rev. Lett. **91**, 182301 (2003).
[19] J. Adams *et al.* [STAR Collaboration], Phys. Rev. Lett. **92**, 052302 (2004).
[20] J. D. Bjorken, FERMILAB-PUB-82-059-THY.
[21] M. Gyulassy and M. Plümer, Phys. Lett. B **243**, 432 (1990).
[22] R. Baier, D. Schiff and B. G. Zakharov, Ann. Rev. Nucl. Part. Sci. **50**, 37 (2000).
[23] M. Gyulassy, I. Vitev, X.-N. Wang and B. W. Zhang, arXiv:nucl-th/0302077, in Quark Gluon Plasma 3, eds. R. C. Hwa and X.-N. Wang (World Scientific, Singapore, 2004).
[24] A. Kovner and U. A. Wiedemann, arXiv:hep-ph/0304151,in Quark Gluon Plasma 3, eds. R. C. Hwa and X.-N. Wang (World Scientific, Singapore, 2004).
[25] X.-N. Wang, Phys. Rept. **280**, 287 (1997).
[26] M. H. Thoma and M. Gyulassy, Nucl. Phys. B **351** (1991) 491.
[27] S. J. Brodsky and P. Hoyer, Phys. Lett. B **298** (1993) 165.
[28] L. D. Landau and I. J. Pomeranchuk, Dokl. Akad. Nauk Ser.Fiz. 92 (1953) 92; A. B. Migdal, Phys. Rev. **103** (1956) 1811.
[29] M. Gyulassy and X.-N. Wang, Nucl. Phys. B **420** (1994)

583. X.-N. Wang, M. Gyulassy and M. Plumer, Phys. Rev. D **51** (1995) 3436.
[30] R. Baier, Y. L. Dokshitzer, S. Peigne and D. Schiff, Phys. Lett. B **345** (1995) 277. R. Baier, Y. L. Dokshitzer, A. H. Mueller, S. Peigne and D. Schiff, Nucl. Phys. B **484** (1997) 265.
[31] B. G. Zakharov, JETP Lett. **63** (1996) 952.
[32] X. F. Guo and X.-N. Wang, Phys. Rev. Lett. **85** (2000) 3591; X.-N. Wang and X. F. Guo, Nucl. Phys. A **696**, 788 (2001).
[33] M. Gyulassy, P. Levai and I. Vitev, Phys. Rev. Lett. **85** (2000) 5535. M. Gyulassy, P. Levai and I. Vitev, Nucl. Phys. B **594** (2001) 371.
[34] U. A. Wiedemann, Nucl. Phys. A **690** (2001) 731.
[35] E. Wang and X.-N. Wang, Phys. Rev. Lett. **89**, 162301 (2002).
[36] C. A. Salgado and U. A. Wiedemann, Phys. Rev. Lett. **89**, 092303 (2002).
[37] E. Wang and X.-N. Wang, Phys. Rev. Lett. **87**, 142301 (2001).
[38] R. Baier, Y. L. Dokshitzer, A. H. Mueller and D. Schiff, Phys. Rev. C **60** (1999) 064902.
[39] X.-N. Wang, Z. Huang and I. Sarcevic, Phys. Rev. Lett. **77** (1996) 231. X.-N. Wang and Z. Huang, Phys. Rev. C **55** (1997) 3047.
[40] B. W. Zhang and X.-N. Wang, Nucl. Phys. A **720**, 429 (2003).
[41] M. Luo, J. Qiu and G. Sterman, Phys. Lett. **B279**, 377 (1992); M. Luo, J. Qiu and G. Sterman, Phys. Rev. D**50**, 1951 (1994); M. Luo, J. Qiu and G. Sterman, Phys. Rev. D**49**, 4493 (1994).
[42] J. Osborne and X.-N. Wang, Nucl. Phys. A **710**, 281 (2002).
[43] A. Airapetian *et al.* [HERMES Collaboration], Eur. Phys. J. C **20**, 479 (2001); V. Muccifora [HERMES Collaboration], arXiv:hep-ex/0106088.
[44] R. Baier, Y. L. Dokshitzer, A. H. Mueller, S. Peigne and D. Schiff, Nucl. Phys. B **484**, 265 (1997).
[45] X.-N. Wang, Phys. Rev. C **61**, 064910 (2000).
[46] X.-N. Wang, Nucl. Phys. A **702**, 238 (2002).
[47] J. Binnewies, B. A. Kniehl and G. Kramer, Z. Phys. C **65**, 471 (1995).
[48] A. D. Martin, R. G. Roberts, W. J. Stirling and R. S. Thorne, Eur. Phys. J. C **4**, 463 (1998).
[49] S. Y. Li and X.-N. Wang, Phys. Lett. B **527**, 85 (2002).
[50] C. Albajar *et al.* [UA1 Collaboration], Nucl. Phys. B **335**, 261 (1990).
[51] F. Abe *et al.* [CDF Collaboration], Phys. Rev. Lett. **61**, 1819 (1988).
[52] K. J. Eskola, V. J. Kolhinen and C. A. Salgado, Eur. Phys. J. C **9**, 61 (1999).
[53] S. Y. Jeon, J. Jalilian-Marian and I. Sarcevic, Phys. Lett. B **562**, 45 (2003).
[54] B. Müller, Phys. Rev. C **67**, 061901 (2003).
[55] R. C. Hwa and C. B. Yang, Phys. Rev. C **67**, 034902 (2003).
[56] R. J. Fries, B. Müller, C. Nonaka and S. A. Bass, Phys. Rev. Lett. **90**, 202303 (2003).
[57] V. Greco, C. M. Ko and P. Levai, Phys. Rev. Lett. **90**, 202302 (2003).
[58] R. C. Hwa and C. B. Yang, arXiv:nucl-th/0403001.
[59] X. F. Zhang and G. I. Fai, arXiv:hep-ph/0306227.
[60] X.-N. Wang, arXiv:nucl-th/0305010.
[61] R. Snellings, arXiv:nucl-ex/0305001.
[62] N. Borghini, P. M. Dinh and J. Y. Ollitrault, Phys. Rev. C **64**, 054901 (2001).
[63] Y. V. Kovchegov and K. L. Tuchin, Nucl. Phys. A **708**, 413 (2002).
[64] B. B. Back *et al.* [PHOBOS Collaboration], Phys. Rev. Lett. **88**, 022302 (2002).
[65] J. D. Bjorken, Phys. Rev. D **27**, 140 (1983).
[66] K. Adcox *et al.* [PHENIX Collaboration], Phys. Rev. Lett. **87**, 052301 (2001).
[67] T. Falter and U. Mosel, Phys. Rev. C **66**, 024608 (2002).
[68] K. Gallmeister, C. Greiner and Z. Xu, Phys. Rev. C **67**, 044905 (2003).
[69] X.-N. Wang, Phys. Lett. B **579**, 299 (2004).
[70] P. F. Kolb, J. Sollfrank and U. W. Heinz, Phys. Rev. C **62**, 054909 (2000).
[71] A. Majumder and X.-N. Wang, arXiv:hep-ph/0402245.
[72] M. M. Aggarwal *et al.* [WA98 Collaboration], Phys. Rev. Lett. **81**, 4087 (1998) [Erratum-ibid. **84**, 578 (2000)]. Eur. Phys. J. C **23**, 225 (2002).
[73] X.-N. Wang, Phys. Rev. Lett. **81**, 2655 (1998).
[74] G. Agakichiev *et al.* [CERES/NA45 Collaboration], arXiv:nucl-ex/0303014.
[75] K. H. Ackermann *et al.* [STAR Collaboration], Phys. Rev. Lett. **86**, 402 (2001).
[76] P. R. Sorensen, Ph.D. Thesis (UCLA), arXiv:nucl-ex/0309003.
[77] S. Pal and S. Pratt, Phys. Lett. B **574**, 21 (2003).
[78] Y. L. Dokshitzer and D. E. Kharzeev, Phys. Lett. B **519**, 199 (2001).
[79] M. Djordjevic and M. Gyulassy, Phys. Lett. B **560**, 37 (2003).
[80] B. W. Zhang, E. Wang and X.-N. Wang, arXiv:nucl-th/0309040.
[81] N. Armesto, C. A. Salgado and U. A. Wiedemann, arXiv:hep-ph/0312106.

Collective Flow Signals the Quark Gluon Plasma

Horst Stöcker

Collective Flow signals the Quark Gluon Plasma *

H. Stöcker

Frankfurt Institute for Advanced Studies (FIAS), and
Institut für Theoretische Physik,
Johann Wolfgang Goethe - Universität,
Robert Mayer Str. 8-10,
60054 Frankfurt am Main, Germany

Abstract

A critical discussion of the present status of the CERN experiments on charm and flow and their interpretation is given. I emphasize the importance of the flow excitation function from 1 to 50 AGeV: the hydrodynamic model predicted the collapse of the v_1-flow and of the v_2-flow at ~ 10 AGeV. At 40 AGeV it has been recently observed. Hadronic rescattering models predict much larger flow than observed. I interpret this as evidence for a first order phase transition at high ρ_B.

A critical discussion of the use of collective flow as a barometer for the equation of state (EoS) of hot dense matter at RHIC follows. Hadronic rescattering models can explain $< 30\%$ of the observed flow, v_2, for $p_T > 1$ GeV/c. I interpret this as evidence for the production of superdense matter at RHIC, with initial pressure way above hadronic pressure, $p > 1$ GeV fm^{-3}. The fluctuations in the flow, v_1 and v_2, should be measured. Ideal Hydrodynamics predicts that they are larger than 50 % due to initial state fluctuations. The QGP coefficient of viscosity may be determined experimentally from the fluctuations observed. The connection of v_2 to jet suppression is examined. It is proven experimentally that the collective flow is not faked by minijet fragmentation and that the away-side jet suppression can only partially ($< 50\%$) be due to hadronic rescattering. I propose upgrades and second generation experiments at RHIC which inspect the first order phase transition in the fragmentation region, i.e. at $\mu_B \approx 400$ MeV, around $y \approx 4-5$, where the collapse of the proton flow analogous to the 40 AGeV data should be seen. The study of Jet-Wake-riding potentials and Bow shocks caused by jets in the QGP formed at RHIC can give further clues on the equation of state (EoS) and transport coefficients of the Quark Gluon Plasma (QGP).

Lattice QCD results [1, 2], Fig. 1, show a crossing, but no first order phase transition to the QGP for vanishing or small chemical potentials, i.e. at the conditions accessible at central rapidities at RHIC full energies.

*Supported by DFG, GSI, BMBF, EU, RIKEN and DOE

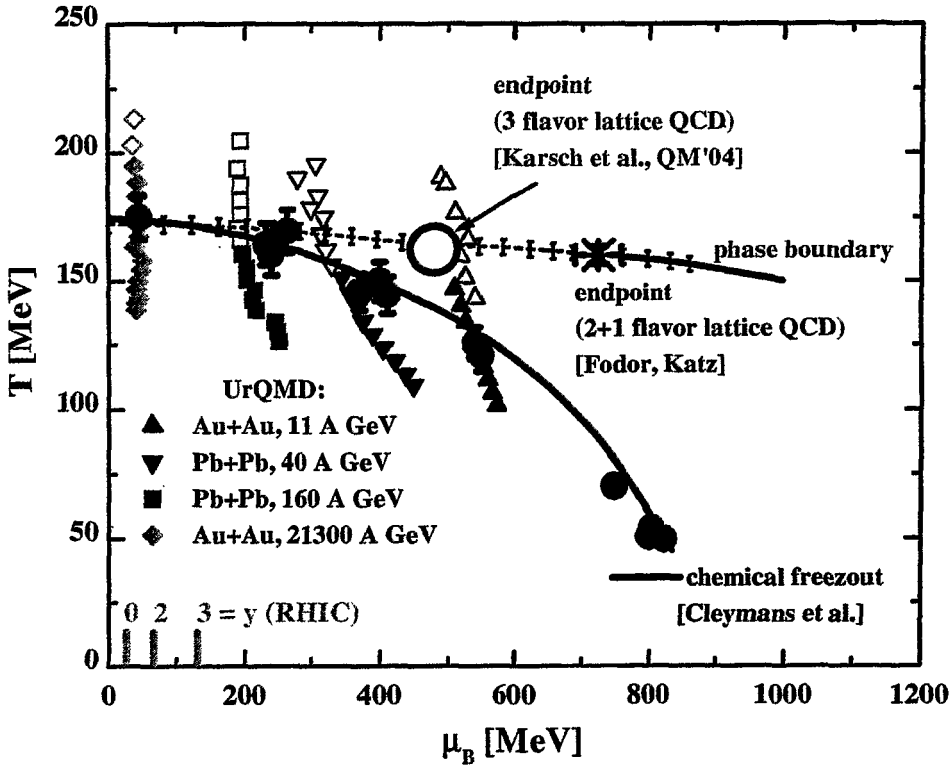

Figure 1: The new phase diagram with the critical end point at $\mu_B \approx 400$ MeV, $T \approx 160$ MeV as predicted by Lattice QCD. In addition, the time evolution, in the $T - \mu$-plane of a central cell in UrQMD calculations [3, 4] are depicted for different bombarding energies. Note that the calculations indicate that $E_{LAB} \lesssim 40$ AGeV are needed to probe to first order phase transition. At RHIC (see insert at μ_B scale) this point is accessible at the fragmentation region only. (Figure taken from [5])

1 Old and new observables for the Quark Gluon Plasma phase transition

A first order phase transition does occur according to [1, 2] only at high baryochemical potentials or densities, i.e. at SIS-300 and lower SPS energies and in the fragmentation region of RHIC, $y \approx 4 - 5$ [6, 7]. The critical baryochemical potential is predicted [1, 2] to be $\mu_B^c \approx 400 \pm 50$ MeV and the critical temperature $T_c \approx 150 - 160$ MeV. We do expect a phase transition also at finite strangeness. Predictions for the phase diagram of strongly interacting matter for realistic non-vanishing net strangeness are urgently needed, to obtain a comprehensive picture of the QCD phase structure. Multi-Strangeness degrees of freedom are very promising probes for the properties of the dense and hot matter [8]. The Strangeness distillation process [9, 10] predicts dynamical de-admixture of s and $\bar{s}$ quarks, which yields unique signatures for QGP creation: high multistrange hyperon-/-matter production, strangelet formation and unusual antibaryon to baryon ratios, to mention a few.

1.1 Thermodynamics in the $T - \mu_B$ plane

A comparison of the thermodynamic parameters T and μ_B extracted from the UrQMD-transport model in the central overlap regime of Au+Au collisions [5] with the QCD predictions is shown in Fig 1. The full dots with errorbars denote the 'experimental' chemical freeze-out parameters - determined from fits to the experimental yields - taken from Ref. [11]. The triangular and quadratic symbols (time-ordered

in vertical sequence) stand for temperatures T and chemical potentials μ_B extracted from UrQMD transport calculations in central Au+Au (Pb+Pb) collisions at RHIC (21.3 A·TeV), 160, 40 and 11 A·GeV [3, 4] as a function of the reaction time (separated by 1 fm/c steps from top to bottom). The open symbols denote nonequilibrium configurations and correspond to T parameters extracted from the transverse momentum distributions, whereas the full symbols denote configurations in approximate pressure equilibrium in longitudinal and transverse direction.

During the nonequilibrium phase (open symbols) the transport calculations show much higher temperatures (or energy densities) than the 'experimental' chemical freeze-out configurations at all bombarding energies ($\geq$ 11 A·GeV). These numbers are also higher than the critical point (circle) of (2+1)f-Lattice QCD calculations by the Bielefeld-Swansea-collaboration [2] (large open circle) and by the Wuppertal-Budapest-collaboration [1] (star shows earlier results [12, 13]). The energy density at μ_c, T_c is on the order of $\approx$ 1 GeV/fm^3. At RHIC energies a cross-over is expected at midrapidity, when stepping down in temperature during the expansion phase of the 'hot fireball'. The baryon chemical potential μ_B for different rapidity intervals at RHIC energies has been obtained from a statistical model analysis by the BRAHMS Collaboration based on measured antihadron to hadron yield ratios [14]. For midrapidity, $\mu_B \simeq 0$, whereas for forward rapidities μ_B increases up to $\mu_B \simeq 130$ MeV at $y = 3$. Thus, only extended forward rapidity measurement ($y \approx 4 - 5$) will allow to probe large μ_B at RHIC. The detectors at RHIC at present offer only a limited chemical potential range. To reach the first order phase transition region at midrapidity, the International Facility at GSI seems to be the right place to go: This situation changes at lower SPS, top AGS, as well as at the future GSI SIS-300 energies: sufficiently large chemical potentials μ_B reached allow for a first order phase transition [15] to the right of the critical point in the (T, μ_B) plane. The transport calculations show high temperatures (high energy densities) in the very early phase of the collisions only. Here, hadronic interactions are weak due to formation time effects and yield little pressure. Diquark, quark and gluon interactions can cure this problem at RHIC.

1.2 *Open charm and charmonia at SPS and RHIC*[16]

Open charm and charmonium production at SPS and RHIC energies has been calculated within the HSD and UrQMD transport approaches using parametrizations for the elementary production channels including the charmed hadrons $D, \bar{D}, D^*, \bar{D}^*, D_s, \bar{D}_s, D_s^*, \bar{D}_s^*$, $J/\Psi, \Psi(2S), \chi_{2c}$ from NN and πN collisions. The latter parametrizations are fitted to PYTHIA calculations [17] above $\sqrt{s} = 10$ GeV and extrapolated to the individual thresholds, while the absolute strength of the cross sections is fixed by the experimental data as described in Ref. [18], for previous works see [19, 20, 21] Backward channels 'charm + anticharm meson $\rightarrow$ charmonia + meson' are treated and detailed balance is employed in a more schematic interaction model with a single parameter or matrix element $|M|^2$ that is fixed by the J/Ψ suppression data from the NA50 collaboration at SPS energies (cf. Ref. [22]).

Charmonium suppression had been proposed as "the clearest" QGP-signature and the community has been riding on this folklore for more than a decade. Hence, these detailed comparisons come as a shock: The $Pb + Pb$ results at 160 A GeV, both from UrQMD and HSD transport dissociation are well in line with the data of the NA50 Collaboration (Fig. 2): the J/Ψ suppression is shown as a function of the transverse energy E_T.

The solid line stands for the HSD result within the comover absorption scenario while the various data points reflect the preliminary NA50 data from the year 2000 (analysis A,B,C). The data have moved so that they agree now with old predictions of the UrQMD model [21] (dashed histogram in Fig. 2). We mention that there might be alternative explanations for J/Ψ suppression, as discussed in Refs. [23, 24] and/or further (dissociation) mechanisms not considered here. However, for the purposes of the present study it is sufficient to point out that

a) no sign of unusual physics can be related to the J/Ψ data and

b) the models employed here (cf. Figs. 6 and 7 in [22]) most likely give upper limits and do not lead to a sizeable re-creation of charmonia by $D + \bar{D}$ channels at SPS energies.

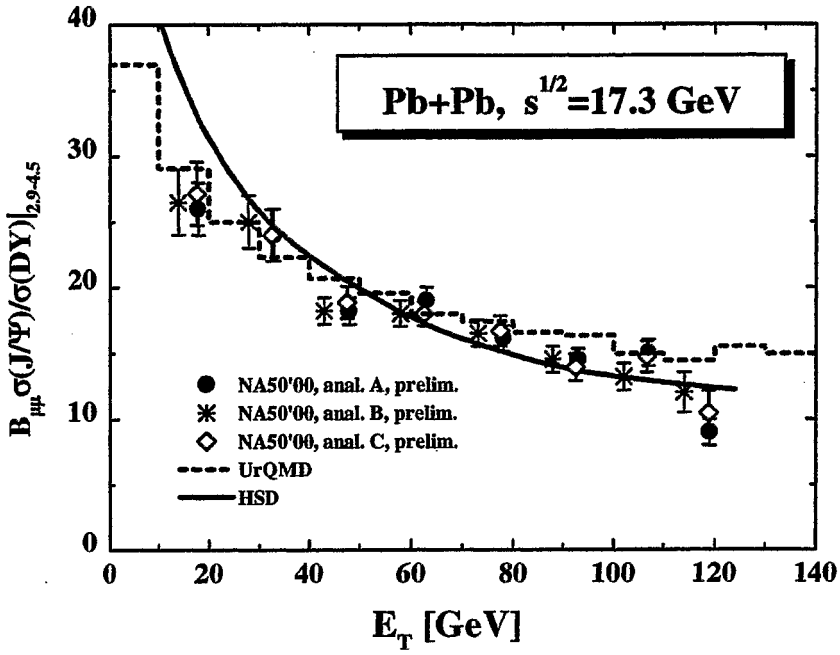

Figure 2: The J/Ψ suppression as a function of the transverse energy E_T in $Pb + Pb$ collisions at 160 A GeV. The solid line shows the HSD result within the comover absorption scenario [22]. The different symbols stand for the NA50 data [25] from the year 2000 (analysis A,B,C) while the dashed histogram is the original UrQMD prediction [21].

At RHIC, central $Au + Au$ collisions at $\sqrt{s} = 200$ GeV will, however, produce multiplicities of open charm pairs about 2 orders of magnitude larger than at 160 A·GeV, such that a much higher J/Ψ reformation rate ($\sim N_{c\bar{c}}^2$) is expected at RHIC energies (cf. Ref. [24]). At RHIC top energy, $\sqrt{s} =$ 200 GeV, the J/Ψ comover dissociation may no longer be important, since the charmonia dissociated in this channel are approximately recreated in the backward channels. Hence, the J/Ψ dissociation at RHIC should be less pronounced than at SPS energies.

The preliminary data of the PHENIX Collaboration [26] allow for a first glance at the situation encountered in $Au + Au$ collisions at $\sqrt{s} = 200$ GeV. Fig. 3 shows the J/Ψ multiplicity per binary collision as a function of the number of participating nucleons, in comparison to the data at midrapidity. The statistics is quite limited, so no final conclusion can presently be drawn. However, the data neither suggest a dramatic enhancement of J/Ψ production nor a complete 'melting' of the charmonia in the QGP phase.

1.3 Historical Interlude

Hydrodynamic flow and shock formation has been proposed early [27, 28] as the key mechanism for the creation of hot and dense matter during relativistic heavy ion collisions. The full three-dimensional hydrodynamical flow problem is much more complicated than the one-dimensional Landau model [29]: the 3-dimensional compression and expansion dynamics yields complex triple differential cross-sections, which give excellent spectroscopic handles on the equation of state: The bounce-off, $v_1(p_T)$, the squeeze-out, $v_2(p_T)$, and the antiflow [30, 31, 32, 33, 34] (third flow component [35, 36]) serve as differential barometers for the properties of compressed, dense matter, from SIS to RHIC. The most employed flow observables are:

$$v_1 = \frac{p_x}{p_T} \tag{1}$$

$$v_2 = \frac{p_x^2 - p_y^2}{p_x^2 + p_y^2}\,. \tag{2}$$

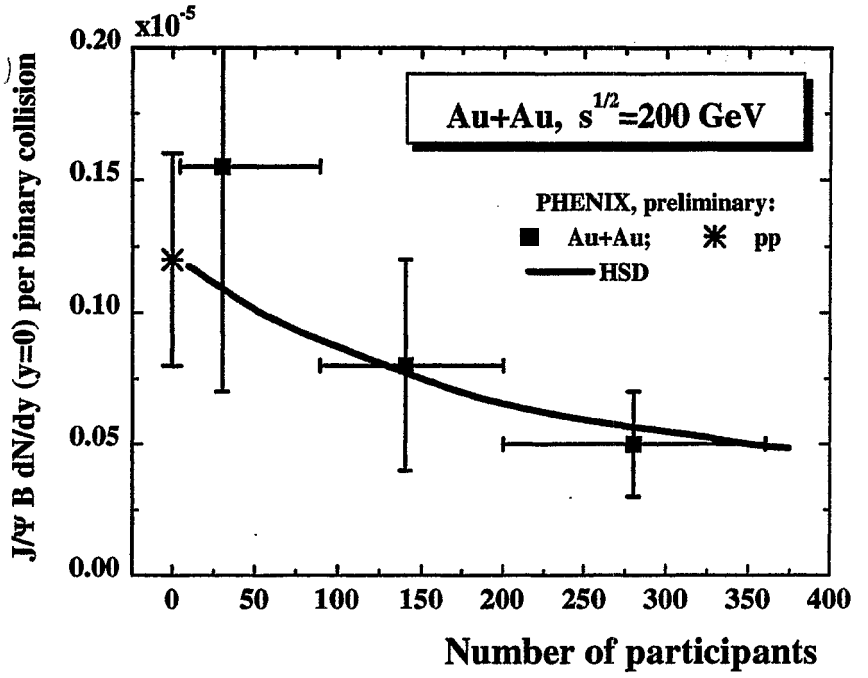

Figure 3: The calculated J/Ψ multiplicity per binary collision – multiplied by the branching to dileptons – as a function of the number of participating nucleons, N_{part}, in comparison to the preliminary data from the PHENIX collaboration [26] for $Au+Au$ and pp reactions (taken from Ref. [22]).

Here, p_x denotes the momentum in x-direction, i.e. the transversal momentum within the reaction plane and p_y the transversal momentum out of the reaction plane. The total transverse momentum is given as $p_T = \sqrt{p_x^2 + p_y^2}$, the z-axis is in the beam direction. Thus, v_1 measures the "bounce-off", i.e. the strength of the directed flow in the reaction plane, and v_2 gives the strength of the second moment of the azimuthal particle emission distribution, the so-called "squeeze-out". [27, 28, 30, 31, 32, 33, 34]. In particular, it has been shown [28, 30, 31, 32, 33, 34] that the disappearence or "collapse" of flow is a direct result of a first order phase transition.

Several hydrodynamic models have been used in the past, starting with the one-fluid ideal hydrodynamic approach. This model predicts far too large flow effects. To obtain a better description of the dynamics, viscous fluid models have been developed [37, 38, 39]. In parallel, so-called three-fluid models, which distinguish between projectile, target and the fireball, have been considered [40]. Here viscosity effects appear only between the different fluids, but not inside one fluid. The aim is to have at our disposal a reliable, three-dimensional, relativistic three-fluid model including viscosity [38, 39].

Flow can be described very elegantly in hydrodynamics. However, also consider microscopic multicomponent (pre-)hadron transport theory, e.g. models like qMD [41], IQMD [42], UrQMD [43] or HSD [44], as control models for viscous hydro and as background models to subtract interesting non-hadronic effects from data. If Hydro with and without quark matter EoS, Hadronic transport models without quark matter but with strings are compared to data, can we learn whether quark matter has been formed? What degree of equilibration has been reached? What does the equation of state look like? How are the particle properties, self energies, cross sections changed? To estimate systematic model uncertainties, the results of the different microscopic transport models also have to be carefully compared. The two robust, hadron based models HSD and UrQMD are considered here.

1.4 Review of SPS and AGS results

Microscopic (pre-)hadronic transport models describe the formation and distributions of many hadronic particles at AGS and SPS rather well [45]. Furthermore, the nuclear equation of state has been extracted by comparing to flow data which are described reasonably well up to AGS energies [46, 47, 48, 35]. Ideal

hydro calculations, on the other hand, predict way too much flow at these energies [37]. Thus, viscosity effects have to be taken into account in hydrodynamics. In particular, ideal hydro calculations are

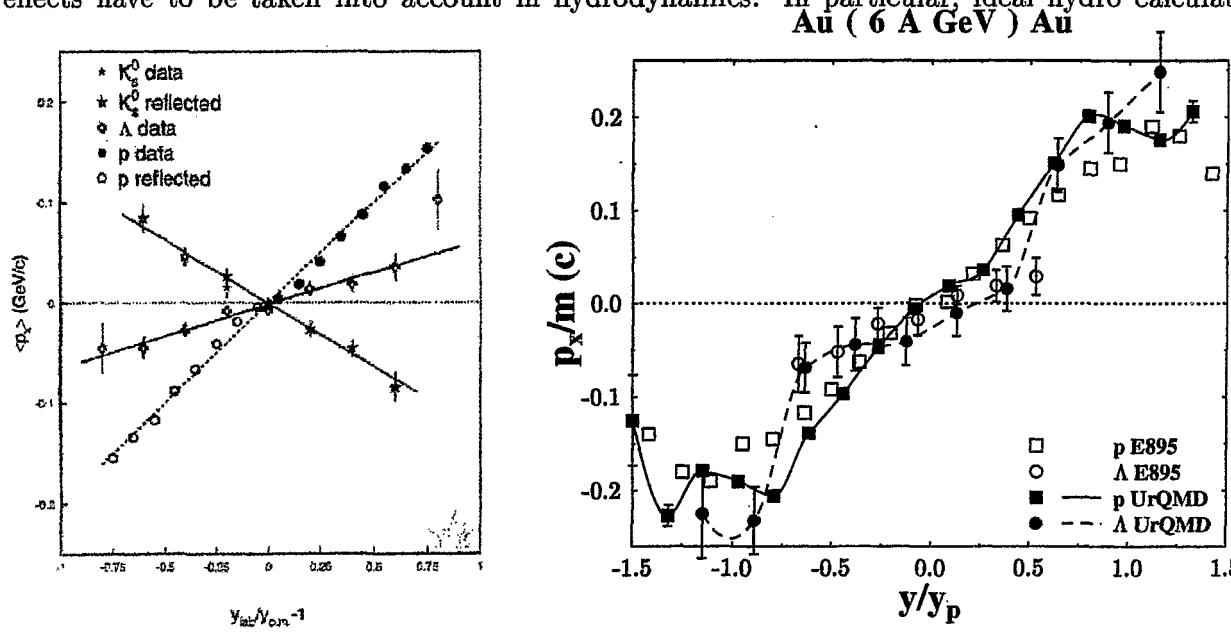

Figure 4: Left: Sideward flow $p_x = v_1 \cdot p_T$ of K, Λ and p's at 6 AGeV as measured by E895 in semi-central collisions at the AGS. Right: Same Directed flow data compared to UrQMD calculations for $b < 7$ fm [48]

factors of two higher than the measured sideward flow at SIS [37] and AGS, while the directed flow p_x/m measurements of the E895 collaboration shows that p and Λ data are reproduced reasonably well [48] (see fig. 4) in UrQMD, i.e. in a hadronic transport theory with reasonable cross-sections, i.e. realistic mean free path. Only ideal hydro calculations predict, however the appearance of a so-called "third flow component" [35] or "antiflow" [49] in central collisions, if, and only if, the matter undergoes a first order phase transition to the QGP: Around midrapidity, the directed flow, $p_x(y)$, of protons develops a negative slope. In contrast, a hadronic EoS without phase transition does not yield such an exotic "antiflow", negative slope, wiggle in the proton flow $v_1(y)$. The ideal hydrodynamic time evolution of the directed flow, p_x/N, for the purely hadronic EoS (Fig. 6 left) does show a clean linear increase of $p_x(y)$, just as the microscopic transport theory (Fig. 4 right) and as the data (Fig. 4 left). For an EoS including a first order phase transition to the QGP (Fig. 6 right), it can be seen, however, that the proton flow value $v_1 \sim p_x/p_T$ collapses . The proton flow collapse occurs around midrapidity. This observation is explained by an antiflow component of protons, which develops when the expansion from the plasma sets in [50].

The ideal hydrodynamic directed proton flow p_x values (Fig. 7) show even negative values between 8 and 20 AGeV. An increase back to positive values is predicted with increasing energy when the compressed QGP is probed. But where is the predicted minimum of the proton flow in the data? The hydro calculations suggest this "softest point collapse" is at $E_{Lab} \approx 8$ AGeV. This has not been verified by the AGS data! However, a linear extrapolation of the AGS data predicts the collapse of the directed proton flow at $E_{Lab} \approx 30$ AGeV (Fig. 7).

Recently, strong evidence for this prediction has been obtained by the low energy 40 AGeV SPS data of the NA49 collaboration [52]: These data clearly exhibit the first occurence of proton "antiflow" around mid-rapidity, in contrast to the AGS data. Thus, at bombarding energies of 30-40 AGeV, a first order phase transition to the baryon rich QGP most likely is observed - the first order phase transition line is crossed. This is the energy region where the new FAIR- facility at GSI will operate. There are

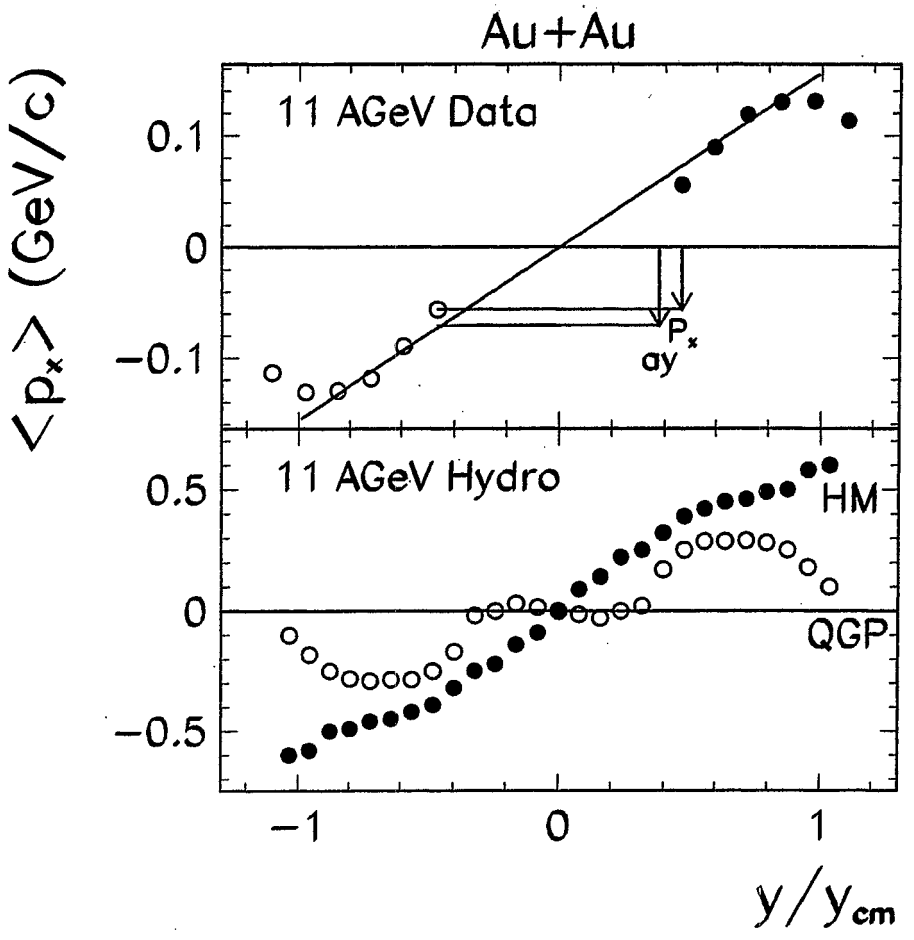

Figure 5: Directed flow from ideal hydrodynamics with and from the Quark Gluon String Model without QGP [35] .

good prospects that the baryon flow collapses and other first order QGP phase transition signals can be studied soon at the lowest SPS energies as well as at the RHIC fragmentation region $y > 4 - 5$. These experiments will enable a detailed study of the first order phase transition at high μ and of the properties of the baryon rich QGP.

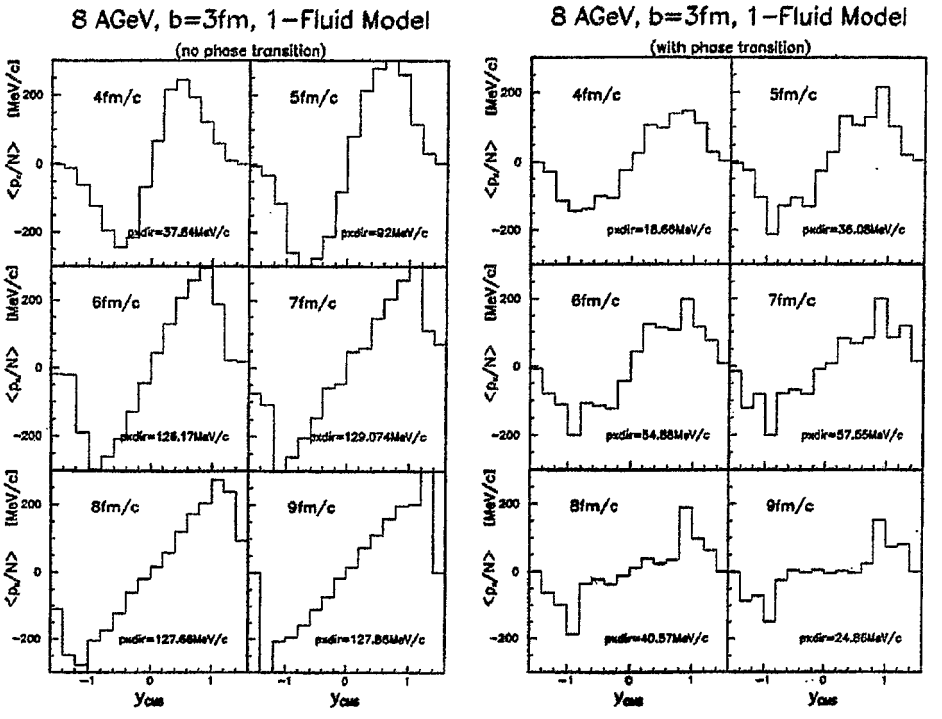

Figure 6: Time evolution of directed flow p_x/N as a function of rapidity for Au+Au collisions at 8 AGeV in the one-fluid model. Left: Hadronic EoS without phase transition. Right: An EoS including a first order phase transition to the QGP is used [49].

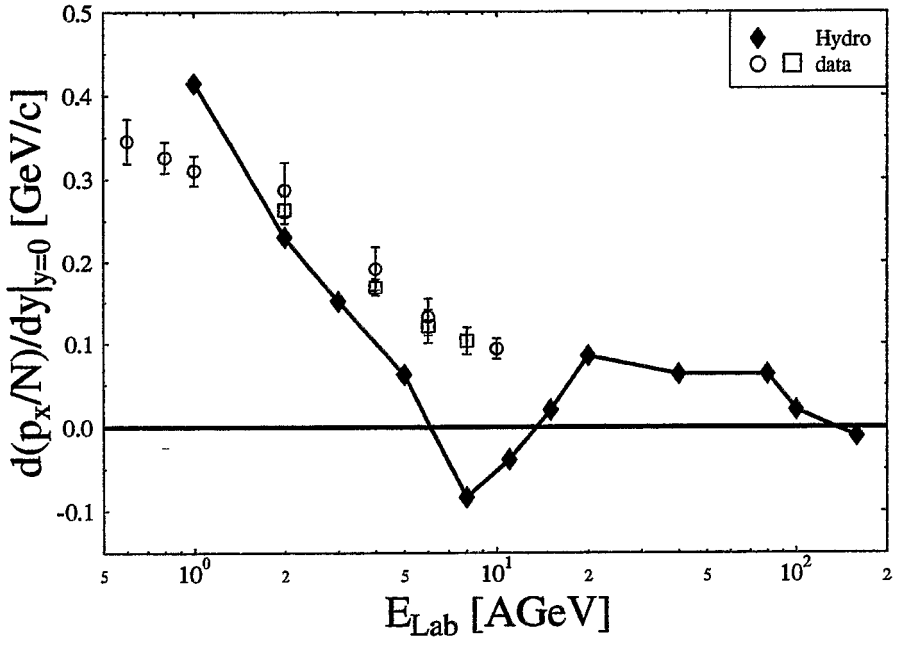

Figure 7: Measured SIS and AGS proton dp_x/dy-slope data compared to a one-fluid hydro calculation. A linear extrapolation of the AGS data predicts the collapse of flow at $E_{Lab} \approx 30AGeV$, i.e. for the lowest SPS- and the upper FAIR- energies at GSI [51]

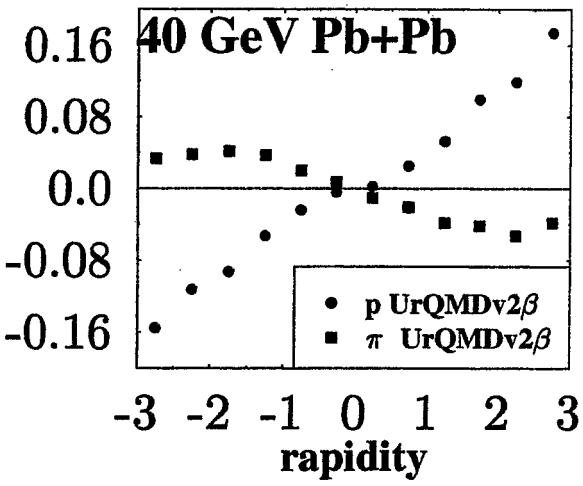

Figure 8: Proton and pion $v_1 = p_x/p_T$ values at 40 AGeV as predicted by the UrQMD model. No proton antiflow is predicted in this hadronic transport theory without phase transition.

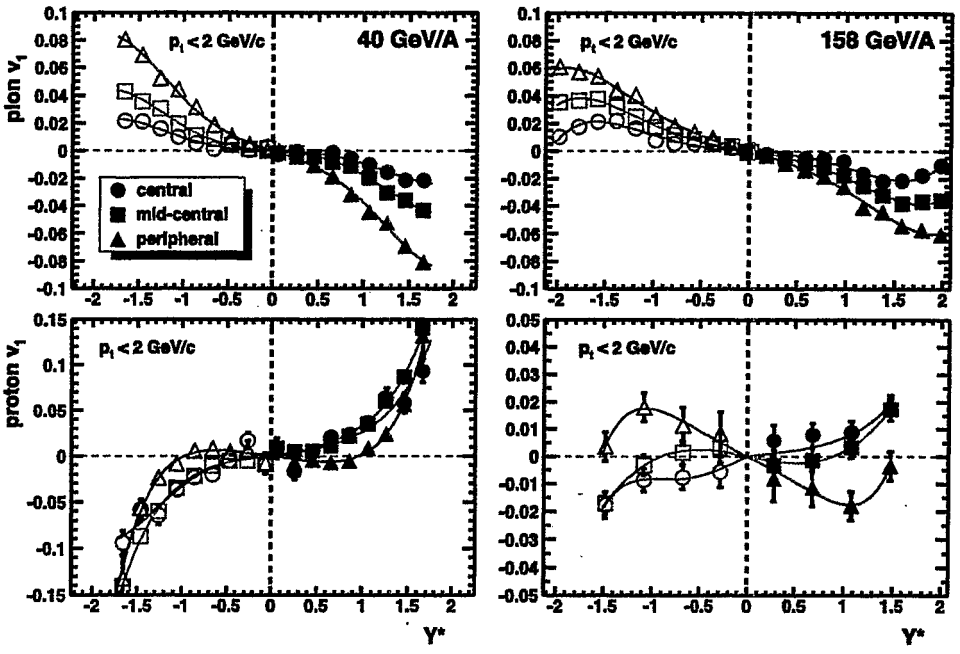

Figure 9: v_1 at SPS, 40 AGeV and 158 AGeV [52] . The proton antiflow is observed in the NA49-experiment even at near central collisions, in contrast to the UrQMD-model (Fig. 8).

2 Proton elliptic flow collapse at 40AGeV - evidence for a first order phase transition at highest net baryon densities

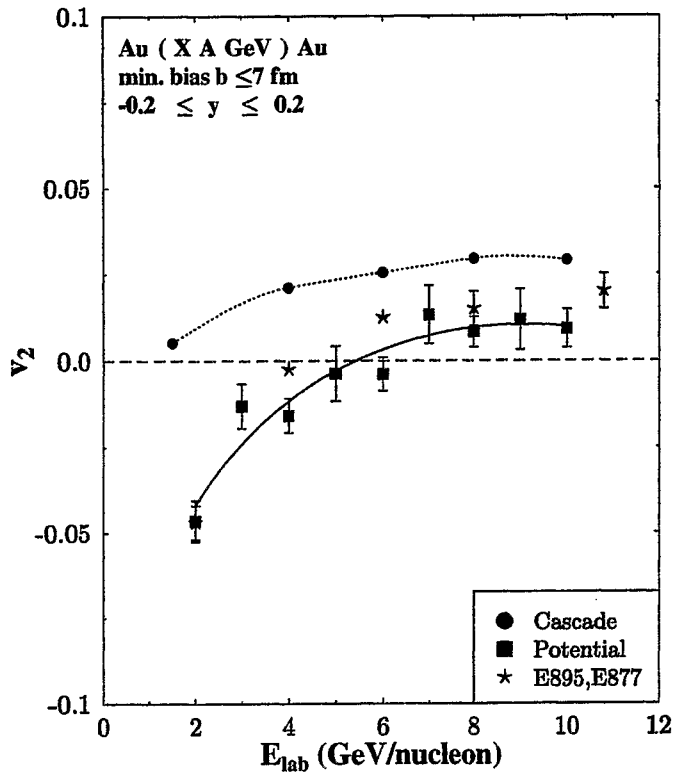

Figure 10: v_2 excitation function of protons at the AGS. The E895-E877 data show the transition from squeeze-out to in-plane proton elliptic flow at 4-5 AGeV; the UrQMD-calculations show the strong sensitivity to the EoS [48].

At SIS energies, microscopic transport models reproduce the data on the excitation function of the proton v_2 quite well: A soft, momentum dependent equation of state [53, 54] seems to account for the data best. The observed proton v_2 is smaller than zero, that corresponds to the squeeze-out predicted by hydrodynamics long ago [27, 28, 30, 31, 32, 33, 34]. The AGS data (Fig. 10) exhibit a transition from squeeze-out to in-plane flow in the midrapidity region. The change in sign of the proton v_2 at 4-5 AGeV is in accord with transport calculations (see the UrQMD calculations in Fig. 10,[48] and references therein). At higher energies, 10-160 AGeV, a smooth increase of the v_2 is predicted from the hadronic transport simulations. The 158 AGeV data of the NA49-collaboration suggest that this smooth increase proceeds between AGS and SPS as predicted. Accordingly, UrQMD predicts considerable (3%) v_2 flow for midcentral and peripheral protons, at 40 AGeV, see Fig.11, [48].

This is in strong contrast to recent NA49 data at 40 AGeV: A sudden collapse of the proton flow is observed, as well for midcentral as for peripheral protons. The collapse of v_2 of protons around midrapidity at 40 AGeV is very pronounced. It is not observed at 158 AGeV. The UrQMD calculations, without a phase transition, show a healthy, but wrong 3% flow of protons - in strong contrast to the data.

A dramatic collapse of the v_1 is also observed by NA49 [52], again around 40 AGeV, where the collapse of v_2 has been observed. This is the highest energy - according to [1, 2] and Fig. 1 - at which a first order phase transition can be reached at the central rapidities of relativistic heavy ion collisions. I therefore conclude that a first order phase transition at the highest baryon densities accessible in nature has been discovered in these energies.

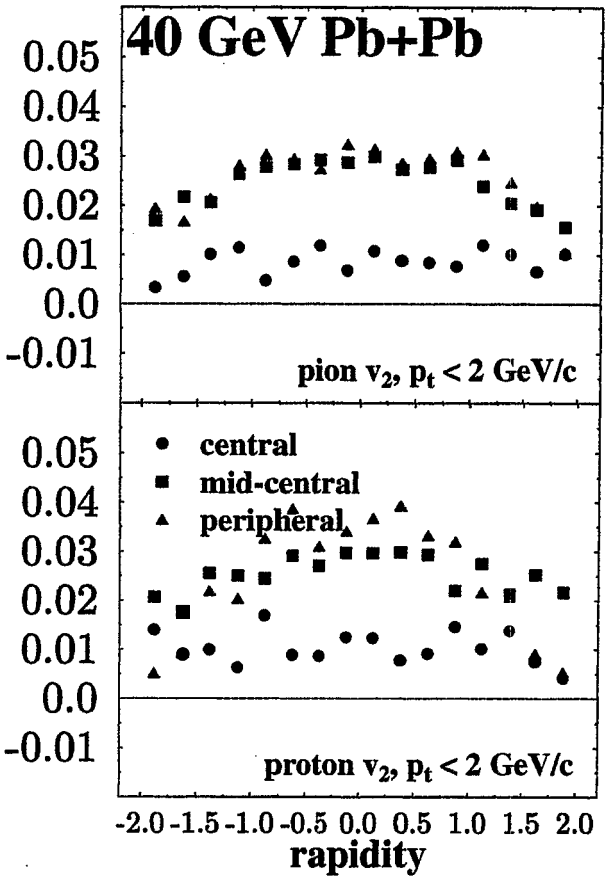

Figure 11: Elliptic flow v_2 of protons (lower frame) and pions (upper frame) versus rapidity for Pb+Pb collisions at 40 AGeV from the UrQMD calculations [48].

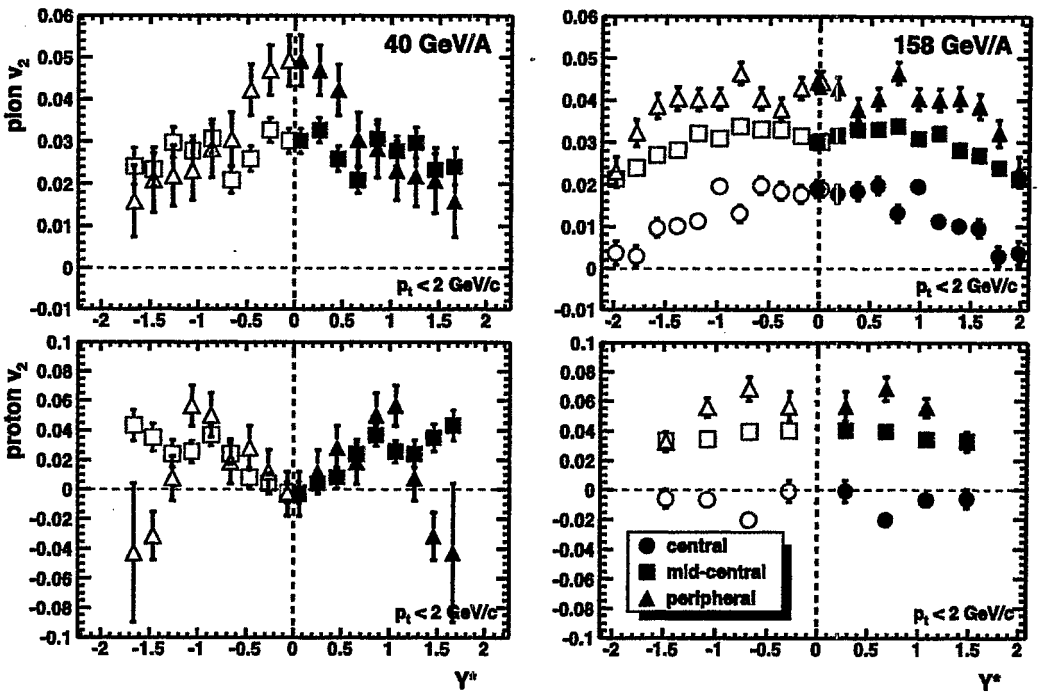

Figure 12: Elliptic flow v_2 of protons collapses versus rapidity at 40 AGeV Pb+Pb collisions [52] measured by NA49 for three centrality bins: central (dots), mid-central (squares) and peripheral (triangles). The solid lines are polynomial fits to the data [52].

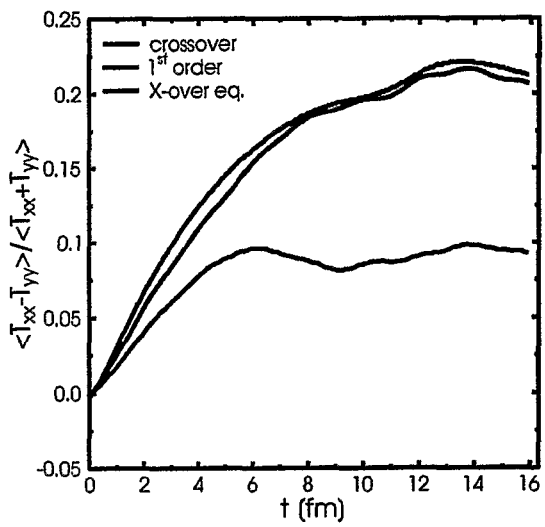

Figure 13: Time evolution of the momentum anisotropy v_2 for a cross over EoS. Both, in- and off-equilibrium calculations shows no drop of the flow - v_2. The calculation with a first order phase transition off-equilibrium shows - on the other hand - the collapse of v_2-flow of protons. Hence, the collapse is only possible for first order transitions [55].

3 Strong collective flow at RHIC signals the QGP

The rapid three body thermalization discovered by Xu and Greiner (see below, Fig. 17) justifies the use of hydrodynamical calculations for the time evolution of the complex four-dimensional expansion of the plasma. However, there is no justification for the use of simple ideal hydrodynamics (i.e. neglecting the important transport coefficients) and simple, smooth initial conditions in hydrodynamics [38, 39, 56]. PHOBOS data at 130 AGeV and 200 AGeV suggest energy independent $v_2(\eta)$ distributions. Furthermore, the observed distribution has a triangular shape. This finding is in in complete disagreement with Bjorken boost invariant hydro predictions [57, 15], which fit only the midrapidity values. The predicted average proton v_2-values obtained from the SPHERIO hydro code with NEXUS initial conditons (Fig. 14, [58]) are factors of two higher than simple smooth initial state hydrodynamic calculations. This indicates that ideal hydro with naive smooth initial conditions as used by many authors do not describe but rather fit the data. Strong viscosity effects can play a role for particles with $p_T < 1.2$ GeV: a decent description of the dynamics requires, however, relativistic viscous hydro simulations [38, 39, 59]. The NexSpherio simulations (Fig. 14, [58]) predict very large e-by-e fluctuations of v_2 caused by the strongly fluctuating initial conditions given by NEXUS. Is this in accord with data? What about the effect on the event plane determination?

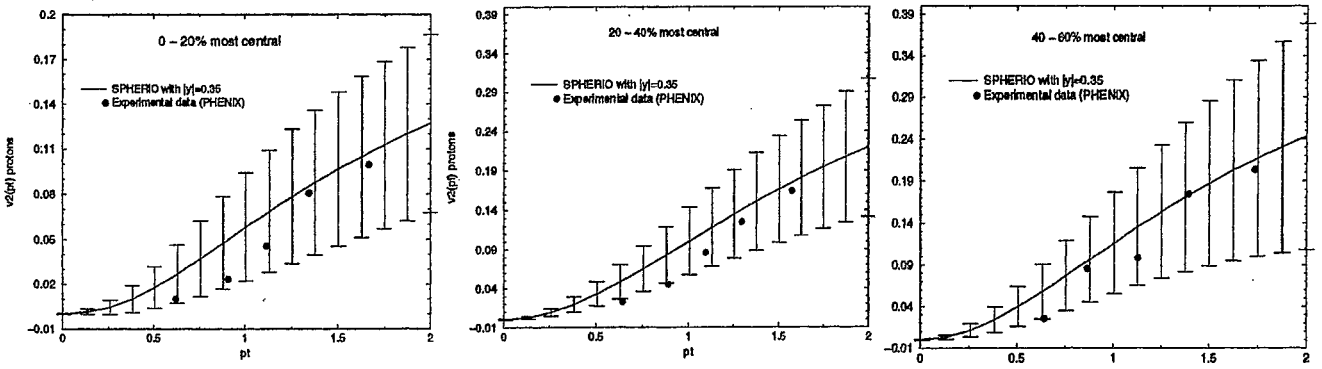

Figure 14: Elliptic flow v_2 of protons as a function of p_T for different centralities. NexSpherio ideal hydro results exhibit about a factor of two higher proton-v_2-values than the PHENIX data up to $p_T = 1$ GeV. Furthermore, the fluctuations in the NEXUS initial conditions for the SPHERIO- ideal hydro simulation reflect in > 50 % fluctuation e-by-e fluctuations of the proton-v_2 values. Only large viscosity effects can damp out the too large v_2 flow itself, as well as the fluctuations in v_2.

Microscopic transport simulations of particle yields, dN/dy distributions, etc. give a good description of the RHIC Au+Au data [22]. The HSD and UrQMD transport approaches are based on string, quark, diquark ($q, \bar{q}, qq, \bar{q}\bar{q}$) as well as hadronic degrees of freedom. At RHIC, UrQMD and HSD yield reasonable abundances of light hadrons, composed of u, d, s quarks[1]. Do they also predict the collective flow properly? The UrQMD prediction did clearly not yield the measured 6% elliptic flow - it is clearly underestimated [61]. Shortening of the formation time [61] can get the model results closer to the data (Fig. 16) but more additional initial pressure, needed to create the missing extra flow, is not justified in the hadronic transport models. At high transverse momenta ($p_T \approx 2GeV$) the v_2-flow is underestimated by a factor of three (see Fig.16) in the HSD model [22]. The microscopic quark-gluon-string model inserts in addition short distance vector repulsion to achieve high flow values [62].

[1]For a more recent survey on hadron rapidity distributions from 2 to 160 A GeV in central nucleus-nucleus collisions within the HSD and UrQMD [60] transport approaches we refer the reader to Ref. [45].

Is a transport approach based on strings and hadronic degrees of freedom adequate in the initial stage of nucleus-nucleus collisions at RHIC energies, where the quark-gluon plasma is formed? Well, the particle abundancies show a rather smooth evolution from SIS to RHIC energies [63, 64]. The effective partonic degrees of freedom in the initial phase are needed to supply the large pressure obviously needed to describe the elliptic flow at RHIC energies. Even 'early' (pre-)hadron formation – as in HSD with $\tau = 0.8$ fm/c – and 'large' (pre-)hadronic interaction cross sections are unsufficient to explain the v_2 flow data. This is demonstrated in Fig. 15, which shows the HSD-calculated elliptic flow v_2 for charged hadrons (solid lines) as a function of the pseudorapidity η (upper part) and as a function of the number of 'participating nucleons' N_{part} (lower part) for $|\eta| \leq 1$ in comparison to the preliminary 'hit-based analysis' data of the PHOBOS Collaboration [65]. The HSD results are very similar to those of the hadronic rescattering model by Humanic et al. [66, 67] which completely ignores formation times and agree with the calculations by Sahu et al. [68] performed within the hadron-string cascade model JAM [69].

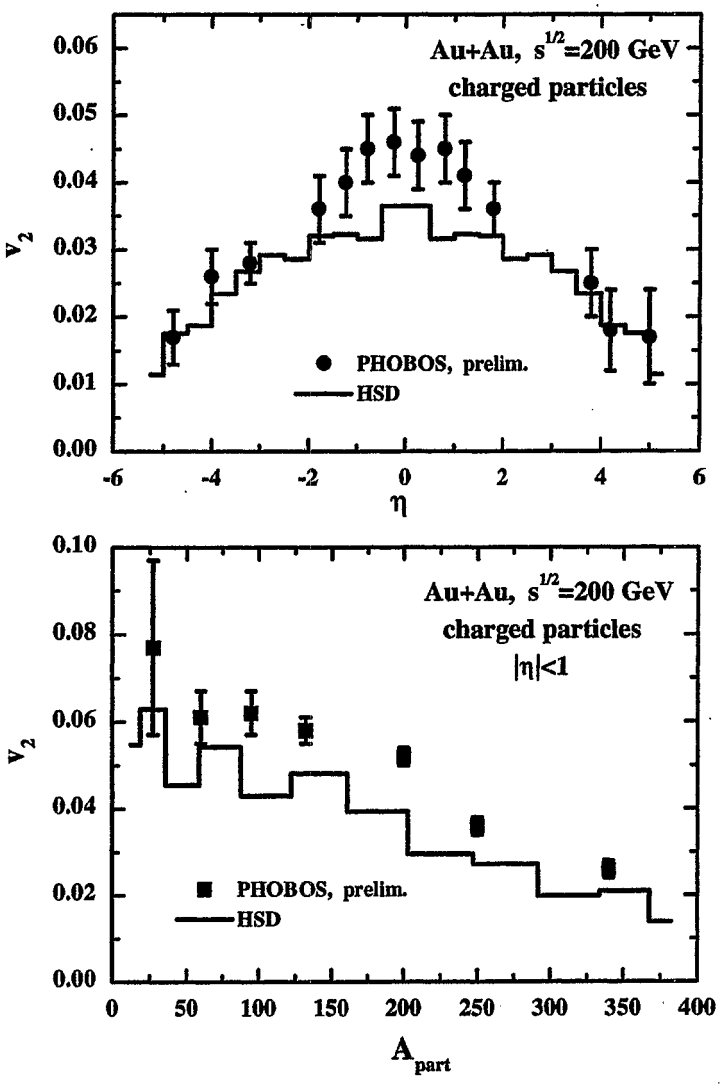

Figure 15: The elliptic flow v_2 for charged hadrons (HSD, solid lines) as a function of pseudorapidity η (upper part) and as a function of the number of 'participating nucleons' A_{part} for $|\eta| \leq 1$ (lower part) for $Au + Au$ collisions at $\sqrt{s} = 200$ GeV, in comparison to the preliminary 'hit-based analysis' data of the PHOBOS Collaboration [65]. Note that in spite of the shortened formation, $\tau \approx 0.8$ fm/c, HSD clearly underpredicts the data even at the moderate p_T-values dominating the p_T integrated v_2-values shown here. At higher p_T-values, Fig. 16, the discrepancy to the data is dramatic.

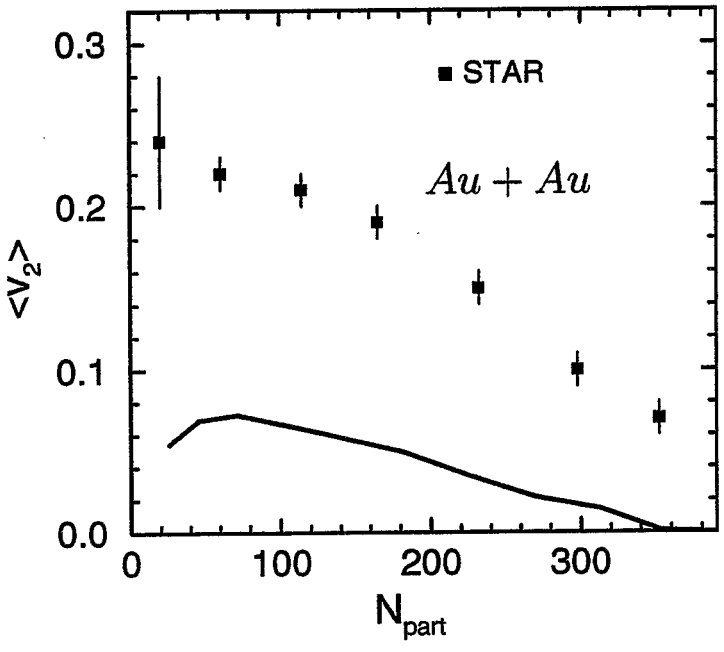

Figure 16: High p_T- v_2 values as a function of N_{part} as measured by STAR are compared to HSD calculations. The v_2 data are more than 5 times higher than the HSD model predictions for the most central collisions [70]

4 Early Thermalization at RHIC - evidence for the QGP

4.1 Elastic and inelastic multi-particle collisions in a parton cascade

To describe the early dynamics of ultrarelativistic heavy ion collisions, and to address the crucial question of thermalization and early pressure build up at RHIC, unexpectedly high elastic parton cross sections of $\sim$ 5–6 mb have been assumed in parton cascades [71, 72] in order to reproduce the elliptic flow $v_2(p_T)$ seen experimentally at RHIC. These cross sections are about 1/9 of the baryon-baryon total cross section ($\sim$ 45 mb) or 1/6 of the meson-baryon cross section ($\sim$ 30 mb), such that the effective cross section for the constituent quarks and antiquarks is roughly the same in the partonic and hadronic phase, tenfold higher than the cross sections calculated in pQCD.

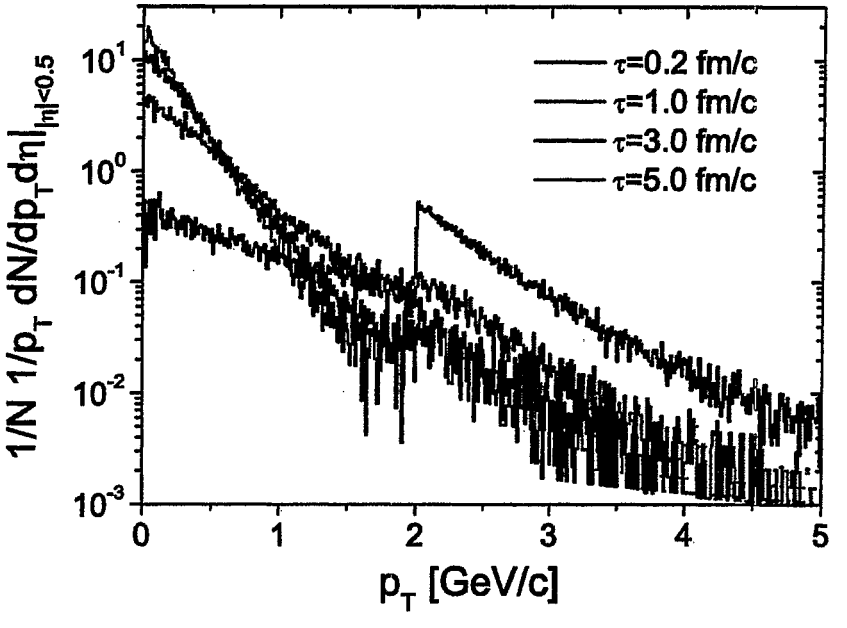

Figure 17: Time evolution of the midrapidity transverse momentum spectrum for a central RHIC collision from the three-dimensional Xu-Greiner-parton cascade simulation [73, 74], prelimenary results are from [75] (including transverse expansion). Only partons residing in a central cylinder of radius $R \leq 5$ fm are plotted. The initial off-equilibrium conditions are given by a minijet distribution, with corresponding overlap function in space-time. At $t = 0$, only minijets with $p_T > 2$ GeV are populated. Energy degradation to lower momenta proceeds by rapid gluon emission within the first fm/c. (Quasi-)kinetic and chemical equilibrium is found up to 4 fm/c. Here longitudinal and transversal hydrodynamic work is done, resulting in a rapid lowering of the temperature by a factor of two. On the other, a part of the initial non-equilibrium high momentum power-law tail of the mini-jet production survives even in this central cell.

This has been a great puzzle until recently, when Xu and Greiner developed a consistent three-body kinetic parton cascade algorithm [73, 74]. These stochastic inelastic ('Bremsstrahlung') $2 \rightarrow 3$ and $3 \rightarrow 2$ collisions, $gg \leftrightarrow ggg$, drive early thermalization, rather than the two body elastic collisions. A quantitative understanding of the early dynamical stages of deconfined matter is finally at reach. Parton cascade analyses incorporating only binary $2 \leftrightarrow 2$ pQCD scattering processes can not build up thermalization and early quasi-hydrodynamic behaviour necessary for achieving sufficient elliptic flow.

The importance of inelastic reactions was raised in the so called 'bottom-up thermalization' picture [76] - gluon multiplication leads to a much faster equilibration.

Xu and Greiner consider - besides gluon- and quark- two-body elementary parton-parton scatterings - for the first time - three-body processes $gg \leftrightarrow ggg$ in leading-order pQCD. They employ effective Landau-Pomeranchuk-Migdal suppression and standard screening masses for the infrared sector of the scattering amplitude.

The early stage of gluon production in the Xu-Greiner (X-G) approach (Fig. 17) leads to an almost immediate kinetic equilibration of the momentum distribution as well as to a rather abrupt lowering of the temperature by soft gluon emission. Detailed balance among gain and loss contributions is reached rapidly. The later, slower evolution is then governed by chemical equilibration of the quark degrees of freedom.

The X-G cascade does allow to study in detail RHIC- collisions with various initial conditions like minijets or color glass condensate. Fig. 17 depicts a preliminary calculation [75] using minijet-initial conditions.

Thermalization and chemical equilibration as proposed in the bottom-up scenario [76] can thoroughly be tested within this approach. The impact parameter dependence on the transverse energy is used to understand elliptic and transverse flow at RHIC within this new kinetic parton cascade with inelastic $3 \rightarrow 2$ and $2 \rightarrow 3$ interactions.

5 How much quenching of high p_T hadrons is due to (pre-) hadronic final state interactions [77]

A (mini-)jet at RHIC can produce hard particles, with p_T above 5 GeV, but must also form soft particles, with p_t around 2 GeV. Jets produced in the center of the plasma zone have to pass first through the free, nearly massless parton phase at very high temperatures, then through the correlated diquark and constituent quarks and finally through the meanwhile hadronic phase. Very high p_T jets with $\gamma > 10$ materialize only far outside of the plasma. Most of the jets which are observed at RHIC are at $p \approx 4 - 5$ GeV. More than 50% of the leading jet particles at $p_t \sim 5\,\mathrm{GeV}$ are baryons. Pion jets of 5 GeV have a $\gamma = 35$, i.e., they form far outside the plasma. However, HSD-Pythia-calculations show that the pions stem from decaying rho-jets. So, rhos and protons of 5 GeV have $\gamma = 5$. Thus, ρ and p-jets hadronize with roughly 50% probability [78, 70] while passing through the expanding bulk matter. All partonic and hadronic models have failed by factors of 5-10 to predict the observed high baryon abundance.

The PHENIX [79] and STAR [80] collaborations reported a suppression of meson spectra for transverse momenta $p_\perp$ above $\sim 3\,\mathrm{GeV}$. This suppression is not observed in d+Au interactions at the same bombarding energy per nucleon [81, 82] and presents clear evidence for the presence of the plasma.

However, it is not clear at present how much of the observed suppression can be attributed to (pre-)hadronic interactions (FSI) [78]. (In-)elastic collisions of (pre-)hadronic high momentum states with some of the bulk (pre-)hadrons in the fireball can contribute in particular to the attenuation of $p_t \approx 5\,\mathrm{GeV}$ transverse momentum hadrons at RHIC [77]: Most of the medium momentum (pre-)hadrons from a ± 5 GeV double jet will materialize inside the dense plasma, their transverse momenta being 0-4 GeV/c. The particles are dominantly rhos, K's and baryons at $p_t > 2.5\,\mathrm{GeV}$ – hence their formation time is $\gamma\tau_F \approx 4$ fm/c in the plasma rest frame. The time for color neutralization can also be very small [83], even of the leading particle, due to gluon emission.

The (pre-)hadronic interactions with the bulk of the (pre-)hadronic comovers then must have clearly an effect: they, too, suppress the p_T-spectrum [78]. (In)elastic reactions of the fragmented (pre-)hadrons with (pre-)hadrons of the bulk system cannot be described by pQCD: the relevant energy scale $\sqrt{s}$ is a few GeV. Such (in-)elastic collisions are very efficient for energy degradation since many hadrons with

lower energies are produced. On the average, 1 to 2 such interactions can account for up to 50% of the attenuation of high $p_\perp$ hadrons at RHIC [78]. Hence, the hadronic fraction of the jet-attenuation had to be addressed.

In [70] the HSD transport approach [44] is employed. Moderate to high transverse momenta (> 1.5 GeV/c) are incorporated by a superposition of $p+p$ collisions described via PYTHIA [17]. In Au+Au collisions, the formation of secondary hadrons is not only controlled by the formation time τ_f, but also by the energy density in the local rest frame. In [70], hadrons are not allowed to be formed if the energy density is above $1\mathrm{GeV/fm}^3$. The interaction of the leading and energetic (pre-)hadrons with the soft hadronic and bulk matter is thus explicitly modeled.

Fig. ?? show the nuclear modification factor [77]

$$R_{\mathrm{AA}}(p_\perp) = \frac{1/N_{\mathrm{AA}}^{\mathrm{event}}\; d^2N_{\mathrm{AA}}/dydp_\perp}{\langle N_{\mathrm{coll}}\rangle\,/\sigma_{pp}^{\mathrm{inelas}}\; d^2\sigma_{pp}/dydp_\perp}\,. \tag{3}$$

for the most central (5% centrality) Au+Au collisions at RHIC.

The Cronin enhancement is visible at all momenta. Hadron formation time effects do play a substantial role in the few GeV region, since heavier hadrons (K's, rhos, protons) are formed 7 times earlier than the rather light pions in the cms frame at fixed transverse momentum due to the lower Lorentz boost $\gamma < 5$. The HSD model is not able to produce the tenfold increase in the observed proton abundance at $p_t \approx 3-5\,\mathrm{GeV}$. It was shown in [70] that for transverse momenta $p_T \geq 6\mathrm{GeV}$ the interactions of formed hadrons are not able to explain the attenuation observed experimentally. However, the ratio R_{AA} is influenced by interactions of formed (pre-)hadrons in the $p_T = 1\ldots5\,\mathrm{GeV/c}$ range [70]. A similar behaviour had also been demonstrated in UrQMD simulations [84].

As pointed out before, the suppression seen in the calculation for larger transverse momentum hadrons is due to the interactions of the leading (pre-)hadrons with target/projectile nucleons and the bulk of low momentum hadrons. It is clear that the experimentally observed suppression can not be quantitatively described by the (pre-)hadronic attenuation of the leading particles [70]. The ratio R_{AA} (3) decreases to a value of about 0.5 at 5 GeV for central collisions, whereas the data are around $R_{\mathrm{AA}} \approx 0.25$.

To check how robust this HSD estimate is, alternative models for the leading pre-hadron cross section have been studied in [70] by adopting a time–dependent, color-transparency-motivated cross section for leading pre-hadrons [85]

$$\sigma_{\mathrm{lead}}(\sqrt{s},\tau) = \frac{\tau-\tau_0}{\tau_f}\sigma_{\mathrm{had}}(\sqrt{s}) \tag{4}$$

for $\tau - \tau_0 \leq \tau_f$, where τ_0 denotes the actual production time, τ_f the formation time, after which the full hadronic cross section is reached.

Within this scenario the attenuation is 35% at $p_T \sim 5\,\mathrm{GeV/c}$ (see figure 19), while the data show more than double the attenuation. Thus, (pre-)hadronic jet interactions cannot provide a quantitative explanation for the jet suppression observed. They do provide, however, a sizable (30−50%) contribution to the jet quenching.

For particles observable with momenta $p_T \geq 4\mathrm{GeV}$, the HSD transport calculation predicts that still 1/3 of the final observed hadrons have suffered one or more interactions, whereas the other 2/3 escape freely, i.e., without any interaction (even for central collisions). This implies that the final high p_T hadrons originate from the surface.

5.1 Angular Correlations of Jets – Can jets fake the large v_2-values observed?

Fig. 20 [70] shows the angular correlation of high p_T particles ($p_{\perp_{Trig}} = 4\ldots6\,\mathrm{GeV/c}, p_\perp = 2\,\mathrm{GeV}\ldots \mathrm{p}_{\perp_{\mathrm{Trig}}}$, $|y| < 0.7$) for the 5% most central Au+Au collisions at $\sqrt{s} = 200$ GeV (solid line) as well as pp re-

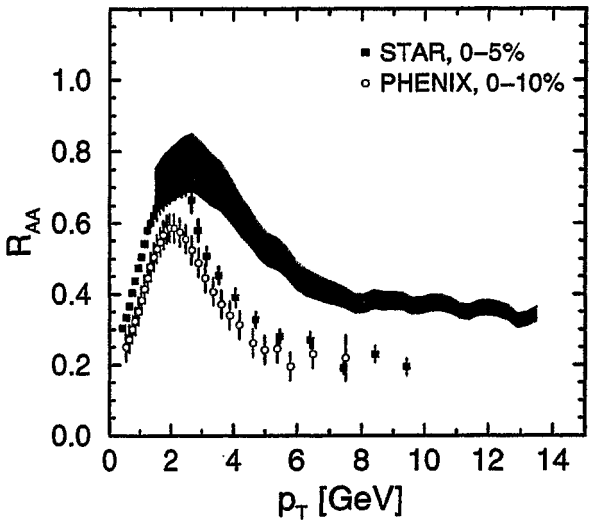

Figure 18: The suppression factor R_{AA} (3) of charged hadrons at 5% (10%) central Au+Au collisions ($\sqrt{s}$=200 GeV) at midrapidity for α = 0.25 to 0.4 (hatched band). The experimental data are from Refs. [26, 86] and show clearly that a partonic suppression is needed (taken from Ref. [70]).

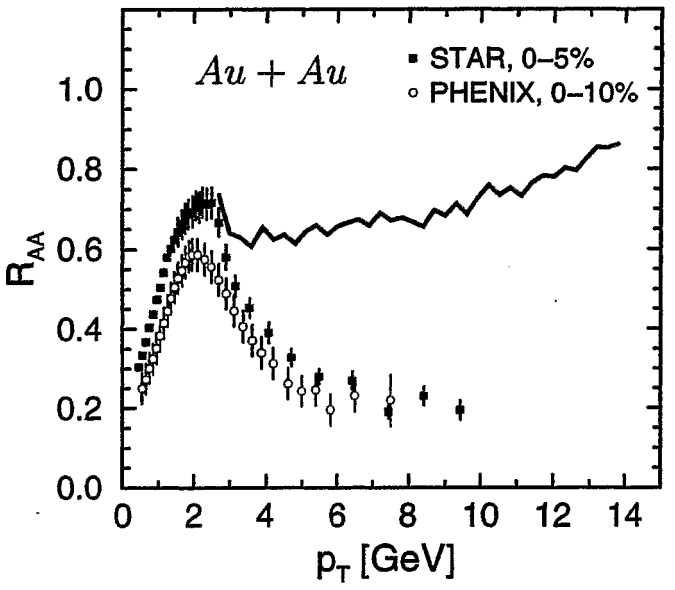

Figure 19: Same as fig. 18, but with a leading cross section according to eq. (4) for the perturbative high $p_\perp$ particles. The observed attenuation is more than double the value!

actions (dashed line) from the HSD-model [70] in comparison to the data from STAR for pp collisions [87]. Gating on high $p_\perp$ hadrons (in the vacuum) yields 'near–side' correlations in AuAu close to the 'near–side' correlations observed for jet fragmentation in the vacuum (pp). This is in agreement with the experimental observation [87]. However, for the away-side jet correlations, CGG get only a ~50% reduction, similar to HIJING, which has only parton quenching and neglects hadron rescattering. Clearly, the observed [87] complete disappearance of the away-side jet (Fig. 20) is not explainable in the HSD-(pre-)hadronic cascade, even with small formation time, 0.8 fm/c. Hence, the correlation data provide another clear proof for the existence of the bulk plasma.

Hence, although (pre-)hadronic final state interactions yield a sizable (−50%) contribution to the high $p_\perp$ suppression effects observed in Au+Au collisions at RHIC, 50 + % of the jet suppression originates from interactions in the plasma phase. The elliptic flow, v_2, for high transverse momentum particles is underestimated by at least a factor of 3 in the HSD transport calculations [70] (see Fig. 15). The experimentally observed proton excess over pions at transverse momenta $p_T > 2.5$ GeV/c cannot be

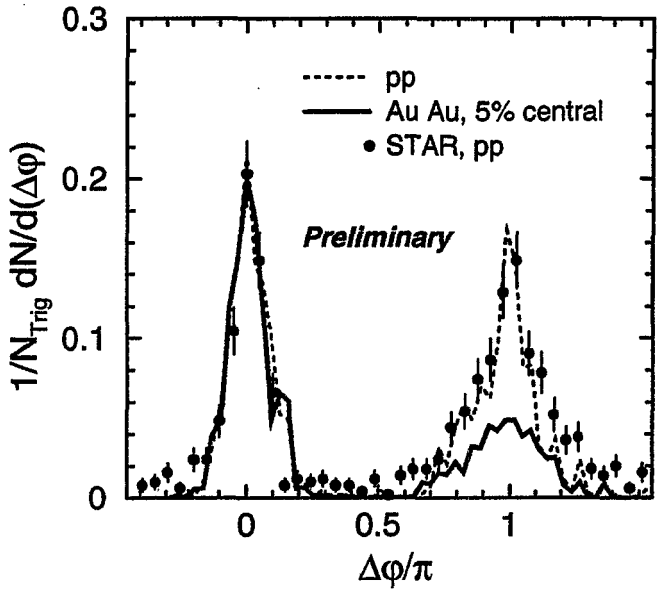

Figure 20: STAR data on near-side and away-side jet correlations compared to the HSD model for p+p and central Au+Au collisions at midrapidity for $p_{\perp_{Trig}} = 4 \ldots 6\,\mathrm{GeV/c}$ and $p_\perp = 2\,\mathrm{GeV/c} \ldots \mathrm{p}_{\perp_{\mathrm{Trig}}}$. [70, 77]

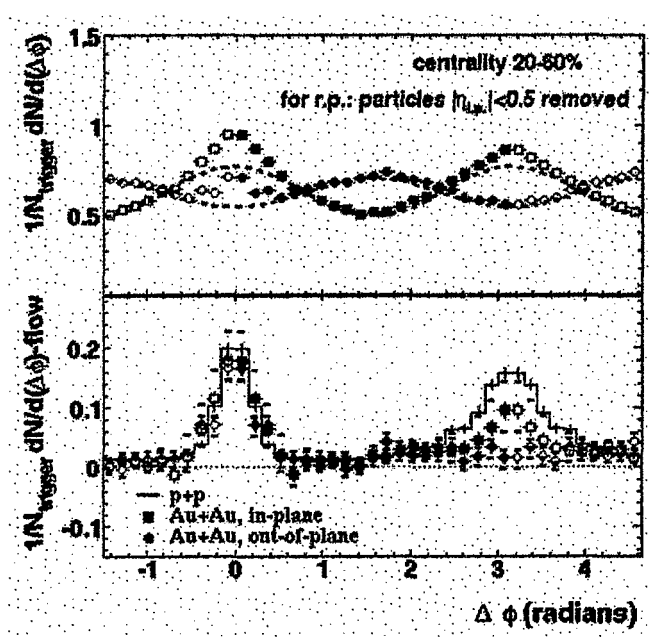

Figure 21: High p_T correlations: in-plane vs. out-of-plane correlations of the probe (jet+secondary jet fragments) with the bulk (v_2 of the plasma at $p_t > 2\,\mathrm{GeV/c}$), prove the existence of the initial plasma state (STAR-collaboration, prelimanary).

explained within the CGG approach–in fact, the proton yield at high p_t is a factor 5-10 too small. This, however, also holds for partonic jet-quenching models. Further experimental data on the suppression of high-momentum hadrons from d+Au and Au+Au collisions, down to $\sqrt{s} = 20$ GeV, are desparately needed to help to separate initial state Cronin effects from final state attenuation and to disentangle the role of partons in the colored parton plasma from those of interacting pre-hadrons in the hot and dense fireball.

Can the attenuation of jets of $p_T \geq 5\,\mathrm{GeV/c}$ actually fake the observed v_2-values at $p_T \approx 2\,\mathrm{GeV/c}$ – due to fragmentation and rescattering, dozens of momentum-degraded hadrons will propagate in the hemisphere defined by the jets – however, their momentum dispersion perpendicular to the jet direction is large, so large, that it could indeed fake what is thought to be the collective flow coming from the high pressure early plasma phase.

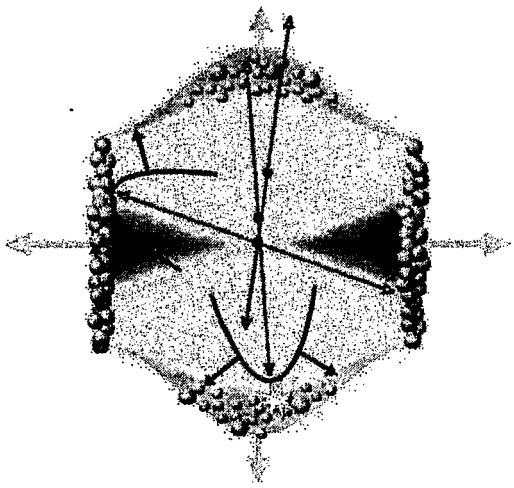

Figure 22: Illustration of jets traveling through the late hadronic stage of the reaction. Only jets from the region close to the initial surface can propagate and fragment in the vacuum [27, 90, 91]. The other jets will interact with the bulk, resulting in wakes with bow waves travelling transversely to the jet axis.

On first sight, Fig.21 shows that this could indeed be the case: the in-plane v_2 correlations are aligned with the jet axis, the away-side bump, usually attributed to collective v_2 flow (dashed line), could well be rather due to the stopped, fragmented and rescattered away-side jet! However, this argument is falsified by the out-of-plane correlations (circles in Fig. 21).

The near-side jet is clearly visible in the valley of the collective flow v_2 distribution. v_2 peaks at $\varphi = \pi/2$ relative to the jet axis! The away-side jet, on the other hand, has completely vanished in the out-of-plane distribution! Where are all the jet fragments gone? Why is there no trace left? Even if the away-side jet fragments completely and is caught stuck in the plasma, leftovers should be detected – at momenta below 2 GeV/c. Hadronic models as well as parton cascades will have a hard time getting to a quantitative agreement with these exciting data.

Let me propose future correlation measurements which can yield spectroscopic information on the plasma.

1. If the plasma were to be a colorelectric plasma, experiments will - in spite of strong plasma damping - be able to search for wake-riding potential effects. The wake of the leading jet particle can trap comoving companions - moving through the plasma in the wake pocket with the same speed (p_T/m) as the leading particle. This can be particular stable for charmed jets due to the deadcone effect, proposed by Kharzeev et al [88]. The deadcone will guarantee little energy loss, i.e. constant velocity of the leading D. The leading D meson will practically have very little momentum degradation in the plasma and therefore the wake potential following the D will be able to capture the equal speed companion, which can be detected [89]

2. One may measure the sound velocity of the expanding plasma by the emission pattern of the plasma particles travelling sideways with respect to the jet axis: The dispersive wave generated by the wake of the jet in the plasma yields preferential emission to an angle (relative to the jet axis) which is given by the ratio of the leading jet particles' velocity, devided by the sound velocity in the hot dense plasma rest frame. The speed of sound for a non-interacting gas of relativistic massless plasma particles is $c_s \approx \frac{1}{\sqrt{3}} \approx 57\% c$, while for a plasma with strong vector interactions, $c_s = c$. Hence, the emission angle measurement can yield information of the interactionsin the plasma.

6 Summary

(a) The NA49-observed collapse of both, v_1- and v_2-collective flow of protons in Pb+Pb collisions at 40 AGeV presents first clear evidence for a first order phase transition in baryon rich dense matter. It will be possible to study the nature of this transition and the properties of the expected chirally restored and deconfined phase both at the forward fragmentation ragion at RHIC, with upgraded and/or second generation detectors, and at the new GSI facility FAIR. According to Lattice QCD results [1, 2], the first order phase transition occurs for chemical potentials above 400 GeV. Fig. 13 shows that the elliptic flow clearly distinguishes between a first order phase transition and a crossover. Thus, the observed collapse of flow, as predicted in [27, 28], is a clear signal for the first order phase transition at the highest baryon densities.

A critical discussion of the use of collective flow as a barometer for the equation of state (EoS) of hot dense matter at RHIC showed that hadronic rescattering models can explain $< 30\%$ of the observed flow, v_2, for $p_T > 1$ GeV/c.

I interpret this as evidence for the production of superdense matter at RHIC, with initial pressure way above hadronic pressure, $p > 1$ GeV fm^{-3}.

The fluctuations in the flow, v_1 and v_2, should be measured. Ideal Hydrodynamics predicts that they are larger than 50 % due to initial state fluctuations. The QGP coefficient of viscosity may be determined experimentally from the fluctuations observed.

The connection of v_2 to jet suppression is examined. It is proven experimentally that the collective flow is not faked by minijet fragmentation and that the away-side jet suppression can only partially ($< 50\%$) be due to hadronic rescattering.

I propose upgrades and second generation experiments at RHIC which inspect the first order phase transition in the fragmentation region, i.e. at $\mu_B \approx 400$ MeV, around $y \approx 4-5$, where the collapse of the proton flow analogous to the 40 AGeV data should be seen.

The study of Jet-Wake-riding potentials and Bow shocks caused by jets in the QGP formed at RHIC can give further clues on the equation of state (EoS) and transport coefficients of the Quark Gluon Plasma (QGP).

I am grateful to E. Bratkovskaya, M. Bleicher00, A. Dumitru, C. Greiner, A. Muronga, K. Paech, M. Reiter, S. Scherer, S. Soff, H. Weber, F. Liu, G. Zeeb, Z. Xu, D. Zschiesche (all J.W. Goethe University, Frankfurt), W. Cassing (J. Liebig University, Giessen), S. Bass (Duke University), B. Tavares, L. Portugal, C. Aguiar, T. Kodama (UFRJ Rio de Janeiro), F. Grassi, Y. Hama, T. Osada, O. Sokolowsci (USP, Sao Paolo), J. Aichelin, C. Hartnack, K. Werner (Subatech Nantes), L.P. Csernai (University Bergen), D. Strottmann (Los Alamos National Lab).

References

[1] Z. Fodor and S. D. Katz. Critical point of qcd at finite t and mu, lattice results for physical quark masses. 2004.

[2] Frithjof Karsch. News from lattice qcd on heavy quark potentials and spectral functions of heavy quark states. 2004.

[3] L. V. Bravina, I. N. Mishustin, J. P. Bondorf, Amand Faessler, and E. E. Zabrodin. Microscopic study of freeze-out in relativistic heavy ion collisions at sps energies. *Phys. Rev.*, C60:044905, 1999.

[4] L. V. Bravina et al. Chemical freeze-out parameters at rhic from microscopic model calculations. *Nucl. Phys.*, A698:383–386, 2002.

[5] E. L. Bratkovskaya et al. Review of qgp signatures: Ideas versus observables. 2004.

[6] R. Anishetty, Peter Koehler, and Larry D. McLerran. Central collisions between heavy nuclei at extremely high- energies: The fragmentation region. *Phys. Rev.*, D22:2793, 1980.

[7] S. Date, M. Gyulassy, and H. Sumiyoshi. Nuclear stopping power at high-energies. *Phys. Rev.*, D32:619, 1985.

[8] P. Koch, B. Muller, and J. Rafelski. Strangeness in relativistic heavy ion collisions. *Phys. Rept.*, 142:167–262, 1986.

[9] C. Greiner, P. Koch, and H. Stöcker. Separation of strangeness from antistrangeness in the phase transition from quark to hadron matter: Possible formation of strange quark matter in heavy ion collisions. *Phys. Rev. Lett.*, 58:1825–1828, 1987.

[10] Carsten Greiner, Dirk-Hermann Rischke, Horst Stöcker, and Peter Koch. The creation of strange quark matter droplets as a unique signature for quark - gluon plasma formation in relativistic heavy ion collisions. *Phys. Rev.*, D38:2797–2807, 1988.

[11] J. Cleymans and K. Redlich. Chemical and thermal freeze-out parameters from 1-a-gev to 200-a-gev. *Phys. Rev.*, C60:054908, 1999.

[12] Z. Fodor, S. D. Katz, and K. K. Szabo. The qcd equation of state at nonzero densities: Lattice result. *Phys. Lett.*, B568:73–77, 2003.

[13] Z. Fodor, S. D. Katz, and A. Ringwald. Relic neutrino masses and the highest energy cosmic rays. *JHEP*, 06:046, 2002.

[14] I. G. Bearden et al. Rapidity dependence of charged antihadron to hadron ratios in au + au collisions at s(nn)**(1/2) = 200-gev. *Phys. Rev. Lett.*, 90:102301, 2003.

[15] Edward V. Shuryak. What have we learned and want to learn from heavy ion collisions at cern sps? *Nucl. Phys.*, A661:119–129, 1999.

[16] W. Cassing, K. Gallmeister, E. L. Bratkovskaya, C. Greiner, and H. Stocker. Dynamics of strange, charm and high momentum hadrons in relativistic nucleus nucleus collisions. 2003.

[17] Torbjorn Sjostrand et al. High-energy-physics event generation with pythia 6.1. *Comput. Phys. Commun.*, 135:238–259, 2001.

[18] W. Cassing, E. L. Bratkovskaya, and A. Sibirtsev. Open charm production in relativistic nucleus nucleus collisions. *Nucl. Phys.*, A691:753–778, 2001.

[19] W. Cassing, E. L. Bratkovskaya, and S. Juchem. Excitation functions of hadronic observables from sis to rhic energies. *Nucl. Phys.*, A674:249–276, 2000.

[20] W. Cassing and E. L. Bratkovskaya. Production and absorption of c anti-c pairs in nuclear collisions at sps energies. *Nucl. Phys.*, A623:570–590, 1997.

[21] C. Spieles et al. Dissociation of j/psi by mesons: Thermal versus nonequilibrium scenario. *J. Phys.*, G25:2351–2359, 1999.

[22] E. L. Bratkovskaya, W. Cassing, and H. Stocker. Open charm and charmonium production at rhic. *Phys. Rev.*, C67:054905, 2003.

[23] Helmut Satz. Colour deconfinement in nuclear collisions. *Rept. Prog. Phys.*, 63:1511, 2000.

[24] L. Grandchamp and R. Rapp. Thermal versus direct j/psi production in ultrarelativistic heavy-ion collisions. *Phys. Lett.*, B523:60–66, 2001.

[25] L. Ramello et al. Results on leptonic probes from na50. *Nucl. Phys.*, A715:243–251, 2003.

[26] J. L. Nagle. Leptonic observables in ultra-relativistic heavy ion collisions. *Nucl. Phys.*, A715:252–261, 2003.

[27] J. Hofmann, H. Stocker, W. Scheid, and W. Greiner. *Report of the workshop on BeV/nucleon collisions of heavy ions - how and why, Bear Mountain, New York, Nov. 29 - Dec. 1, 1974 (BNL-AUI 1975).*

[28] J. Hofmann, H. Stocker, U. W. Heinz, W. Scheid, and W. Greiner. Possibility of detecting density isomers in high density nuclear mach shock waves. *Phys. Rev. Lett.*, 36:88–91, 1976.

[29] L.D. Landau and E.M. Lifshitz. *Fluid Mechanics.* Pergamon Press, New York, 1959.

[30] H. Stocker, J. Hofmann, J. A. Maruhn, and W. Greiner. Shock waves in nuclear matter - proof by circumstantial evidence. *Progress in Particle and Nuclear Physics*, 4:133, 1980.

[31] H. Stocker, J. A. Maruhn, and W. Greiner. Collective sideward flow of nuclear matter in violent high- energy heavy ion collisions. *Phys. Rev. Lett.*, 44:725, 1980.

[32] H. Stocker, C. Riedel, Y. Yariv, L. P. Csernai, G. Buchwald, G. Graebner, J. A. Maruhn, W. Greiner, M. Gyulassy K. Frankel, B. Schurmann, G. Westfall, J. D. Stevenson, J. R. Nix, and D. Strottman. Nuclear fluid dynamics versus intranuclear cascade - possible evidence for collective flow in central high-energy nuclear collisions. *Phys. Rev. Lett.*, 47:1807, 1981.

[33] H. Stocker et al. Jets of nuclear matter from high-energy heavy ion collisions. *Phys. Rev.*, C25:1873–1876, 1982.

[34] H. Stöcker and W. Greiner. High-energy heavy ion collisions: Probing the equation of state of highly excited hadronic matter. *Phys. Rept.*, 137:277–392, 1986.

[35] L. P. Csernai and D. Rohrich. Third flow component as qgp signal. *Phys. Lett.*, B458:454, 1999.

[36] L. P. Csernai et al. Phase transitions in high energy heavy-ion collisions. 2004.

[37] W. Schmidt et al. Viscosity and the equation of state in high energy heavy- ion reactions. *Phys. Rev.*, C47:2782–2793, 1993.

[38] Azwinndini Muronga. Dissipative relativistic fluid dynamics for nuclear collisions. *Heavy Ion Phys.*, 15:337–347, 2002.

[39] Azwinndini Muronga. Causal theories of dissipative relativistic fluid dynamics for nuclear collisions. *Phys. Rev.*, C69:034903, 2004.

[40] J. Brachmann et al. Non-equilibrium fluid-dynamics in the early stage of ultrarelativistic heavy-ion collisions. *Nucl. Phys.*, A619:391–412, 1997.

[41] M. Hofmann et al. Nonequilibrium dynamics of a hadronizing quark-gluon plasma. 1999.

[42] C. Hartnack et al. Quantum molecular dynamics: A microscopic model from unilac to cern energies. *Nucl. Phys.*, A495:303c–320c, 1989.

[43] S. A. Bass, M. Gyulassy, H. Stöcker, and W. Greiner. Signatures of quark-gluon-plasma formation in high energy heavy-ion collisions: A critical review. *J. Phys.*, G25:R1–R57, 1999.

[44] W. Cassing and E. L. Bratkovskaya. Hadronic and electromagnetic probes of hot and dense nuclear matter. *Phys. Rept.*, 308:65–233, 1999.

[45] H. Weber, E. L. Bratkovskaya, W. Cassing, and H. Stocker. Hadronic observables from sis to sps energies: Anything strange with strangeness? *Phys. Rev.*, C67:014904, 2003.

[46] A. Andronic et al. Directed flow in au+au, xe+csi and ni+ni collisions and the nuclear equation of state. *Phys. Rev.*, C67:034907, 2003.

[47] A. Andronic et al. Differential directed flow in au + au collisions. *Phys. Rev.*, C64:041604, 2001.

[48] Sven Soff, Steffen A. Bass, Marcus Bleicher, Horst Stoecker, and Walter Greiner. Directed and elliptic flow. 1999.

[49] J. Brachmann. *Kollektiver Fluss im Dreifluessigkeitenmodell.* PhD thesis, J. W. Goethe Universität Frankfurt am Main, 2000.

[50] J. Brachmann et al. Antiflow of nucleons at the softest point of the eos. *Phys. Rev.*, C61:024909, 2000.

[51] K. Paech, M. Reiter, A. Dumitru, H. Stocker, and W. Greiner. On the observation of phase transitions in collisions of elementary matter. *Nucl. Phys.*, A681:41–48, 2001.

[52] C. Alt et al. Directed and elliptic flow of charged pions and protons in Pb + Pb collisions at 40-A-GeV and 158-A-GeV. *Phys. Rev.*, C68:034903, 2003.

[53] A. Andronic et al. Transition from in-plane to out-of-plane azimuthal enhancement in au + au collisions. *Nucl. Phys.*, A679:765–792, 2001.

[54] A. Andronic. Elliptic flow and equation of state in heavy ion collisions at sis energies. *Nucl. Phys.*, A661:333–336, 1999.

[55] K. Paech, H. Stocker, and A. Dumitru. Hydrodynamics near a chiral critical point. *Phys. Rev.*, C68:044907, 2003.

[56] Derek A. Teaney. Viscosity and thermalization. 2004.

[57] Ulrich Heinz and Peter F. Kolb. Rapidity dependent momentum anisotropy at rhic. 2004.

[58] C. E. Aguiar, Yogiro Hama, T. Kodama, and T. Osada. Event-by-event fluctuations in hydrodynamical description of heavy-ion collisions. *Nucl. Phys.*, A698:639–642, 2002.

[59] Azwinndini Muronga. Shear viscosity coefficient from microscopic models. *Phys. Rev.*, C69:044901, 2004.

[60] F. Weber. *Pulsars as Astrophysical Laboratories for Nuclear and Particle Physics.* IoP, Bristol, 1999.

[61] Marcus Bleicher and Horst Stocker. Anisotropic flow in ultra-relativistic heavy ion collisions. *Phys. Lett.*, B526:309–314, 2002.

[62] E. Zabrodin, L. Bravina, C. Fuchs, and A. Faessler. Microscopic description of anisotropic flow in relativistic heavy ion collisions. 2004.

[63] J. L. Nagle and T. S. Ullrich. Heavy ion experiments at rhic: The first year. 2002.

[64] B. B. Back et al. Global observations from phobos. *Nucl. Phys.*, A715:65–74, 2003.

[65] Steven Manly et al. Flow and bose-einstein correlations in au au collisions at rhic. *Nucl. Phys.*, A715:611–614, 2003.

[66] T. J. Humanic. Can hadronic rescattering explain the large elliptic flow and small hbt radii seen at rhic? 2002.

[67] R. Bellwied, H. Caines, and T. J. Humanic. Time dependence of chemical freeze-out in relativistic heavy ion collisions. *Phys. Rev.*, C62:054906, 2000.

[68] P. K. Sahu, N. Otuka, and A. Ohnishi. Systematic study of elliptic flow at rhic energy. 2002.

[69] Y. Nara, N. Otuka, A. Ohnishi, K. Niita, and S. Chiba. Study of relativistic nuclear collisions at ags energies from p + be to au + au with hadronic cascade model. *Phys. Rev.*, C61:024901, 2000.

[70] W. Cassing, K. Gallmeister, and C. Greiner. Suppression of high transverse momentum hadrons at rhic by (pre-) hadronic final state interactions. *Nucl. Phys.*, A735:277–299, 2004.

[71] Bin Zhang, C. M. Ko, Bao-An Li, Zi-Wei Lin, and Subrata Pal. J/psi production in relativistic heavy ion collisions from a multi-phase transport model. *Phys. Rev.*, C65:054909, 2002.

[72] Denes Molnar and Miklos Gyulassy. Saturation of elliptic flow at rhic: Results from the covariant elastic parton cascade model mpc. *Nucl. Phys.*, A697:495–520, 2002.

[73] Z. Xu and C. Greiner. Elastic and inelastic multiplication collisions in a parton cascade treated in an unified manner, 2004. publication in preparation.

[74] Z. Xu. PhD thesis, Universität Giessen, 2004.

[75] C. Greiner, S. Juchem, and Z. Xu. Aspects of non-equilbrium quantum field theory in heavy ion collisions. 2004.

[76] R. Baier, Alfred H. Mueller, D. Schiff, and D. T. Son. 'bottom-up' thermalization in heavy ion collisions. *Phys. Lett.*, B502:51–58, 2001.

[77] W. Cassing, K. Gallmeister, and C. Greiner. Quenching of high p(t) hadrons by (pre-)hadronic fsi at rhic. 2004.

[78] K. Gallmeister, C. Greiner, and Z. Xu. Quenching of high p(t) hadron spectra by hadronic interactions in heavy ion collisions at rhic. *Phys. Rev.*, C67:044905, 2003.

[79] S. S. Adler et al. High-p(t) charged hadron suppression in au + au collisions at s(nn)**(1/2) = 200-gev. *Phys. Rev.*, C69:034910, 2004.

[80] J. Adams et al. Transverse momentum and collision energy dependence of high p(t) hadron suppression in au + au collisions at ultrarelativistic energies. *Phys. Rev. Lett.*, 91:172302, 2003.

[81] S. S. Adler et al. Absence of suppression in particle production at large transverse momentum in s(nn)**(1/2) = 200-gev d + au collisions. *Phys. Rev. Lett.*, 91:072303, 2003.

[82] J. Adams et al. Evidence from d + au measurements for final-state suppression of high p(t) hadrons in au + au collisions at rhic. *Phys. Rev. Lett.*, 91:072304, 2003.

[83] B. Z. Kopeliovich, J. Nemchik, E. Predazzi, and A. Hayashigaki. Nuclear hadronization: Within or without? 2003.

[84] S. A. Bass et al. Last call for rhic predictions. *Nucl. Phys.*, A661:205–260, 1999.

[85] L. Gerland, L. Frankfurt, M. Strikman, H. Stocker, and W. Greiner. Charmonium suppression: Interplay of hadronic and partonic degrees of freedom. *Nucl. Phys.*, A663:1019–1022, 2000.

[86] C. Adler et al. Measurement of inclusive antiprotons from au + au collisions at s(nn)**(1/2) = 130-gev. *Phys. Rev. Lett.*, 87:262302, 2001.

[87] C. Adler et al. Disappearance of back-to-back high p(t) hadron correlations in central au + au collisions at s(nn)**(1/2) = 200-gev. *Phys. Rev. Lett.*, 90:082302, 2003.

[88] D Kharzeev. private communication.

[89] W. Schafer, H. Stocker, B. Muller, and W. Greiner. Mach cones induced by fast heavy ions in electron plasma. *Z. Phys.*, A288:349, 1978.

[90] H. G. Baumgardt et al. Shock waves and mach cones in fast nucleus-nucleus collisions. *Z. Phys.*, A273:359–371, 1975.

[91] D. H. Rischke, H. Stocker, and W. Greiner. Flow in conical shock waves: A signal for the deconfinement transition? *Phys. Rev.*, D42:2283–2292, 1990.

Searching Evidence for the Color Glass Condensate at RHIC

J.-P. Blaizot and F. Gelis

Searching Evidence for the Color Glass Condensate at RHIC

Jean-Paul Blaizot, François Gelis

Service de Physique Théorique[1]
Bât. 774, CEA/DSM/Saclay
91191, Gif-sur-Yvette Cedex, France

Abstract

This contribution discusses the phenomenon of parton saturation, the color glass picture of hadronic wavefuntions, and their relevance in the early stages of nucleus-nucleus collisions. Evidence for the color glass condensate in the presently available RHIC data is critically reviewed.

1 Introduction

The degrees of freedom involved in the early stages of a nucleus-nucleus collision at sufficiently high energy are partons, mostly gluons, whose density grows as the energy increases (i.e., when x, their momentum fraction, decreases). This growth of the number of gluons in the hadronic wave functions is a phenomenon which has been well established at HERA. One expects however that it should eventually "saturate" when non linear QCD effects start to play a role.

The existence of such a saturation regime has been predicted long ago, together with estimates for the typical transverse momenta where it sets in. But it is only during the last decade that equations providing a complete dynamical description of the saturated regime have been obtained. A remarkable feature which emerges from the solution of these equations is that the dense, saturated system of partons to be found in hadronic wave functions at high energy has universal properties, the same for all hadrons or nuclei. It follows that the early stages of hadronic collisions at sufficiently high energies are governed by universal wave functions ("color glass condensate"), whose properties could in principle be calculated from QCD. This is a very exciting perspective which fully justifies the active search for evidence of this novel regime of QCD both at HERA and at RHIC.

It is expected that the saturation regime sets in earlier (i.e., at lower energy) in collisions involving large nuclei than in those involving protons. In fact, the

[1]URA 2306 du CNRS.

parton densities in the central rapidity region of a Au-Au collision at RHIC are not too different from those measured in deep inelastic scattering at HERA. There is however one important difference: while at HERA these densities result from gluon evolution, at RHIC there is little evolution, at least in the central rapidity region, and the large densities result mostly from the additive contributions of the participant nucleons. Of course, one has the possibility at RHIC to explore various situations. In particular the study of dA collisions in the fragmentation region of the deuteron gives access to a regime where final state interactions should play a minor role and where quantum evolution could be significant. Indeed, very exciting results have been obtained in this regime.

One may worry that at present energies, the conditions for saturation are at best marginally satisfied. Nevertheless a successful phenomenology based on the saturation picture has been developed over the last few years, both at RHIC and at HERA. We shall review in this report some of the experimental findings providing evidence for the color glass picture. It should be emphasized that the field is still in a rapidly evolving phase, most theoretical analysis are incomplete, so that conclusions reached today can at best be considered as tentative. Before we go into this phenomenological discussion, we shall start by a brief (and incomplete) historical perspective, to emphasize the remarkable theoretical developments of the last decade.

2 The infancy of the idea of saturation

An important feature of partonic interactions is that they involve only partons with comparable rapidities. Let us then consider the interaction between a nucleus and some external probe and consider what happens when one boosts the projectile nucleus, increasing its rapidity in successive steps. In the first step, the valence constituents become Lorentz contracted in the longitudinal direction while the time scale of their internal motions is Lorentz dilated. In addition, the boost reveals new vacuum fluctuations coupled to the boosted valence partons. Such fluctuations are not Lorentz contracted in the longitudinal direction, and represents the dynamical degrees of freedom; they are the partons that can interact with the probe. Making an additional step in rapidity would freeze these fluctuations, while making them Lorentz contracted as well. But the additional boost also produces new quantum fluctuations, which become the new dynamical variables. This argument can be repeated, and one arrives at the picture of a high-energy projectile containing a large number of frozen, Lorentz contracted partons (the valence partons, plus all the quantum fluctuations produced in the previous boosts), and partons which have a small rapidity, are not Lorentz contracted and can interact with the probe. This space-time description was developed before the advent of QCD (see for instance [1]; in Bjorken's lectures [2], one can actually foresee the modern interpretation of parton evolution as a renormalization group evolution *a la* Wilson on which the color glass formalism is based).

Of course, such a space-time picture, which was deduced from rather general

field theoretical considerations, can now be understood in terms of QCD. In fact, shortly after QCD was established as the theory of strong interaction, quantitative equations were established, describing the phenomenon outlined above [3–8]. In particular, the equation derived by Balitsky, Fadin, Kuraev and Lipatov [3,4] describes the growth of the non-integrated gluon distribution in a hadron as it is boosted towards higher rapidities. Experimentally, an important

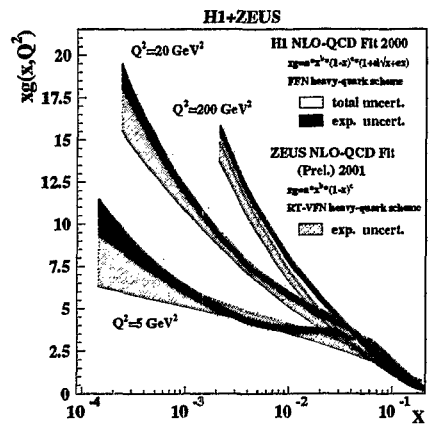

Figure 1: The gluon structure function in a proton measured at HERA.

increase of the number of gluons at small x has indeed been observed in the Deep Inelastic Scattering experiments performed at HERA (see fig. 1), down to $x \sim 10^{-4}$. Such a growth raises a problem: if it were to continue to arbitrarily small x, it would induce an increase of hadronic cross-sections as a power of the center of mass energy, in violation of unitarity bounds.

However, as noticed by Gribov, Levin and Ryskin in [9], the BFKL equation includes only branching processes that increase the number of gluons ($g \to gg$ for instance), but not the recombination processes that could reduce the number of gluons (like $gg \to g$). While it may be legitimate to neglect the recombination process when the gluon density is small, this cannot remain so at arbitrarily high density: a saturation mechanism of some kind must set in. Treating the partons as ordinary particles, one can get a crude estimate of the onset of saturation from a simple mean free path argument. The recombination cross-section for gluon with transverse momentum Q is roughly given by

$$\sigma \sim \frac{\alpha_s(Q^2)}{Q^2}\,, \tag{1}$$

while the number of such gluons per unit of transverse area is given by

$$\rho \sim \frac{xG(x,Q^2)}{\pi R^2}\,, \tag{2}$$

where R is the radius of the hadron and x the momentum fraction of the considered gluons. Saturation sets in when $\rho\sigma \sim 1$, or equivalently for:

$$Q^2 = Q_s^2 \,, \quad \text{with } Q_s^2 \sim \alpha_s(Q_s^2)\frac{xG(x,Q_s^2)}{\pi R^2} \,. \tag{3}$$

The momentum scale that characterizes this new regime, Q_s, is called the saturation momentum [10]. Partons with transverse momentum $Q > Q_s$ are in a dilute regime; those with $Q < Q_s$ are in the saturated regime.

A more refined argument for the onset of saturation was given in [11], where recombination is associated with a higher twist correction to the DGLAP equation. More generally, one may view the saturation momentum Q_s as the scale at which QCD non linear effects become important. This occurs when field fluctuations are such that gluon kinetic energies become comparable to their interaction energies, that is when $\langle(\partial A)^2\rangle \sim \alpha_s\langle(A^2)^2\rangle$, where $\langle A^2\rangle$ denotes the fluctuations of the gauge fields. Since the relevant dynamics is in the transverse plane, the magnitude of the gradient is fixed by the transverse momentum Q. As for the magnitude of the gauge field fluctuations, $\langle A^2\rangle$, they can be estimated from the particle number density in the transverse plane, i.e. $\langle A^2\rangle \sim \rho$, with ρ given in eq. (2). The condition $\langle(\partial A)^2\rangle \sim \alpha_s\langle(A^2)^2\rangle$ translates then into $Q^2 \sim \alpha_s\langle A^2\rangle$, which is eq. (3) above. Note that at saturation, naive perturbation theory breaks down, even though $\alpha_s(Q_s)$ may be small if Q_s is large: the saturation regime is a regime of weak coupling, but large density.

Early estimates of Q_s in nucleus-nucleus collisions were given in [12], and do not differ much from more modern ones [13]. But, as we have already emphasized, what has changed dramatically over the last decade is that we do not have only access to the boundary of the saturation region, we now have a complete dynamical picture of the saturation region. Before we turn to a short introduction to these new developments, let us indicate some expected characteristics of the saturated regime.

Note first that the saturation momentum increases as the gluon density increases. This may come from an increase of the gluon structure function as x decreases. The increase of the density may also come from the coherent contributions of several nucleons in a nucleus. In large nuclei, one expects $Q_s^2 \propto \alpha_s A^{1/3}$, where A is the number of nucleons in the nucleus.

There is another feature. Consider the number of partons occupying a small disk of radius $1/Q_s$ in the transverse plane. This is easily estimated by combining eqs. (2) and (3); one finds this number to be proportional to $1/\alpha_s$. In such conditions of large numbers of quanta, classical field approximations may become relevant to describe the nuclear wave-functions.

3 Modern formulation: the color glass condensate

Once one enters the saturated regime the evolution of the parton distributions can no longer be described by a linear equation such as the BFKL equation. One

of the major breakthrough of the last ten years is that non linear equations have been obtained which allow us to follow the evolution of the partonic systems form the dilute regime to the dense, saturated, regime. These take different, equivalent, forms, generically referred to as the JIMWLK equation.

The color glass formalism, which provides the most complete physical picture, relies on the separation of the degrees of freedom in a high-energy hadron into frozen partons and dynamical fields, as discussed above. In the original McLerran and Venugopalan model [14–16], the fast partons are frozen, Lorentz contracted, color sources flying along the light-cone, and constitute a density of color charge $\rho(\boldsymbol{x}_\perp)$. Conversely, the low x partons are described by classical gauge fields $A^\mu(x)$ determined by solving the Yang-Mills equations with the source given by the frozen partonic configuration. An average over all acceptable configurations must be performed.

The weight of a given configuration is a functional $W_{x_0}[\rho]$ of the density ρ which depends on the separation scale x_0 between the modes which are described as frozen sources, and the modes which are described as dynamical fields. As one lowers this separation scale, more and more modes are included among the frozen sources, and therefore the functional W_{x_0} evolves with x_0 according to a renormalization group equation [17–26].

This evolution equation for $W_{x_0}[\rho]$ has been derived in [17–26] and reads

$$\frac{\partial W_{x_0}[\rho]}{\partial \ln(1/x_0)} = \frac{1}{2}\int_{\vec{x}_\perp,\vec{y}_\perp} \frac{\delta}{\delta\rho_a(\vec{x}_\perp)}\chi_{ab}(\vec{x}_\perp,\vec{y}_\perp)\frac{\delta}{\delta\rho_b(\vec{y}_\perp)}W_{x_0}[\rho]\,, \tag{4}$$

where the kernel $\chi_{ab}(\vec{x}_\perp,\vec{y}_\perp)$ depends on the color density ρ only via Wilson lines:

$$U(\boldsymbol{x}_\perp) \equiv \mathcal{P}\exp\left[-ig\int_{-\infty}^{+\infty} dz^- A^+(z^-,\boldsymbol{x}_\perp)\right]\,. \tag{5}$$

Here $\mathcal{P}$ denotes an ordering along the x^- axis, A^+ is the classical color field of the hadron moving close to the speed of light in the $+z$ direction. The field A^+ depends implicitly on the frozen sources, i.e. on the color charge density $\rho(\boldsymbol{x}_\perp)$.

This functional evolution equation can be rewritten as an infinite hierarchy of equations for correlation functions of the ρ's, or equivalently of the U's. For instance, the correlator $\mathrm{tr}\langle U^\dagger(\boldsymbol{x}_\perp)U(\boldsymbol{y}_\perp)\rangle$ of two Wilson lines has an evolution equation that involves a correlator of four Wilson lines. If one assumes that this 4-point correlator can be factored into a product of two 2-point functions, one obtains a closed equation for the 2-point function, called the Balitsky-Kovchegov [19,21] equation:

$$\frac{\partial \mathrm{tr}\langle U^\dagger(\boldsymbol{x}_\perp)U(\boldsymbol{y}_\perp)\rangle_{x_0}}{\partial\ln(1/x_0)} = -\frac{\alpha_s}{2\pi^2}\int_{\boldsymbol{z}_\perp}\frac{(\boldsymbol{x}_\perp-\boldsymbol{y}_\perp)^2}{(\boldsymbol{x}_\perp-\boldsymbol{z}_\perp)^2(\boldsymbol{y}_\perp-\boldsymbol{z}_\perp)^2}$$
$$\times\Big[N_c\mathrm{tr}\langle U^\dagger(\boldsymbol{x}_\perp)U(\boldsymbol{y}_\perp)\rangle_{x_0} - \mathrm{tr}\langle U^\dagger(\boldsymbol{x}_\perp)U(\boldsymbol{z}_\perp)\rangle_{x_0}\mathrm{tr}\langle U^\dagger(\boldsymbol{z}_\perp)U(\boldsymbol{y}_\perp)\rangle_{x_0}\Big] \tag{6}$$

When the density of color charge ρ is small, one can expand the Wilson line U in powers of ρ. Eq. (6) becomes then[2] a linear evolution equation for the

[2]The same is true of eq. (4), because in this limit the kernel χ_{ab} becomes quadratic in ρ.

correlator $\langle \rho(\boldsymbol{x}_\perp)\rho(\boldsymbol{y}_\perp)\rangle_{x_0}$, or equivalently for the unintegrated gluon density, which is nothing but the BFKL equation.

The opposite limit, at very small x_0 (where the color charge density is large – far inside the saturation region), also leads to significant simplifications. Indeed, since the exponent in the Wilson lines is then a large quantity, one can use a Random Phase Approximation in which the correlators of Wilson lines are small. The solution is a Gaussian (albeit non-local in the transverse coordinates) [27]:

$$W_{x_0}[\rho] = \exp\Big[-\int_{\boldsymbol{x}_\perp,\boldsymbol{y}_\perp} \frac{\rho(\boldsymbol{x}_\perp)\rho(\boldsymbol{y}_\perp)}{2\mu^2(\boldsymbol{x}_\perp-\boldsymbol{y}_\perp,x_0)}\Big]\,. \tag{7}$$

This formula is not valid to arbitrarily short distances $|\boldsymbol{x}_\perp - \boldsymbol{y}_\perp| \to 0$ (this domain is the realm of high Q^2 physics, controlled by DGLAP evolution).

Like with the BFKL or DGLAP evolution equations, the initial condition for the evolution is truly a non-perturbative input. One can in principle try to model it, and then adjust the parameters of the model to fit experimental data. A simple model is that proposed by McLerran and Venugopalan, in which the initial $W_{x_0}[\rho]$ is a local Gaussian:

$$W_{x_0}[\rho] = \exp\Big[-\int_{\boldsymbol{x}_\perp} \frac{\rho(\boldsymbol{x}_\perp)\rho(\boldsymbol{x}_\perp)}{2\mu^2}\Big]\,. \tag{8}$$

At this point, one should stress that testing the predictions of the Color Glass Condensate in principle requires to test both the properties of the evolution with rapidity and the initial condition.

It is also important to note that the gaussians of eqs. (7) and (8) do not have the same status in the CGC framework: eq. (8) is one particular model for the initial condition at moderately small x, while eq. (7) is the asymptotic regime reached at very small x regardless of the initial condition. The latter is therefore a property of the small x evolution itself. The MV model requires an infrared cutoff at the scale Λ_{QCD}. This is because assuming a truly local Gaussian distribution ignores the fact that color neutralization occurs on distance scales smaller than the nucleon size ($\sim \Lambda_{QCD}^{-1}$): two ρ's can only be uncorrelated if they are at transverse coordinates separated by at least the distance scale of color neutralization. In the asymptotic solution of eq. (7), there is no infrared problem because the color neutralization is built in the dependence of $\mu^2(\boldsymbol{x}_\perp - \boldsymbol{y}_\perp, x_0)$ on the transverse coordinates. Color neutralization in fact occurs on distance scales of the order of $Q_s^{-1}(x_0)$ [27]. This is the physical origin of the universality of the saturated regime.

4 Phenomenological predictions

4.1 Geometrical scaling

In the $(\ln(1/x), \ln(p_\perp))$ plane, the saturation domain is defined by the condition $\Lambda_{QCD} \ll p_\perp \lesssim Q_s(x)$. In this region, one expects that observables (made

dimensionless by scaling out the appropriate power of $p_\perp$) depending a priori on both x and $p_\perp$ scale like functions of the unique variable $p_\perp/Q_s(x)$. This property is called "geometrical scaling" in the literature. It has been shown by Iancu, Itakura and McLerran in [28] that this scaling property holds in a much larger domain, whose upper bound is $p_\perp \lesssim Q_s(x)^2/\Lambda_{QCD}$. This region has been labeled "extended scaling region" in figure 2. Technically, the reason

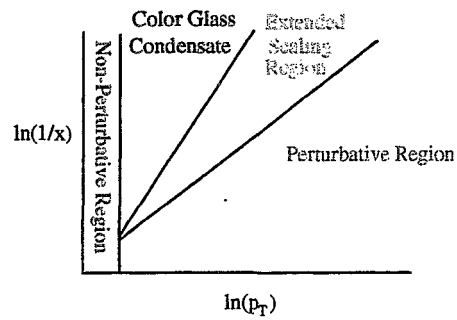

Figure 2: The scaling region in the $(\ln(1/x), \ln(p_\perp))$ plane.

why this scaling survives outside of the saturation domain is that the (linear) BFKL equation that controls the evolution in x when $p_\perp \gtrsim Q_s(x)$ preserves for a while the scaling properties inherited from the physics of the saturation region (which affects the BFKL evolution via a boundary condition at $p_\perp = Q_s(x)$).

Such a scaling has been searched for in the data of the DIS experiments at HERA, and it turns out that one can indeed represent all the small x ($x < 10^{-2}$) data points for the structure function $F_2(x, Q^2)$ as a single function of the variable $\tau \equiv Q^2/Q_s^2(x)$ with

$$Q_s^2(x) \equiv Q_0^2 \left(\frac{x_0}{x}\right)^\lambda . \tag{9}$$

This is illustrated by the plot of figure 3. The parameter Q_0 is set to 1 GeV, while $x_0 \approx 3.10^{-4}$ and $\lambda \approx 0.29$ are determined through a fit to the data [29]. By studying BFKL evolution to next-to-leading order, Triantafyllopoulos has obtained a value of λ in good agreement with that observed [30]. Note however that this scaling is not by itself a proof of the color glass condensate picture, since it does not depend much on the detailed underlying dynamics.

4.2 Structure functions and diffraction in DIS

In an appropriate frame, and at leading order in α_s, the cross section for the interaction of a virtual photon with a proton takes the following factorized form:

$$\sigma_{\gamma^* p}(x, Q^2) = \int_0^1 dz \int d^2\boldsymbol{r}_\perp \left|\psi(Q^2, z, \boldsymbol{r}_\perp)\right|^2 \sigma_{\text{dipole}}(x, \boldsymbol{r}_\perp) . \tag{10}$$

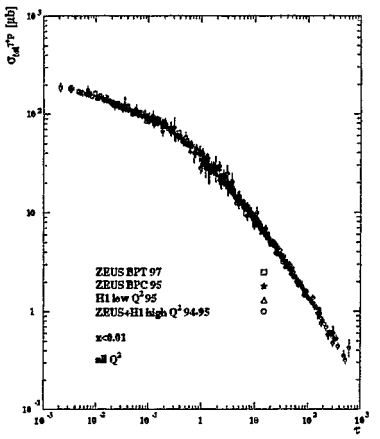

Figure 3: The $\gamma^* p$ cross-section at HERA, plotted against $\tau \equiv Q^2/Q_s^2(x)$.

In this formula, $\psi(Q^2, z, \boldsymbol{r}_\perp)$ is the Fock component of the virtual photon light-cone wave function that corresponds to a $q\bar{q}$ dipole of size $\boldsymbol{r}_\perp$; it depends on the invariant mass Q^2 of the photon, on the transverse size $\boldsymbol{r}_\perp$ of the $q\bar{q}$ dipole, and on the fraction z of the photon longitudinal momentum taken by the quark. The other factor in this formula, $\sigma_{\rm dipole}(x, \boldsymbol{r}_\perp)$, is the total dipole-proton cross-section. It can be expressed in terms of a correlator of Wilson lines:

$$\sigma_{\rm dipole}(x, \boldsymbol{r}_\perp) = \frac{2}{N_c} \int d^2\boldsymbol{X}_\perp \mathrm{tr}\left[1 - \left\langle U(\boldsymbol{X}_\perp + \frac{\boldsymbol{r}_\perp}{2}) U^\dagger(\boldsymbol{X}_\perp - \frac{\boldsymbol{r}_\perp}{2})\right\rangle\right] , \quad (11)$$

where the average is taken over the color field of the proton.

Several models for this dipole cross-section have been used in the literature in order to fit HERA data. Golec-Biernat and Wüsthoff have used a very simple parameterization [31,32]

$$\sigma_{\rm dipole}(x, \boldsymbol{r}_\perp) = \sigma_0 \left[1 - e^{-\frac{1}{4}Q_s^2(x) r_\perp^2}\right], \quad (12)$$

which has led to good results for describing the data at $x < 10^{-2}$ and moderate Q^2. In this formula, the scale $Q_s(x)$ was taken to be of the form given in eq. (9). This model fails however at large Q^2. This aspect was improved in [33], where the dipole cross-section is parameterized in a way that reproduces pQCD for small dipoles. Note that these approaches, even if they are inspired by saturation physics, do not derive the dipole cross-section from first principles. Recently, Iancu, Itakura and Munier [34] derived an expression of the dipole cross-section from the color glass condensate framework, and obtained a good fit of HERA data with a small number of free parameters.

One can express in a similarly factorized form the diffractive $\gamma^* p$ cross-section, where the exchange between the dipole and the target is color singlet.

In fact, since the dipole cross-section involved in eqs. (10) and (11) is the total cross-section, one can use the optical theorem to deduce from it the forward elastic scattering amplitude:

$$\mathcal{M}_{\text{elastic}}(x, \boldsymbol{r}_\perp, t=0) = \frac{i}{N_c} \int d^2\boldsymbol{X}_\perp \text{tr}\left[1 - \left\langle U(\boldsymbol{X}_\perp + \frac{\boldsymbol{r}_\perp}{2}) U^\dagger(\boldsymbol{X}_\perp - \frac{\boldsymbol{r}_\perp}{2})\right\rangle\right] , \tag{13}$$

assuming that this amplitude is predominantly imaginary. This can then be used to obtain for the diffractive DIS cross-section at $t = 0$ an expression involving the *square* of the total dipole-proton cross-section[3]:

$$\left.\frac{d\sigma^D_{\gamma^* p}(x, Q^2)}{dt}\right|_{t=0} = \frac{1}{16\pi} \int_0^1 dz \int d^2\boldsymbol{r}_\perp \left|\psi(Q^2, z, \boldsymbol{r}_\perp)\right|^2 \sigma^2_{\text{dipole}}(x, Q^2) . \tag{14}$$

By using in this formula the total dipole cross-section fitted to the inclusive F_2, one obtains a good description of the measured diffractive DIS cross-section [31,32]. Note however that keeping only the $q\bar{q}$ component of the photon wave function is a good approximation only when the invariant mass of the diffractively produced object is not too large. For large masses, one needs to consider also the $q\bar{q}g$ component.

4.3 Particle multiplicities at RHIC

In the framework of saturation models, predictions have been made for global observables like the total number of produced particles per unit of rapidity $dN/d\eta$. This can be studied as a function of the collision energy, the centrality of the collision, and the rapidity.

The Color Glass Condensate may provide a dynamical justification rooted in QCD for many general features of particles production in hadronic interactions. This may be the case in particular for the phenomenon of "limiting fragmentation", i.e., the expectation that the rapidity distribution in the fragmentation region becomes independent of the collision energy at high energy. Evidence for such a behavior has indeed been observed by the PHOBOS collaboration, as is illustrated in figure 4. Here, one has plotted the rapidity distribution $dN/d\eta'$ of produced particles in Au-Au collisions as a function of the rapidity relative to the incoming beam rapidity $\eta' \equiv \eta - \eta_{\text{beam}}$. When one increases the beam energy, one sees that $dN/d\eta'$ is the same at large η' for all energies. The particles produced at some given (large) energy are those that would have been produced at lower energies plus new particles produced at a lower rapidity. An early interpretation of such a phenomenon in the language of the CGC has been proposed by Jalilian-Marian [36]. The interpretation suggested there is that in the fragmentation region of one of the nuclei (η' around zero), this nucleus is a dilute partonic system while the other nucleus is in a saturated state. The rise

[3]Another way in which this relation is stated in the literature is that in order to obtain the diffractive part of a cross-section, one should average the scattering amplitude over the configurations of the frozen sources *before* squaring the amplitude.

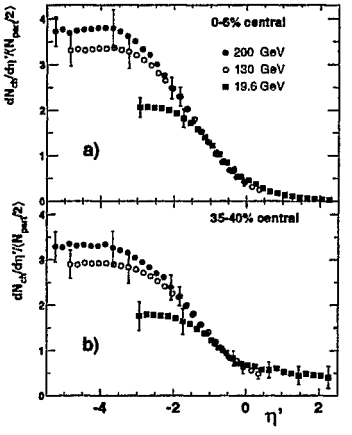

Figure 4: Particle multiplicity at RHIC for different collision energies, plotted against the rapidity of the produced particle relative to the rapidity of the beam $\eta' \equiv \eta - \eta_{\text{beam}}$ [35].

in multiplicity when one decreases η' is then attributed to the growth of the parton distribution in the dilute nucleus. One should emphasize however that no detailed quantitative analysis of the data presented in figure 4 has yet been done in this framework.

In comparing more quantitative predictions of the color glass formalism for $dN/d\eta$ to experimental data, it is important to keep the following points in mind. First, the color glass condensate can only predict the distribution of initial gluons, set free typically at a proper time $\tau \sim Q_s^{-1}$. Between this early stage and the final chemical freeze-out, the system undergoes several non-trivial steps: kinetic and chemical equilibration (possibly with additional parton production), hadronization, etc., which are most often ignored in calculations based on the color glass condensate. Secondly, even the calculation of the initial gluon production is a highly non-trivial task. It involves, in principle, solving the classical Yang-Mills equations in the presence of the color densities describing the distribution of frozen sources in both projectiles. This has been achieved analytically only for proton-nucleus collisions, when the color charge density inside the proton is assumed to be weak [37–39]. In the case of nucleus-nucleus collisions, two kinds of calculations have been performed:

(i) *Ab initio* numerical calculations [40–43] that solve exactly the Yang-Mills equations for AA collisions. The average over the color charge densities in the projectiles is performed by assuming that the distributions $W_{x_0}[\rho]$ are given by the MV model, i.e. by the gaussian of eq. (8). Quantum evolution effects are therefore not included. Note that when one calculates $dN/d\eta$ at $\eta = 0$, the typical x probed in the wave function of the nuclei is about $x \sim 10^{-2}$. Such

calculations can therefore be used to test the validity of the gaussian model[4] for $W_{x_0}[\rho]$ at $x_0 \sim 10^{-2}$ as well as the non-linear dynamics of the classical field.

(ii) Approximate analytical calculations of the initial gluon spectrum [44]. These calculations assume $k_\perp$-factorization, although such a property is so far unproven for the collision of two dense projectiles. The non-integrated gluon

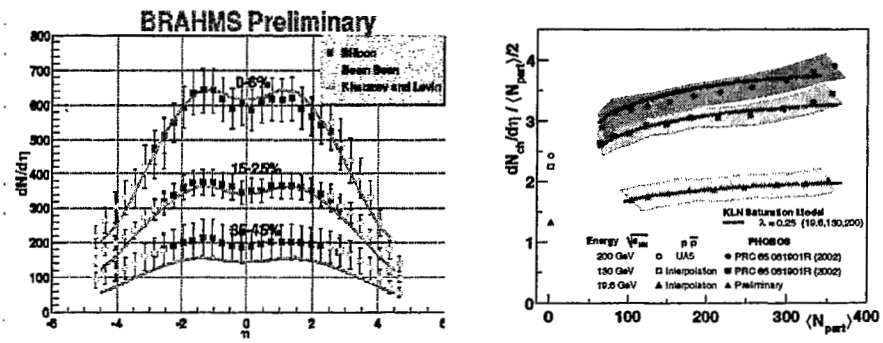

Figure 5: The number of particles per unit of rapidity in AA collisions, as a function of rapidity for different centralities (left plot) and as a function of centrality at different energies (right plot). From [44] .

distribution in the nuclei is taken to be of the form $\varphi(k_\perp) \sim 1/\alpha_s$ for $k_\perp \ll Q_s(x)$ and $\varphi(k_\perp) \sim Q_s^2(x)/k_\perp^2$ for $k_\perp \gg Q_s(x)$ (saturation appears through the fact that the gluon distribution does not diverge like $k_\perp^{-2}$ at small $k_\perp$). The rapidity dependence in this model is governed by that of $Q_s(x)$, eq. (9), where the exponent λ can be taken from the study of the scaling properties in the HERA data. The overall normalization factor, as well as the value of Q_s at a certain fixed energy, were fitted on RHIC data at $\sqrt{s} = 130$ GeV. A prediction was then made in [44] for the value of $dN/d\eta$ at $\sqrt{s} = 200$ GeV, which is in good agreement with experimental results, as illustrated in figure 5. One should also mention the fact that the value of $Q_s^2(x)$ one needs in this approach in order to reproduce the measured $dN/d\eta$, of the order of 2 GeV^2, is relatively large compared to Λ_{QCD}; this may perhaps be taken as an encouraging indication for the validity of the overall picture.

Note that the residual dependence on the number of participants in the quantity $N_{\rm part}^{-1} dN/d\eta$ calculated by Kharzeev, Levin and Nardi, comes entirely from the scale dependence of the strong coupling constant, as follows:

$$\frac{1}{N_{\rm part}} \frac{dN}{d\eta} \sim \frac{1}{\alpha_s(Q_s^2)} \sim \ln(Q_s^2/\Lambda_{QCD}^2) \,. \tag{15}$$

However, strictly speaking, since the gluon multiplicity is obtained by solving the *classical* Yang-Mills equations, there is no running of α_s at this level of

[4]Since the gluon multiplicity depends only on the correlator $\langle A^\mu(x) A^\nu(y) \rangle$, only one moment of the distribution $W_{x_0}[\rho]$ is tested by this observable. One could certainly imagine different models for this distribution that give the same value for this particular correlator.

approximation. Certainly the running of α_s will come together with next-to-leading-order corrections, but it is at this point an ad hoc prescription. Since other interpretations of these same data, based on soft physics, are possible [45], it is unclear whether what we are "seeing" in the right hand panel of figure 5 is indeed the running of $\alpha_s(Q_s^2)$ induced by the variation of the saturation scale with centrality.

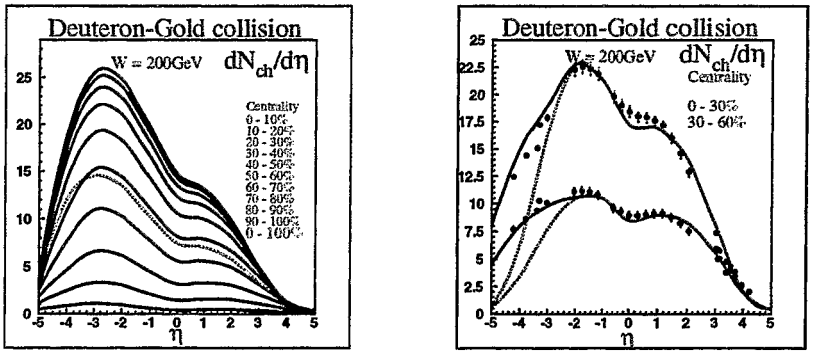

Figure 6: The number of particles per unit of rapidity in dA collisions, as predicted in [46].

Such analysis of multiplicity distributions were extended to the case of deuteron-nucleus collisions [46], with results in fair agreement with RHIC data[5] as illustrated in figure 6.

4.4 Spectra of produced particles

4.4.1 $p_\perp$ dependence

The saturation regime is characterized by a single scale, the saturation momentum Q_s, and as was the case for DIS, one may look for scaling laws in various observables. An attempt has been made to identify such a scaling in the transverse mass distributions of produced particles [47]: it has been found that the spectra for different species of particles are well represented by a single function of $m_\perp/Q_s$. The centrality dependence of the scaling parameter Q_s^2 was found in rough agreement with $Q_s^2 \sim N_{\text{part}}^{1/3} \sim A^{1/3}$. It should be emphasized however, that the hadrons whose spectra are measured have certainly undergone many reinteractions, so that their spectra are unlikely to reflect directly the initial momentum distribution of the color glass. Thus the interpretation of the m_t scaling in the saturation picture is unconvincing.

In the case of deuteron-gold collisions, one does not expect final state interactions to play a dominant role. All the medium effects responsible for

[5]In the first version of this study, there was a discrepancy with the measured multiplicities, which seems to have been pinned down to a problem with the Glauber determination of the number of participants.

the difference between pA and pp collisions may in fact be taken into account in the color glass condensate. The produced partons hadronize then by the same mechanisms as in the vacuum, and their spectrum can be calculated by convoluting the partonic cross-section with the usual fragmentation functions. Moreover, since the calculation of the gluon spectrum only involves the correlator $\langle U(0)U^\dagger(\boldsymbol{x}_\perp)\rangle$ [38,48,49,39], one can in principle determine it from the dipole cross-section used in DIS [50]. A numerical calculation of the spectrum of hadrons produced in dA collisions has been performed in this approach in [51], with results in fairly good agreement with the spectrum measured at RHIC in dA collisions.

The situation is far more complicated in the case of nucleus-nucleus collisions. Indeed, the gluons which emerge from the color glass shortly after the initial impact (typically at a proper time of the order of $Q_s^{-1} \sim 0.2$ fm) will interact strongly and may form a hot and dense medium (a quark-gluon plasma?). These interactions will presumably modify the gluon spectrum: the momentum distribution will become more isotropic and the hard tail of the spectrum will be suppressed by parton energy loss. These additional effects are not taken in to account in the color glass, which merely provides the initial condition for the subsequent evolution of the system.

By assuming that local thermalization is achieved quickly, one can use hydrodynamics to describe this evolution. One may adjust the initial conditions so that integrated quantities like the local energy density match those predicted in saturation models. Such a strategy has been used by Eskola, Niemi, Ruuskanen and Rasanen [52,53], who predicted hadron spectra in good agreement with the observed ones for $p_\perp \lesssim 2$ GeV. One should however keep in mind that this kind of test is by construction only sensitive to integrated quantities predicted by the CGC rather than to the detailed shape of the spectrum: indeed, the very assumption that thermalization occurs means that the system has lost memory of the initial momentum distribution except for the local energy density.

This remark implies that dA collisions are certainly much better suited than AA collisions in order to test the predictions of the color glass condensate, because the details of the system at early times are carried out to the final state almost unaltered. One should therefore be able to perform more direct tests of the CGC ideas in the context of dA collisions.

4.4.2 Anisotropy

Another interesting quantity to look at is the so-called "elliptic flow", which signals the existence of a significant pressure in the transverse direction [54], that converts the original spatial anisotropy into an anisotropy in momentum space.

This has been estimated by Krasnitz, Nara and Venugopalan [55] from the numerical solution of the classical Yang-Mills equations. The growth of the anisotropy with time is similar to what happens in hydrodynamical models, [55] and the full v_2 is attained after a time of the order of the size R of the system.

The v_2 obtained at late times in the color glass condensate framework[6] is plotted in figure 7. One can see that although it is not in quantitative agreement with

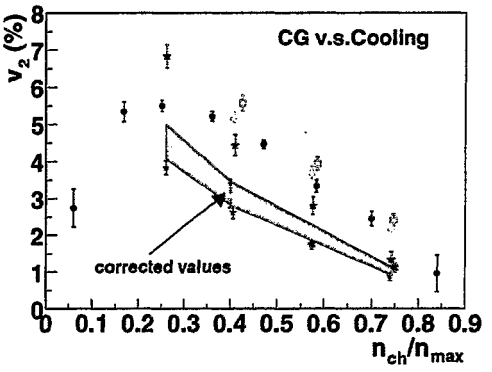

Figure 7: The centrality dependence of v_2 from the classical gluon production (green band). The black filled dots are STAR data.

the data, it has the correct order of magnitude and reproduces qualitatively the dependence on the multiplicity (i.e. on the centrality). However, the dependence of v_2 on the transverse momentum is in clear disagreement with the RHIC data: the color glass condensate predicts that v_2 has a maximum at small momentum and then falls to zero at large momentum, while the measured v_2 increases monotonously up $p_\perp \sim 2$ GeV and remains almost constant at higher momenta. This discrepancy is probably the sign that there are strong final state interactions which drastically change the distribution in $p_\perp$ of the produced gluons.

4.5 Ratios of spectra: R_{AA}, R_{dA}

The comparison of the $p_\perp$ spectra in AA or dA to the corresponding ones in pp collisions is usually done through the following ratio:

$$R_{AA} \equiv \frac{\left.\frac{dN}{dyd^2\boldsymbol{p}_\perp}\right|_{AA}}{N_{\rm coll}\left.\frac{dN}{dyd^2\boldsymbol{p}_\perp}\right|_{pp}}\,, \quad R_{dA} \equiv \frac{\left.\frac{dN}{dyd^2\boldsymbol{p}_\perp}\right|_{dA}}{N_{\rm coll}\left.\frac{dN}{dyd^2\boldsymbol{p}_\perp}\right|_{pp}}\,, \tag{16}$$

where $N_{\rm coll}$ is the number of binary collisions. For the production of high $p_\perp$ particles, expected to scale like the number of binary collisions, these ratios should be unity. These ratios have been measured at RHIC both for AA and dA collisions.

[6]This is of course a somewhat academic exercise since the description of the system in terms of classical fields breaks down for times that are large compared to Q_s^{-1}. However, it is instructive to see that this model, which does not rely on the assumption of thermalization, produces a v_2 of comparable magnitude to the v_2 obtained in hydrodynamical expansion over similar time-scales.

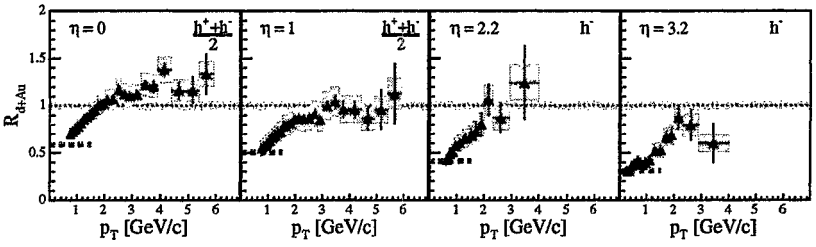

Figure 8: The ratio R_{dA} measured at RHIC by the BRAHMS collaboration at several rapidities (positive rapidities correspond to the fragmentation region of the deuteron) [56].

In AA collisions at central rapidity ($\eta = 0$), the measured R_{AA} is much smaller than one (around 0.2) in central collisions, even at $p_\perp$'s as high as 10 GeV, and approaches one from below as one goes to more and more peripheral collisions. However, at the values of x probed by gluon production at mid-rapidity ($x \sim 10^{-2}$ for $p_\perp \sim 1$ GeV), where one expects the distribution $W_{x_0}[\rho]$ to be given by the McLerran-Venugopalan model (eq. (8)), the R_{AA} predicted in the color glass condensate at a time of the order of Q_s^{-1} has a maximum larger than 1 at small $p_\perp$ and then goes to one from above as $p_\perp$ increases [57]. This maximum of R_{AA} in the MV model is interpreted as a manifestation of the multiple (elastic) rescatterings of the produced gluon, which tend to redistribute the $p_\perp$ spectrum by depleting the small $p_\perp$'s and enhancing the high $p_\perp$'s (Cronin effect). The observed suppression of R_{AA} therefore requires final state effects, and is naturally interpreted as energy loss of the high $p_\perp$ partons as they go through the dense medium formed in AA collisions.

At much smaller values of x, which can be probed by looking at particle production at large rapidity, one expects the distribution $W_{x_0}[\rho]$ to reach the asymptotic form of eq. (7). It has been found that with such a distribution of color sources, the color glass condensate leads to a suppression of the ratios R_{AA} or R_{dA} [58] (see the plots of figure 9, taken from [59]). However, in order to disentangle this suppression which is an initial state effect (because it comes from the "wave function" of the projectiles) from the energy loss, one needs an experiment in which one has no significant final state effects, like dA collisions. The ratio R_{dA} measured by the BRAHMS experiment is shown in figure 8 [56]. One can see at $\eta = 0$ a very different behavior than for AA collisions: the ratio R_{dA} has a maximum above one and seems to go to one from above at high $p_\perp$. As one increases the rapidity of the observed particles, one can see the ratio R_{dA} drop very fast and eventually become consistently smaller than one. Such a behavior with rapidity was predicted in [59] (see the figure 9), where the evolution of the ratio R_{dA} was evaluated by evolving the unintegrated gluon distribution in a nucleus using the Balitsky-Kovchegov equation, starting from the McLerran-Venugopalan model at large x. Similar results were obtained in [60] using a toy model for the gluon distribution inspired from the color

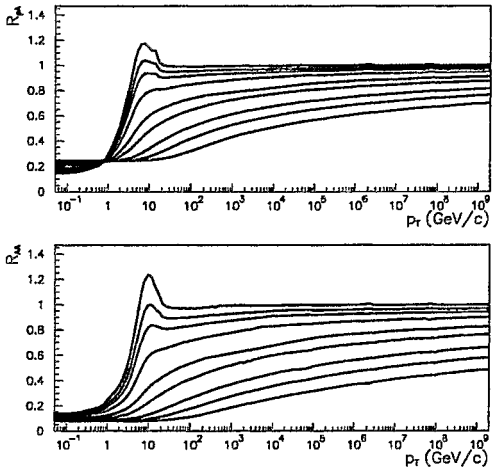

Figure 9: Evolution of the ratios R_{AA} and R_{dA} with rapidity in the color glass condensate framework. The initial condition is the McLerran-Venugopalan model. Note that the calculation of R_{AA} assumed $k_\perp$-factorization.

glass condensate, and in [39] were the two distributions of frozen sources given in eqs. (7) and (8) were used in order to compute the ratio R_{dA}. The onset of the suppression of the ratio R_{dA} as one increases the rapidity was studied analytically in [61], where it was shown that the rapid suppression seems is due to the fact that the gluon distribution evolves faster in a proton than it does in a nucleus, because the nucleus reaches the saturation regime earlier. So far, the color glass condensate is the only framework in which one reproduces, at least qualitatively, both the the Cronin effect at central rapidities and its suppression at forward rapidities.

5 Discussion and outlook

Considerable theoretical progress has been made over the last ten years in understanding the physics that governs the wave function of a hadron at high energy. Not only has one acquired a fairly intuitive picture that is universally applicable to all hadrons at high energy, but an operational framework has been developed in which many phenomena can be described quantitatively. One is now in principle able to study and make predictions in the entire $x, k_\perp$ plane (with the exception of the truly non-perturbative region $k_\perp \lesssim \Lambda_{QCD}$), with non-perturbative physics entering only as an initial condition for otherwise known evolution equations.

With the realization that the characteristic scale that governs high energy hadronic interactions, the saturation momentum Q_s, is enhanced by the size

of the projectiles in collisions involving nuclei, RHIC can be viewed as a place of choice in order to test these ideas and confront them to data. An indeed the phenomenology based on saturation physics has been quite successful in describing what is observed at RHIC. Whenever relevant comparisons with data can be made (global observables in AA collisions, spectra in dA collisions), the tests are successful. In cases of marked disagreement, like with the elliptic flow, one understands that the discrepancy comes from using the color glass picture beyond its domain of applicability.

One may ask whether the predictions which have been tested so far are distinctive features of the color glass condensate that cannot be reasonably explained by other models. Naturally, the more precise the question, the more discriminatory the answer. Because in AA collisions the final state interactions are important, only global observables are preserved from early times to the final state. Therefore AA collisions are in general not ideal for direct tests of the color glass condensate (many global features of AA collisions are present in any reasonable model of hadronic interactions, and thus not characteristic of the color glass condensate). Collisions involving a small projectile, like dA collisions, where effects of final state interactions can be minimized, at least in some kinematical domains, are much better suited. And indeed the suppression of the ratio R_{dA} at forward rapidities could turn out to be such a distinctive measurement, since no other model has been able so far to provide a natural explanation of what is observed. This is also one instance where non trivial quantum evolution could be playing a significant role. What is missing for this to become a real test is a detailed calculation of this effect that would go beyond the many qualitative approaches performed so far. Clearly, doing such calculations, as well as getting more precise data, is of utmost importance.

From comparisons with data, one has also learned that final state interactions are generally very important in AA collisions, and many observables do not simply reflect the properties of the partonic system produced in the early stages. The color glass condensate only provides the initial condition for a subsequent evolution of the system leading possibly to the formation of a quark-gluon plasma. Understanding whether and how thermalization happens presents interesting theoretical challenges (see [62,63] for two recent works on the subject) and is of utmost importance for giving a solid theoretical basis to present descriptions of AA collisions.

As a final remark, oriented towards the future, one may note that many of the phenomena uncovered at RHIC, should become more clearly visible at the LHC. There, with center of mass energies of 5.5 TeV for AA collisions, the typical value of x at mid-rapidity will be about 5.10^{-4} and values as small as 10^{-5} could be reached at forward rapidities. This corresponds roughly to values of Q_s^2 ranging from 5 GeV^2 to 14 GeV^2. Such large values of the saturation momentum make the coupling constant α_s smaller than at RHIC, giving firmer grounds to the weak coupling expansion used in the color glass condensate framework. A corollary of this is that the gluon occupation number in the saturation region will be larger, making the classical description also more justified.

Acknowledgements

We would like to thank E. Iancu and A.H. Mueller for their careful reading of this manuscript.

References

[1] R.P. Feynman, *Photon-Hadron Interactions*, Frontiers in Physics, W.A. Benjamin, (1972).

[2] J.D. Bjorken, Lecture Notes in Physics, **56**, Springer, Berlin (1976).

[3] E.A. Kuraev, L.N. Lipatov, V.S. Fadin, Sov. Phys. JETP **45**, 199 (1977).

[4] I. Balitsky, L.N. Lipatov, Sov. J. Nucl. Phys. **28**, 822 (1978).

[5] V.N. Gribov, L.N. Lipatov, Sov. J. Nucl. Phys. **15**, 438 (1972).

[6] V.N. Gribov, L.N. Lipatov, Sov. J. Nucl. Phys. **15**, 675 (1972).

[7] G. Altarelli, G. Parisi, Nucl. Phys. **B 126**, 298 (1977).

[8] Yu. Dokshitzer, Sov. Phys. JETP **46**, 641 (1977).

[9] L.V. Gribov, E.M. Levin, M.G. Ryskin, Phys. Rept. **100**, 1 (1983).

[10] A.H. Mueller, Nucl. Phys. **B 558**, 285 (1999).

[11] A.H. Mueller, J-W. Qiu, Nucl. Phys. **B 268**, 427 (1986).

[12] J.P. Blaizot, A.H. Mueller, Nucl. Phys. **B 289**, 847 (1987).

[13] A.H. Mueller, Talk given at QM2002, Nantes, France, July 2002, Nucl. Phys. **A 715**, 20 (2003).

[14] L.D. McLerran, R. Venugopalan, Phys. Rev. **D 49**, 2233 (1994).

[15] L.D. McLerran, R. Venugopalan, Phys. Rev. **D 49**, 3352 (1994).

[16] L.D. McLerran, R. Venugopalan, Phys. Rev. **D 50**, 2225 (1994).

[17] J. Jalilian-Marian, A. Kovner, A. Leonidov, H. Weigert, Nucl. Phys. **B 504**, 415 (1997).

[18] J. Jalilian-Marian, A. Kovner, A. Leonidov, H. Weigert, Phys. Rev. **D 59**, 014014 (1999).

[19] I. Balitsky, Nucl. Phys. **B 463**, 99 (1996).

[20] Yu.V. Kovchegov, Phys. Rev. **D 54**, 5463 (1996).

[21] Yu.V. Kovchegov, Phys. Rev. **D 61**, 074018 (2000).

Other RBRC Scientific Articles Proceedings Volumes:

Volume 1 **Prospects for Spin Physics at RHIC**
Gerry Bunce, Naohito Saito, Jacques Soffer, Werner Vogelsang
July 2000

Volume 2 **Status Report on the Calculation of ε'/ε**
RBRC-Brookhaven-Columbia Collaboration
November 2000

Volume 3 **Scientific Presentations: 7th Meeting of the Management Steering Committee of the RIKEN BNL Collaboration, RIKEN, Wako, Japan, February 13-14, 2001**

Volume 4 **CP Violation in K Decay From Lattice QCD**
Thomas Blum and Robert Mawhinney
RBRC-Brookhaven-Columbia QCDSP Collaboration
July 26, 2001

Volume 5 **Scientific Presentations: 8th Meeting of The Management Steering Committee of The RIKEN BNL Collaboration, RIKEN, Wako, Japan, March 11-12, 2002**

Volume 6 **BNL/RIKEN RHIC Spin Physics Symposium**
RIKEN BNL Research Center Fifth Anniversary Celebration, April 30, 2002

Volume 7 **Reflections on My Contributions to Particle Physics and Recent Experimental Results from RHIC**
N. P. Samios
Dubna, Russia, January 18, 2002

Volume 8 **RBRC/CCAST Symposium on Spin Physics, Lattice QCD and RHIC Physics, CCAST, Beijing, China,**
April 7, 2003